UNIQUE GLYCOLYTIC PATHWAY ENZYMES AS MOLECULAR TARGETS FOR NOVEL ANTI-CRYPTOSPORIDIAL DRUGS

BY

SHAHBAZ MANZOOR KHAN

DISSERTATION

Submitted in partial fulfillment of the requirements
for the degree of Doctor of Philosophy in VMS-Pathobiology
in the Graduate College of the
University of Illinois Urbana-Champaign, 2023

Urbana, Illinois

Doctoral Committee:

Associate Professor William H. Witola, Chair and Director of Research
Professor Weiping Zhang
Professor Federico A. Zuckermann
Associate Professor Prabhakara P. Reddi

ABSTRACT

The intracellular protozoan parasite of the genus *Cryptosporidium* is among the leading causes of waterborne diarrheal disease outbreaks throughout the world. The parasite is transmitted by ingestion of infective oocysts that are highly stable in the environment and resistant to almost all conventional disinfection methods and water treatments. Control of the parasite infection is exceedingly difficult due to the excretion of large numbers of oocysts in the feces of infected individuals that contaminate the environment and serve as a source of infection for susceptible hosts including humans and animals. Drug development against the parasite is challenging owing to its limited genetic tractability, absence of conventional drug targets, unique intracellular location within the host, and the paucity of robust cell culture platforms for continuous parasite propagation. Despite the high prevalence of the parasite, the only United States Food and Drug Administration (FDA)-approved treatment for *Cryptosporidium* infections is nitazoxanide, which has shown moderate efficacy in immunocompetent patients. More importantly, no effective therapeutic drugs are available for treating severe, potentially life-threatening cryptosporidiosis in immunodeficient patients, young children, and neonatal livestock. Several compounds have been tested for both *in vitro* and *in vivo* efficacy against the disease. However, to date, only a few experimental compounds have been subjected to clinical trials in natural hosts, and among those none have proven efficacious. Thus, safe, inexpensive, and efficacious drugs are urgently required to reduce the ever-increasing global cryptosporidiosis burden especially in low-resource countries.

The long-term goal of this study is to unveil validated lead-compound combinations for developing new effective drugs for treating *C. parvum* infection in humans and livestock. *C. parvum* possesses greatly simplified and curtailed metabolic and biochemical pathways in

comparison to other apicomplexan parasites. Owing to the nonexistence of tricarboxylic acid cycle and ATP generating oxidative phosphorylation, *C. parvum* depends heavily on glycolysis for energy production. In the glycolytic pathway of *C. parvum*, the last two reaction steps that lead to the generation of metabolic energy (ATP) are catalyzed by a plant-type *C. parvum* pyruvate kinase (CpPyK), and a bacterial-type *C. parvum* lactate dehydrogenase (CpLDH). CpLDH and CpPyK are significantly different from their mammalian counterparts, making them ideal molecular targets for developing safe and efficacious anti-cryptosporidial drugs. In our previous studies, we have found that inhibitors of CpLDH enzyme can stop growth of the parasite and prevent disease in infected mouse models. In the present study, we developed a CpPyK enzyme-based assay and identified several compounds with *in vitro* inhibitory activity against the recombinant CpPyK enzyme. We used a series of *in vitro* cytotoxicity and parasite growth inhibition assays to study the safety and anti-cryptosporidial efficacy of these CpPyK-inhibitors. Safety and effectiveness of identified compounds was further validated in an immunocompromised mouse infection model to select non-toxic compounds, NSC234945 and NSC252172, with high *in vivo* efficacy against the parasite.

Herein, we also investigated the anti-cryptosporidial synergistic activities of CpLDH- and CpPyK-inhibitors in *C. parvum*-infected mammalian cells using multiple synergism assessment methods: curve-shift analysis, combination-index method, dose-reduction index analysis, and isobologram analysis. Synergy analysis of *in vitro* dose-response data identified combinations of CpLDH- and CpPyK-inhibitors with strong synergistic effects against the growth and survival of *C. parvum*. The combinations that showed synergistic activity were evaluated for safety and efficacy against *C. parvum* using an *in vivo* mouse infection model. In immunocompromised mice, NSC303244+NSC158011, and NSC252172+NSC158011 compound combinations

demonstrated improved effectiveness in reducing *C. parvum* oocyst numbers, and alleviated the intestinal damage caused by cryptosporidiosis at doses lower than those required for individual compounds. Notably, the NSC303244+NSC158011 combination proved to be effective in completely eradicating the infection in immunocompromised mice, without any subsequent relapse.

Although combination therapy has proven effective in treating other related apicomplexan diseases, minimal efforts have been made to evaluate drug combinations against cryptosporidiosis. Our study has discovered combinations of compounds that effectively inhibit two crucial catalytic steps involved in metabolic energy production in *C. parvum* with enhanced efficacy against the parasite. Collectively, the results of this study will have an overall positive and significant impact in the challenging field of *Cryptosporidium* drug discovery by generating a new class of highly active and safe therapeutic leads for treating cryptosporidiosis in vulnerable human and animal populations.

ACKNOWLEDGMENTS

First, and most importantly, praise and thanks be to Allah (God), the most merciful, the most gracious, for giving me the inspiration, wisdom, strength, and endurance to complete this dissertation.

I would like to take this opportunity to express my deepest gratitude and appreciation to all those who have supported and guided me throughout the course of my research:

First and foremost, I am immensely grateful to my supervisor, Dr. William Witola, for his expert guidance and constant support throughout this research endeavor. His insightful feedback and continuous encouragement have been invaluable in shaping the direction and content of this research. I thank him for giving me an opportunity to work in his laboratory and supporting me financially during my graduate studies.

I am immensely grateful to my doctoral advisory committee members, Dr. Weiping Zhang, Dr. Federico Zuckermann, and Dr. Prabhakara Reddi, for their valuable insights, constructive comments, and thoughtful suggestions during the various stages of my research.

I am also thankful to all faculty members, staff, and fellow graduate students of the Department of Pathobiology, University of Illinois Urbana-Champaign for providing a stimulating academic environment for research and learning. My special thanks go out to Karen Nichols for her immense role in the smooth operation of departmental activities and for taking care of any administrative issues that I faced during my degree program.

I want to thank all past and present graduate students of the Witola Lab: Xuejin Zhang, Mukthar Mia, Muhammad Rashid Bajwa, Abdur Rehman Azam, and Akansha Singh, who have offered their encouragement, insightful discussions, and assistance throughout this thesis.

I would also like to express my heartfelt thanks to my parents for their prayers, love, and encouragement throughout my academic journey. Your belief in me has been my constant motivation, and I am forever grateful for your endless support.

Lastly, I would like to acknowledge the moral support of my family, whose understanding, and patience have been my pillars of strength throughout this journey, and whose sacrifices have enabled me to pursue my academic goals.

Thank you all for being an integral part of this milestone in my academic career. Your contributions have made this journey both rewarding and memorable.

To my beloved children, Myra, and Rayan

I dedicate this thesis to you as a symbol of my deep appreciation for your sacrifices

TABLE OF CONTENTS

CHAPTER 1: LITERATURE REVIEW

1.1 INTRODUCTION

1.1.1 History.

The intracellular protozoan parasite *Cryptosporidium* is one of the most common parasitic pathogens causing enteric disease in humans and in a broad range of animals worldwide (Chalmers, 2014). First recognized and described briefly in 1907 by Ernest Tyzzer in the gastric glands of the common mouse (Tyzzer, 1907), *Cryptosporidium* was later described in greater detail in 1910, again from histological preparations from the murine gastric mucosa (Tyzzer, 1910). Tyzzer proposed the name *Cryptosporidium muris* for the parasite (Tyzzer, 1907; 1910). In 1912, Tyzzer described another species with smaller oocysts than those of *C. muris* in the small intestine of experimentally infected laboratory mice, which he named *Cryptosporidium parvum* (Tyzzer, 1912). Although *Cryptosporidium* was subsequently identified in a wide range of domesticated animals, this genus of parasites only gained importance in the 1970s (after almost 7 decades from its initial discovery), when the parasite was found to be linked to gastrointestinal disease in humans and farm animals (Panciera et al., 1971; Meuten et al., 1974; Meisel et al., 1976; Nime et al., 1976). In the 1980s, cryptosporidiosis gained more widespread recognition after reports of fatal cryptosporidiosis in AIDS patients (Soave et al., 1984), zoonotic cryptosporidiosis in immunocompetent and immunodeficient humans (Current et al., 1983), waterborne human diarrheal outbreaks (D'Antonio et al., 1985; Hayes et al., 1989), and diarrheal disease in children (Sallon et al., 1988) and animals (Tzipori et al., 1980; Moon and Bemrick, 1981; Angus et al., 1982).

Part of this chapter has been published as a review article in Frontiers in Cellular and Infection Microbiology. The original citation is: Khan, S.M., and Witola, W.H. (2023). Past, current, and potential treatments for cryptosporidiosis in humans and farm animals: A comprehensive review. *Front Cell Infect Microbiol* 13**,** 1115522. doi: 10.3389/fcimb.2023.1115522. PubMed PMID: 36761902.

In 1993, *Cryptosporidium* caused the largest documented drinking water outbreak in US history, which affected an estimated 403,000 people in Milwaukee, Wisconsin, and resulted in over $96 million in combined healthcare costs and productivity losses (Mac Kenzie et al., 1994; Hoxie et al., 1997; Corso et al., 2003). The enormity of the Milwaukee outbreak sparked concern among the public and attracted generous funds for *Cryptosporidium* research from governmental agencies all over the world during the next decade. This resulted in further advances in our knowledge about the basic biology of the parasite and the development of reliable molecular detection tools for estimating the global burden of the disease.

1.1.2 Life Cycle.

The life cycle of *Cryptosporidium* is direct and complex (Figure 1.1), consisting of both asexual multiplication and sexual reproduction phases within a single host that culminate in the production of environmentally resistant oocysts (Current and Garcia, 1991). Following ingestion of sporulated thick-walled oocysts, four infectious sporozoites are released from each oocyst upon exposure to host-derived signals such as low pH, warm body temperature, and the presence of digestive enzymes and/or bile salts in the gastrointestinal tract (Fayer and Leek, 1984; Reduker and Speer, 1985). The sporozoites exhibit gliding motility, attach to the apical surface of intestinal epithelial cells, and then actively invade the host cell membrane to form an intracellular but extracytoplasmic parasitophorous vacuole (Current and Reese, 1986; Wetzel et al., 2005). Within the vacuole, sporozoites mature into trophozoites, which undergo three rounds of asexual proliferation by merogony to produce meronts with eight merozoites, followed by a single generation of sexual stages. Merozoites emerging from the third round of merogony are thought to initiate the sexual cycle and differentiate into either a microgamont (male) or a macrogamont (female) stage upon host cell reinvasion (English et al., 2022). Microgametes

released from the microgamont penetrate and fertilize macrogamonts to form diploid zygotes. The zygotes undergo meiosis and sporogony generating either thin-walled or thick-walled oocysts, each containing four haploid sporozoites (Current and Reese, 1986). Thick-walled oocysts containing two-layered membranes are environmentally resistant and are passed out of the body in feces, where they are immediately infectious for other susceptible hosts. Thin-walled oocysts rupture in the intestinal lumen, releasing naked infectious sporozoites that autoinfect other enteric cells to ensure continued infection of the same host.

1.1.3 Transmission.

In general, cryptosporidiosis is transmitted through the fecal-oral route (Figure 1.1) and contact with animals, manure or contaminated food and water is believed to lead to infections in humans (Xiao et al., 2004). Transmission in animals mainly occurs via ingestion of oocysts excreted by infected animals, especially neonates in overcrowded or mixed housing facilities. Manure produced by livestock, especially cattle, is an important source of infection to both animals and people and it has been estimated that the global *Cryptosporidium* load in livestock manure is approximately 3.2×10^{23} oocysts per year (Vermeulen et al., 2017). Oocysts are highly stable in the environment and resistant to almost all conventional disinfection methods and water treatments such as chlorination (Fayer et al., 2000). Indeed, these persistent parasites have been found to be responsible for majority of the global protozoal water outbreaks that occurred from 2004–2010 (Karanis, 2018) and pose the biggest pathogen threat to the water industry (Chalmers, 2012). In the United States, exposure to treated recreational water such as swimming pools and water playgrounds was responsible for nearly 35% of the reported cryptosporidiosis outbreaks resulting in almost 57% cases during 2009–2017 (Gharpure et al., 2019). In addition to treated recreational water, contact with infected cattle (~15%), and contact with infected persons

in childcare settings (~13%) were the other predominant causes of these outbreaks (Gharpure et al., 2019). *Cryptosporidium* is also recognized as an important foodborne pathogen, being responsible for more than 40 documented foodborne outbreaks to date, and more than 8 million cases of foodborne illnesses annually (Zahedi and Ryan, 2020). However, these numbers may be highly under-reported due to the lack of proper surveillance and the difficulties in tracing the source of foodborne disease outbreaks. Food can be contaminated at any point along the food production chain (during processing, distribution, or preparation) by direct contact with infected food handlers or by indirect exposure to water, preparation surfaces, equipment, or utensils contaminated with oocysts. Raw unpasteurized milk, unpasteurized apple cider, and salads are most associated with foodborne outbreaks of cryptosporidiosis (Gharpure et al., 2019; Zahedi and Ryan, 2020).

1.2 CRYPTOSPORIDIOSIS GLOBAL DISEASE BURDEN IN HUMANS AND ANIMALS

Cryptosporidium spp. enjoy high parasitic success due to their wide host range, low infective threshold, high excretion of resistant oocysts from infected individuals, and water-borne route of transmission (Innes et al., 2020). Protozoa of this genus are associated with diarrheal disease throughout the world with a higher incidence in developing countries (Shirley et al., 2012). Cryptosporidiosis is a major cause of public health concern in developed countries as well, with reported cases on the rise mainly due to the leading role of *Cryptosporidium* in causing waterborne outbreaks (Gharpure et al., 2019). Unfortunately, the global burden of cryptosporidiosis is likely to be underestimated, due to the lack of cheap and consistent methods of diagnosis, under-recognized disease in immunocompetent patients, lack of proper surveillance in developed countries, and difficulties observed in measuring the impact of the disease in poor-resource areas. Many infected individuals either do not exhibit symptoms or exhibit mild

symptoms due to a self-limiting illness, and such infections often go unrecognized. There is a wide range of disease severity that is affected by the host's age, nutritional, and immune status, and perhaps by the parasite species and subtype (Shirley et al., 2012). Differences in sensitivity of methods, type of diagnostics used, and study populations have resulted in a large variation in burden estimates for diarrhea from *Cryptosporidium* infection in humans and animals. However, recent advances in knowledge and the development of highly sensitive and superior diagnostic and typing tools have improved our understanding of the epidemiology and true burden of the disease.

1.2.1 Humans.

Out of the currently documented 44 species of *Cryptosporidium*, *Cryptosporidium hominis* (*C. hominis*) and *Cryptosporidium parvum* (*C. parvum*) are responsible for most human infections (Ryan et al., 2021a). While *C. hominis* is primarily anthroponotic and only infects humans, *C. parvum* is a zoonotic parasite that can be transmitted between humans and animals. Apart from *C. hominis* and *C. parvum*, 21 other *Cryptosporidium* species and genotypes including *C. meleagridis*, *C. felis*, *C. canis*, *C. ubiquitum*, *C. cuniculus*, *C. ditrichi*, *C. erinacei*, *C. fayeri*, *C. scrofarum*, *C. tyzzeri*, *C. viatorum*, *C. muris*, *C. andersoni*, *C. suis*, *C. bovis*, *C. occultus*, *C. xiaoi*, horse genotype, chipmunk genotype I, skunk genotype, and mink genotype have also been reported in humans (Ryan et al., 2021a).

Cryptosporidiosis is considered a high-risk and often lethal opportunistic disease for patients with compromised immune systems such as those suffering from HIV/AIDS (O'Connor R et al., 2011) or those receiving organ transplants (Danziger-Isakov, 2014; Bhadauria et al., 2015). The global prevalence of *Cryptosporidium* in HIV/AIDS patients was 10.09% during the period from 2007 to 2017 (Wang et al., 2018). However, the greatest burden of cryptosporidiosis

occurs among young children living in less developed countries. *Cryptosporidium* prevalence is higher in such areas that lack proper sanitation facilities, mainly drinking water and sewage, which led the World Health Organization (WHO) to include it in the water sanitation and health program (WHO, 2009). Several epidemiological studies conducted in the previous decade have estimated the disease burden of diarrheal pathogens in developing countries. In the Global Enteric Multicenter Study (GEMS) conducted at seven sites in sub-Saharan Africa and South Asia, *Cryptosporidium* was found to be the main cause of linear growth faltering and the second leading cause of moderate-to-severe diarrhea in infants (0–11 months of age) (Kotloff et al., 2013; Nasrin et al., 2021). *Cryptosporidium* infection was also associated with a higher risk of mortality in diarrheic children aged 12–23 months who were admitted to hospitals (Kotloff et al., 2013). The 2016 Global Burden of Diseases, Injuries, and Risk Factors study (GBD) identified *Cryptosporidium* as a leading cause of diarrheal mortality in children younger than 5 years old with an estimated loss of 4.2 million disability-adjusted life years (DALYs) (Collaborators, 2018). However, this study focused on acute illness alone, and as such, the number increased to 12.9 million DALYs, when long-term-effects of cryptosporidiosis such as growth retardation and cognitive defects were also considered (Khalil et al., 2018). Furthermore, the MAL-ED (Etiology, Risk Factors, and Interactions of Enteric Infections and Malnutrition and the Consequences for Child Health and Development Project) study carried out at eight sites in South America, sub-Saharan Africa, and Asia, found that *Cryptosporidium* along with four other pathogens exhibited the highest attributable burdens of diarrhea in community clinics in the first year of life (Platts-Mills et al., 2015).

1.2.2 Cattle.

At least four main *Cryptosporidium* species infect cattle: *C. parvum, C. bovis, C. ryanae,* and *C. andersoni* (Lindsay et al., 2000; Santin et al., 2004; Fayer et al., 2005; Fayer et al., 2008), although other species have also been reported in sporadic cases, including *C. felis, C. hominis, C. suis, C. canis, C. scrofarum, C. tyzzeri, C. serpentis*, and *C. occultus* (formerly known as the *C. suis*-like genotype) (Robertson et al., 2014; Santin, 2020). The occurrence of *C. parvum, C. bovis, C. ryanae,* and *C. andersoni* in cattle follows an age-related pattern: the zoonotic *C. parvum* infects mostly pre-weaned calves, *C. bovis* and *C. ryanae* are found mostly in post-weaned calves, whereas *C. andersoni* is the predominant species found in heifers and adults (de Graaf et al., 1999; Santin et al., 2004; Fayer et al., 2006; Santin et al., 2008; Khan et al., 2010).

Cryptosporidiosis is one of the most important global causes of diarrhea in neonatal farm ruminants including calves. *Cryptosporidium* parasites invade intestinal epithelial cells and cause severe mucosal erosion resulting in villus shortening and fusion, and hypertrophy of crypts at small intestinal sites that lead to impaired digestion and increased intestinal permeability (Tzipori et al., 1983). The resulting diarrhea causes high production losses including mortality, reduced live weight gain, veterinary costs, and the added feeding and rearing costs for affected animals with slowed growth rates (Innes et al., 2020; Santin, 2020; Shaw et al., 2020). Cryptosporidiosis is recognized as endemic in cattle worldwide and the prevalence of bovine cryptosporidiosis varies substantially between countries, age groups, and studies, ranging from 11.7 to 78%, with the highest incidence reported in pre-weaned calves (Santin et al., 2004; Watanabe et al., 2005; Fayer et al., 2006; Maddox-Hyttel et al., 2006; Trotz-Williams et al., 2007; Khan et al., 2010; Amer et al., 2013; Thomson et al., 2017; Hatam-Nahavandi et al., 2019). An 18-month longitudinal study that focused on 2,545 dairy heifer calves from birth to weaning at 104 dairy operations in 13 US states identified at least 1 calf positive for *Cryptosporidium* at almost all

operations (Urie et al., 2018b). Furthermore, the overall prevalence of *Cryptosporidium* in pre-weaned heifer calves was 43.1% with the disease more prevalent among young calves less than 2 weeks of age (63.3%) compared with calves older than 6 weeks (9.1%) (Urie et al., 2018a).

1.2.3 Small Ruminants.

Of the species infecting small ruminants, *C. parvum, C. ubiquitum, and C. xiaoi* are the most frequently detected species (Fayer and Santin, 2009; Fayer et al., 2010; Santin, 2020). In addition, *C. andersoni, C. bovis, C. ryanae, C. hominis, C. fayeri, C. baileyi*, and *C. suis* have been identified sporadically in sheep and goats (Hatam-Nahavandi et al., 2019; Santin, 2020).

Cryptosporidium causes significant morbidity and mortality in neonatal lambs and goat kids (de Graaf et al., 1999; Wright and Coop, 2007). Diarrhea resulting in reduced productivity and growth has been associated with *Cryptosporidium* infections in lambs and kids (Paraud and Chartier, 2012; Jacobson et al., 2016; Jacobson et al., 2018). *Cryptosporidium* shedding was also associated with less carcass weight and lowered dressing percentage in both symptomatic and apparently asymptomatic sheep on Australian farms (Jacobson et al., 2016). A wide range of *Cryptosporidium* prevalence based on microscopy and molecular detection methods has been reported in small ruminants worldwide ranging from 12.5% to 77.4% in lambs (Causape et al., 2002; Ryan et al., 2005; Castro-Hermida et al., 2007; Goma et al., 2007; Santin et al., 2007; Geurden et al., 2008) and from 4.8% to 70.8% in goat kids (Noordeen et al., 2001; Watanabe et al., 2005; Castro-Hermida et al., 2007; Goma et al., 2007; Geurden et al., 2008). As in cattle, *Cryptosporidium* oocysts are found mostly in feces of very young animals (1−3 weeks of age), with a lower incidence in older animals (de Graaf et al., 1999; Noordeen et al., 2001; Causape et al., 2002; Santín and Trout, 2007).

1.2.4 Pigs.

The most common species and subtypes found in pigs are *C. parvum*, *C. suis*, and *C. scrofarum* formerly known as *Cryptosporidium* pig genotype II (Zahedi and Ryan, 2020), although *C. muris* and *C. tyzzeri* have also been reported occasionally (Robertson et al., 2014). As seen in ruminants, *Cryptosporidium* species tend to generally follow an age-related pattern: *C. suis* is more commonly found in piglets whereas starter pigs and fatteners primarily host *C. scrofarum* (Petersen et al., 2015).

There is a huge disparity in prevalence rates (0.1% to 100%) reported from all over the world (Robertson et al., 2014). Nonetheless, it is obvious that prevalence and intensity of infection is predominant in younger animals than older ones (Maddox-Hyttel et al., 2006; Petersen et al., 2015). While natural or experimental infections with the pig-adapted species, *C. suis* and *C. scrofarum*, are usually asymptomatic and cause mild or no illness (Robertson et al., 2014), experimental infection of piglets with either *C. parvum* or *C. hominis* results in watery diarrhea, anorexia, mucosal lesions, and increased mortality (Tzipori et al., 1994; Theodos et al., 1998; Lee et al., 2017).

1.3 TREATMENT OPTIONS IN HUMANS AND ANIMALS: THE PAST AND CURRENT STATE OF AFFAIRS

Immunocompromised patients, neonatal animals, and young children, especially malnourished ones are the most vulnerable to cryptosporidiosis, and hence, are the ones in most urgent need for effective therapeutics. Although cryptosporidiosis causes a self-limiting diarrheal illness in immunocompetent humans, patients do face a considerable risk for longer-term sequelae, especially in low-income countries. Additionally, *Cryptosporidium* infections in adult animals can lead to reduced production and result in economic losses to the livestock and food industry. As such, there is an urgent need for the development of safe, inexpensive, and

efficacious drugs to reduce the ever-increasing worldwide burden of this disease. However, despite the widespread occurrence of the parasite, current effective treatment and prophylactic options for human and animal *Cryptosporidium* infections are virtually non-existent.

1.3.1 Humans.

Several drugs with *in vitro* and *in vivo* anti-*Cryptosporidium* activity have been tested against human cases of cryptosporidiosis in uncontrolled/controlled clinical trials, open label/blinded studies, and case reports. These include macrolides, rifamycin derivatives, letrazuril, paromomycin, nitazoxanide, clofazimine, and other pharmacological agents (Table 1.1). In addition to drugs having direct anti-parasitic activity, other medications that augment the host immunity or ameliorate the symptoms/pathology of cryptosporidiosis have also been tested for the management of the disease (Table 1.2). However, unfortunately most of these treatments showed limited efficacy and inconsistent results when tested in the most susceptible target population including immunocompromised individuals and young children.

1.3.1.1 Nitazoxanide.

Thus far, nitazoxanide is the only drug approved by the United States Food and Drug Administration (FDA) for the treatment of cryptosporidiosis in immunocompetent human patients (Checkley et al., 2015). Nitazoxanide is a member of the thiazole class of drugs that was initially developed as a veterinary anthelmintic but was later reported to have broad-spectrum activity against parasites, viruses, and bacteria. This drug acts by inhibiting the pyruvate:ferredoxin/flavodoxin oxidoreductase (PFOR), an enzyme essential for the anaerobic energy metabolism of various microorganisms (Hoffman et al., 2007). However, the exact mechanism of action against *Cryptosporidium* remains questionable since these parasites encode a unique PFOR with a fused C-terminal cytochrome P450 domain (Rotte et al., 2001).

Interestingly, nitazoxanide was shown to inhibit the growth of *C. parvum* by more than 90% at a concentration of 10 µg/ml (32 µM) in cell culture but was ineffective in the anti-IFN-γ-conditioned SCID mouse model of cryptosporidiosis even at high doses (Theodos et al., 1998). Furthermore, nitazoxanide has also been found to be ineffective in other immunodeficient or immunocompromised animal models of cryptosporidiosis, questioning the true efficacy of the drug (Lee et al., 2017; Jumani et al., 2018).

Various randomized placebo-controlled studies have found nitazoxanide to be helpful in treating cryptosporidiosis in adults and children without HIV resulting in reduced duration of both diarrhea and oocyst shedding (Rossignol et al., 2001; Amadi et al., 2002; Rossignol et al., 2006; Hussien et al., 2013; Abaza et al., 2016). Studies conducted in Egyptian immunocompetent adults and children demonstrated significantly higher clinical and parasitological cure rates compared with the placebo-treated groups (Rossignol et al., 2001; Rossignol et al., 2006). In a randomized controlled trial involving malnourished children in Zambia, nitazoxanide treatment for 3 days yielded a partial but significantly better cure than placebo (Amadi et al., 2002). Recent controlled trials have also reported complete clinical and parasitological recovery in most immunocompetent children with cryptosporidiosis (Hussien et al., 2013; Abaza et al., 2016).

However, a meta-analysis of seven randomized controlled trials involving 169 participants with cryptosporidiosis confirmed the absence of obvious evidence of efficacy of nitazoxanide in HIV-seropositive patients (Abubakar et al., 2007). A course of nitazoxanide does not appear to improve the resolution of diarrhea and parasitological outcome in HIV-infected and immunocompromised patients (Doumbo et al., 1997; Rossignol et al., 1998; Amadi et al., 2002; Zulu et al., 2005; Amadi et al., 2009; Abaza et al., 2016). In the first randomized controlled trial of this drug in adult HIV patients with cryptosporidiosis, better overall parasite clearance rates

were seen in the treated group compared with the placebo one, but significant differences were only seen in those with CD4+ T-cell counts above 50/mm^3 (Rossignol et al., 1998). Other randomized placebo-controlled trials conducted by Amadi and others in HIV-positive children in Zambia have also documented no beneficial effect of nitazoxanide over placebo in terms of clinical and parasitological cure rates or mortality (Amadi et al., 2002; Amadi et al., 2009). Moreover, only moderate efficacy was achieved in a study of cryptosporidiosis in immunocompromised children even after prolonged nitazoxanide treatment of up to 28 days (Abaza et al., 2016). While prolonged therapy with higher doses of the drug is somewhat effective in treating cryptosporidiosis in patients with compromised immunity, normal prescribed doses and short-term duration of therapy are inadequate for preventing recurrence of disease symptoms after treatment discontinuation (Abraham et al., 2008; Krause et al., 2012; Ali et al., 2014; Bhadauria et al., 2015; Demonchy et al., 2021). Therefore, it is evident that nitazoxanide therapy is clearly futile in treating cryptosporidiosis in advanced AIDS patients and other severely immunocompromised patients.

Lack of efficacy in immunocompromised animal models and humans suggests that a healthy host immune system is essential to the effectiveness of nitazoxanide. Nitazoxanide treatment has been recently shown to result in broad amplification of the host cell innate immune response to viral infections, including an increase in interferon activities (Jasenosky et al., 2019). If an immune defect renders the host incapable of generating an interferon-γ-dependent response, nitazoxanide would be expected to be ineffective in such immunocompromised hosts (Theodos et al., 1998; Jumani et al., 2018), given the importance of these innate responses in controlling *Cryptosporidium* at its initial stages of infection (McDonald et al., 2013). Similarly, lack of curative effect of nitazoxanide in advanced AIDS patients (with low CD4+ T-cell counts)

suffering from chronic cryptosporidiosis can be explained by the fact that adaptive immunity plays a crucial role in clearing the parasites completely from the infected host (Mead, 2014). Thus, the efficacy of nitazoxanide seems to be closely related to both the innate and adaptive immune status of the host.

1.3.1.2 Paromomycin.

Another well studied drug, a poorly absorbed aminoglycoside paromomycin, has been investigated against cryptosporidiosis in three published controlled trials (White et al., 1994; Hewitt et al., 2000; Hussien et al., 2013), but results have been highly divergent and mostly discouraging. Paromomycin, like other aminoglycoside antibiotics, inhibits protein synthesis by binding to the 30S ribosomal subunit and shows broad spectrum activity against bacteria and some protozoa (Lin et al., 2018). Several uncontrolled trials and case studies in AIDS patients suffering from cryptosporidiosis have reported favorable clinical outcomes after paromomycin treatment (Gathe et al., 1990; Clezy et al., 1991; Armitage et al., 1992; Danziger et al., 1993; Fichtenbaum et al., 1993; Wallace et al., 1993; Bissuel et al., 1994; Scaglia et al., 1994; Hashmey et al., 1997). However, the patient responses in most cases were short-lived and continuous maintenance therapy was required to prevent frequent relapses after treatment discontinuation suggesting that complete parasitological cure was not achieved in these cases. Children suffering from cryptosporidiosis have been reported to respond favorably after treatment with paromomycin, although the overall clinical and parasitological response is reduced as compared to nitazoxanide or azithromycin (Trad et al., 2003; Vandenberg et al., 2012; Hussien et al., 2013).

1.3.1.3 Macrolides.

Macrolides are a class of antibiotics that disrupt bacterial protein synthesis by binding to the 50S subunit of the ribosome (Lin et al., 2018). Among the macrolides tested for efficacy against human cryptosporidiosis, azithromycin remains the most studied. In a multi-center, placebo-controlled, double-blind study, preliminary data analysis revealed no significant improvement in clinical symptoms and oocyst numbers in azithromycin-treated AIDS patients with cryptosporidiosis (Soave et al., 1993). Interestingly, however, a statistically significant decrease in cryptosporidial oocyst shedding was reported in patients with appropriate azithromycin serum concentrations (Soave et al., 1993). By contrast, azithromycin was found to have no therapeutic or prophylactic efficacy in the management of cryptosporidial diarrhea in AIDS patients (Blanshard et al., 1997; Holmberg et al., 1998). While short-term azithromycin treatment for cryptosporidiosis was unable to achieve total parasitological clearance and prevent relapses in AIDS patients, long-term and low dose maintenance therapy was associated with noticeable clinical and parasitological benefits (Dionisio et al., 1998; Kadappu et al., 2002). Nevertheless, azithromycin seems to be more effective in treating children with cryptosporidiosis. Prompt clinical improvement and high parasite clearance rates have been reported after azithromycin therapy in both immunocompetent and immunocompromised children (Vargas et al., 1993; Hicks et al., 1996; Allam and Shehab, 2002; Trad et al., 2003).

Clarithromycin has been tested in humans with AIDS for prophylactic effectiveness against cryptosporidiosis. But studies have reported conflicting results with some indicating a highly protective effect against the development of cryptosporidiosis (Jordan, 1996; Holmberg et al., 1998) while others concluding that the drug is not useful in preventing cryptosporidiosis in this patient population (Fichtenbaum et al., 2000). Similarly, spiramycin has also shown inconsistent results in treating cryptosporidiosis in controlled and uncontrolled trials involving

infants (Saez-Llorens et al., 1989; Wittenberg et al., 1989) and adult patients (Woolf et al., 1987; Moskovitz et al., 1988) with reports of acute intestinal injury in some patients receiving high doses of the drug (Weikel et al., 1991). Another macrolide, roxithromycin has proven effective in uncontrolled studies of AIDS patients with cryptosporidial enteritis. However, complete parasite clearance was only achieved in half of the treated patients and the results were not compared with a placebo-treated control group (Sprinz et al., 1998; Uip et al., 1998).

1.3.1.4 Rifamycin Derivatives.

Rifamycins are a group of drugs that are highly active against mycobacterial infections. Members of this antibiotic class inhibit RNA synthesis by selective binding of the bacterial DNA-dependent RNA polymerase (Hartmann et al., 1967). Several uncontrolled studies have evaluated rifamycin derivatives, namely rifabutin and rifaximin, for prophylactic and therapeutic efficacy respectively, against cryptosporidiosis in HIV-infected humans. Rifabutin has been found to be highly effective in preventing the development of cryptosporidiosis in AIDS patients receiving chemoprophylaxis for *Mycobacterium avium* complex infection (Holmberg et al., 1998; Fichtenbaum et al., 2000). Similarly, some studies have demonstrated a significant clinical and parasitological benefit of rifaximin, a poorly absorbed rifamycin, in the treatment of cryptosporidiosis in solid organ transplant recipient patients (Burdese et al., 2005) and a small number of HIV-infected adults and children with CD4+ T-cell counts ranging from <50 cells/mm^3 to >200 cells/mm^3 (Amenta et al., 1999; Gathe et al., 2008). Thus, these results warrant the testing of these drugs in larger randomized controlled clinical trials for confirmation of anti-*Cryptosporidium* efficacy.

1.3.1.5 Benzene Acetonitrile Derivatives.

Diclazuril and letrazuril have been both shown to be active against *Eimeria* species, parasites closely related to *Cryptosporidium*, although the exact mode of action of these drugs is currently unknown. Yet, diclazuril failed to show any obvious effect in severe cryptosporidiosis in adults with HIV infection (Connolly et al., 1990). In another study, a single patient showed both clinical and parasitological response to diclazuril treatment but the infection was less severe and the patient also received antiretroviral therapy during and after the treatment course (Menichetti et al., 1991). Additionally, letrazuril, the p-fluor analog of diclazuril, shows only partial efficacy against advanced AIDS-related cryptosporidial diarrhea (Harris et al., 1994; Loeb et al., 1995; Blanshard et al., 1997) and treated patients develop temporary drug-related side-effects including abnormal liver function tests and skin rashes that tend to resolve after treatment discontinuation (Murdoch et al., 1993; Harris et al., 1994; Loeb et al., 1995).

1.3.1.6 Miscellaneous Antimicrobials.

1.3.1.6.1 Clofazimine.

Clofazimine, an FDA-approved antimycobacterial drug primarily used to treat leprosy, was found to be effective against both *C. parvum* and *C. hominis in vitro* and showed promising efficacy against *C. parvum* in a mouse model (Love et al., 2017). Interestingly, the mechanism of action of clofazimine as an anti-mycobacterial drug is not well understood. A recent randomized controlled clinical trial tested the efficacy of the drug in enrolled patients with advanced HIV infection and *Cryptosporidium*-associated diarrhea. The findings of the study, however, failed to demonstrate any effectiveness of clofazimine in reducing fecal parasite shedding and stool frequency in immunocompromised patients (Iroh Tam et al., 2021). Moreover, unexpected adverse events were higher in the clofazimine-treated patients as compared to the placebo control group.

1.3.1.6.2 Miltefosine.

Like clofazimine, miltefosine an anti-*Leishmania* drug, has also shown promising *in vitro* efficacy against *C. parvum* as per anecdotal observations but its specific mode of action is not entirely known. This drug, however, showed modest clinical improvement without evidence of oocyst clearance in treated HIV-infected malnourished individuals (Sinkala et al., 2011). Furthermore, adverse events including hepatic dysfunction and renal failure were observed in some patients, leading to premature termination of the phase-1–phase-2 trial.

1.3.1.6.3 Albendazole.

Albendazole is a broad-spectrum anthelmintic drug that is known to bind to β-tubulin and inhibit microtubule assembly in helminth worms (Lacey, 1988). This benzimidazole derivative was shown to have a significant effect on the duration of diarrhea in a randomized, controlled trial in HIV-seropositive patients with persistent diarrhea (Kelly et al., 1996). Later, another study assessed the effect of albendazole on *C. parvum* and other intracellular protozoa including *Isospora* and microsporidia in HIV-positive patients and found the drug to exhibit complete *C. parvum* clearance when used at doses higher than the normal prescribed dose (Zulu et al., 2002). However, the number of HIV patients with cryptosporidiosis in this study was very small as compared to patients infected with other protozoa, and the results cannot be considered credible due to the lack of an untreated control group for comparison. Nevertheless, it does seem that albendazole has some activity against *Cryptosporidium* at high doses (Fayer and Fetterer, 1995), but, to the best of our knowledge, no other study has evaluated albendazole for anti-*Cryptosporidium* efficacy in immunocompromised humans.

1.3.1.7 Other treatments.

Although most studies on the treatment of cryptosporidiosis have been carried out by repurposing the use of antibacterial drugs, some studies have tested other treatments with alternate modes of action such as immune cell extracts, immunoglobulins, hyperimmune colostrum, somatostatin analogs, and highly active antiretroviral therapy (HAART) (Table 1.2).

1.3.1.7.1 Immunotherapy.

Passive immunotherapy by oral administration of immunoglobulins derived from bovine colostrum or human serum was shown to be effective in *Cryptosporidium*-infected immunosuppressed humans in several open-label uncontrolled studies and case reports (Tzipori et al., 1987; Ungar et al., 1990; Borowitz and Saulsbury, 1991; Rump et al., 1992; Shield et al., 1993; Floren et al., 2006), but results obtained from randomized double-blind controlled studies have been disappointing (Nord et al., 1990; Okhuysen et al., 1998). Similarly, treatment of AIDS-associated cryptosporidial diarrhea by oral administration of cellular extracts prepared from lymphocytes obtained from immunized calves produced mixed results (Louie et al., 1987; McMeeking et al., 1990).

1.3.1.7.2 Somatostatin Analogs.

Somatostatin analogs including octreotide and vapreotide have been reported to improve secretory diarrhea by inhibiting the motility and secretions of the gastro-intestinal tract. Patients with AIDS-related chronic diarrhea, especially those without specific pathogens, may benefit from treatment with this class of drugs. However, these agents have mostly been ineffective or partially effective in reducing the fecal output in *Cryptosporidium*-associated diarrhea in HIV-infected patients and show no parasitological cure (Cook et al., 1988; Katz et al., 1988; Clotet et

al., 1989; Cello et al., 1991; Romeu et al., 1991; Girard et al., 1992; Liberti et al., 1992; Moroni et al., 1993).

1.3.1.7.3 Highly Active Antiretroviral Therapy (HAART).

Cryptosporidiosis is typically a self-limiting illness in immunocompetent individuals, and therefore, immune reconstitution by restoring CD4+ T-cell levels in particular, is an essential part of the disease management strategy in the immunocompromised (Flanigan et al., 1992). HIV-infected patients with CD4+ T-cell counts below 200/mm^3 tend to be susceptible to a higher frequency of cryptosporidial infections highlighting the relationship of these opportunistic pathogens with the immune status of an individual (de Oliveira-Silva et al., 2007; Tuli et al., 2008; Adamu et al., 2013; Nsagha et al., 2016; Cerveja et al., 2017; Amoo et al., 2018). The use of HAART in HIV-infected patients has significantly reduced the global frequency and severity of cryptosporidiosis in this patient population (Le Moing et al., 1998; Call et al., 2000; Conti et al., 2000; Ives et al., 2001; Babiker et al., 2002; Bachur et al., 2008; Missaye et al., 2013). HAART re-establishes CD4+ T-cell counts and inhibits viral replication using a combination of nucleoside reverse transcriptase inhibitors (NRTIs), non-nucleoside reverse transcriptase inhibitors (NNRTIs), and HIV protease inhibitors. However, chronic diarrhea at initiation of HAART in HIV-positive patients has been associated with increased early mortality, emphasizing the need for early anti-retroviral therapy before the onset of diarrhea (Dillingham et al., 2009). Most studies involving HAART for the treatment of cryptosporidiosis have used HIV protease inhibitors either individually or in combination with other antiretrovirals to successfully treat the disease with major clinical and parasitological benefits (Grube et al., 1997; Bobin et al., 1998; Carr et al., 1998; Foudraine et al., 1998; Miao et al., 1999; Miao et al., 2000). Such a therapy may exert its pharmacological effect against AIDS-associated cryptosporidiosis both by

restoration of circulating CD4+ T-cell counts and direct inhibition of *Cryptosporidium* proteases (Mele et al., 2003; Pantenburg et al., 2009). But individuals with other causes of weakened immunity, including primary immunodeficiency, immunosuppressive therapy in organ transplant recipients, and chemotherapy in cancer patients, remain at high risk of severe cryptosporidiosis.

1.3.1.8 Combination therapy.

Several combination therapies involving the use of either nitazoxanide or paromomycin in conjunction with macrolides, rifamycin derivatives, or HAART have shown promising efficacy for cryptosporidiosis in small uncontrolled trials and case studies with both clinical improvement and parasite elimination in a range of affected immunocompromised individuals (Table 1.3). However, these results need to be replicated in large, controlled trials before any definite conclusions can be drawn regarding the efficacy of such combinations. Huang and colleagues conducted a randomized placebo-controlled trial to investigate the therapeutic effects of acetylated spiramycin and garlicin on *Cryptosporidium* infection in institutionalized drug users. Although the combination treatment achieved high parasitological cure rates, this study was carried out in asymptomatic *Cryptosporidium* carriers without ascertaining the HIV/immune status of the enrolled individuals, and therefore has limited clinical significance (Huang et al., 2015).

Certain clinical case reports have documented favorable clinical and parasitological outcomes in HIV-infected and organ transplant recipient patients diagnosed with extra-intestinal and intestinal cryptosporidiosis, after antimicrobial combination therapy with azithromycin and paromomycin (Palmieri et al., 2005; Meamar et al., 2006; Denkinger et al., 2008). In a small open-label, uncontrolled study, patients with AIDS (<100 CD4+ T-cells/mm^3) and chronic cryptosporidiosis, showed a marked improvement in stool frequency and a significant decrease

in fecal excretion of *Cryptosporidium* oocysts in response to azithromycin/paromomycin combination therapy (Smith et al., 1998). However, follow-up study after the completion of treatment revealed the persistence of chronic, mild diarrhea in some patients.

Complete resolution of diarrhea as well as elimination of the parasite has been reported in immunosuppressed children and adults suffering from cryptosporidiosis after dual therapy with azithromycin and nitazoxanide (Legrand et al., 2011; Bakliwal et al., 2021; Dupuy et al., 2021). Additionally, triple therapy involving azithromycin, nitazoxanide, and paromomycin or rifaximin led to complete clinical and parasitological cure with no relapse in renal transplant patients (Hong et al., 2007; Tomczak et al., 2022). Another study successfully treated cryptosporidiosis in a pediatric renal transplant patient using a triple therapy consisting of spiramycin, nitazoxanide, and paromomycin (Acikgoz et al., 2012).

Moreover, quite a few small uncontrolled studies suggest that a combination of antimicrobials and HAART (especially with protease inhibitors) dramatically accelerates the clinical response in AIDS patients suffering from cryptosporidiosis (Maggi et al., 2000; Schmidt et al., 2001; Moling et al., 2005). But data from randomized controlled trials is required to support these results given the self-limiting nature of the disease. Nevertheless, increasing evidence has demonstrated that combination therapy achieves better clinical and microbiological resolution rates than monotherapy for the treatment of cryptosporidiosis in immunocompromised patients (Maggi et al., 2000; Bhadauria et al., 2015; Lanternier et al., 2017; Bakliwal et al., 2021; Tomczak et al., 2022).

1.3.2 Animals.

Numerous antimicrobial compounds have been screened and evaluated for efficacy against naturally acquired and experimentally induced cryptosporidiosis in animals (Table 1.4),

albeit with limited success. Most of the tested drugs exhibit only partial prophylactic and therapeutic efficacy in reducing oocyst excretion and disease severity in affected animals. Thus far, no effective currently licensed therapeutics are available in the United States for *Cryptosporidium* infections in animals (Santin, 2020; Zahedi and Ryan, 2020). Alternatively, several supportive and immunological therapies have also been tested for the management of cryptosporidiosis in livestock (Table 1.5), but none have shown promise in changing the course of the disease.

1.3.2.1 Anticoccidials.

1.3.2.1.1 Halofuginone Lactate.

Halofuginone lactate, a prolyl-tRNA synthetase inhibitor, is a synthetic quinazolinone coccidiostat primarily used in veterinary medicine for the prevention and treatment of *Eimeria* infections in avian species. This medication is licensed for veterinary use in cattle against cryptosporidiosis in several European countries as well as Canada, although it is not labeled for use in the United States. Halofuginone lactate has a narrow safety index and is contraindicated in dehydrated animals suffering from diarrhea: clinical signs typical of cryptosporidiosis in neonatal animals. Hence, this drug is not suitable for therapeutic purposes and is generally used as a prophylactic to prevent cryptosporidial diarrhea in newborn farm animals. Recently, Brainard and others conducted a systematic review of literature and used meta-analysis to evaluate key outcomes such as oocyst shedding, diarrhea, mortality, and weight gain for the treatment of calf cryptosporidiosis with halofuginone lactate. The authors concluded that prophylactic halofuginone treatment was associated with significantly lower incidence of oocyst shedding, diarrhea burden, and mortality especially when the treatment was started early in life (Brainard et al., 2021). Furthermore, Giadinis et al. conducted two extensive field trials in

Greece and found the drug to be effective in preventing and treating cryptosporidiosis, and reducing deaths associated with the disease in neonatal lambs and goat kids (Giadinis et al., 2007; Giadinis et al., 2008).

A number of early reports suggested that halofuginone showed effectiveness in protecting young ruminants from severe cryptosporidiosis, but relapses occurred after treatment discontinuation in calves (Villacorta et al., 1991; Naciri et al., 1993; Peeters et al., 1993; Lefay et al., 2001), lambs (Naciri and Yvore, 1989; Causapé et al., 1999), and goat kids (Chartier et al., 1999), questioning the effectiveness of the preventative treatment. Moreover, although halofuginone lactate treatment reduces oocyst shedding in infected animals, it fails to provide complete protection and cure, implying that treatment along with good animal husbandry practices including individual housing, proper hygiene measures, and suitable disinfection are required to prevent environmental contamination and disease transmission among animals on farms (Joachim et al., 2003; Jarvie et al., 2005; Klein, 2008; De Waele et al., 2010; Trotz-Williams et al., 2011; Keidel and Daugschies, 2013). Likewise, a few studies also showed some efficacy in reducing excretion of *Cryptosporidium* oocysts in treated animals as compared to untreated controls, but no significant effect on the prevalence of diarrhea or body weight gain was noted (Causapé et al., 1999; Lallemand et al., 2006; Trotz-Williams et al., 2011; Almawly et al., 2013). Interestingly, preventive treatment with halofuginone lactate was also found to be associated with reduced weight gain in calves (Niine et al., 2018; Velez et al., 2019). Thus, the preventive and therapeutic effectiveness of halofuginone lactate in animals remains controversial.

1.3.2.1.2 Decoquinate.

Decoquinate is a quinolone coccidiostat most used for controlling coccidiosis in ruminants and poultry. This drug inhibits the mitochondrial respiration by blocking electron transport in *Eimeria* parasites (Wang, 1976). Decoquinate produces limited-to-no clinical and parasitological response when used preventatively before the development of signs and symptoms of cryptosporidiosis in experimentally or naturally infected calves (Redman and Fox, 1993; Moore et al., 2003; Lallemand et al., 2006). However, it significantly reduces oocyst shedding and severity of cryptosporidiosis in neonatal kids, but without complete eradication of infection (Mancassola et al., 1997; Ferre et al., 2005).

1.3.2.1.3 Lasalocid.

Lasalocid is an ionophore antibiotic and a coccidiostat that is commonly used as a feed additive for promoting growth and preventing coccidiosis in ruminants. This drug has been used as a prophylactic or therapeutic to treat *Cryptosporidium* infections in calves. Based on anecdotal reports, short-term dosing (3-4 days) of lasalocid (6-15 mg/kg/day) was effective in treating severe cryptosporidiosis in calves (Gobel, 1987a; b; Sahal et al., 2005). However, mortality and serious side effects resulting from lasalocid toxicosis have been described in animals when long-term therapy or a dose higher than the label dose was used as a preventative for cryptosporidiosis (Moon et al., 1982; Benson et al., 1998). More recently however, Murakoshi and others demonstrated a highly beneficial effect of lasalocid, without any side effects, when used at a lower dose (3 mg/kg/day) to prevent calf cryptosporidiosis. But the treatment was not found to be protective after the 7-day dosing period (Murakoshi et al., 2014).

1.3.2.1.4 Sulfonamides.

Sulfonamides are broadly active antimicrobial agents that inhibit dihydropteroate synthase, an enzyme involved in folate synthesis (Henry, 1943). They have been widely used in veterinary medicine to prevent coccidiosis and treat bacterial infections in animals and poultry. More recently, the FDA has limited the use of these drugs in food animals to prevent the spread of antimicrobial resistance and preserve their effectiveness in humans (FDA, 2012). In any case, prophylactic or therapeutic treatment of natural or experimental cryptosporidiosis with a variety of sulfonamides and potentiated sulfonamides including sulfadimidine, sulfadimethoxine, and cotrimoxazole (trimethoprim in combination with sulfamethoxazole) has failed miserably in calves (Moon et al., 1982; Fischer, 1983; Fayer, 1992; Joachim et al., 2003; Nasir et al., 2013) and goat kids (Naciri et al., 1984; Koudela and Bokova, 1997).

1.3.2.2 Paromomycin.

In addition to humans, paromomycin has also been extensively tested for anti-*Cryptosporidium* efficacy in various food animals. However, as has been the case in humans, results have been varied and the treatment failed to achieve complete parasitological cure in most studies. Prophylactic administration of paromomycin was found to decrease the duration and severity of diarrhea as well as the duration and intensity of oocyst shedding in calves experimentally infected with *C. parvum* (Fayer and Ellis, 1993). Similar positive results were reported in a controlled-blind field trial of natural infection in calves, but the treated group started shedding oocysts and developed diarrhea after the treatment withdrawal (Grinberg et al., 2002). However, paromomycin does seem to be more effective in small ruminants. Treatment has been shown to reduce both cryptosporidial oocyst output and severity of clinical signs, when used prophylactically in neonatal goat kids (Mancassola et al., 1995; Chartier et al., 1996; Johnson et al., 2000) and therapeutically in neonatal lambs (Viu et al., 2000). This agent was also

proven to be therapeutically effective against moderate cryptosporidiosis but ineffective against severe cryptosporidiosis in infected gnotobiotic piglets (Tzipori et al., 1994; Theodos et al., 1998). However, paromomycin, like many aminoglycosides, is potentially nephrotoxic and detrimental effects on growth have been observed after treatment in young animals (Viu et al., 2000). In addition, the drug is expensive and therefore, its use in agricultural animals is impractical.

1.3.2.3 Nitazoxanide.

Nitazoxanide, the only licensed treatment available in humans, has also been tested for efficacy in animal cryptosporidiosis, although reports on treatment outcomes have been conflicting. While Ollivett and others found this medication to significantly reduce the duration of oocyst shedding and clinical severity in experimentally infected calves as compared to the placebo treated group (Ollivett et al., 2009), another controlled study found no prophylactic or therapeutic effect of nitazoxanide on clinical appearance or oocyst excretion in calves infected with *C. parvum* (Schnyder et al., 2009). Furthermore, while nitazoxanide reduced oocyst shedding in experimentally challenged newborn goat kids, no reduction in mortality rates or improvement in weight gains were recorded in the treated groups compared with the control group (Viel et al., 2007). Importantly, the authors of this study suggested that the mortalities seen in kid neonates in the nitazoxanide treated groups were caused by severe drug toxicity (Viel et al., 2007). In the gnotobiotic piglet diarrhea model, nitazoxanide demonstrated only partial efficacy at high doses in reducing *C. parvum* oocyst shedding, induced drug-related diarrhea, and was not as effective as paromomycin (Theodos et al., 1998). In another study performed in the same animal model but infected with *C. hominis*, nitazoxanide reduced diarrhea and oocyst

shedding in only the initial phase of treatment and had no clinical or parasitological effect at the later stages of the disease (Lee et al., 2017).

1.3.2.4 Macrolides.

Macrolides have been evaluated as anti-*Cryptosporidium* agents in a range of animals. Azithromycin significantly suppressed *Cryptosporidium* oocyst shedding and resulted in significant clinical improvement and weight gain in naturally infected dairy calves when used as a therapeutic at high doses, but high costs of treatment are a concern (Elitok et al., 2005). Similar reports of azithromycin efficacy against *C. parvum* infection in calves (Nasir et al., 2013) and a buffalo calf (Maurya et al., 2016) have also been published. Treatment of gnotobiotic neonatal piglets infected with *C. hominis* alleviated clinical disease only for the first few days and azithromycin treated piglets exhibited no reduction of oocyst excretion compared with untreated animals (Lee et al., 2017). In combination with nitazoxanide, azithromycin led to significant clinical improvement in infected piglets but did not eliminate oocyst excretion after producing a transient initial reduction in oocyst shedding in treated animals (Lee et al., 2017).

Experience with other macrolides has also been mixed. While tilmicosin failed to prevent severe cryptosporidiosis in newborn kids raised on a commercial dairy goat farm (Paraud et al., 2010), tylosin was found to be therapeutically effective in reducing fecal oocyst excretion and clinical signs of disease in naturally infected calves (Duru et al., 2013).

1.3.2.5 Other Treatments.

1.3.2.5.1 Immunotherapy.

Passive immunotherapy using bovine colostrum or bovine serum concentrate containing specific antibodies to *Cryptosporidium* provided only partial protection against cryptosporidiosis by reducing duration of diarrhea and oocyst shedding in experimentally infected calves (Fayer et

al., 1989; Slacek et al., 1996; Hunt et al., 2002). However, much better protection from *Cryptosporidium* infection was noted in some studies after prophylactic oral administration of bovine/ovine colostrum comprising of anti-cryptosporidial antibodies in infected calves and lambs (Naciri et al., 1994; Perryman et al., 1999; Askari et al., 2016; Kacar et al., 2022). Moreover, therapeutic administration of hyperimmune colostrum-immunoglobulin in experimentally infected gnotobiotic piglets reduced oocyst shedding but had little-to-no effect on diarrhea and intestinal mucosal damage caused by the parasite (Tzipori et al., 1994). Similarly, preventive treatment of experimentally induced calf cryptosporidiosis by recombinant bovine interleukin-12 (rBoIL-12) or lymphocyte extracts from immunized calves failed to provide prophylaxis (Fayer et al., 1987; Pasquali et al., 2006).

1.3.2.5.2 Adsorbents.

Oral intestinal adsorbents have been used worldwide as a remedy to treat diarrhea of various causes. A product consisting of activated charcoal and wood vinegar was found to be highly effective in treating experimental *C. parvum* infection in calves (Watarai et al., 2008) and provided partial protection to newborn kids against natural infection (Paraud et al., 2011). More recently, activated charcoal also showed a partial curative effect on neonatal calf diarrhea caused mainly by *C. parvum* at a commercial calf-raising farm (Ross et al., 2021). Similarly, another adsorbent clinoptilolite also demonstrated a good prophylactic and therapeutic effect against *C. parvum* in experimentally infected lambs (Dinler Ay et al., 2021). These adsorbents seem to be effective against cryptosporidial infections probably because of their potential to adsorb and thereby trap parasites and prevent host cell invasion. Although this adsorption principle has been demonstrated in an *in vitro* adsorption test (Watarai et al., 2008), the same needs to be confirmed in further *in vivo* studies.

1.3.2.5.3 Polysaccharides.

Cyclodextrins are cyclic oligosaccharides that are commonly used as drug excipients to enhance the solubility, safety, stability, and bioavailability of drugs. After showing some unexpected activity against *C. parvum* experimental infection in mice, β-cyclodextrin has been tested for both prophylactic as well as therapeutic efficacy against cryptosporidiosis in young ruminants with results showing that the preventive effect is greater than the curative one. While β-cyclodextrin showed partial efficacy in reducing diarrhea and oocyst shedding in naturally infected calves (Castro-Hermida et al., 2001a), this drug reduced mortality and produced an even better clinical and parasitological response in infected lambs under field conditions (Castro-Hermida et al., 2001b). Another drug of this class, α-cyclodextrin was tested for prophylactic effectiveness in experimentally infected neonatal kids and showed some reduction in the intensity of infection and oocyst shedding, but almost half treated kids died probably due to drug-related side effects (Castro-Hermida et al., 2004).

Chitosan, a natural linear polysaccharide has also been investigated for efficacy in *C. parvum* infected lambs. Therapeutic treatment after the onset of disease improved clinical signs and fecal consistency, and reduced oocyst excretion, but did not eliminate cryptosporidiosis completely in treated lambs (Aydogdu et al., 2019).

Researchers have suggested various modes of action of polysaccharides such as cyclodextrins and chitosan in controlling viral, bacterial, and parasitic infections that involve use of their antimicrobial properties, osmotic properties, and cholesterol-sequestering ability, among others (Aydogdu et al., 2019; Braga, 2019). It is likely that, in the case of *Cryptosporidium*, these polysaccharides might form a protective film over the intestinal surface due to their adhesive properties, which may act as a physical barrier and prevent cell invasion by parasites. However,

to date, the exact mechanism of action of these pharmaceutical agents against *Cryptosporidium* remains unknown.

1.3.2.5.4 Natural Plant-Based Products.

Various natural products like phytogenic extracts, essential oils, and phytobiotics have been used to treat animal cryptosporidiosis, but with unconvincing results. A randomized controlled study evaluated allicin, a sulfur-containing component of garlic, in experimentally infected neonatal calves and found it to have no effect on the duration of diarrhea or weight gain in treated calves (Olson et al., 1998). Another study conducted in Israel showed that a concentrated pomegranate extract feed supplement partially reduced clinical signs and fecal oocyst counts in natural calf cryptosporidiosis (Weyl-Feinstein et al., 2014). Similarly, experimentally infected calves receiving plant-based isoquinoline alkaloids as feed additive suffered from less intense diarrhea for a shorter period but shed similar number of oocysts daily compared with the control group (Mendonca et al., 2021). Furthermore, administration of essential oils or essential oil-based phytogenic products to newborn calves also failed to produce any preventive effect on parasite shedding in infected calves (Katsoulos et al., 2017; Volpato et al., 2019).

1.3.2.5.5 Probiotics.

A few animal studies suggest some potential for the use of probiotics for prophylactic treatment of cryptosporidiosis, though bacterial mechanisms involved in protection against *Cryptosporidium* infection are not known. Daily oral administration of lactic acid producing bacteria for 10 consecutive days to *C. parvum* infected dairy calves had limited effect on clinical signs and no effect on parasite abundance (Harp et al., 1996; Fernandez et al., 2020), although a partial reduction in the severity of diarrhea, prevalence of cryptosporidial infection, and oocyst

excretion was noted when probiotics combined with phytobiotics were dispensed to calves under field conditions (Stefańska et al., 2021). Likewise, feeding of yeast fermentation products had no clinical and parasitological benefits in bovine cryptosporidiosis (Velez et al., 2019).

1.3.2.5.6 Miscellaneous Treatments.

Apart from drugs that have a direct anti-parasitic effect, other medications that have no known anti-*Cryptosporidium* activity but act by improving the symptoms of cryptosporidiosis have also been tested in animals. Such drugs might show some reduction of parasite load in young animals probably by relieving the symptoms of disease and allowing natural host immunity to develop and act against the infection. One such anti-inflammatory drug, Bobel-24, was unable to completely prevent or treat experimentally induced *C. parvum* infection in neonatal lambs but showed some prophylactic efficacy in reducing the duration and intensity of oocyst shedding and the presence of diarrhea (Castro-Hermida et al., 2008). Also, preventive administration of anti-IL-10 egg yolk antibodies for 11 days had no effect on the prevalence of *Cryptosporidium* infection in calves reared under field conditions (Raabis et al., 2018). In another study, administration of glucagon-like peptide 2 or artificial sweetener therapy before a low-level experimental *C. parvum* exposure reduced severity of diarrhea, fecal oocyst excretion, and intestinal pathology in neonatal calves (Connor et al., 2017).

1.4 NEW POTENTIAL TREATMENTS FOR HUMANS AND ANIMALS

So far, no satisfactory prophylactics or therapeutics are available for the prevention or treatment of severe cryptosporidiosis in humans and animals. The limited progress made in this field can be directly attributed to the limited genetic tractability of *Cryptosporidium*, lack of conventional apicomplexan targets, as well as the unique intracellular but extracytoplasmic location within the host cells. Furthermore, the lack of reliable cell culture platforms and limited

availability of technical tools to study the parasite in biological systems, lead to an inadequate knowledge about the host-parasite interactions (Checkley et al., 2015; Innes et al., 2020). Nevertheless, breakthrough genetic modification of the parasite that has been made recently has advanced *Cryptosporidium* research, although the approach is complicated compared to methods developed for other apicomplexan parasites, as it requires the passage of the transgenic parasites in laboratory animals (Vinayak et al., 2015). Importantly, some significant progress has been made in generating genetically modified *C. parvum* strains *in vitro*, using mouse-derived intestinal organoid cultures grown in a modified air-liquid-interface system, that enables the completion of the life cycle and produces viable oocysts that are infectious in cell culture and immunocompromised mice (Wilke et al., 2019; Wilke et al., 2020). Indeed, recent advances in genetic manipulation and culture of *Cryptosporidium* have resulted in substantial progress in anti-*Cryptosporidium* drug discovery in recent years, and several compounds of preclinical, lead, and late lead status have emerged from target-based and phenotypic screens and are currently in development (Love and Choy, 2021).

C. parvum infects both humans and cattle as natural hosts, with the human disease closely resembling the one found in neonatal calves (Santín and Trout, 2007). Thus, the use of the neonatal calf infection model is highly recommended for assessment of efficacy of candidate compounds before advancement to human clinical trials and should ensure the safety and efficacy of promising compounds in both humans and livestock. Recently some compounds have shown promising efficacy in treating cryptosporidiosis in natural animal host models including the neonatal calf model without any major safety issues. These include bumped kinase inhibitors (BKIs), pyrazolopyridine-based KDU731, triazolopyradizine MMV665917, benzoxaborole AN7973, and compound 2093 (Table 1.4).

1.4.1 Bumped Kinase Inhibitors.

BKIs inhibit the *Cryptosporidium parvum* calcium-dependent protein kinase 1 (CpCDPK1), an enzyme that is essential for host cell invasion and does not have any mammalian analogs (Van Voorhis et al., 2021). Recent studies have assessed novel BKIs as a possible cure for cryptosporidiosis. In one study, Lendner et al. evaluated a bumped kinase inhibitor BKI-1294 for efficacy against *C. parvum* in experimentally infected neonatal calves and concluded that BKI-1294 reduced oocyst shedding but had no effect on diarrhea and dehydration in treated calves (Lendner et al., 2015). In another study, Schaefer and others demonstrated that BKI-1294 significantly improved clinical appearance, diarrhea, and parasitological outcomes but failed to eliminate diarrhea and other clinical symptoms of bovine cryptosporidiosis (Schaefer et al., 2016). Nonetheless, another CpCDPK1 inhibitor, BKI-1369, has emerged as an encouraging lead compound for anti-*Cryptosporidium* therapy in animals (Van Voorhis et al., 2021). This compound has shown promising efficacy against cryptosporidiosis in both the *C. parvum* infected neonatal calf, and the *C. hominis* infected gnotobiotic piglet models (Hulverson et al., 2017; Lee et al., 2018). Unfortunately, these BKIs possess potent human *Ether-à-go-go*-Related *Gene* (hERG) inhibitory activity, which is associated with a potentially fatal disorder called long QT syndrome and cardiotoxicity in humans, effectively removing them from the anti-cryptosporidial drug development pipeline for humans (Van Voorhis et al., 2021). Nevertheless, BKI-1369 displayed both efficacy and safety in the neonatal calf model with a 30-fold reduction in total oocyst excretion and, therefore, calls for additional development as an anti-*Cryptosporidium* therapeutic for cattle (Hulverson et al., 2017).

1.4.2 KDU731.

The pyrazolopyridine derivative KDU731 is another promising anti-cryptosporidial drug candidate that inhibits the enzymatic activity of *Cryptosporidium* lipid kinase PI(4)K

(phosphatidylinositol-4-OH-kinase) and is active against both *C. parvum* and *C. hominis*. Oral treatment with KDU731 resulted in significant reduction in oocyst shedding, duration of severe diarrhea, and dehydration without any adverse drug-related effects in neonatal calves experimentally infected with *C. parvum* (Manjunatha et al., 2017). Intriguingly, KDU731 displayed limited systemic exposure in pharmacokinetic analysis of the drug in *C. parvum*-infected calves, suggesting that systemic exposure may not be important for therapeutic efficacy.

1.4.3 MMV665917.

Recently, a piperazine derivative MMV665917 with an unknown molecular mechanism of action (MMOA), was identified within the open access "Malaria Box" collection of antimalarial compounds and found to have potent *in vitro* activity against both *C. parvum* and *C. hominis* in addition to excellent *in vivo* anti-*Cryptosporidium* efficacy in mouse models of acute (IFN-γ KO) and chronic (NSG) cryptosporidiosis (Jumani et al., 2018). This compound was later tested in the neonatal calf model of cryptosporidiosis by Stebbins and colleagues and treatment resulted in rapid resolution and reduced duration of diarrhea, as well as a 94% reduction in total fecal excretion of cryptosporidial oocysts in treated calves compared with the control group (Stebbins et al., 2018). In another study conducted in the gnotobiotic piglet model, MMV665917 was shown to significantly reduce fecal *C. hominis* oocyst shedding, intestinal lesions, parasite colonization, and severity of diarrhea, compared with untreated control piglets (Lee et al., 2019). Unfortunately, like BKIs, this promising compound shows partial hERG inhibition and is potentially cardiotoxic in humans. However, similarities between the modes of action of BKIs and MMV665917 cannot be drawn based on this finding since hERG inhibition is generally an off-target effect and several compounds with diverse structures and modes of action are known to promiscuously block this channel (Witchel, 2011). Hence, studies to determine the MMOA of

MMV665917 are needed to aid further lead optimization efforts to reduce the affinity for hERG binding.

1.4.4 AN7973.

Another compound that has been discovered by phenotypic screening of an antimalarial compound library for *Cryptosporidium* growth inhibitors is the 6-carboxamide benzoxaborole AN7973 (Lunde et al., 2019). Like MMV665917, AN7973 is active against both *C. parvum* and *C. hominis* in cell culture and shows promising efficacy in both the acute and chronic murine models of cryptosporidiosis but does not have a validated target in *Cryptosporidium*. In the calf clinical model of cryptosporidiosis, AN7973 demonstrated exceptional efficacy in reducing the total parasite fecal excretion by >90% with complete elimination of diarrhea and significant reduction in dehydration in treated calves. Furthermore, the compound possesses favorable safety, stability, and pharmacokinetic characteristics and does not inhibit hERG, a major liability for development of other potential anti-cryptosporidial therapeutics including BKIs and MMV665917 for the human disease (Lunde et al., 2019).

1.4.5 Compound 2093.

Aminoacyl-tRNA synthetase inhibitors have emerged as promising therapeutic candidates for targeting protein synthesis in *Cryptosporidium* for the development of anti-cryptosporidial drugs (Jain et al., 2017; Baragana et al., 2019; Buckner et al., 2019; Vinayak et al., 2020). Amongst these compounds, only the potent *Cryptosporidium parvum* methionyl-tRNA synthetase (CpMetRS) inhibitor, compound 2093, has been tested in the neonatal calf efficacy model of cryptosporidiosis so far (Hasan et al., 2021). In dairy calves experimentally infected with *C. parvum*, compound 2093 initially reduced total oocyst shedding, diarrhea, and dehydration during the first 4 days of infection but most treated calves relapsed later with a

severe progressive disease indicating the likely emergence of drug resistance. Sequencing analysis of parasite DNA extracted from feces of relapsed animals revealed the presence of two mutant parasite strains with different single amino acid substitutions in the *CpMetRS* genomic locus that potentially conferred MetRS inhibitor resistance. Further genome editing, structural modeling, and enzymatic studies confirmed the spontaneous emergence of drug resistant *Cryptosporidium* parasites, an alarming finding that demands immediate attention (Hasan et al., 2021).

1.4.6 Other compounds.

In addition to the above discussed compounds, several other promising compounds have been unveiled in the last few years and found to be effective in both *in vitro* and mouse models of cryptosporidial infection. These include but are not limited to benzoxaboroles (Swale et al., 2019; Bellini et al., 2020), 5-aminopyrazole-4-carboxamide-based BKIs (Huang et al., 2019), *C. parvum* prolyl-tRNA synthetase (CpPRS) inhibitors (Jain et al., 2017), *C. parvum* lysyl-tRNA synthetase (CpKRS) inhibitors (Baragana et al., 2019), *C. parvum* phenylalanyl-tRNA synthetase (CpPheRS) inhibitors (Vinayak et al., 2020), piperazine derivatives (Oboh et al., 2021), and glycolytic enzyme inhibitors (Li et al., 2019). However, demonstration of efficacy and safety of these compounds in the neonatal calf and gnotobiotic piglet infection models is essential before further advancement to the next stages of development. Nevertheless, availability of multiple potential anti-cryptosporidial compounds is advantageous as a diverse pool of candidate compounds would be needed to account for the high attrition rate that is typical of drug development programs.

1.5 VACCINE DEVELOPMENT

Since efficacious anti-cryptosporidial drug options are currently lacking, vaccines could be a relevant option for the control of this disease. However, there are currently no vaccines available to prevent cryptosporidiosis. In any case, humans and animals with healthy immune systems suffer from a mild self-limiting illness and improve without treatment. Therefore, it is unclear whether vaccination is justified in these patient groups. However, vaccination could be particularly useful in preventing cryptosporidiosis in neonatal animals, immunocompromised individuals, and malnourished children living in underdeveloped countries. An effective vaccine should provide rapid long-lasting immunity in vaccinated individuals and minimize disease in livestock with a reduction in shedding of oocysts in feces thereby preventing the spread of the disease. A degree of cross-protective immunity against multiple species and subtypes, albeit less possible, will also be beneficial. The most viable strategy would be to vaccinate cattle, as they are the most significant contributors to contaminated manure globally (Vermeulen et al., 2017). However, it might be difficult to generate protective immunity in neonatal calves rapidly enough through active vaccination (Thomson et al., 2017). Therefore, passive immunization by transfer of anti-*Cryptosporidium* antibodies from immunized dams to calves through colostrum is a feasible alternate approach to protect them during the early days of life (Innes et al., 2020). Several immunogenic *Cryptosporidium* antigens, such as gp15, Cp15, and Cp23 that are involved in attachment or penetration of host cells, are being explored as vaccine candidates especially in the form of a multivalent vaccine, incorporating multiple antigens or antigenic epitopes (Mead, 2014; Innes et al., 2020). However, a major obstacle to the development of vaccines is our current limited understanding of the protective immune response against *Cryptosporidium* infection (Checkley et al., 2015).

1.6 UNIQUE ENERGY METABOLISM IN *CRYPTOSPORIDIUM PARVUM*

Arguably the most important milestone in *Cryptosporidium* research was achieved at the beginning of the 21st century with the availability of the genome sequences of *C. parvum* IOWA (Abrahamsen et al., 2004) and *C. hominis* TU502 (Xu et al., 2004) isolates. The successive launch of the CryptoDB (http://cryptodb.org/) database (Puiu et al., 2004) provided researchers with easy online access to these annotated genome sequences as well as functional genomic, transcriptomic, and proteomic data of *Cryptosporidium*. This enabled researchers to unveil and study unique biological features in this opportunistic parasite such as the presence of a highly streamlined metabolism and reduced biosynthetic pathways, loss of apicoplast and functional mitochondria along with their respective genomes. These findings provided an explanation for the restricted number of classical drug targets in *C. parvum* and its resistance to several drugs that typically work against other apicomplexan parasites.

Energy production in most eukaryotic cells involves breakdown of glucose in the cytoplasm by glycolysis, and subsequent transport of pyruvate into the mitochondria for electron transfer by oxidative phosphorylation. However, *C. parvum* lacks functional mitochondria along with the genes encoding for enzymes of the Krebs cycle and the electron transport chain. Furthermore, this parasite is incapable of de novo synthesis of most nutrients, including amino acids, nucleosides and fatty acids (Zhu, 2007). Consequently, the parasite depends heavily, if not solely, on the anaerobic oxidation of glucose via the glycolytic pathway for metabolic energy production. *C. parvum* either salvages glucose and other simple sugars from the host or acquires them by degradation of polysaccharides, including amylopectin and amylose. Glycolysis begins with the activation of hexose sugar (glucose or fructose) by *C. parvum* hexokinase (CpHK) and ends with the production of pyruvate in the presence of *C. parvum* pyruvate kinase (CpPyK), which is rapidly converted to lactate by *C. parvum* lactate dehydrogenase enzyme (CpLDH) with

the regeneration of cofactor NAD+ that is cycled back so that glycolysis can continue (Figure 1.2). In *C. parvum*, a total of 3 net ATP molecules are produced from a single hexose by the glycolytic pathway in comparison to the typical net production of 2 ATP molecules by glycolysis seen in most eukaryotes. This is because the *C. parvum* genome encodes a pyrophosphate-dependent phosphofructokinase that helps reduce ATP consumption unlike the ATP-dependent phosphofructokinase expressed in most aerobic cells (Denton et al., 1996). Pyruvate is converted to acetyl-CoA by a bifunctional pyruvate, pyruvate:NADP+ oxidoreductase (PNOR), which contains a unique pyruvate:ferredoxin oxidoreductase (PFOR) domain fused with a cytochrome P450 domain (Rotte et al., 2001). Acetyl-CoA can be further metabolized to produce organic acid end-products such as ethanol and acetate by the aldehyde dehydrogenase and acetate-CoA ligase enzymes respectively (Zhu, 2007).

1.7 HYPOTHESIS AND OBJECTIVES OF THE THESIS

1.7.1 Hypothesis.

Genome sequencing of *C. parvum* shows that this parasite lacks the Krebs cycle and cytochrome-based respiration, suggesting that it depends solely on the glycolytic pathway for metabolic energy production (Abrahamsen et al., 2004). Importantly, the final glycolytic reactions in the parasite are catalyzed by two crucial enzymes, CpPyK, a “plant-like” pyruvate kinase enzyme, and CpLDH, a “bacterial-type” lactate dehydrogenase enzyme, that result in the production of pyruvate, lactate, and high-energy molecules like ATP and NADH. Therefore, these unique glycolytic enzymes are excellent drug targets for this parasite. Consistent with this notion, our previous studies have provided genetic evidence for the critical role of CpLDH in the growth and development of the parasite *in vitro* and *in vivo* (Witola et al., 2017; Zhang et al., 2018). Further, we have successfully identified specific inhibitors of the CpLDH enzyme that

exhibit both *in vitro* and *in vivo* efficacy against *C. parvum* (Li et al., 2019). However, CpLDH has a relatively higher expression in extracellular stages (oocysts, sporozoites, and merozoites) of the parasite life cycle as opposed to intracellular stages. On the other hand, CpPyK is highly expressed in intracellular stages suggesting that this enzyme is critical for energy metabolism in these stages (Mirhashemi et al., 2018; Tandel et al., 2019). Therefore, we hypothesize that simultaneous inhibition of CpPyK and CpLDH can completely disrupt the energy metabolism in all parasite stages leading to severe defects in the growth and replication of the parasite.

1.7.2 Objectives.

Objective 1: To clone and functionally characterize putative CpPyK.

***Overview*:** We cloned the coding sequence of CpPyK, expressed the recombinant protein in a bacterial expression system, and purified the expressed putative CpPyK protein in native form using affinity chromatography. Using purified CpPyK, we developed a luminescence-based pyruvate kinase activity assay and validated the concentration-dependent enzymatic activity of the recombinant protein. We confirmed the pyruvate kinase activity of recombinant CpPyK and determined its enzymatic kinetic parameters including the Michaelis constant (K_m) and maximum velocity (V_{max}).

Objective 2: To identify specific inhibitors against CpPyK enzymatic activity.

***Overview*:** Using the CpPyK enzymatic assay, we screened a chemical compound library obtained from the National Cancer Institute and identified several specific *in vitro* inhibitors of the catalytic activity of recombinant CpPyK. We derived their half-maximal enzyme inhibitory concentrations (IC_{50}) against CpPyK. We determined the cytotoxic effects of candidate inhibitors on a mammalian intestinal cell line and derived their half-maximal cytotoxic concentrations (CC_{50}) using a colorimetric cytotoxicity assay.

Objective 3: To test the efficacy of CpPyK-inhibitors in killing *C. parvum in vitro* and *in vivo*.

***Overview*:** To identify efficacious lead-compounds for potential anti-cryptosporidial drug development, we used parasite growth inhibition assays to investigate the *in vitro* efficacy of non-toxic CpPyK-inhibitors. We identified CpPyK-inhibitors that inhibited the growth of *C. parvum* in infected cell cultures and calculated their half-maximal effective concentrations (EC_{50}). We tested the anti-cryptosporidial efficacy of the identified effective compounds in infected immunocompromised mice using quantitative PCR (qPCR) of fecal DNA and histopathological analyses of the intestinal tissue samples of treated and untreated mice. We identified CpPyK-inhibitors that reduced the oocyst load and prevented pathological lesions of cryptosporidiosis in infected mice at low non-toxic doses.

Objective 4: To derive combinations of CpLDH- and CpPyK-inhibitors that are safe and efficacious against *C. parvum* infection.

***Overview*:** Using a fixed-ratio model of combination, we combined CpLDH- and CpPyK-inhibitors to produce multiple compound mixtures. We used an *in vitro* colorimetric assay to evaluate the cytotoxicity of these compound combinations in mammalian cells. We evaluated the *in vitro* anti-cryptosporidial efficacy of non-toxic concentrations of individual compounds and combinations using *C. parvum* growth inhibition assays and analyzed the dose-response data by multiple approaches to identify synergistic compound combinations. We tested the synergistic compound combinations in the immunocompromised mouse model of cryptosporidiosis to determine their effect on disease progression during treatment and after withdrawal of treatment. We identified combinations of CpLDH- and CpPyK-inhibitors with improved anti-

cryptosporidial activity at low doses compared with individual inhibitors in the mouse infection model.

1.8 FIGURES AND TABLES

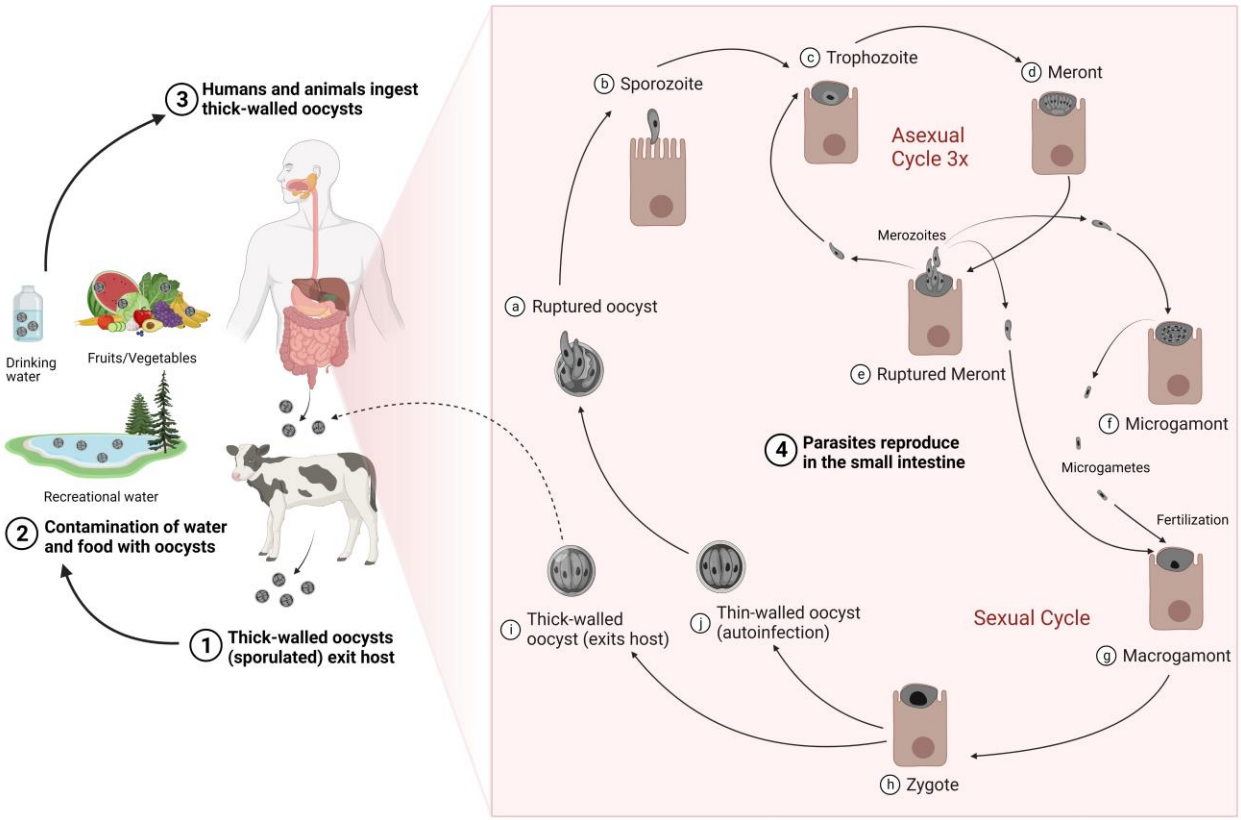

Figure 1.1: Life Cycle and Transmission of *Cryptosporidium*. Thick-walled sporulated oocysts are released in the feces of infected hosts (1) that contaminate food and water sources (2). Transmission occurs mainly by ingestion of contaminated water or food by susceptible hosts (3). Following ingestion, oocyst ruptures (4a) to release four sporozoites (4b). Sporozoites exhibit gliding motility, enter the host epithelial cells, and mature into trophozoites (4c), which undergo three rounds of asexual multiplication to produce meronts (4d) that invariably release eight merozoites (4e). Merozoites released from the third round of asexual proliferation give rise to the sexual stages upon reinvasion of host cells: the male microgamonts (4f) and the female macrogamonts (4g). Microgametes released from the microgamont penetrate and fertilize macrogamonts to form diploid zygotes (4h). The zygotes undergo meiosis and sporogony generating either thin-walled (4i) or thick-walled (4j) oocysts, each containing four haploid sporozoites. Thick-walled oocysts are released into the lumen of the intestine and excreted into the environment, where they are instantly infectious. The thin-walled oocysts, in contrast, excyst to cause autoinfection in the same host. Adapted with modification from (CDC, 2019). Created with BioRender.com.

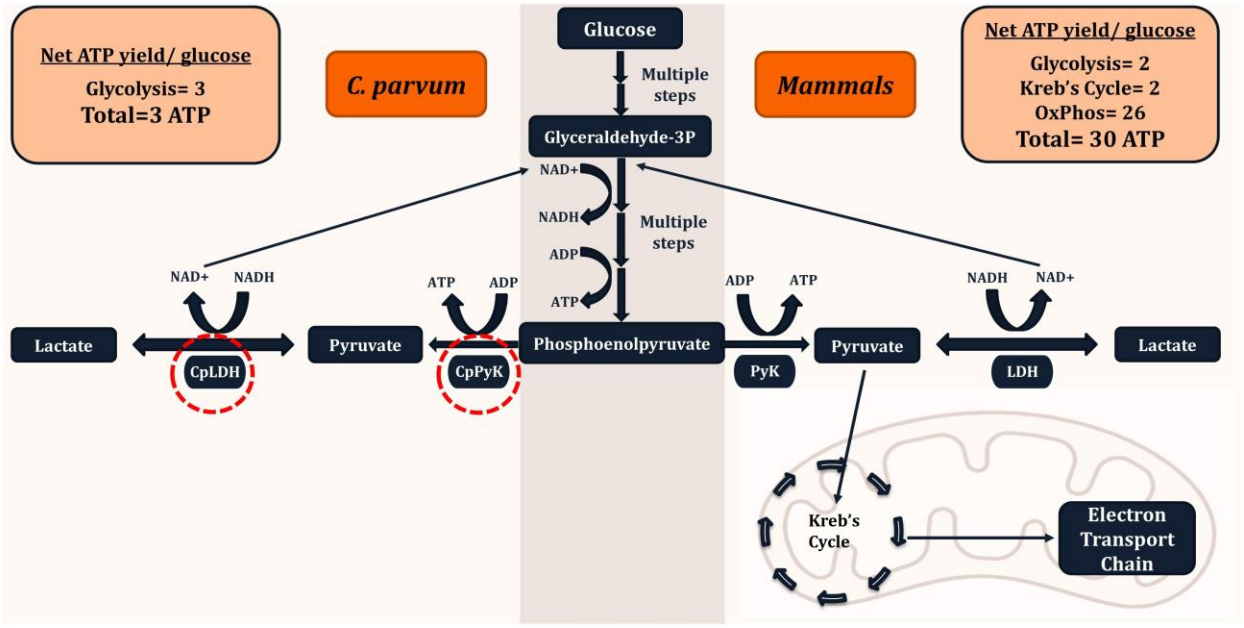

Figure 1.2: The role of CpPyK and CpLDH in the unique glycolytic pathway of *C. parvum* with a side-by-side comparison with the mammalian energy metabolism pathways. Abbreviations: ADP, Adenosine diphosphate; ATP, Adenosine Triphosphate; CpLDH, *C. parvum* lactate dehydrogenase; CpPyK, *C. parvum* pyruvate kinase; NAD+, Oxidized Nicotinamide adenine dinucleotide; NADH, Reduced Nicotinamide adenine dinucleotide; LDH, Lactate dehydrogenase; PyK, Pyruvate Kinase.

Table 1.1: Efficacies of treatments tested against cryptosporidiosis in human patients.

Drug	Age and health status of patients	Number of individuals	Study type	Reference	Treatment type	Efficacy	
						Clinical Cure	Parasitological Cure
Albendazole	Adults with advanced AIDS (CD4+ cell counts >200/mm^3)	4	OL	(Zulu et al., 2002)	Therapeutic	+	+
Azithromycin	Adults with AIDS	85	R, DB, PC	(Soave et al., 1993)	Therapeutic	±	±
	Children on chemotherapy for cancer	2	CR	(Vargas et al., 1993)	Therapeutic	+	±
	Children with AIDS	4	CR	(Hicks et al., 1996)	Therapeutic	+	+
	Adults with AIDS	14	OL	(Blanshard et al., 1997)	Therapeutic	-	-
		13	OL, DC	(Dionisio et al., 1998)	Therapeutic	±	±
		54	RCR	(Holmberg et al., 1998)	Prophylactic	-	-
		41	R, OL, DC	(Kadappu et al., 2002)	Therapeutic	+	±
	Immunocompetent children	43	OL, AC	(Allam and Shehab, 2002)	Therapeutic	+	+
	Children on chemotherapy for cancer	2	CR	(Trad et al., 2003)	Therapeutic	+	+
Clarithromycin	Adults with AIDS	353	RCR	(Jordan, 1996)	Prophylactic	+	+
	Adults with AIDS	312	RCR	(Holmberg et al., 1998)	Prophylactic	+	+
	Adults with advanced AIDS	530	RCR	(Fichtenbaum et al., 2000)	Prophylactic	-	-
Clofazimine	Adults with advanced AIDS	20	R, DB, PC	(Iroh Tam et al., 2021)	Therapeutic	-	-
Diclazuril	Adults with AIDS	9	OL	(Connolly et al., 1990)	Therapeutic	-	-
		1	CR	(Menichetti et al., 1991)	Therapeutic	±	±
Letrazuril	Adults with advanced AIDS	1	CR	(Murdoch et al., 1993)	Therapeutic	+	+
		14	OL	(Harris et al., 1994)	Therapeutic	±	±
		35	OL	(Loeb et al., 1995)	Therapeutic	±	±
		10	OL	(Blanshard et al., 1997)	Therapeutic	±	±
Miltefosine	Malnourished adults with AIDS	7	OL	(Sinkala et al., 2011)	Therapeutic	±	-
Nitazoxanide	Adults with advanced AIDS	12	OL	(Doumbo et al., 1997)	Therapeutic	±	±
	Adults with AIDS	66	R, DB, PC	(Rossignol et al., 1998)	Therapeutic	±	±
	Immunocompetent adults and children	99	R, DB, PC	(Rossignol et al., 2001)	Therapeutic	+	±
	Malnourished HIV-seronegative children	47	R, DB, PC	(Amadi et al., 2002)	Therapeutic	±	±
	Malnourished HIV-seropositive children	49				-	-

Table 1.1 (cont.)

Nitazoxanide	Adults with AIDS	207	R, DB, PC	(Zulu et al., 2005)	Therapeutic	-	-
	Immunocompetent adults and adolescents	86	R, DB, PC	(Rossignol et al., 2006)	Therapeutic	+	+
	Children and adults with AIDS	357	CU, OL	(Rossignol, 2006)	Therapeutic	±	±
	Children with AIDS	3	CU, CR	(Abraham et al., 2008)	Therapeutic	+	+
	Children with AIDS	52	R, DB, PC	(Amadi et al., 2009)	Therapeutic	-	-
	Pediatric solid organ transplant recipients	6	RCR	(Krause et al., 2012)	Therapeutic	+	+
	Immunocompetent children	135	R, OL, AC, PC	(Hussien et al., 2013)	Therapeutic	+	+
	Immunocompetent adults	58	OL	(Ali et al., 2014)	Therapeutic	±	±
	Adult renal transplant recipients	13	RCR	(Bhadauria et al., 2015)	Therapeutic	±	±
	Immunocompetent children	60	R, DB, PC	(Abaza et al., 2016)	Therapeutic	+	+
	Immunocompromised children	60				±	±
	Adults on chemotherapy for cancer	2	CR	(Demonchy et al., 2021)	Therapeutic	±	±
Paromomycin	Adults with AIDS	12	RCR	(Gathe et al., 1990)	Therapeutic	±	±
		5	CR	(Clezy et al., 1991)	Therapeutic	±	±
		5	CR	(Armitage et al., 1992)	Therapeutic	±	±
		1	CR	(Danziger et al., 1993)	Therapeutic	±	±
		7	RCR	(Fichtenbaum et al., 1993)	Therapeutic	±	±
		6	CR	(Wallace et al., 1993)	Therapeutic	±	±
		24	OL	(Bissuel et al., 1994)	Therapeutic	±	±
		35	OL	(Scaglia et al., 1994)	Therapeutic	±	±
		10	R, DB, PC	(White et al., 1994)	Therapeutic	+	+
		44	OL	(Flanigan et al., 1996)	Therapeutic	±	±
		20	OL	(Blanshard et al., 1997)	Therapeutic	±	±
		70	RCR	(Hashmey et al., 1997)	Therapeutic	±	±
		35	R, DB, PC	(Hewitt et al., 2000)	Therapeutic	-	-
	Children on chemotherapy for cancer	3	CR	(Trad et al., 2003)	Therapeutic	+	±
	Immunocompetent children	38	OL	(Vandenberg et al., 2012)	Therapeutic	±	±
		135	R, OL, AC, PC	(Hussien et al., 2013)	Therapeutic	±	±

Table 1.1 (cont.)

Roxithromycin	Adults with AIDS	24	OL	(Sprinz et al., 1998)	Therapeutic	+	±
		22	OL	(Uip et al., 1998)	Therapeutic	+	±
Rifabutin	Adults with AIDS	214	RCR	(Holmberg et al., 1998)	Prophylactic	+	+
	Adults with advanced AIDS	650	RCR	(Fichtenbaum et al., 2000)	Prophylactic	+	+
Rifaximin	Adults and children infected with HIV (CD4+ cell counts >200/mm^3)	10	OL	(Amenta et al., 1999)	Therapeutic	+	+
	Adult solid organ transplant recipient	1	CR	(Burdese et al., 2005)	Therapeutic	+	+
	Adults with AIDS (CD4+ cell counts <50 cells/mm^3)	5	CR	(Gathe et al., 2008)	Therapeutic	+	+
Spiramycin	Adult with AIDS	1	N of 1 trial	(Woolf et al., 1987)	Therapeutic	-	-
	Immunocompromised adults	37	CU, OL	(Moskovitz et al., 1988)	Therapeutic	+	±
	Immunocompetent infants	44	DB, PC	(Saez-Llorens et al., 1989)	Therapeutic	+	+
	Malnourished infants	39	R, DB, PC	(Wittenberg et al., 1989)	Therapeutic	-	-
	Adults with AIDS	31	CR	(Weikel et al., 1991)	Therapeutic	-	-

Notes:
1. AC, active-controlled; DB, double-blind; CU, compassionate use; CR, case report; DC, dose comparison; OL, open-label; PC, placebo-controlled; R, randomized; RCR, retrospective case review.
2. "+" = complete resolution; "-" = no demonstrable activity; "±" = partial resolution or relapse after treatment discontinuation.

Table 1.2: Other immunological and supportive treatments tested for efficacy against cryptosporidiosis in human patients.

Drug	Age and health status of patients	Number of individuals	Study type	Reference	Treatment type	Efficacy	
						Clinical Cure	Parasitological Cure
Bovine leukocyte extract	Adults and a child with AIDS	8	CR	(Louie et al., 1987)	Therapeutic	±	±
	Adults with AIDS	14	R, DB, PC	(McMeeking et al., 1990)	Therapeutic	+	+
Human serum immune globulin	Child on chemotherapy for cancer	1	CR	(Borowitz and Saulsbury, 1991)	Therapeutic	+	+
Hyperimmune bovine colostrum	Immunocompromised children and adult	3	CR	(Tzipori et al., 1987)	Therapeutic	+	±
	Adults with AIDS	5	R, DB, PC	(Nord et al., 1990)	Therapeutic	±	±
		1	CR	(Ungar et al., 1990)	Therapeutic	+	+
	Immunodeficient children and adults	7	OL	(Rump et al., 1992)	Therapeutic	+	+
	Adults with AIDS	7	OL	(Plettenberg et al., 1993)	Therapeutic	±	±
	Child infected with HIV	1	CR	(Shield et al., 1993)	Therapeutic	+	+
	Adults with AIDS	20	OL	(Greenberg and Cello, 1996)	Therapeutic	±	-
	Immunocompetent adults	16	R, DB, PC	(Okhuysen et al., 1998)	Prophylactic	±	±
	Adults with AIDS	20	OL	(Floren et al., 2006)	Therapeutic	+	NR
Somatostatin analogs (octreotide and vapreotide)	Adults with AIDS	1	CR	(Cook et al., 1988)	Therapeutic	+	-
		1	CR	(Katz et al., 1988)	Therapeutic	+	-
		4	CR	(Clotet et al., 1989)	Therapeutic	±	-
		15	OL	(Cello et al., 1991)	Therapeutic	±	-
		18	OL	(Romeu et al., 1991)	Therapeutic	±	-
		21	OL	(Girard et al., 1992)	Therapeutic	±	-
		4	OL	(Liberti et al., 1992)	Therapeutic	±	-
		13	OL	(Moroni et al., 1993)	Therapeutic	±	-
HIV protease inhibitor (indinavir or saquinavir)	Adults with advanced AIDS (CD4+ count < 50/mm^3)	1	CR	(Grube et al., 1997)	Therapeutic	+	+
		5	OL	(Bobin et al., 1998)	Therapeutic	+	+
		2	R, OL	(Foudraine et al., 1998)	Therapeutic	+	+
HAART including HIV protease inhibitor	Adults with AIDS (CD4+ count < 400/mm^3)	4	OL	(Carr et al., 1998)	Therapeutic	+	+

Table 1.2 (cont.)

HAART including HIV protease inhibitor	Adults with advanced AIDS (CD4+ count < 50/mm^3)	3	CR	(Miao et al., 1999; Miao et al., 2000)	Therapeutic	+	+

Notes:
1. DB, double-blind; CR, case report; NR, not reported; OL, open-label; PC, placebo-controlled; R, randomized.
2. "+" = complete resolution; "-" = no demonstrable benefit; "±" = partial resolution or relapse after treatment discontinuation.

Table 1.3: Efficacies of various combination therapies tested against human cryptosporidiosis.

Drug combination	Age and health status of patients	Number of individuals	Study type	Reference	Treatment type	Efficacy	
						Clinical Cure	Parasitological Cure
Acetylspiramycin + garlicin	Asymptomatic adult drug users	151	R, PC	(Huang et al., 2015)	Therapeutic	-	+
Azithromycin + paromomycin	Adults with AIDS	11	OL	(Smith et al., 1998)	Therapeutic	+	±
	Adult with AIDS	1	CR	(Palmieri et al., 2005)	Therapeutic	+	+
	Adult with AIDS	1	CR	(Meamar et al., 2006)	Therapeutic	+	+
	Adult liver transplant recipient	1	CR	(Denkinger et al., 2008)	Therapeutic	+	+
Azithromycin + paromomycin + nitazoxanide	Pediatric renal transplant recipient	1	CR	(Hong et al., 2007)	Therapeutic	+	+
Azithromycin + nitazoxanide	Adult allogeneic hematopoietic stem cell transplant recipients	5	OL	(Legrand et al., 2011)	Therapeutic	+	+
	Child on chemotherapy for cancer	1	CR	(Bakliwal et al., 2021)	Therapeutic	+	+
	Immunosuppressed child with CD40L deficiency	1	CR	(Dupuy et al., 2021)	Therapeutic	+	+
Azithromycin + nitazoxanide + rifaximin	Adult renal transplant recipient	1	CR	(Tomczak et al., 2022)	Therapeutic	+	+
Clarithromycin + rifabutin	Adults with advanced AIDS	451	RCR	(Fichtenbaum et al., 2000)	Prophylactic	±	±
Antiretrovirals + Paromomycin, Spiramycin, or Azithromycin	Adults with AIDS (CD4+ count $< 180/mm^3$)	45	RCR	(Maggi et al., 2000)	Therapeutic	+	+
HAART + Paromomycin	Adults with advanced AIDS (CD4+ count $< 50/mm^3$)	1	CR	(Schmidt et al., 2001)	Therapeutic	+	+
HAART + Glutamine + Azithromycin + Paromomycin		1	CR	(Moling et al., 2005)	Therapeutic	+	±
Nitazoxanide + fluoroquinolone	Adult renal transplant recipients	21	RCR	(Bhadauria et al., 2015)	Therapeutic	+	+
Spiramycin + paromomycin + nitazoxanide	Pediatric renal transplant recipient	1	CR	(Acikgoz et al., 2012)	Therapeutic	+	+

Notes:
1. DB, double-blind; CR, case report; OL, open-label; PC, placebo-controlled; R, randomized; RCR, retrospective case review.
2. "+" = complete resolution; "-" = no demonstrable activity; "±" = partial resolution or relapse after treatment discontinuation.

Table 1.4: Anti-cryptosporidial efficacies of various antimicrobial and novel treatments in farm animals and natural host animal models.

Therapeutic agent	Animal species and age	Number of individuals	Type of infection	Reference	Treatment type	Efficacy	
						Clinical Cure	Parasitological Cure
Aminoacyl-tRNA synthetase inhibitor Compound 2093	Neonatal calves	6	Experimental	(Hasan et al., 2021)	Therapeutic	±	±
Azithromycin	Neonatal calves	50	Natural	(Elitok et al., 2005)	Therapeutic	+	±
		25	Natural	(Nasir et al., 2013)	Therapeutic	NR	±
	Gnotobiotic piglets	40	Experimental	(Lee et al., 2017)	Therapeutic	±	-
	Buffalo calf	1	Natural	(Maurya et al., 2016)	Therapeutic	+	NR
Benzoxaborole AN7973	Neonatal calves	17	Experimental	(Lunde et al., 2019)	Therapeutic	+	+
Bumped Kinase Inhibitor 1294	Neonatal calves	18	Experimental	(Lendner et al., 2015)	Prophylactic	±	±
		24	Experimental	(Schaefer et al., 2016)	Therapeutic	±	+
Bumped Kinase Inhibitor 1369	Neonatal calves	7	Experimental	(Hulverson et al., 2017)	Therapeutic	+	+
	Gnotobiotic piglets	18	Experimental	(Lee et al., 2018)	Therapeutic	+	+
Decoquinate	Neonatal calves	30	Experimental	(Redman and Fox, 1993)	Prophylactic	±	±
		43	Experimental	(Moore et al., 2003)	Prophylactic	-	-
		90	Natural	(Lallemand et al., 2006)	Prophylactic	-	-
	Neonatal goat kids	20	Experimental	(Mancassola et al., 1997)	Prophylactic	+	±
		64	Natural	(Ferre et al., 2005)	Prophylactic	±	±
Halofuginone lactate	Neonatal calves	150	Natural	(Villacorta et al., 1991)	Prophylactic	+	±
		20	Experimental	(Naciri et al., 1993)	Prophylactic	+	±
		70	Natural and experimental	(Peeters et al., 1993)	Prophylactic	+	±
		158	Natural	(Lefay et al., 2001)	Prophylactic	+	±
		152	Natural	(Joachim et al., 2003)	Metaphylactic	±	±
		31	Natural	(Jarvie et al., 2005)	Prophylactic	±	±
		90	Natural	(Lallemand et al., 2006)	Prophylactic	-	±
		260	Natural	(Klein, 2008)	Prophylactic	±	±
					Therapeutic	±	±
		32	Natural	(De Waele et al., 2010)	Prophylactic	+	±
		513	Natural	(Trotz-Williams et al., 2011)	Prophylactic	±	±

Table 1.4 (cont.)

Halofuginone lactate	Neonatal calves	45	Natural	(Almawly et al., 2013)	Prophylactic	-	-
		149	Natural	(Keidel and Daugschies, 2013)	Metaphylactic	±	±
		530	Natural	(Meganck et al., 2015)	Prophylactic	±	±
		144	Natural	(Niine et al., 2018)	Prophylactic	±	-
		20	Natural	(Aydogdu et al., 2018)	Therapeutic	±	±
		123	Natural	(Velez et al., 2019)	Prophylactic	-	±
	Neonatal lambs	12	Experimental	(Naciri and Yvore, 1989)	Prophylactic	+	+
		5			Therapeutic	+	±
		28	Natural	(Causapé et al., 1999)	Prophylactic	-	±
					Therapeutic	±	±
		1170	Natural	(Giadinis et al., 2007)	Prophylactic	+	±
					Therapeutic	+	+
	Neonatal goat kids	69	Natural	(Chartier et al., 1999)	Prophylactic	±	±
		2240	Natural	(Giadinis et al., 2008)	Prophylactic	+	+
					Therapeutic	+	+
		44	Experimental	(Petermann et al., 2014)	Prophylactic	±	±
Lasalocid	Neonatal calves	10	Experimental	(Moon et al., 1982)	Prophylactic	±	±
		11	Natural	(Sahal et al., 2005)	Therapeutic	+	±
		12	Natural	(Murakoshi et al., 2014)	Prophylactic	+	±
Nitazoxanide	Neonatal calves	20	Experimental	(Ollivett et al., 2009)	Therapeutic	+	±
		9	Experimental	(Schnyder et al., 2009)	Prophylactic	-	-
					Therapeutic	-	-
	Neonatal goat kids	47	Experimental	(Viel et al., 2007)	Prophylactic	NR	±
	Gnotobiotic piglets	31	Experimental	(Theodos et al., 1998)	Therapeutic	-	±
		40	Experimental	(Lee et al., 2017)	Therapeutic	±	±
Paromomycin	Neonatal calves	16	Experimental	(Fayer and Ellis, 1993)	Prophylactic	+	+
		20	Natural	(Grinberg et al., 2002)	Prophylactic	±	±
		20	Natural	(Aydogdu et al., 2018)	Therapeutic	±	±
	Neonatal goat kids	19	Experimental	(Mancassola et al., 1995)	Prophylactic	+	+
		30	Natural	(Chartier et al., 1996)	Prophylactic	+	±
		55	Natural	(Johnson et al., 2000)	Prophylactic	+	+

Table 1.4 (cont.)

Paromomycin	Neonatal lambs	36	Natural	(Viu et al., 2000)	Therapeutic	±	+
	Gnotobiotic piglets	21	Experimental	(Tzipori et al., 1994)	Therapeutic	±	±
		31	Experimental	(Theodos et al., 1998)	Therapeutic	+	±
Triazolopyradizine MMV665917	Neonatal calves	13	Experimental	(Stebbins et al., 2018)	Therapeutic	+	+
	Gnotobiotic piglets	28	Experimental	(Lee et al., 2019)	Therapeutic	+	±
Pyrazolopyridine KDU731	Neonatal calves	13	Experimental	(Manjunatha et al., 2017)	Therapeutic	+	+
Sulfonamides	Neonatal calves	59	Natural	(Fischer, 1983)	Prophylactic	-	-
					Therapeutic	-	-
		13	Experimental	(Fayer, 1992)	Prophylactic	-	-
		152	Natural	(Joachim et al., 2003)	Metaphylactic	-	-
		25	Natural	(Nasir et al., 2013)	Therapeutic	NR	-
	Neonatal goat kids	24	Experimental	(Koudela and Bokova, 1997)	Prophylactic	-	-
					Therapeutic	-	-
Tilmicosin	Neonatal goat kids	22	Natural	(Paraud et al., 2010)	Prophylactic	-	-
Tylosin	Neonatal calves	23	Natural	(Duru et al., 2013)	Therapeutic	+	±

Notes:
1. NR, not reported.
2. “+” = complete cure; “-” = no demonstrable effect; “±” = partial cure or relapse after treatment discontinuation.

Table 1.5: Alternate treatments tested for efficacy against cryptosporidiosis in farm animals and natural host animal models.

Drug	Animal species and age	Number of individuals	Type of infection	Study	Treatment type	Efficacy	
						Clinical Cure	Parasitological Cure
α-cyclodextrin	Neonatal goat kids	20	Experimental	(Castro-Hermida et al., 2004)	Prophylactic	±	±
β-cyclodextrin	Neonatal calves	12	Natural	(Castro-Hermida et al., 2001a)	Prophylactic	+	±
					Therapeutic	±	±
	Neonatal lambs	53	Natural	(Castro-Hermida et al., 2001b)	Prophylactic	+	+
					Therapeutic	+	±
Activated charcoal	Neonatal calves	258	Natural	(Ross et al., 2021)	Therapeutic	±	±
Activated charcoal + wood vinegar	Neonatal calves	6	Experimental	(Watarai et al., 2008)	Therapeutic	+	+
	Neonatal goat kids	40	Natural	(Paraud et al., 2011)	Prophylactic	±	±
Anti-IL-10 egg yolk antibody	Neonatal calves	133	Natural	(Raabis et al., 2018)	Prophylactic	-	-
Artificial sweetener/ Glucagon-like peptide	Neonatal calves	24	Experimental	(Connor et al., 2017)	Prophylactic	±	±
Bobel-24 (anti-inflammatory drug)	Neonatal lambs	37	Experimental	(Castro-Hermida et al., 2008)	Prophylactic	±	±
					Therapeutic	±	-
Bovine/ Ovine colostrum	Neonatal calves	12	Experimental	(Fayer et al., 1989)	Prophylactic	±	±
		30	Experimental	(Slacek et al., 1996)	Prophylactic	±	±
		12	Experimental	(Perryman et al., 1999)	Prophylactic	+	+
		10	Experimental	(Askari et al., 2016)	Prophylactic	+	+
		30	Natural	(Kacar et al., 2022)	Prophylactic	+	+
	Neonatal lambs	32	Experimental	(Naciri et al., 1994)	Prophylactic	+	±
	Gnotobiotic piglets	21	Experimental	(Tzipori et al., 1994)	Therapeutic	-	-
Bovine interleukin-12 (recombinant)	Neonatal calves	20	Experimental	(Pasquali et al., 2006)	Prophylactic	-	-
Bovine serum concentrate	Neonatal calves	24	Experimental	(Hunt et al., 2002)	Prophylactic	±	±
Bovine leukocyte extract	Neonatal calves	9	Experimental	(Fayer et al., 1987)	Prophylactic	-	-
Clinoptilolite	Neonatal lambs	30	Experimental	(Dinler Ay et al., 2021)	Prophylactic	+	+
					Therapeutic	+	+
Chitosan	Neonatal lambs	32	Experimental	(Aydogdu et al., 2019)	Therapeutic	±	±
Phytogenic extracts and essential oils	Neonatal calves	43	Experimental	(Olson et al., 1998)	Prophylactic	-	-
		41	Natural	(Weyl-Feinstein et al., 2014)	Prophylactic	+	±
		91	Natural	(Katsoulos et al., 2017)	Prophylactic	±	-
		30	Natural	(Volpato et al., 2019)	Prophylactic	-	-
		26	Experimental	(Mendonca et al., 2021)	Prophylactic	±	±

Table 1.5 (cont.)

Probiotics (lactic acid producing bacteria)	Neonatal calves	134	Natural	(Harp et al., 1996)	Prophylactic	-	-
		30	Natural	(Fernandez et al., 2020)	Prophylactic	±	-
		44	Natural	(Stefańska et al., 2021)	Prophylactic	±	±
Yeast fermentation products	Neonatal calves	123	Natural	(Velez et al., 2019)	Prophylactic	-	-

Note: "+" = complete cure; "-" = no demonstrable effect; "±" = partial cure or relapse after treatment discontinuation.

CHAPTER 2: *CRYPTOSPORIDIUM PARVUM* PYRUVATE KINASE INHIBITORS WITH *IN VIVO* ANTI-CRYPTOSPORIDIAL EFFICACY

2.1 ABSTRACT

Cryptosporidium parvum is a highly prevalent protozoan parasite that causes diarrheal disease in humans and animals worldwide. Thus far, the moderately effective nitazoxanide is the only drug approved by the United States Food and Drug Administration for treating cryptosporidiosis in immunocompetent humans. However, no effective drug exists for the severe disease seen in young children, immunocompromised individuals, and neonatal livestock. *C. parvum* lacks the Krebs cycle and the oxidative phosphorylation steps, making it dependent solely on glycolysis for metabolic energy production. Within its glycolytic pathway, *C. parvum* possesses two unique enzymes, the bacterial-type lactate dehydrogenase (CpLDH) and the plant-like pyruvate kinase (CpPyK), that catalyze two sequential steps for generation of essential metabolic energy. We have previously reported that inhibitors of CpLDH are effective against *C. parvum*, both *in vitro* and *in vivo*. Herein, we cloned the open reading frame of the CpPyK gene, expressed the recombinant CpPyK protein in bacteria, and purified it in native form using nickel-affinity chromatography. Further we developed an *in vitro* luminescence-based CpPyK enzymatic assay and found that the recombinant CpPyK protein showed concentration-dependent enzymatic catalytic activity and followed Michaelis-Menten kinetics with respect to both its substrates, phosphoenolpyruvate (PEP) and adenosine diphosphate (ADP). We used the *in vitro* enzymatic assay to screen a chemical compound library for inhibitors of CpPyK's activity. The identified inhibitors were tested (at non-toxic concentrations) for efficacy against *C. parvum* using *in vitro* assays, and an *in vivo* mouse infection model. We identified six CpPyK-inhibitors that blocked *in vitro* growth and

---

Part of this chapter has been published as a research article in Frontiers in Microbiology. The original citation is: Khan, S.M., Zhang, X., and Witola, W.H. (2022). *Cryptosporidium parvum* Pyruvate Kinase Inhibitors With *in vivo* Anti-cryptosporidial Efficacy. *Front Microbiol* 12**,** 800293. doi: 10.3389/fmicb.2021.800293. PubMed PMID: 35046922.

proliferation of *C. parvum* at low micromolar concentrations (EC_{50} values ranging from 10.29 to 86.01 μM) that were nontoxic to host cells. Among those six compounds, two (NSC252172 and NSC234945) were found to be highly efficacious against cryptosporidiosis in immunocompromised mice at a dose of 10 mg/kg body weight, with very significant reduction in parasite load and amelioration of intestinal pathologies. Together, these findings have unveiled inhibitors for an essential molecular target in *C. parvum* and demonstrated their efficacy against the parasite *in vitro* and *in vivo*. These inhibitors are, therefore, potential lead-compounds for developing efficacious treatments for cryptosporidiosis.

2.2 INTRODUCTION

Intracellular eukaryotic protozoan parasites belonging to the genus *Cryptosporidium* are members of the phylum Apicomplexa. Out of the currently documented 42 species of *Cryptosporidium* (Zahedi and Ryan, 2020), *Cryptosporidium parvum* is recognized as the major zoonotic species responsible for diarrheal infections in animals and humans worldwide (Ryan et al., 2014; Thomson et al., 2017). In particular, *C. parvum* is the most frequently identified enteric pathogen in pre-weaned calves (Cho et al., 2013), causing substantial morbidity resulting in weight loss and delayed growth (Thomson et al., 2017; Shaw et al., 2020). Among humans in developing countries, *Cryptosporidium* is the main cause of linear growth faltering and the second leading cause of moderate-to-severe diarrhea in infants (0 to 11 months of age) and a major cause of mortality and stunted growth in the second year of life (Kotloff et al., 2013; Nasrin et al., 2021). Cryptosporidiosis is regarded as a high-risk and often fatal opportunistic infection for immunocompromised patients such as those suffering from HIV/AIDS (O'Connor R et al., 2011) or those receiving organ transplants (Danziger-Isakov, 2014; Bhadauria et al., 2015).

The life cycle of *C. parvum* consists of the asexual replication phase and the sexual reproduction phase leading to generation of infectious oocysts that persist in the environment (Fayer et al., 2000). While *C. parvum* has been recognized as an important etiological agent of diarrhea for over 4 decades (Navin and Juranek, 1984), neither fully effective therapeutic drugs nor prophylactic vaccines are currently available. Nitazoxanide, the only drug approved for treatment of cryptosporidiosis in immunocompetent human patients, is ineffective in the most susceptible populations including young children and immunocompromised individuals (Checkley et al., 2015). Further, there is no effective treatment available for *C. parvum* infections in cattle (Santin, 2020). Thus, there is an urgent need for the development of efficacious anti-cryptosporidial drugs.

Owing to the lack of genes encoding components of conventional apicomplexan drug targets such as the apicoplast, tricarboxylic acid cycle, and the ATP-generating classical respiratory chain (Abrahamsen et al., 2004), drugs developed against various other apicomplexan parasites are ineffective against cryptosporidiosis. Nevertheless, the parasite possesses other unique pathways that are essential for its growth and replication within the host. Notably, *C. parvum* lacks a functional mitochondrion, making it dependent on glycolysis for metabolic energy (Abrahamsen et al., 2004; Zhu, 2007). The glycolytic enzymes, therefore, are potential targets for developing therapeutics against *C. parvum*, provided that adequate parasite-versus-host selectivity is attained. Of interest are *C. parvum* pyruvate kinase (CpPyK), a plant-like pyruvate kinase enzyme, and *C. parvum* lactate dehydrogenase (CpLDH), a bacterial-type lactate dehydrogenase enzyme (Abrahamsen et al., 2004), that sequentially catalyze the last two glycolytic reactions to produce pyruvate and lactate, respectively, with generation of metabolic energy (ATP).

Previously, we have provided genetic evidence for the critical role of CpLDH in growth, infectivity, and multiplication of *C. parvum*, both *in vitro* and *in vivo* (Witola et al., 2017; Zhang et al., 2018). We have also identified CpLDH-inhibitors that show antiparasitic activity against *C. parvum*, both *in vitro* and *in vivo* (Li et al., 2019). Herein, we undertook a chemical library screen to identify specific inhibitors for the enzymatic activity of recombinant CpPyK (rCpPyK) protein. Using mammalian cell culture infection assays and *in vivo* mouse infection models, we have demonstrated that some of those CpPyK-inhibitors possess anti-cryptosporidial activity at low tolerable doses. Collectively, our results make a compelling case for further development of the identified glycolytic pathway inhibitors into the next generation of efficacious anti-cryptosporidial drugs.

2.3 RESULTS

2.3.1 Enzymatic activity and kinetics of rCpPyK protein.

Primary amino acid sequence alignment between the *C. parvum* and the human pyruvate kinase revealed a low alignment score of around 37 (Figure 2.1A). Moreover, phylogenetic analysis of various pyruvate kinases belonging to apicomplexan, plant, animal, and bacterial origins showed that the CpPyK is more closely related to plant-like pyruvate kinases than mammalian pyruvate kinases (Figure 2.1B). Collectively, these analyses agreed with previous findings (Abrahamsen et al., 2004) and suggested that the unique pyruvate kinase encoded by the *C. parvum* genome may be an attractive drug target.

The 1581 bp long open reading frame of the CpPyK gene translates into a 526 amino acid protein with an estimated molecular weight of 56.4 kDa and an isoelectric point of 6.78 (http://cryptodb.org). We sequenced the cloned CpPyK coding sequence amplified from *C. parvum* cDNA and observed a 100% homology when aligned with the nucleotide sequence

reported in genome databases (CryptoDB gene ID: cgd1_2040; GenBank accession number: XM_628040). To analyze the activity of the CpPyK protein in catalyzing the transfer of a phosphate group from phosphoenolpyruvate to ADP, we expressed CpPyK as a His-tagged protein and nickel affinity column chromatography-purified it in its native form. The purified rCpPyK protein containing the vector-derived hexahistidine tag (His-tag) was of the expected molecular size of approximately 57 kDa (Figure 2.2A). Using the ATP detection-based CpPyK enzymatic assay (Figure 2.2B), we found that rCpPyK protein depicted concentration- and pH-dependent catalytic activity with optimal activity at 6 ng/µl and pH 7.5, respectively (Figures 2.2C, D). The catalytic activity of the recombinant protein was consistent with Michaelis-Menten kinetics on the substrate (phosphoenolpyruvate) and the co-substrate (ADP) (Figure 2.3), with kinetic parameters (K_m and V_{max}) that were comparable to those previously reported for CpPyK (Denton et al., 1996) (Table 2.1).

2.3.2 Identification of non-toxic CpPyK-inhibitors.

To identify selective inhibitors for the rCpPyK catalytic activity, we screened a library consisting of 1424 chemical compounds using the *in vitro* CpPyK enzymatic assay. We identified 70 compounds that displayed substantial *in vitro* inhibition (> 30%) of the rCpPyK catalytic activity at a concentration of 50 µM (Figure 2.4). In addition, there were several other compounds that exhibited low inhibitory activity (< 30%) against rCpPyK, but for logistical reasons were not pursued further in order to limit the number of compounds that were subsequently investigated in detail. The remaining compounds either had no effect or augmented the activity of rCpPyK and were also not analyzed further.

Prior to the evaluation of rCpPyK-inhibitors for *in vitro* anti-cryptosporidial effect, we tested them for cytotoxicity against the human ileocecal colorectal adenocarcinoma cell line

(HCT-8) that was used for *in vitro* culture of *C. parvum*. The cytotoxic effect of compounds in HCT-8 cells was evaluated by quantifying the cleavage of the tetrazolium salt (WST-1) to formazan by metabolically active cells (Figure 2.5A). In the initial cytotoxicity screen, of the 70 rCpPyK-inhibitors, 44 depicted low cytotoxicity (< 25%) after 24 hours of treatment of the cell cultures with the inhibitors at a concentration of 50 μM, and those compounds were, therefore, selected for *in vitro* efficacy studies (Figure 2.5B). On the other hand, the remaining 26 compounds were found to inhibit the host cells' viability by more than 25% and were thus not pursued further due to potential toxicity issues.

2.3.3 rCpPyK-inhibitors with *in vitro* anti-*Cryptosporidium* efficacy.

To determine the effect of rCpPyK-inhibitors on the intracellular growth and replication of *C. parvum*, we performed *in vitro* infection and treatment assays using HCT-8 cell monolayers to culture *C. parvum* (Figure 2.6A). rCpPyK-inhibitors that were found to be non-toxic to host cells at 50 μM were screened initially at 25 μM (half the concentration used for primary cytotoxicity screening) to evaluate their *in vitro* efficacy against *C. parvum*. All experimental data were normalized with DMSO-treated wells and paromomycin-treated (Marshall and Flanigan, 1992) wells that represented negative and positive treatment controls, respectively. Among the 44 compounds tested, a total of six compounds (NSC234945, NSC252172, NSC636718, NSC303244, NSC638080, and NSC11437) exhibited significant inhibitory effect on the *in vitro* proliferation and viability of *C. parvum* when compared to the untreated parasites after 48 hours of culture (Figure 2.6B). We selected those compounds for secondary analysis using varying concentrations of each compound at different time-points of infection to determine their *in vitro* anti-cryptosporidial half-maximal effective concentration (EC_{50}) values. To start with, the selected compounds were analyzed at varying concentrations (ranging from 0 to 1000

μM) for *in vitro* cytotoxicity against uninfected HCT-8 cells using the WST-1 cell proliferation assay, and the half-maximal cytotoxic concentration (CC_{50}) values were derived (Table 2.2). As a guide, for each compound, the highest concentration that was tested for anti-cryptosporidial activity did not exceed 50% of its CC_{50} value.

To determine the compounds' concentration-dependent effect against *C. parvum in vitro*, each compound was tested by adding it to the HCT-8 cells culture shortly before or 2 hours after infection with *C. parvum* sporozoites in order to assess the effect of the compound on host cell invasion by the parasites, and the effect of the compound on intracellular parasites, respectively. When the cultures were analyzed by an immunofluorescence assay after 48 hours post-infection (PI), all six compounds (NSC234945, NSC252172, NSC636718, NSC303244, NSC638080 and NSC11437) showed a significant ($P < 0.05$) concentration-dependent inhibitory effect on the proliferation of intracellular *C. parvum* parasites in HCT-8 cells in comparison with the control infected cultures without compound treatment (Figures 2.7A-F). The treatment of infected HCT-8 cultures resulted in concentration-dependent decreases in parasite viability regardless of whether the compound (NSC234945, NSC252172, NSC636718, and NSC11437) treatment commenced at 0 hours PI or 2 hours PI (without any notable significant difference between the two time points of treatment). However, compounds NSC303244 and NSC638080 showed higher potency when treatment commenced at 0 hours PI than at 2 hours PI, suggesting that exposure of the sporozoites to the compounds prior to host cell invasion reduced their viability and led to a reduction in the number of parasites that invaded the cells. The EC_{50} values derived from the dose-response curves for the compounds, when compared to their CC_{50} values, showed that compounds NSC638080 and NSC303244 had the best selectivity indices (Table 2.2), suggesting that they had good safety margin with regard to toxicity in mammalian cells, but with

best potencies at low EC_{50} concentrations against *C. parvum*. Compounds NSC636718 and NSC234945 had the least selectivity indices, suggesting a narrower safety margin (Table 2.2).

2.3.4 rCpPyK-inhibitors with *in vivo* efficacy against *C. parvum* infection.

Based on the *in vitro* infection and treatment assay results described above, we selected NSC638080 and NSC303244 for *in vivo* testing (Figure 2.8), because of their high selectivity indices (SIs) that implied wider safety margins in terms of toxicity to mammalian cells. While NSC252172 had a comparatively lower SI, it was also selected for *in vivo* testing because of its relatively high *in vitro* potency against *C. parvum* (Table 2.2). Additionally, even though NSC234945 had comparatively lower SI, it was also selected for *in vivo* testing because of its high solubility in DMSO, which facilitated its use at high doses reconstituted in relatively small volumes of DMSO. NSC11437 was not pursued further because of its low solubility and difficulties in sourcing sufficient amounts for *in vivo* use. Additionally, NSC636718 was also not pursued further because it had the lowest SI and low *in vitro* anti-cryptosporidial efficacy in comparison to other compounds.

Prior to use in mice, the targeted highest dose of 10 mg/kg was tested for tolerability in uninfected mice. For the selected 4 compounds (NSC638080, NSC303244, NSC252172 and NSC234945) the dose of 10 mg/kg daily oral administration did not induce any toxicity signs (changes from normal physical activity, respiration, body temperature, feeding pattern, body posture, fur condition or occurrence of death) over 8 days of treatment. However, for the initial evaluation of the compounds' anti-*Cryptosporidium* efficacy in mice, a lower dose of 2.5 mg/kg was used for NSC638080, NSC303244, and NSC252172, while 5 mg/kg of NSC234945 was used. This was because, compared to the other three compounds, NSC234945 had depicted an *in vitro* EC_{50} concentration that was 2-3-fold higher, suggesting lower potency. Paromomycin was

used as a positive control drug at 1000 mg/kg once daily orally (Griffiths et al., 1998). The load of *C. parvum* oocysts shed in mice feces was determined by using real time PCR quantification of the *C. parvum* 18s rRNA gene. As expected, all the infected mice started shedding detectable levels of *C. parvum* oocysts in their feces by day 3 PI, indicating that at the time point (day 3 PI) when treatment commenced, the infection was patent in all the infected mice. From day 5 PI onwards, there were significantly progressive increases in oocysts load in the feces of the untreated mice, peaking at about 2.1×10^7 oocysts per gram feces on day 10 PI (Figure 2.9A). By day 8 PI, all the mice in the untreated infected group had become visibly sick, showing signs of progressive disease including rough hair coat, hunched back, reluctance to move, and weight loss. In comparison, from day 5 PI onwards, mice in the groups treated with test compounds or paromomycin all maintained lower loads of oocysts in their feces when compared to the untreated mice (Figure 2.9A). By day 9 PI, there was a notable difference in oocysts load among the different compound treatments, with NSC234945 and paromomycin depicting significantly ($P < 0.05$) lower oocysts loads than the other treatments and the untreated group (Figure 2.9A). By day 10 PI (when the oocyst load peaked) compounds treatment groups had 2-6-fold lower oocysts loads than the untreated group, with compound NSC234945 showing the highest potency, followed by paromomycin, NSC25172, NSC303244 and NSC638080, in that order (Figure 2.9A). Consistent with the lower oocysts counts, when compared to the untreated, mice from all the treated groups depicted relatively normal physical parameters including activity, posture, and appetite. Because the untreated mice became moribundly ill by day 10 PI, for ethical considerations, all mice were sacrificed on day 11 PI and intestinal samples submitted for histopathology.

Because NSC234945 and NSC252172 showed higher potency than the rest of the compounds, we tested them further at a higher dose of 10 mg/kg to determine if they would depict dose-dependent efficacy. Intriguingly, this increase in dose led to about 3-fold reduction in oocysts load by day 9 PI when compared to the untreated mice (Figure 2.9B). And by day 10 PI, both NSC234945 and NSC252172 had about 9-fold lower oocysts load than the untreated mice (Figure 2.9B), indicating that higher dose increased the compounds' *in vivo* efficacy against *C. parvum*. Noteworthy, the higher dose (10 mg/kg) of NSC234945 and NSC252172 showed about 2.5-fold higher potency than paromomycin (1000 mg/kg) by day 10 PI (Figure 2.9B). These mice were also sacrificed on day 11 PI and the distal small intestines submitted for histopathology.

C. parvum colonizes mostly the distal small intestines, causing villous atrophy, erosion, and ulceration of the intestinal mucosa. As such, we performed histopathological examination of sections of the small intestines resected from the distal part of the small intestines. As expected, while uninfected mice had normal intestinal mucosa, infected untreated mice had microscopic lesions characterized by severe villous atrophy, mucosal erosion, hypertrophy of the crypts of Lieberkuhn, and infiltration of inflammatory cells (Figure 2.10). In contrast, treatment of infected mice with the compounds evidently ameliorated the effects of *C. parvum* infection in the intestinal mucosa, with NSC234945 showing the best efficacy, followed by NSC252172 (Figure 2.10). These findings were consistent with the significantly lower oocysts loads attributed to NSC234945 and NSC252172 treatments. Notably, NSC303244 and NSC638080, though having lower efficacy than NSC234945 and NSC252172, still reduced intestinal pathology in a comparative manner to paromomycin (Figure 2.10).

2.4 DISCUSSION

An ideal approach to developing effective and safe drugs against parasites is through targeting the disruption of the activity of the parasite's unique molecules that are essential for its survival. The complete and annotated genome sequence of *C. parvum* indicates that, while the parasite lacks genes for conventional molecular drug targets found in other important protozoan parasites, it has several genes encoding unique plant-like and bacterial-like enzymes that catalyze potentially essential biosynthetic and metabolic pathways (Abrahamsen et al., 2004). Importantly, *C. parvum* lacks the tricarboxylic acid cycle and the oxidative phosphorylation steps for generation of metabolic energy (ATP) (Abrahamsen et al., 2004), making the parasite solely dependent on anaerobic respiration (glycolytic pathway) for the generation of ATP which is critical for its survival and pathogenesis in the host (Witola et al., 2017; Zhang et al., 2018). Previous studies have highlighted the importance of glycolytic enzymes such as glucose-6-phosphate isomerase (CpGPI) and hexokinase (CpHK) as potential drug targets for the treatment of cryptosporidiosis (Eltahan et al., 2018; Eltahan et al., 2019). Furthermore, we have found that inhibitors for *C. parvum*'s unique bacterial-type lactate dehydrogenase (CpLDH) in the parasite's glycolytic pathway can stop growth of the parasite and prevent disease in infected mice models (Li et al., 2019). Herein, we targeted the *C. parvum* pyruvate kinase (CpPyK) enzyme that catalyzes the step immediately upstream of the CpLDH catalytic step. CpPyK serves as the key metabolic control in *C. parvum*'s glycolytic cycle, in that it catalyzes the irreversible conversion of phosphoenolpyruvate to pyruvate and generates ATP (Berg et al., 2002).

We cloned and sequenced the coding sequence of CpPyK from *C. parvum* cDNA and found it to have significantly low homology to mammalian pyruvate kinases, consistent with the previous reports that it differs both functionally and structurally from its mammalian counterparts (Denton et al., 1996; Cook et al., 2012). We established an *in vitro* enzymatic assay

in which we used natively purified recombinant CpPyK as the enzyme to catalyze the dephosphorylation of phosphoenolpyruvate to pyruvate and production of ATP. Using this assay, we validated that CpPyK follows Michaelis-Menten saturation kinetics, consistent with previous observations (Denton et al., 1996). By using this CpPyK enzyme-based *in vitro* assay, we screened a chemical compound library and identified specific inhibitors for the catalytic activity of CpPyK, suggesting that those compounds could also potentially block the activity of the *bona fide* CpPyK in the parasites, leading to loss of metabolic energy for the parasite. Given that mammalian cells possess pyruvate kinases, we first determined the CpPyK-inhibitors' cytotoxicity (CC_{50}) concentrations in order to guide our selection of the concentrations for the *in vitro* anti-cryptosporidial assays. From these assays we identified CpPyK-inhibitors (NSC234945, NSC252172, NSC636718, NSC303244, NSC638080, and NSC11437) that had no toxicity to mammalian cells at their effective concentrations against the activity of CpPyK. These findings corroborated reports that CpPyK has distinct functional as well as structural properties when compared to mammalian pyruvate kinases, suggesting that CpPyK-inhibitors may not affect mammalian pyruvate kinases because of their divergent structural differences (Fothergill-Gilmore and Michels, 1993; Entrala and Mascaro, 1997). Additionally, mammals seem to be less sensitive to the inhibition of glycolysis because, unlike *C. parvum*, they possess multiple pyruvate kinase isoforms, a fully functional Krebs cycle, and the ability to use alternative energy sources including amino acids and fatty acids (Fothergill-Gilmore and Michels, 1993).

We then determined the *in vitro* anti-cryptosporidial efficacy of the candidate compounds in infected HCT-8 monolayers and identified compounds (NSC234945, NSC252172, NSC636718, NSC303244, NSC638080, and NSC11437) that had concentration-dependent inhibitory effect against the growth and proliferation of *C. parvum* parasites at low micromolar

concentrations that were not toxic to mammalian host cells. Notably, the selectivity indices (SI) of the six test compounds ranged from 3.2 to 69.0, indicating that they were all efficacious against *C. parvum* at concentrations that were tolerable to host mammalian cells (Kaminsky et al., 1996). The infection-treatment assays we used involved infecting HCT-8 cells with excysted *C. parvum* sporozoites that infect host cells and transform into proliferative merozoites, a process that requires metabolic energy. Therefore, by inhibiting the activity of CpPyK, the inhibitors blocked the key enzyme for the generation of metabolic energy, thereby curtailing the growth and replication of intracellular *C. parvum*. Paromomycin, which was used as a positive control drug in this study, has a reported *in vitro* anti-*Cryptosporidium* EC_{50} of 450 µM (Li et al., 2019). Comparatively, the six compounds that showed *in vitro* efficacy against *C. parvum* all had much lower EC_{50} values (ranging from 10.29 – 86.01 µM), suggesting better efficacy than paromomycin.

The interferon-gamma knockout (IFN-γ KO) mouse, which is highly susceptible to *C. parvum* infection, is a widely used acute infection model for evaluating compounds for *in vivo* anti-*Cryptosporidium* efficacy. Typically, *C. parvum*-infected IFN-γ KO mice develop gastrointestinal disease, characterized by extensive lower intestinal epithelial cells infection and severe mucosal damage, with associated clinical signs including depression, anorexia, weight loss, and death within 2 to 4 weeks (Griffiths et al., 1998). Treatment of *C. parvum*-infected IFN-γ KO mice with paromomycin has been shown to significantly limit parasite load and clinical disease, and to prevent death (Griffiths et al., 1998). Therefore, we used the IFN-γ KO mice to test the CpPyK-inhibitors for *in vivo* efficacy against *C. parvum*. We found that treatment of the infected mice with compounds NSC252172, NSC303244, NSC638080 (at dose of 2.5 mg/kg) or NSC234945 (at a dose of 5 mg/kg) led to a significant reduction in the load of *C. parvum* oocysts

shed in mice's feces, and prevented manifestation of clinical disease and intestinal pathology in a manner that was comparable to treatment with paromomycin at 1000 mg/kg. Comparatively, NSC252172 and NSC234945 depicted better efficacy, while NSC638080 had the least efficacy. Interestingly, at a higher dose of 10 mg/kg (that was tolerable in mice), both NSC252172 and NSC234945 showed significantly better efficacy than paromomycin at 1000 mg/kg. These findings corroborated the *in vitro* efficacy results, thus positioning CpPyK-inhibitors as promising lead-compounds for the development of efficacious anti-cryptosporidial drugs.

Lipinski's and Veber's rules describe a set of key physicochemical properties that determine the probability of drug candidates to be orally bioavailable in humans (Lipinski et al., 2001; Veber et al., 2002). The chemical structures of the CpPyK-inhibitors (NSC234945, NSC252172, NSC636718, NSC303244, NSC638080, and NSC11437) with anti-cryptosporidial efficacy all conform to the Lipinski's and Veber's rules for the accepted criteria for drug-likeness, including their molecular masses, hydrophobicity, hydrogen bond donors/acceptors, rotatable bonds, and polarity, as listed in Table 2.3. *Cryptosporidium* spp. are minimally invasive, and their development is restricted to an unusual intracellular but extra-cytoplasmic location in the host epithelial cells (Guerin and Striepen, 2020). Therefore, an orally active anti-cryptosporidial drug must effectively penetrate both host and parasite membranes to reach its intended target in the parasite. It is well known that octanol-water partition coefficients, cLog(*P*), provide a good estimate of a compound's lipophilicity, which is a good measure of its ability to penetrate cellular membranes, including gastrointestinal absorption (Artursson and Karlsson, 1991). Generally, more lipophilic drugs tend to diffuse faster into the lipid cell membranes, suggesting that the relatively high cLog(*P*) value of 4.4 for NSC252172 (Table 2.3 entailed enhanced lipophilicity, and thus likely favored its bioavailability *in vivo,* making it reach its

intended molecular target in substantial amounts. However, too high cLog(*P*) may be counterproductive as it can negatively impact aqueous solubility and target molecule binding. Thus, the relatively lower cLog(*P*) value of 1.2 for compound NSC234945 would tend to maintain its aqueous solubility for optimized drug-likeness and anti-parasitic potency. Additionally, a molecule's topological polar surface area (Å) value that is lower than 80 tends to improve the drug-likeness for a molecule. Interestingly, all the compounds we found to have anti-cryptosporidial efficacy had Å values that were significantly lower than 80 (Table 2.3).

Structure-wise, the diversity of the aromatic/heteroaromatic portion among the CpPyK-inhibitors extends to dihydroquinazoline (NSC303244), dihydronaphthalenone (NSC252172), and 3,5-dipyridyl-triazole (NSC234945) skeletons (Figure 2.11). It is noteworthy that the aforementioned structural motifs are very often found in various approved medications and biologically active natural products, e.g. anthraquinone (Malik and Muller, 2016), and others representing the so-called 'privileged scaffolds' often utilized in library design and drug discovery (Welsch et al., 2010; Alagarsamy et al., 2018; Aggarwal and Sumran, 2020). Most importantly, these scaffolds are highly amenable to structural modification for the synthesis of derivatives with enhanced potency and safety. In conclusion, the impressive anti-cryptosporidial efficacy and safety, both *in vitro* and *in vivo*, for the CpPyK-inhibitors identified in the current study provide excellent starting compounds for the development of the much-needed novel anti-cryptosporidial therapeutics for both humans and animals.

2.5 MATERIAL AND METHODS

2.5.1 Sequence alignment and phylogenetic analysis of pyruvate kinases.

Amino acid sequences of the *C. parvum* pyruvate kinase (Accession no. XP_628040.1) and the human pyruvate kinase (Accession no. CAA39849.1) were retrieved from the National

Center for Biotechnology Information (NCBI) database and aligned using Clustal W (Larkin et al., 2007). The phylogenetic relationship among various pyruvate kinases was examined using a dataset of 13 representative amino acid sequences that included 4 apicomplexan, 2 plant, 5 animal, and 2 bacterial sequences. Evolutionary analyses were conducted in MEGA11 (Tamura et al., 2021). Multiple sequence alignments of pyruvate kinases were done using the Clustal W program and a neighbor-joining phylogenetic tree was constructed using a 1000 bootstrap value. The evolutionary distances were computed using the Poisson correction method and all ambiguously aligned positions were removed for each sequence pair.

2.5.2 *C. parvum* propagation and oocyst purification.

The AUCP-1 isolate of *C. parvum* was maintained and propagated by repeated passage in Holstein bull calves. Oocysts were purified from freshly collected calf feces by sequential sieve filtration, Sheather's sugar flotation (Current, 2018), and discontinuous sucrose density gradient centrifugation (Arrowood and Sterling, 1987). Purified oocysts were washed and stored at 4°C in phosphate buffered saline (PBS) and used within 3 months of initial purification from feces, when viability remained above 75% as judged by excystation. Sporozoites were excysted from *C. parvum* oocysts following a previously described procedure (Kuhlenschmidt et al., 2016). Briefly, about 1×10^8 purified *C. parvum* oocysts were suspended in 500 µl of PBS and treated with an equal volume of 40% commercial laundry bleach for 10 minutes at 4˚C. The oocysts were washed four times in PBS containing 1% (w/v) bovine serum albumin (BSA), resuspended in Hanks balanced salt solution (HBSS), and then incubated at 37˚C for 60 minutes. An equal volume of warm 1.5% sodium taurocholate in HBSS was added to the oocysts followed by further incubation at 37˚C for 60 minutes with occasional shaking. The excysted sporozoites were collected by centrifugation, washed in supplemented PBS, and resuspended in RPMI-1640

medium containing 10% fetal bovine serum (FBS). The sporozoites were separated from oocyst shells and unexcysted oocysts by filtering the suspension through a sterile 5 μm syringe filter (Millex™, Millipore). Purified sporozoites were enumerated with a hemocytometer and used immediately for the infection of cell monolayers.

2.5.3 Cloning and expression of rCpPyK protein.

cDNA was prepared from total RNA extracted from the AUCP-1 isolate of *C. parvum* and the CpPyK coding sequence (Genbank accession number XM_628040) was PCR-amplified from the cDNA using the primer pair 5'-*CTCGAG***ATG**ATTTCAAACGATCA-3' (Forward, with the *XhoI* restriction site italicized and start codon in bold) and 5'-*GGATCC***TTA**GGGGCACCTAACTAT- 3' (Reverse, with the *BamHI* site italicized and stop codon in bold) for site-directed cloning at the *XhoI*/*BamHI* site of the pET-15b expression vector (Novagen) in frame with the N-terminal hexahistidine tag (His-tag). The recombinant expression vector was sequenced to confirm identity, amplified in the K12 strain of *Escherichia coli* cells (NEB® Turbo; New England Biolabs), and transformed into protein expression BL21-CodonPlus (DE3)-RIL *E. coli* (Agilent Technologies). Transformed *E. coli* were cultured at 37˚C in Luria broth medium containing 100 μg/ml ampicillin and 34 μg/ml chloramphenicol to an absorbance of 0.6-0.8 at a wavelength of 600 nm, and protein expression was induced by addition of 1 mM isopropyl-β-D-thiogalactopyranoside. Bacterial cells were pelleted by centrifugation and resuspended in lysis buffer (50 mM NaH_2PO_4, 300 mM NaCl, 10 mM imidazole, pH 8.0) containing a 1× EDTA-free protease inhibitor cocktail, 600 units benzonase, and 30 kU lysozyme (EMD Millipore). The resuspended bacteria were lysed by sonication on ice and the cleared soluble fraction of the lysate was clarified by centrifugation at 13000 rpm. The His-tagged recombinant protein was purified under native conditions by nickel-affinity

chromatography according to the manufacturer's instructions (Novagen). The wash buffer contained 50 mM NaH_2PO_4, 300 mM NaCl, and 20 mM imidazole, pH 8.0, while the elution buffer was composed of 50 mM NaH_2PO_4, 300 mM NaCl, and 250 mM imidazole, pH 8.0. An ultrafiltration centrifugal protein concentrator with a molecular weight cut-off of 30K (Thermo Scientific) was used to remove imidazole and concentrate the protein in dialysis buffer containing 5 mM Hepes–KOH (pH 7.8) and 0.5 mM DTT. The purity and concentration of the recombinant protein were evaluated by SDS/PAGE and a Qubit™ Protein Assay Kit (Life Technologies), respectively.

2.5.4 CpPyK enzyme activity and kinetics.

The *in vitro* enzymatic activity of the rCpPyK protein was determined by quantitating the amount of ATP produced by the transfer of a phosphate group from phosphoenolpyruvate to ADP in the presence of varying concentrations of the recombinant protein. A typical assay contained 0.5 mM phosphoenolpyruvate, 0.6 mM ADP, 50 mM Tris buffer pH 7.5, 60 mM $MgSO_4$, 100 mM KCl, and varying concentrations of rCpPyK incubated for 3 hours at room temperature. The ATP generated was detected in a reaction volume of 50 µl in white opaque-walled 96 well plates by the luciferase-based Cell Titer-Glo 2.0 reagent (Promega) following the manufacturer's instructions. The enzyme kinetics of rCpPyK were determined by using varying phosphoenolpyruvate (0 to 8 mM) and ADP (0 to 2 mM) concentrations in an enzymatic reaction catalyzed by a fixed concentration of the recombinant protein (6 ng/µl). In all assays, reaction mixtures without rCpPyK were included as negative controls. Three independent assays were performed for each experiment, and samples were run in triplicate. The luminescence generated was recorded using a multi-mode microplate reader (Spectra Max iD3; Molecular Devices,

USA). GraphPad PRISM® v8 software was used to fit the Michaelis-Menten model directly to the substrate-velocity data to determine the enzymatic kinetic parameters for rCpPyK.

2.5.5 Screening compounds for inhibitory activity against CpPyK.

The Diversity Set VI chemical library (Table 2.4) was obtained from the National Cancer Institute (NCI)/Developmental Therapeutics Program (DTP) Open Repository collection of chemical compounds (http://dtp.cancer.gov). Compounds were individually reconstituted in molecular biology grade dimethyl sulfoxide (DMSO) from Sigma-Aldrich and stored at -20°C. From the library, 1424 compounds were screened in 96-well plates using the rCpPyK catalyzed enzyme assay to identify potential CpPyK-inhibitors. The reactions were performed in 50 µl reaction volume containing 0.5 mM phosphoenolpyruvate, 0.6 mM ADP, 50 mM Tris buffer pH 7.5, 60 mM $MgSO_4$, 100 mM KCl, 6 ng/µl of rCpPyK protein with or without compound. The concentration of DMSO in all reaction mixtures was 1% (v/v). Control reactions without rCpPyK protein were included for background subtraction. Following 3 hours of incubation at room temperature, an equal volume of the Cell Titer-Glo 2.0 reagent was added to each well, and the luminescence produced was recorded as relative luminescence units (RLU) after 10 minutes of incubation using a multi-mode microplate reader (Spectra Max iD3; Molecular Devices, USA). The mean percent inhibition (MPI) of rCpPyK activity by each compound was derived by dividing the difference in luminescence (RLU) between the compound-treated wells and the DMSO-treated wells by the luminescence of the DMSO-treated wells and multiplying the product by 100:

$$\text{MPI} = [(\text{Mean RLU}_{\text{DMSO-treated}} - \text{Mean RLU}_{\text{Compound-treated}}) \div \text{Mean RLU}_{\text{DMSO-treated}}] \times 100.$$

Half-maximal inhibitory concentration (IC_{50}) values were determined by applying a non-linear regression analysis curve fit to the mean dose-response data for varying concentrations of each compound using GraphPad PRISM® v8. Reactions were performed in triplicate and repeated at least thrice.

2.5.6 *In vitro* compound cytotoxicity assays.

Compounds were tested for cytotoxicity in human ileocecal colorectal adenocarcinoma cells (HCT-8 [HRT-18]; ATCC® CCL-244™, RRID:CVCL_2478) by using the cell proliferation reagent WST-1 (Roche) according to the manufacturer's protocol. The WST-1 assay is a quantitative colorimetric assay for measurement of metabolically active cells. This assay is based on the reduction of the tetrazolium salt (WST-1) by viable cells. About 5×10^4 HCT-8 cells were seeded per well in 96-well plates and grown overnight in 200 µl of RPMI-1640 medium (without phenol red) (Gibco) supplemented with 2.5 g/L of glucose, 1 mM sodium pyruvate, 1.5 g/L of sodium bicarbonate, 10% heat-inactivated FBS (Gibco), and 1× Antibiotic-Antimycotic (Gibco) at 37°C with 5% CO_2 in a humidified incubator. Upon reaching 80 - 90% confluency, cells were treated with the chemical compounds reconstituted in DMSO for 24 hours. The volume of DMSO was kept below 1% of the total culture volume in all the wells to avoid DMSO cytotoxicity. Control wells received equivalent volumes of DMSO used in the reconstituted compounds. After 24 hours of culture, 10 µl of the WST-1 reagent was added to each well, and the plates were incubated for 1 hour at 37°C with 5% CO_2 under dark conditions. The plates were shaken thoroughly and 150 µl of the medium from each well was transferred to a new clear flat-bottom black 96-well plate (Corning). Absorbance was read at a test wavelength of 440 nm and a reference wavelength of 690 nm using a multi-mode microplate reader (Spectra Max iD3; Molecular Devices, USA). The mean percent toxicity (MPT) of each compound was derived by

dividing the difference in absorbance (OD) between the compound-treated cells and the DMSO-treated cells by the absorbance from the DMSO-treated cells and multiplying the product by 100:

$$MPT = [(\text{Mean } OD_{\text{DMSO-treated}} - \text{Mean } OD_{\text{Compound-treated}}) \div \text{Mean } OD_{\text{DMSO-treated}}] \times 100.$$

The half-maximal cytotoxic concentration (CC_{50}) values were determined by using non-linear regression analysis in GraphPad PRISM® v8. Assays were performed in triplicate and repeated three times.

2.5.7 *In vitro* testing of anti-*Cryptosporidium* activity of CpPyK-inhibitors.

HCT-8 cells were grown to confluency in supplemented RPMI-1640 medium in 96-well plates. Once confluent, the cells were infected with 10^5 freshly excysted *C. parvum* sporozoites per well, immediately followed by the addition of anti-CpPyK compounds (reconstituted in DMSO) to one set of wells. Control infected cells were treated with DMSO volumes equivalent to those used for the compound-treated cultures. Paromomycin reconstituted in distilled sterile water, served as a positive control at a concentration of 200 μM. The cell monolayers were processed by a direct immunofluorescence assay (Witola et al., 2017) after 48 h of culture at 37°C with 5% CO_2. Briefly, the medium was removed from the culture wells, and the cells were washed two times with PBS before fixation with pre-chilled methanol-acetic acid (9:1) for 5 minutes at room temperature. Residual fixative was removed by rinsing the wells with PBS. Cells were rehydrated and permeabilized by washing twice with a buffer containing 0.1% Triton X-100, 0.35 M NaCl, and 0.13 M Tris-base, pH 7.6. Normal goat serum (5% in PBS) was used as a blocking agent, and the cell monolayer was stained with a fluorescein-labeled anti-*C. parvum* polyclonal antibody (Sporo-Glo™; Waterborne, Inc.) overnight at 4˚C. The stained cells

were washed twice with PBS followed by the addition of 200 µl water to each well. Plates were then imaged with an inverted fluorescence microscope using a 20× objective. The fluorescence generated by intracellular *C. parvum* parasites was quantified from 9 microscopic fields per well of a 96-well plate using the batch process function in ImageJ version v1.50 (NIH, USA) after setting a threshold for the detection of parasites. Control wells with uninfected monolayers were included for background subtraction. Experiments were performed in triplicate and repeated at least three times.

Anti-*Cryptosporidium* EC_{50} values of CpPyK-inhibitors were determined by performing *in vitro C. parvum* infection assays as described above, with the exception that varying concentrations of compounds were used to treat infected HCT-8 cell cultures. One set of wells with confluent HCT-8 cells received CpPyK-inhibitors immediately after *C. parvum* infection, while the same compounds were added to the other set of wells 2 hours post-infection (PI). Control infected cells were treated with varying volumes of DMSO equivalent to the ones used for the compound-treated cultures. Cell monolayers were processed for immunofluorescence analysis after 48 hours of incubation as described above. Samples were run in triplicate and three independent assays were performed. EC_{50} values were calculated using non-linear regression analysis of the mean dose-response curve data in GraphPad PRISM® v8.

2.5.8 *In vivo* testing of the anti-*Cryptosporidium* efficacy of CpPyK-inhibitors.

Eight weeks old male IFN-γ KO mice (B6.129S7-*Ifng*^{tm1Ts}/J) were purchased from The Jackson Laboratory, USA, and allowed to quarantine and acclimatize for 1 week before the commencement of experiments. Before the start of the infection assays in mice, the tolerability of each inhibitor was determined by daily oral gavage with varying dosages (0 to 10 mg/kg mouse bodyweight) in groups of mice (n = 3 mice per group) for 8 days. During this period, mice

were monitored daily for any changes in physical and mental activity, feeding, body weight, body temperature, fur condition, and body posture. The highest dose of each inhibitor that did not produce any signs of toxicity during the 8-day monitoring period was used as the maximum dose limit for subsequent *in vivo* infection studies. Mice were divided into infected and uninfected groups (n = 3 mice per group) and each individual mouse was housed in a separate cage lined with sterile gauze bedding. Each mouse from the infected group was infected by oral gavage administration of 10^4 *C. parvum* AUCP-1 isolate oocysts suspended in 50 µl of PBS. Beginning day 3 PI, groups of mice were orally treated with CpPyK-inhibitors (at the specified doses), sham (100 µl of 5% DMSO in PBS), or 1000 mg/kg paromomycin (in sterile water) once daily for a total of 8 days. Fecal pellets were collected daily in individual sterile 15 ml tubes and submerged in an equivalent volume of PBS containing a cocktail of penicillin (100 units/ml), streptomycin (100 µg/ml), chloramphenicol (34 µg/ml), and amphotericin (0.25 µg/ml), and stored at 4°C until use. Three independent replicate infection assays were performed. Mice were sacrificed at day 11 PI, and 5 cm of the distal small intestine just anterior to the cecum was resected and submerged in 10% neutral buffered formalin and submitted for histopathological processing in the Comparative Biosciences Histology Laboratory at the University of Illinois at Urbana-Champaign. Briefly, intestinal tissues preserved in 10% neutral buffered formalin were washed in 70% ethanol, embedded in paraffin, and sectioned transversely at a thickness of 5 µm. Sections were stained with hematoxylin and eosin. The slides were imaged using a Zeiss microscope fitted with a color camera.

2.5.9 Quantitative analysis of *C. parvum* oocysts load in mice feces.

DNA was isolated from 250 mg of feces collected from individual mice using the QIAamp® PowerFecal® Pro DNA kit (Qiagen, USA) following the manufacturer's protocol.

Oocysts load per gram of feces was measured by quantitative real time PCR (qPCR) analysis of the Cp18s rRNA gene (GenBank accession number AF164102) using gene-specific primers: 5'-CTGCGAATGGCTCATTATAACA-3' (Forward) and 5'-AGGCCAATACCCTACCGTCT-3' (Reverse), described previously (Parr et al., 2007). To generate a quantification standard curve, fecal samples were obtained from uninfected mice and spiked with 10^8 *C. parvum* oocysts per gram of feces, followed by isolation of DNA as described above. Ten-fold serial dilutions of the extracted DNA were made and used as quantification standards for qPCR. *C. parvum* oocysts load quantification for the test mice was performed using DNA samples from the infected feces. Each 20 µl qPCR reaction contained 10 µl of PowerUp™ SYBR™ Green Master Mix (Applied Biosystems, USA), 500 nM of each primer, and 2 µl of DNA template. After 2 minutes of initial denaturation at 95°C, 40 cycles of denaturation at 95°C for 15 seconds and annealing/extension at 60°C for 1 minute were performed in a 7500 Real-Time PCR System (Applied Biosystems, USA). The oocyst load per gram of feces was derived by the 7500-system software using the generated quantification standard curves (Figure 2.12).

2.5.10 Statistical Analysis.

Statistical analyses were done by two-way analysis of variance (ANOVA) with the Tukey's multiple comparison post-hoc test using GraphPad PRISM® v8. *P* values of 0.05 or less were considered significant.

2.5.11 Ethics.

Animal study protocols were approved by the University of Illinois Institutional Animal Care and Use Committee under protocol numbers 21091 and 20036 for the use of Holstein calves and mice respectively. All experiments involving the use of animals were carried out in strict compliance with the recommendations and guidelines in the United States Department of

Agriculture Animal Welfare Act and the National Institute of Health Public Health Service Policy on the Humane Care and Use of Animals. All efforts were made to minimize the pain and suffering of animals.

2.6 FIGURES AND TABLES

A

```
CLUSTAL 2.1 Multiple Sequence Alignment
Sequences (1:2) Aligned. Score: 37.2624

CpPyK          MISNDHLKR------LASTSAVMSCTLGKATCLGMDKICS-PLADNDVTQRKTQIICTIG  53
Human_PyK      -MSKPHSEAGTAFIQTQQLHAAMADT-------FLEHMCRLDIDSPPITARNTGIICTIG  52
                :*: * :         .  *.*: *         ::::*   : .  :* *:* ******
CpPyK          PSCNNVESLIGLIDKGMSVARLNFSHGDHESHFKTLQNIREAAKARP-----HSTVGIML  108
Human_PyK      PASRSVETLKEMIKSGMNVARLNFSHGTHEYHAETIKNVRTATESFASDPILYRPVAVAL  112
               *:...**:*  :*..**.********* ** * :*::*:* *:::       :  *.: *
CpPyK          DTKGPEIRTGMLEGGK--PIELKAGQTLKITTDYSMLG--NSECISCSYSLLPKSVQIGS  164
Human_PyK      DTKGPEIRTGLIKGSGTAEVELKKGATLKITLDNAYMEKCDENILWLDYKNICKVVEVGS  172
               **********:::*.    :*** * ***** * : :   :.: :  .*. : * *::**
CpPyK          TVLIADGSLSTQVLEIGDDFIVCKVLNSVTIGERKNMNLPGCKVHLPIIGDKDRHDIVDF  224
Human_PyK      KIYVDDGLISLQVKQKGADFLVTEVENGGSLGSKKGVNLPGAAVDLPAVSEKDIQDL-KF  231
               .: : ** :* ** : * **:* :* *. ::*.:*.:****. *.** :.:** :*: .*
CpPyK          ALKYNLDFIALSFVQNGADVQLCRQIISENTQYSNGIPSSIKIISKIENLEGVINFDSIC  284
Human_PyK      GVEQDVDMVFASFIRKASDVHEVRKVLGEK-------GKNIKIISKIENHEGVRRFDEIL  284
               .:: ::*::  **:::.:**:  *:::.*:         ..********* *** .**.*
CpPyK          SESDGIMVARGDLGMEIPPEKIFVAQKCMISKCNVAGKPVVTATQMLESMIKSNRPTRAE  344
Human_PyK      EASDGIMVARGDLGIEIPAEKVFLAQKMMIGRCNRAGKPVICATQMLESMIKKPPPTRAE  344
               . ************:*** **:*:*** **.:** *****: **********.  *****
CpPyK          MTDVANAVLDGSDCVMLSGETANGAFPFDAVNVMSRVCAQAETCIDYPVLYHAIHSSVPK  404
Human_PyK      GSDVANAVLDGADCIMLSGETAKGDYPLEAVRMQHLIAREAEAAIYHLQLFEELRRLAPI  404
                :*********:**:*******:* :*::**.:   :. :**:.* :  *:. ::  .*
CpPyK          PVAVPEAIACSAVESAHDVNAKLIITITETGNTARLISKYRPSQTIIACTAKPEVARGLK  464
Human_PyK      TSDPTEATAVGAVEASFKCCSGAIIVLTKSGRSAHQVARYRPRAPIIAVTRNPQTARQAH  464
                    ** * .***::..  :  **.:*::*.:*: :::***   *** * :*:.**  :
CpPyK          IARGVKTYVLNSIHH------SEVVISNALALAKEESLIESGDFAIAVHGVKESCPGSCN  518
Human_PyK      LYRGIFPVLCKDPVQEAWAEDVDLRVNFAMNVGKARGFFKKGDVVIVLTGWRPG-SGFTN  523
               : **:   : :.  :       :: :. *: :.* ..::::.**..*.: * : .  *  *
CpPyK          LMKIVRCP   526
Human_PyK      TMRVVPVP   531
                *::*  *
```

B

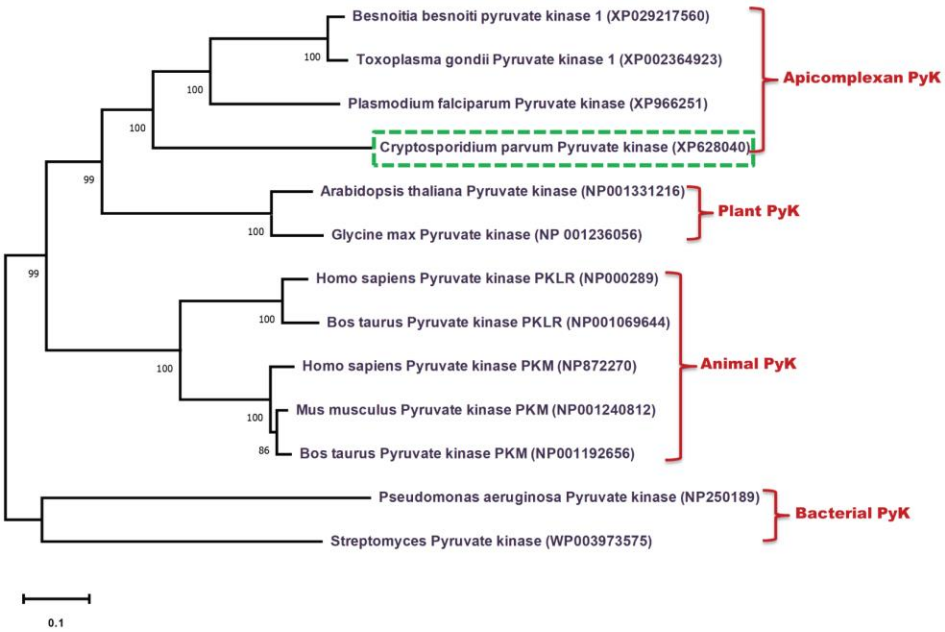

Figure 2.1: Comparison of CpPyK protein with other pyruvate kinases. (A) Primary amino acid sequence alignment between CpPyK and human PyK using the Clustal W program.

Figure 2.1 (cont.)

(B) Phylogenetic analysis of CpPyK with other apicomplexan, plant, animal, and bacterial pyruvate kinases. All sequences were aligned with Clustal W, and the evolutionary tree was built in MEGA 11 using the neighbor-joining method. Bootstrap analyses of 1000 replicates were conducted, and values above 50% are shown on the branches. Accession numbers of amino acid sequences retrieved from the NCBI database are indicated in parentheses against each pyruvate kinase.

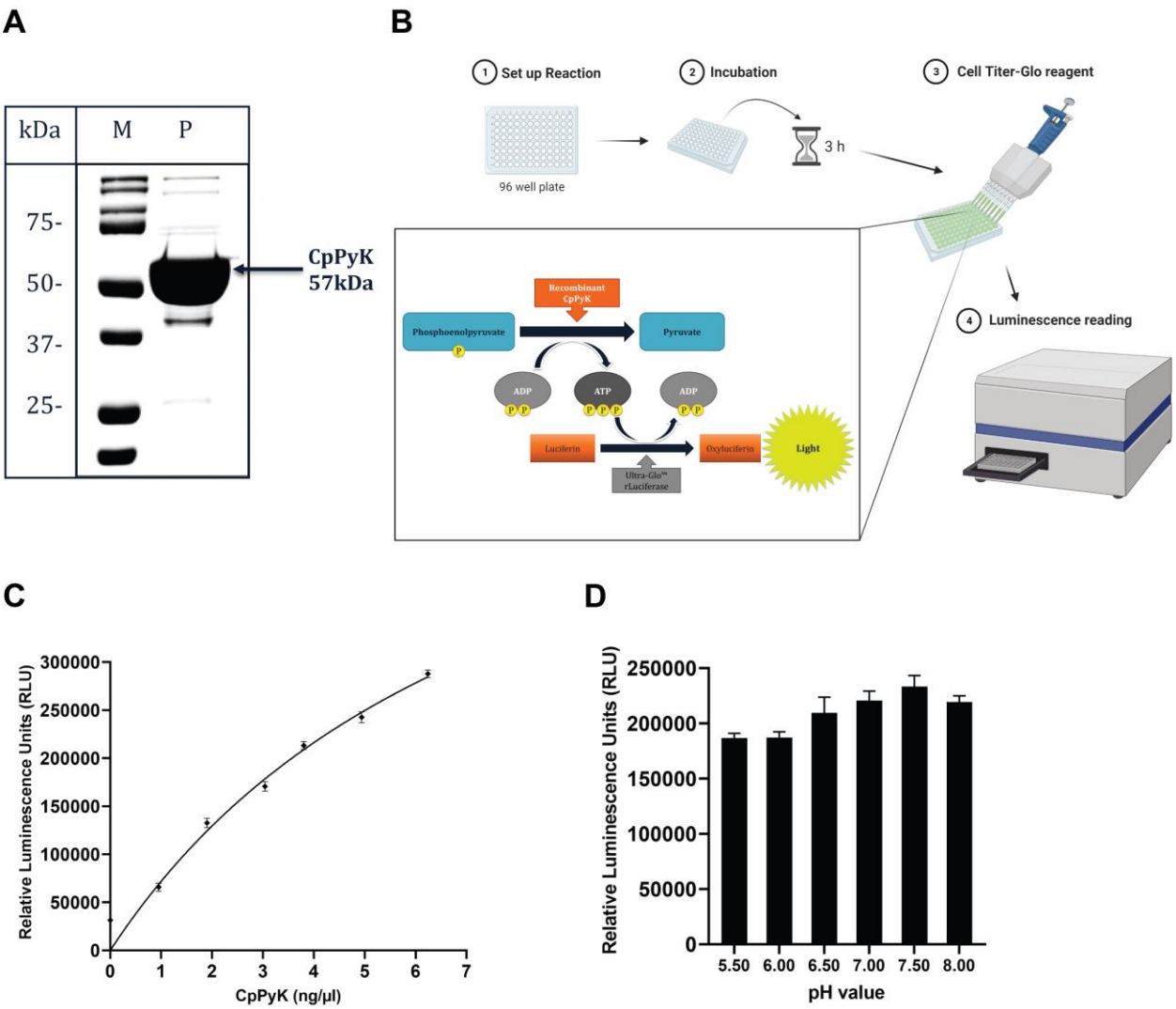

Figure 2.2: Analysis of the enzymatic activity of rCpPyK protein. (A) Illustration of the *in vitro* assay for the dephosphorylation of phosphoenolpyruvate to pyruvate using rCpPyK protein as the catalytic enzyme. The reaction is coupled to a luciferase assay involving the utilization of the generated ATP to phosphorylate luciferin to oxyluciferin whose luminescence is detected by a plate reader. (B) SDS-PAGE analysis of the nickel affinity column chromatography purified rCpPyK protein stained with Coomassie blue (Lane M: protein ladder; Lane P: CpPyK protein with the expected band size indicated at about 57 kDa). Effect of (C) increasing concentrations and (D) pH on the enzymatic activity of the recombinant CpPyK protein. The data shown represent the mean of three independent experiments with standard deviation (SD) error bars. Abbreviations: ADP, Adenosine diphosphate; ATP, Adenosine triphosphate; CpPyK, *C. parvum* pyruvate kinase. Created with BioRender.com.

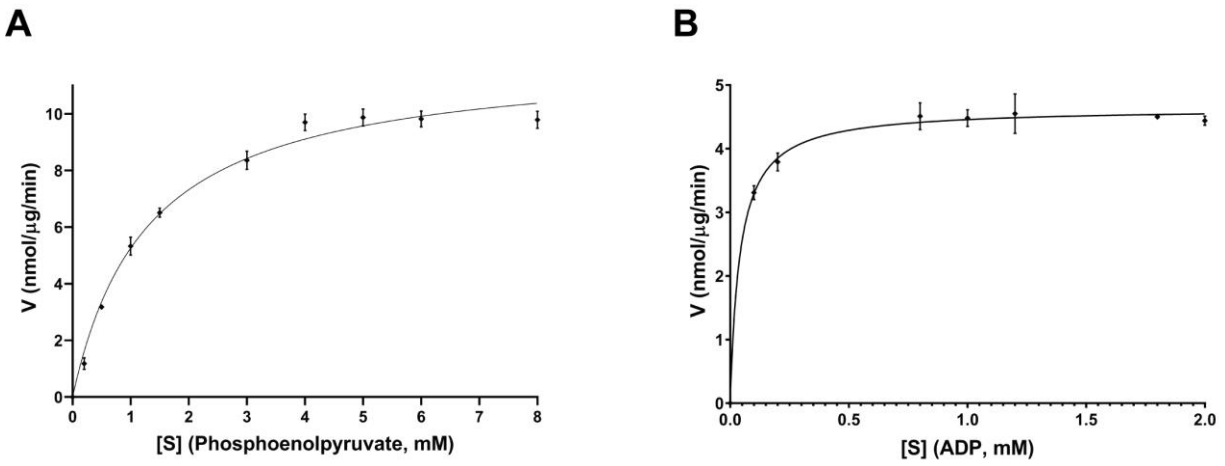

Figure 2.3: Enzyme kinetics of CpPyK. Michaelis-Menten kinetics of rCpPyK on the substrate (A) phosphoenolpyruvate and on the co-substrate (B) ADP, respectively. The data shown represent the mean of three independent experiments with standard deviation (SD) error bars. Abbreviations: ADP, Adenosine diphosphate; V, the velocity of the reaction.

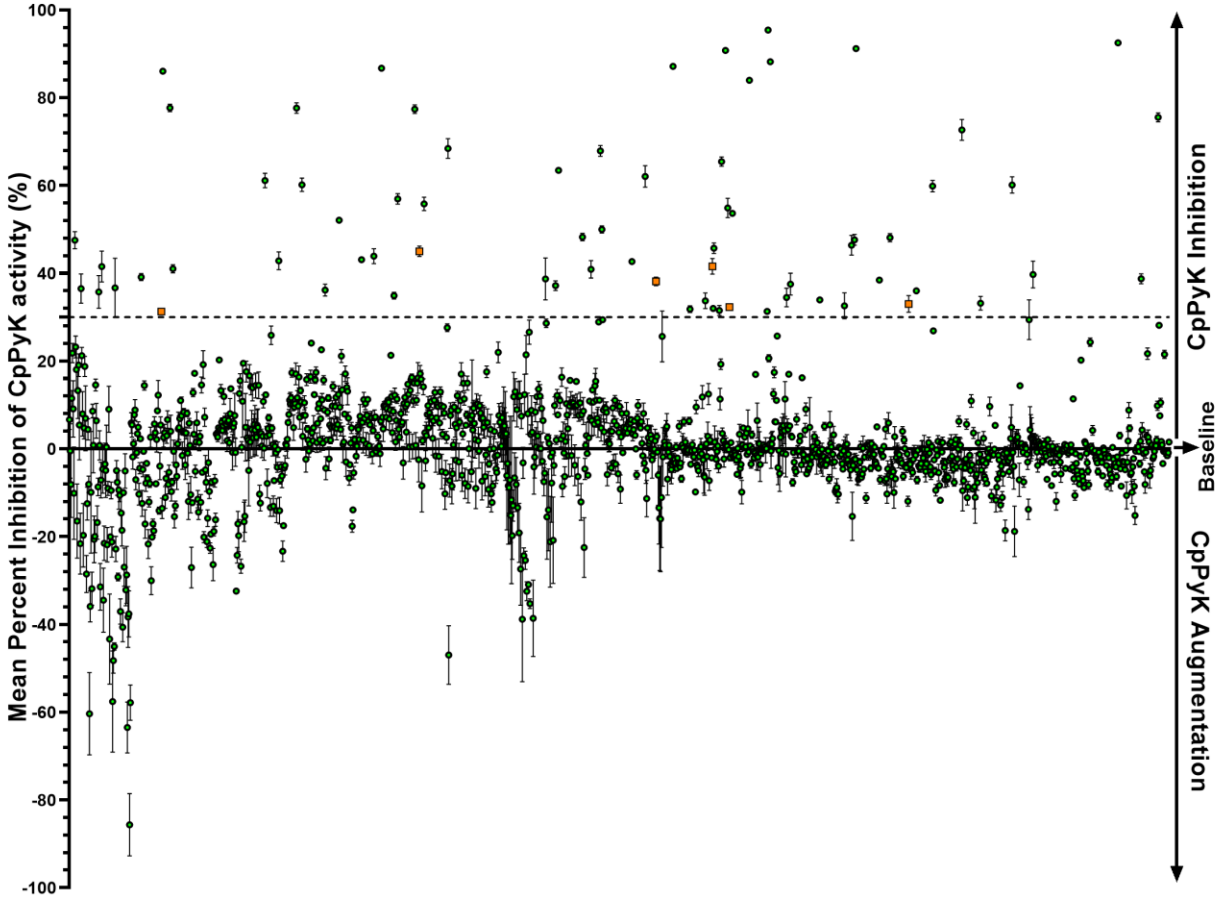

Figure 2.4: Effect of compounds from the NCI Diversity Set VI chemical library on the catalytic activity of rCpPyK protein. Individually reconstituted compounds were used at a final concentration of 50 μM in the CpPyK catalyzed reaction for the transfer of a phosphate group from phosphoenolpyruvate to ADP, yielding pyruvate and ATP. The mean percent inhibition of rCpPyK activity by each compound was derived by dividing the difference in luminescence between the compound-treated wells and the DMSO-treated wells by the luminescence of the DMSO-treated wells and multiplying the product by 100. The baseline mean percent inhibition of 0 was for the reaction without compound, but with an equivalent volume of DMSO used to reconstitute the compounds. Compounds with mean percent inhibition values greater than 0 were designated as inhibitors of the activity of rCpPyK, while those with mean percent inhibition values less than 0 were classified as augmenters. The orange squares indicate the 6 top hits found to have significant inhibitory effect on the *in vitro* growth of *C. parvum* as shown in Figure 2.6B. Each reaction was performed in triplicate, and the data shown represent the mean of three independent experiments. Bars represent standard errors of the mean (SEM).

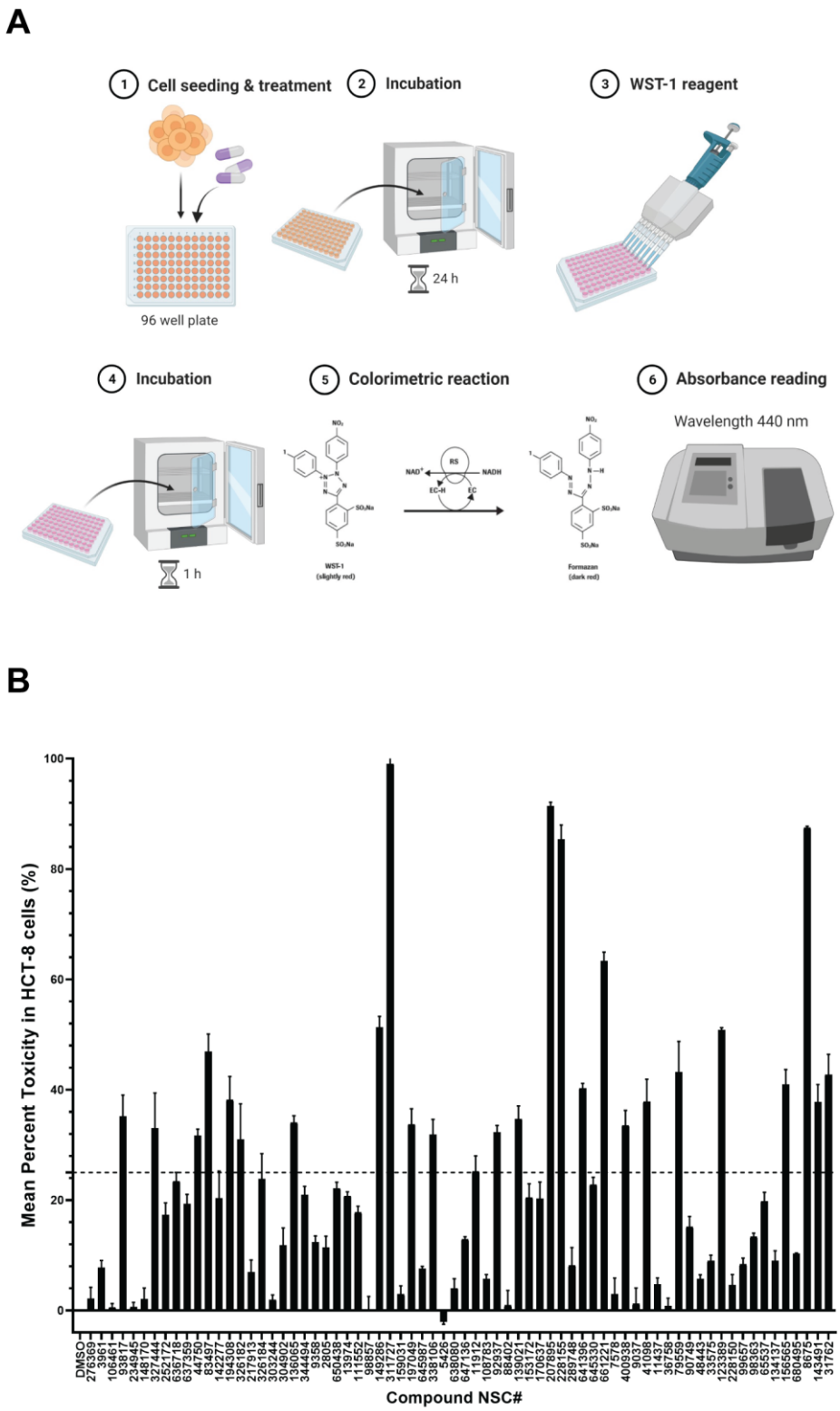

Figure 2.5: Mean percent toxicity (MPT) values of test compounds in HCT-8 cells. (A) Individually reconstituted compounds were incubated with uninfected HCT-8 cells for 24 hours at a final concentration of 50 μM. Control wells without chemical compound, but in which

Figure 2.5 (cont.)

equivalent volumes of DMSO (chemical compound solvent) were added were also set up. Following 24 hours of culture, a colorimetric assay using the cell proliferation reagent WST-1 was used for the quantification of cell viability. (B) The mean percent toxicity value of each compound was derived by dividing the difference in absorbance between the compound-treated cells and the DMSO-treated cells by the absorbance from the DMSO- treated cells and multiplying the product by 100. The baseline mean percent toxicity of 0 was for the reaction without compound, but with an equivalent volume of DMSO used to reconstitute the compounds. Each reaction was performed in triplicate, and the data shown represent the mean of three independent experiments. Bars represent standard errors of the mean (SEM). Created with BioRender.com.

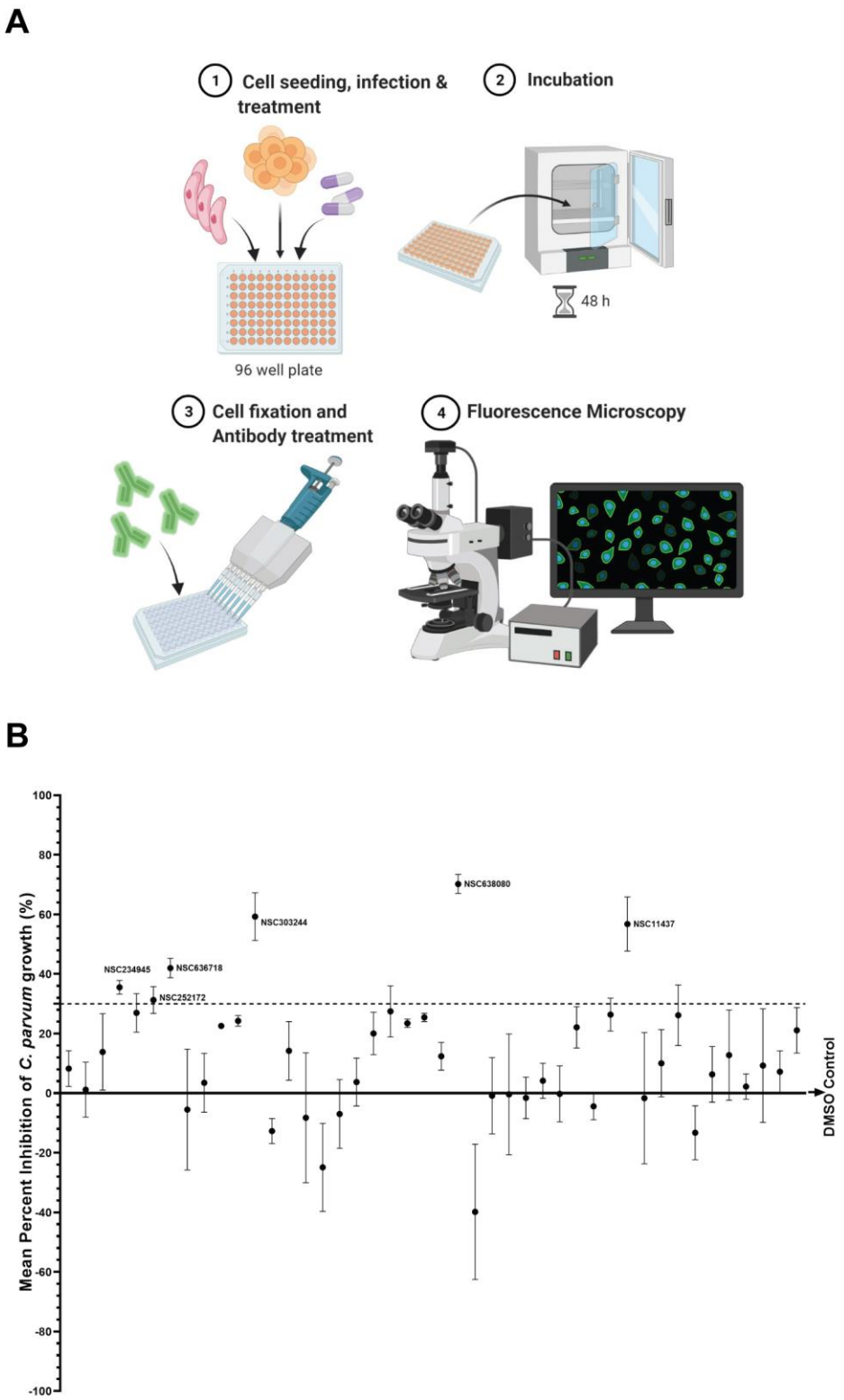

Figure 2.6: Analysis of the effect of rCpPyK-inhibitors on the *in vitro* growth of *C. parvum* in HCT-8 cells. (A) Equal amounts of freshly excysted sporozoites of *C. parvum* were inoculated into HCT-8 cells in culture and compounds at 25 µM concentration were added immediately

Figure 2.6 (cont.)

after infection. Control infected cells were treated with volumes of DMSO equivalent to those used in the compound-treated cultures. Paromomycin reconstituted in distilled sterile water was added to a separate set of wells as a positive control at 200 μM final concentration. The cultures were analyzed for parasite infectivity and proliferation by an immunofluorescence assay after 48 hours of incubation. (B) The fluorescence generated by intracellular *C. parvum* parasites was quantified and used to calculate the mean percent parasite inhibition values for each compound. The data shown represent the mean of three independent experiments. Bars represent standard errors of the mean (SEM). Created with BioRender.com.

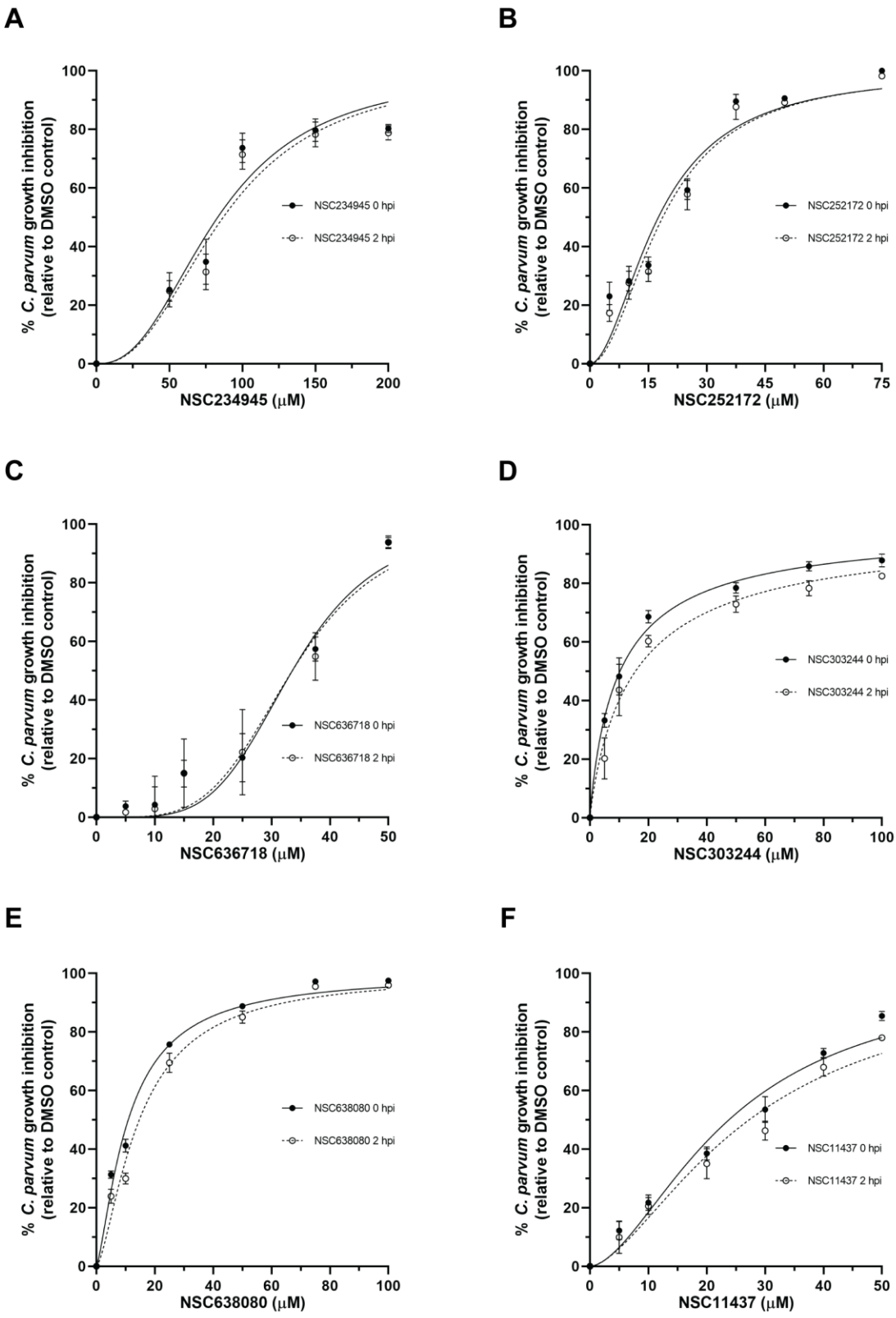

Figure 2.7: Effect of varying concentrations of rCpPyK-inhibitors on the growth of *C. parvum* in HCT-8 cells. Equal amounts of freshly excysted sporozoites of *C. parvum* were inoculated into

Figure 2.7 (cont.)

HCT-8 cells in culture and varying concentrations of (A) NSC234945, (B) NSC252172, (C) NSC636718, (D) NSC303244, (E) NSC638080, and (F) NSC11437 were added at the time of infection (solid line) or added 2 hours post-infection (PI) (dashed line). Control infected cells were treated immediately PI with volumes of DMSO equivalent to those used in the compound-treated cultures. After 48 hours, the cultures were analyzed for parasite proliferation by immunofluorescence assays. The fluorescence generated by intracellular *C. parvum* merozoites was quantified and used to calculate the mean percent parasite inhibition values of each compound concentration relative to the DMSO-treated controls. The data shown represent the mean of three independent experiments. Bars represent standard errors of the mean (SEM).

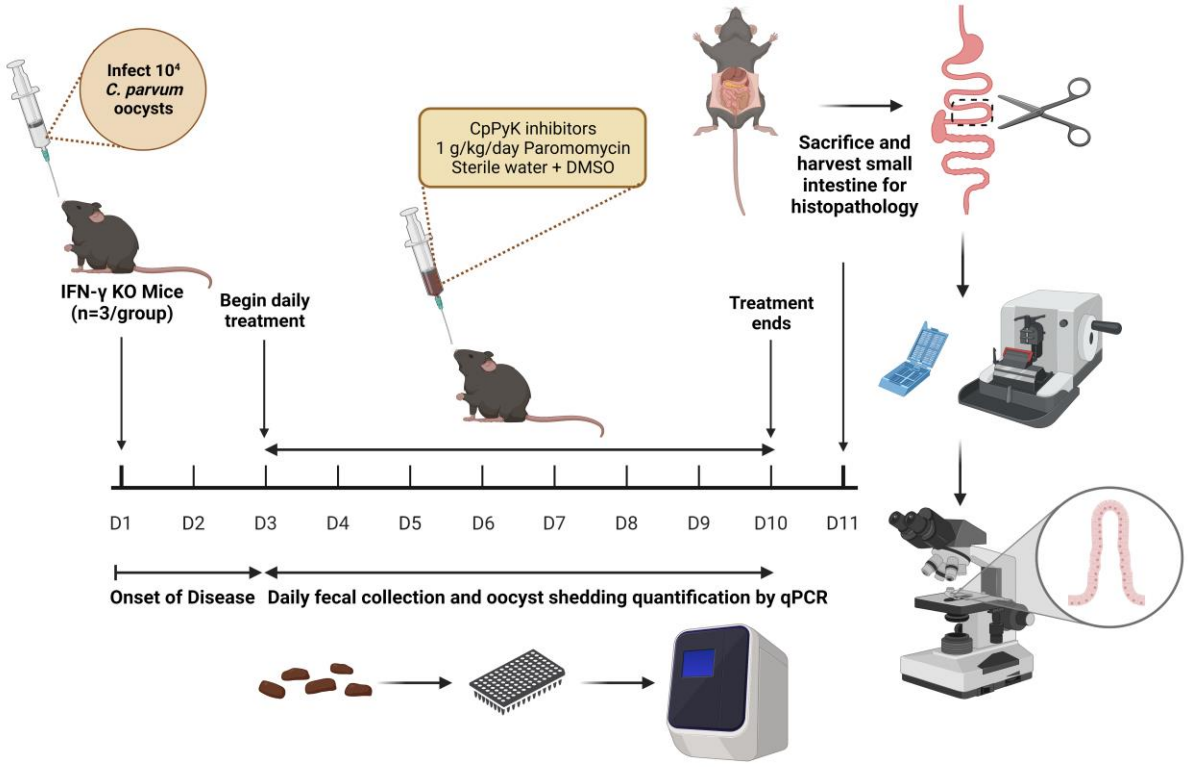

Figure 2.8: Immunocompromised mouse model of acute cryptosporidiosis. Male IFN-γ KO mice (3 animals per group) were infected by oral administration of 10^4 *C. parvum* oocysts. On days 3 to 10 post-infection, mice were treated with CpPyK-inhibitors, paromomycin, or the compound vehicle. Fecal parasite shedding was monitored by qPCR analysis during the entire treatment period. Mice were sacrificed at day 11 post-infection for histopathological analysis of lesions of cryptosporidiosis in harvested intestinal samples. Created with BioRender.com.

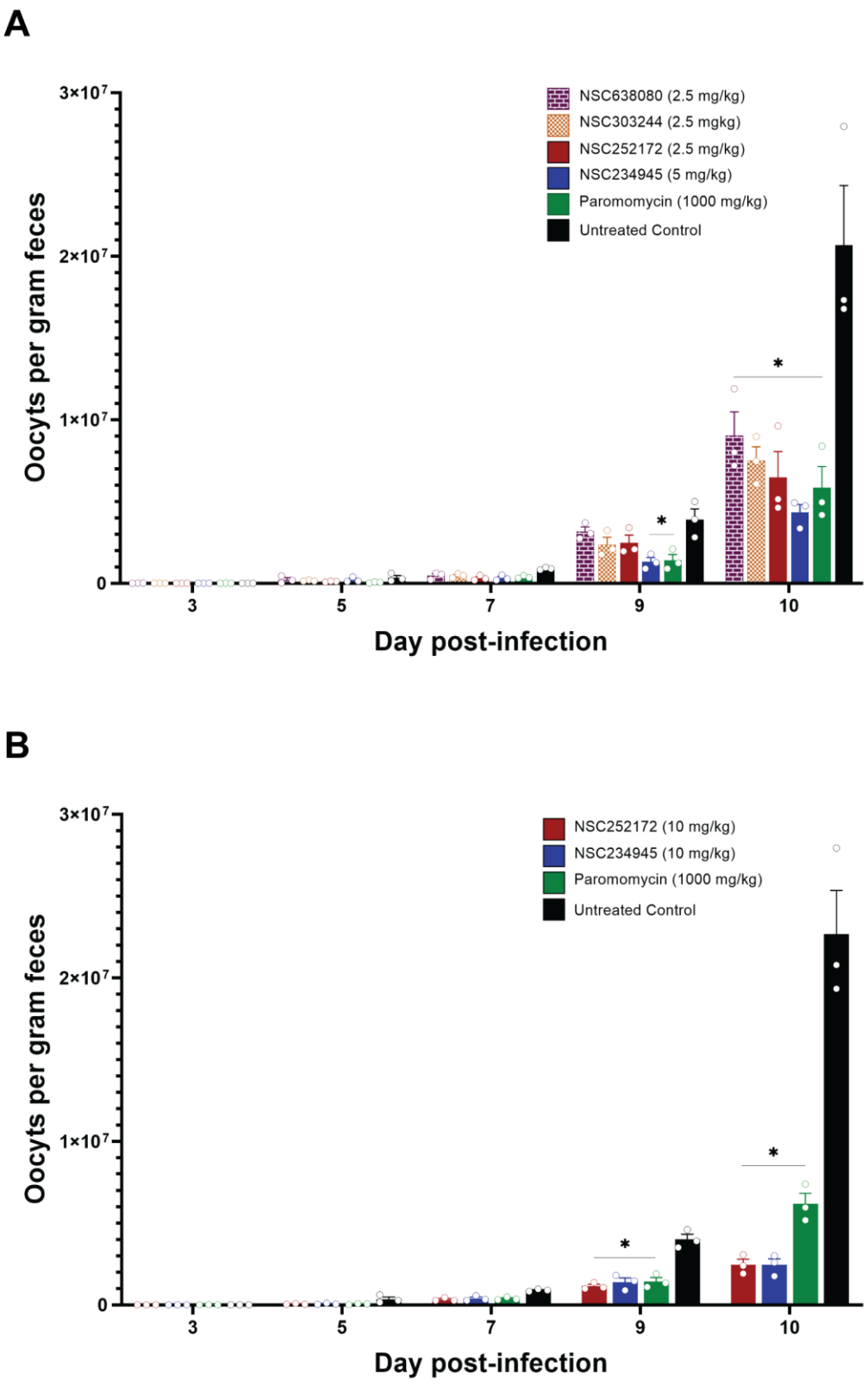

Figure 2.9: Real-time PCR quantification of the load of *C. parvum* oocysts in fecal samples of infected mice treated with or without rCpPyK-inhibitors. Infected IFN-γ KO mice were treated

Figure 2.9 (cont.)

with (A) 2.5 mg/kg NSC638080, 2.5 mg/kg NSC303244, 2.5 mg/kg NSC252172 or 5 mg/kg NSC234945, and (B) 10 mg/kg NSC252172 or 10 mg/kg NSC234945. In both experiments (A and B) paromomycin at 1000 mg/kg was used as positive control treatment, while the untreated control group of mice was administered an equivalent volume of the solvent used to reconstitute the test compounds (5% DMSO in water). Oocyst shedding per gram of feces was measured by qPCR of the *C. parvum* 18S rRNA gene, and the equivalent oocysts per gram feces were derived using a standard curve. The data shown represent the means for fecal oocysts load from 3 mice per group. Bars represent standard errors of the mean (SEM) with level of statistical significance as compared to the untreated control mice indicated by asterisk (*, $P < 0.05$).

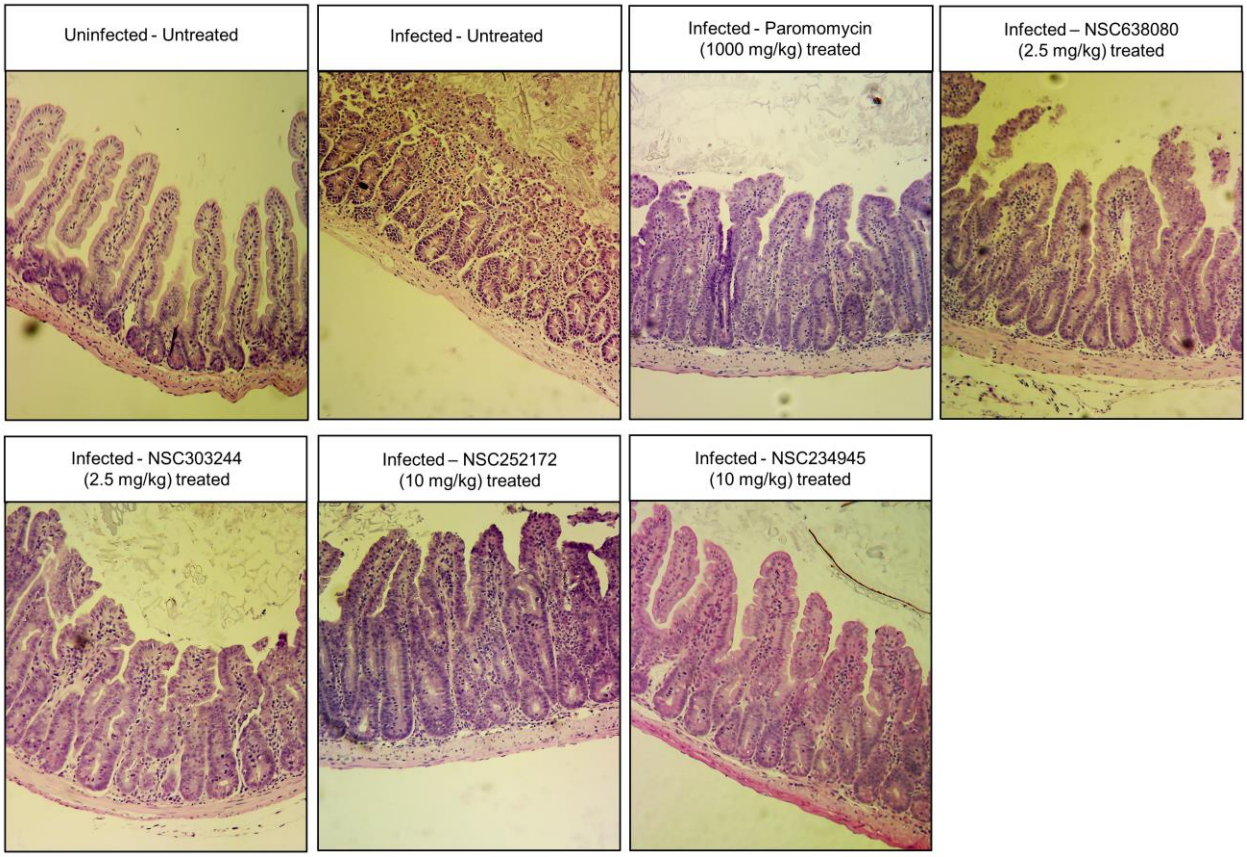

Figure 2.10: Histological analysis of the distal small intestines of mice infected with *Cryptosporidium parvum* with or without treatment. Male IFN-γ KO mice (n = 3 per group) were infected with 10^4 *C. parvum* oocysts, and from the third day post-infection, daily oral treatment was commenced with NSC638080 (2.5 mg/kg), NSC303244 (2.5 mg/kg), NSC252172 (10 mg/kg), NSC234945 (10 mg/kg), or paromomycin (1000 mg/kg). The untreated-uninfected control group of mice was administered an equivalent volume of the solvent used to reconstitute the test compounds (5% DMSO in water). After day 11 post-infection, mice were sacrificed, and the distal small intestinal tissue processed for histology and stained with hematoxylin and eosin. The uninfected-untreated control mice's samples depicted intact intestinal epithelium with prominent villi. The infected–untreated mice depicted denuded villi, infiltration of inflammatory cells and hypertrophy of crypts. In contrast, samples from infected mice treated with the test compounds or paromomycin had notably reduced pathological changes (intact intestinal epithelium with prominent villi), especially treatment with compounds NSC252172 and NSC234945. The images are representative of samples analyzed from 3 mice per treatment group.

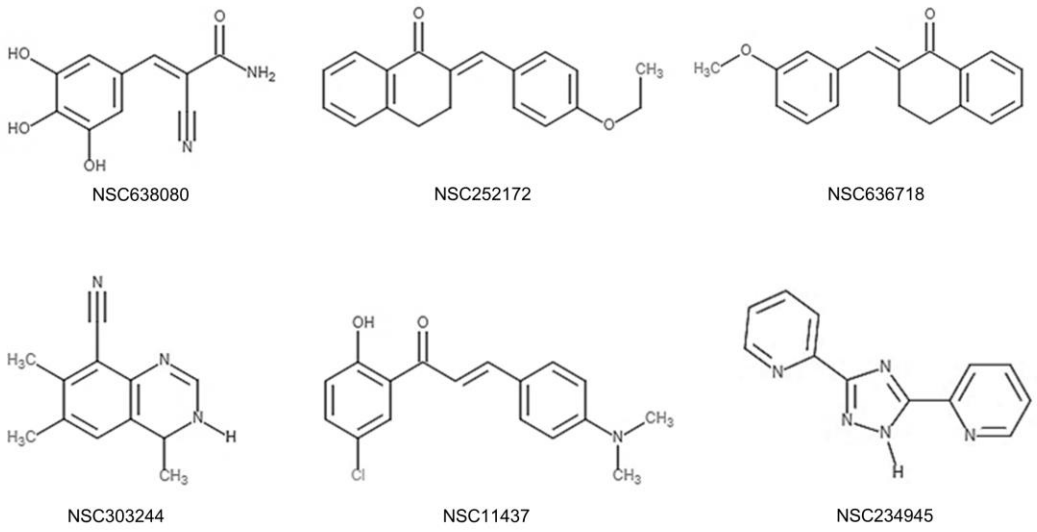

Figure 2.11: Chemical structures of the inhibitors for CpPyK enzyme that have anti-cryptosporidial efficacy.

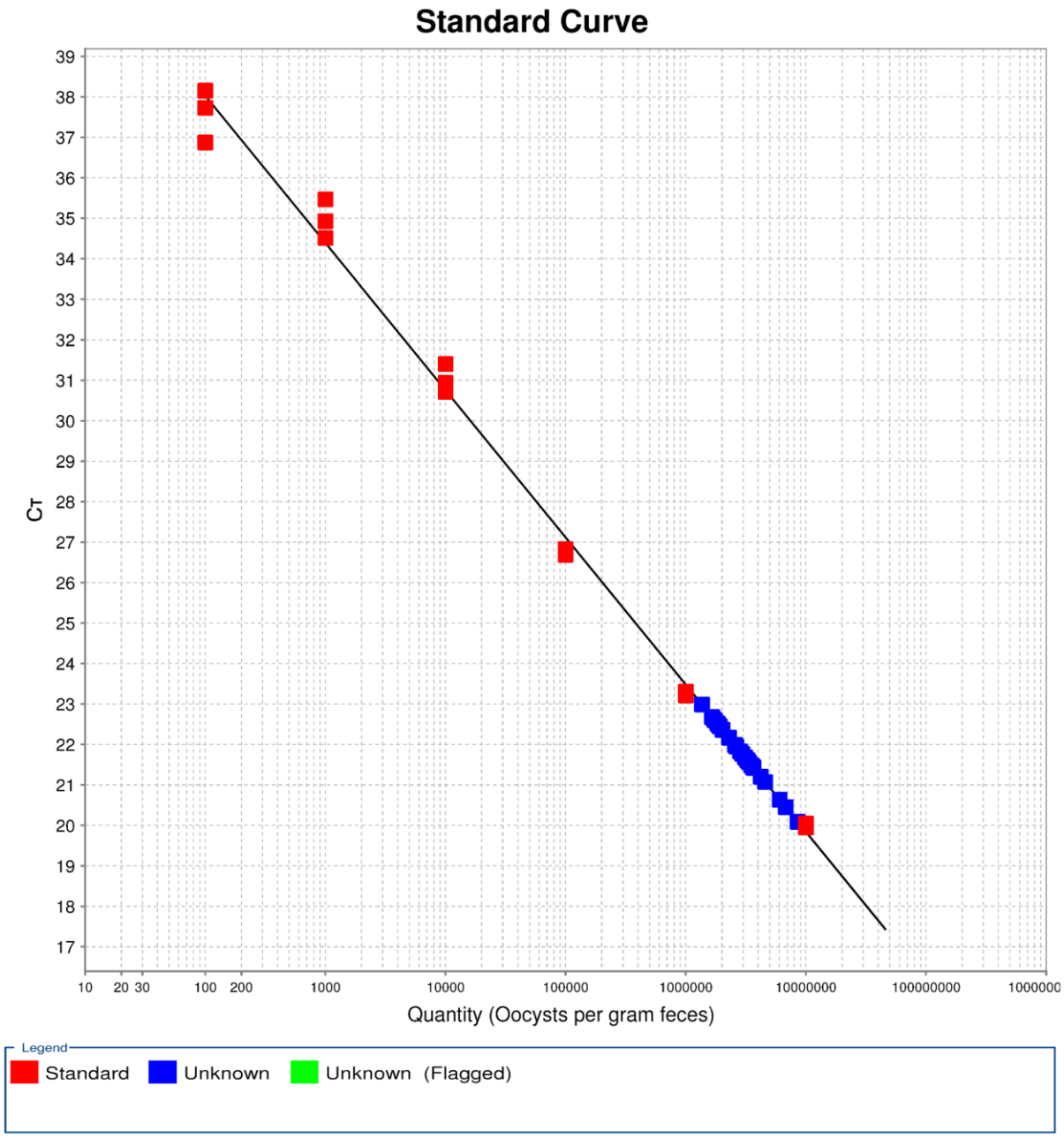

Figure 2.12: A representative standard curve generated by the 7500-system software for quantification of *C. parvum* oocyst load from fecal samples.

Table 2.1: rCpPyK enzyme kinetic parameters on substrates.

Parameter	Phosphoenolpyruvate	ADP
V_{max} (nmol/µg/min)	12.05 (6.82[a])	4.64
K_m (mM)	1.29 (0.32[a])	0.04

[a]Reported by (Denton et al., 1996)

Table 2.2: Enzyme inhibition, cytotoxicity, *in vitro* efficacy, and selective index values of selected compounds.

Compound	**Enzyme inhibition IC_{50} (µM)**	**HCT-8 CC_{50} (µM)**	**Anti-*C. parvum* EC_{50} (µM)**		**Selectivity Index (CC_{50}/EC_{50})**
			0 h PI	**2 h PI**	
NSC234945	234.9	432.1	86.01	89.58	5.02
NSC252172	123.3	266.5	17.61	18.73	15.10
NSC636718	116.7	106.5	33.78	33.56	3.15
NSC303244	242.5	660.2	10.29	15.79	64.15
NSC638080	97.14	749.6	10.87	14.68	68.96
NSC11437	156.1	612.5	23.80	27.27	25.73

Table 2.3: Physicochemical properties of identified CpPyK-inhibitors (adapted from: *https://pubchem.ncbi.nlm.nih.gov*).

NSC number	IUPAC name	Molecular formula	Molecular weight	cLog(*p*)	Number of Hydrogen bond donors	Number of Hydrogen bond acceptors	Number of rotatable bonds	Polar surface area (Å²)
234945	2-(3-pyridin-2-yl-1*H*-1,2,4-triazol-5-yl)pyridine	$C_{12}H_9N_5$	223.23	1.2	1	4	2	67.4
252172	(2*E*)-2-[(4-ethoxyphenyl)methylidene]-3,4-dihydronaphthalen-1-one	$C_{19}H_{18}O_2$	278.3	4.4	0	2	3	26.3
636718	(2*E*)-2-[(3-methoxyphenyl)methylidene]-3,4-dihydronaphthalen-1-one	$C_{18}H_{16}O_2$	264.3	4.1	0	2	2	26.3
303244	4,6,7-trimethyl-1,4-dihydroquinazoline-8-carbonitrile	$C_{12}H_{13}N_3$	199.25	1.6	1	2	0	48.2
638080	(*E*)-2-cyano-3-(3,4,5-trihydroxyphenyl)prop-2-enamide	$C_{10}H_8N_2O_4$	220.18	0.1	4	5	2	128
11437	(*E*)-1-(5-chloro-2-hydroxyphenyl)-3-[4-(dimethylamino)phenyl]prop-2-en-1-one	$C_{17}H_{16}ClNO_2$	301.8	4.6	1	3	4	40.5

Table 2.4: Diversity Set VI chemical compounds.

NSC Number	Molecular Weight	Molecular Formula	Mean CpPyK Inhibition (%)	SEM (%)
479	267	C15H13N3O2	0.6	2.8
1014	341	C22H19N3O	20.6	0.8
1451	239.28	C13H13N5	5.5	2.8
1614	446.63	C27H42O5	-0.5	0.3
1620	215.21	C10H9N5O	-4.4	1.3
1751	224	C8H16O7	-6.8	0.8
1847	262	C12H10N2O3S	17.1	1.9
2561	240	C12H16O5	3.6	1.4
2805	246.26	C14H14O4	86.0	0.4
3001	214	C11H18O4	4.0	3.7
3064	328	C16H16N4O4	-0.4	6.1
3076	265.32	C15H15N5	9.8	2.1
3193	270	C12H18N2O3S	-1.6	3.8
3247	275	C8H10AsNO5	7.2	1.8
3323	375	C23H25N3O2	-4.2	2.0
3391	554	C23H26N2O4.C7H13NO3	-4.7	0.6
3753	304.36	C15H16N2O3S	-2.6	1.1
3961	228	C11H8N4S	31.3	0.7
4263	225	C12H7N3O2	4.5	3.8
4292	380.44	C19H12N2O3S2	0.8	1.0
4429	296.29	C12H12N10	8.8	1.3
4921	214	C10H6N4O2	3.6	1.4
5053	335	C19H15N4.Cl	0.2	0.3
5157	395.41	C22H21NO6	-1.7	1.4
5426	258.23	C14H10O5	57.0	1.2
5476	334	C18H26N2O2S	-3.5	0.7
5564	275	C16H21NO3	9.6	1.9
5836	362	C17H18N2O3S2	0.9	1.8
5856	448.56	C23H20N4O2S2	-0.9	1.0
5907	463	C22H18N2O2.2C2H4O2	0.5	0.9
5995	213	C12H11N3O	-1.8	2.8
6101	330	C20H26O4	-5.0	1.4
6137	263	C8H7BrO5	10.9	1.4
6145	286	C20H14O2	15.9	2.0
6268	318.33	C18H14N4O2	11.3	4.0
6731	254	C17H18O2	4.8	2.4
6821	289	C19H15NO2	7.1	0.4

Table 2.4 (cont.)

6844	292.29	C18H12O4	4.5	2.9
6866	232	C10H11Cl2NO	2.3	0.3
6910	250	C13H18N2O3	-21.6	3.3
7218	293	C17H15N3O2	21.3	0.7
7419	393	C13H15Cl5N2O	-11.1	1.7
7420	298	C13H16BrNO2	4.5	1.6
7436	304.41	C16H20N2O2S	1.1	2.3
7572	278	C13H14N2O3S	3.8	2.8
7578	343	C21H13NO4	45.7	1.2
7745	268	C13H16O6	15.0	0.6
7867	294	C12H9Cl2N5	14.7	0.7
7962	284	C18H20O3	-8.4	6.0
8090	247	C17H13NO	-7.9	0.6
8179	203	C9H9N5O	2.6	2.2
8481	208	C12H16O3	-9.7	2.2
8675	492	C31H42N3.Cl	92.5	0.1
8813	238	C10H14N4O3	4.8	2.8
8816	252	C11H16N4O3	0.8	2.9
9032	364	C25H20N2O	0.5	0.3
9037	336.3	C19H12O6	65.4	1.1
9064	204	C9H16O5	8.1	0.8
9341	237	C12H15NO4	1.2	1.0
9358	226	C13H14N4	39.1	0.8
9461	202	C6H4BrNO2	-12.1	1.2
9782	282	C19H22O2	8.2	3.0
9852	240	C14H12N2O2	-5.3	1.7
10091	240	C14H12N2O2	2.1	2.9
10173	278	C15H18O5	10.1	0.8
10211	287	C19H13NO2	9.8	0.9
10416	243	C18H13N	3.6	2.0
10428	204	C12H12O3	-7.6	0.8
10768	255	C12H17NO5	11.9	1.2
10865	260	C12H9AsO2	8.5	1.0
10995	241	C10H9BrO2	6.9	0.3
11023	268	C16H16N2O2	14.1	1.8
11149	235	C13H11ClO2	-1.0	4.7
11150	235	C13H11ClO2	7.7	1.4
11275	266	C12H18N4O3	10.8	1.3

Table 2.4 (cont.)

11276	266	C12H18N4O3	7.1	1.8
11296	286	C14H14N4O3	2.7	2.7
11307	314	C16H18N4O3	-7.7	0.8
11437	302	C17H16ClNO2	32.3	0.5
11624	277	C12H9ClN4S	5.9	1.6
11643	288	C14H14ClN5	-1.7	4.1
11664	295	C17H21N5	12.9	1.1
11667	474.16	C18H14Br2N6	-0.9	1.2
11668	385.25	C18H14Cl2N6	-11.0	5.9
11826	228	C10H8N6O	-12.4	3.0
11881	390	C23H23N3OS	-12.0	2.0
11891	225	C9H7NO2S2	-7.9	0.9
11912	274	C19H18N2	68.4	2.2
11991	226	C14H14N2O	8.7	0.4
12028	286	C17H22N2O2	-2.6	4.8
12262	314	C18H22N2O3	-5.8	0.5
12488	271	C15H11ClN2O	14.9	1.7
12544	320	C15H10ClNO3S	2.7	0.3
12628	321	C8H8AsNO8	-0.4	0.9
12633	275	C8H10AsNO5	-5.2	2.3
12644	289	C9H12AsNO5	-0.5	3.9
12646	267	C10H10AsNO3	17.5	1.3
12650	322	C12H11AsN2O4	-1.7	0.7
12666	364	C14H13AsN2O5	-2.7	0.8
12865	405	C20H24N2O2.BrH	-1.1	0.5
13051	407	C24H23ClN2O2	4.3	1.7
13151	259	C15H11ClO2	3.9	1.7
13156	314.36	C15H14N4O2S	-1.8	2.9
13176	318	C22H26N2	1.6	3.7
13248	290	C16H20ClN3	9.9	2.5
13294	430	C22H15Cl3N2O	-7.3	0.7
13345	254	C10H10N2O4S	-47.0	6.7
13434	269	C12H15NO6	4.8	5.0
13487	379	C27H26N2	-0.8	2.2
13579	268	C12H10ClNO2S	11.4	1.4
13616	327.47	C20H29N3O	3.5	1.3
13653	218	C12H10O4	-11.1	2.5
13658	264	C14H16O5	7.6	12.6

Table 2.4 (cont.)

13785	267	C10H10AsNO3	9.8	2.4
13791	447	C12H11As2NO8	0.6	0.4
13800	254	C10H10N2O4S	6.0	3.1
13974	247	C16H13N3	41.0	0.9
14142	327	C16H17N5O3	-2.0	0.7
14303	222	C10H14N4O2	-6.3	3.0
14304	222	C10H14N4O2	11.0	0.4
14311	263	C12H17N5O2	-8.8	5.8
14380	266	C12H18N4O3	-1.7	1.5
14396	284	C15H16N4O2	-5.2	3.9
14398	299	C15H17N5O2	-7.2	3.8
14506	332	C17H33O4P	0.1	1.6
14540	219	C8H14NO4P	-12.0	4.1
14974	396	C20H28O8	-1.5	0.6
15358	293	C12H11N3O4S	12.1	1.0
15359	264	C12H12N2O3S	-7.8	3.5
15362	227	C13H13N3O	8.9	2.4
15364	242	C13H14N4O	-4.7	1.7
15372	235	C16H13NO	2.6	2.3
15571	246	C7H7AsO5	12.2	3.4
15784	266	C17H12ClN	4.2	6.2
15910	451	C10H6Cl6O5S	1.0	0.1
16416	234	C14H18O3	-6.8	1.6
16437	368	C24H16O4	-7.0	1.8
16722	302	C16H14O6	0.5	0.8
16736	362.34	C18H18O8	-3.8	1.7
16813	216	C15H20O	-0.6	2.5
17055	280	C17H12O4	-3.4	6.0
17128	348	C21H29FO3	0.9	0.6
17129	242	C10H14N2O3S	7.6	4.3
17148	286	C6H8ClN3O4S2	8.2	1.2
17339	213	C14H15NO	-12.3	0.6
17355	357	C20H23NO5	0.8	1.5
17362	266	C17H14O3	-9.2	4.1
17507	253	C13H19NO4	-4.5	3.3
18883	349	C22H24N2S	-0.6	1.3
19061	385.25	C18H14Cl2N6	-8.7	1.2
19063	230	C6H6N4S3	5.8	1.1

Table 2.4 (cont.)

19096	222	C10H14N4O2	-7.0	2.3
19108	244	C11H8N4OS	-0.6	0.5
19115	217	C11H15N5	-30.0	3.2
19123	305	C12H9ClN6O2	-0.5	4.0
19125	276	C12H10ClN5O	3.3	1.1
19136	273.72	C13H12ClN5	7.6	3.0
19141	288	C14H14ClN5	8.7	3.5
19487	220	C10H12N4S	-14.1	0.8
19637	226	C13H10N2O2	3.0	1.7
19803	464.38	C21H20O12	-4.2	1.1
19824	275.35	C19H17NO	5.4	0.5
19962	274	C17H22O3	9.2	1.8
19970	499	C27H34N2O7	-1.5	0.5
19990	770	C40H51NO14	4.7	0.8
20045	205	C13H19NO	-15.4	2.6
20192	386	C21H39NO5	-6.3	5.2
20618	258	C13H14N4S	13.0	3.0
20619	258	C13H14N4S	-3.2	3.6
21034	237	C10H7NO6	-1.5	3.1
21333	260	C15H20N2O2	6.9	3.7
21603	290	C20H34O	-3.4	0.7
21678	232	C10H12N6O	0.7	2.2
21683	292	C16H16N6	-5.4	1.8
21709	279	C12H17N5O3	9.6	0.4
21710	277	C13H19N5O2	8.8	0.9
21725	244	C15H20N2O	3.7	4.6
21970	268	C21H16	8.9	3.9
22070	306	C17H22O5	11.0	0.1
22801	280	C17H16N2O2	-3.0	4.2
22806	262	C15H22N2O2	7.8	0.9
22881	266	C18H18O2	5.7	2.2
22939	224	C12H20N2O2	-0.9	1.2
23123	240	C14H12N2O2	14.5	1.1
23247	237	C13H11N5	-20.1	0.4
23248	227	C13H13N3O	-4.0	3.1
23672	222	C10H8ClN3O	6.7	2.0
23715	265	C12H19N5O2	3.2	2.2
23895	221	C12H15NO3	-13.0	1.1

Table 2.4 (cont.)

23906	201	C8H13ClN4	3.9	0.8
24032	310	C22H18N2	2.9	3.3
24035	227	C13H13N3O	-10.4	4.1
24113	369	C21H21ClN2S	2.4	1.6
24951	350	C21H22N2O3	0.1	1.8
25368	216	C11H20O4	3.5	1.6
25435	310.29	C18H15O3P	1.8	1.2
25457	348.4	C24H16N2O	1.4	0.5
25673	347	C17H12Cl2N2O2	-3.5	0.2
25678	277.32	C18H15NO2	-7.4	4.3
25740	298.32	C11H14N4O4S	-0.1	2.8
26112	306	C13H8Cl4	4.1	3.0
26113	318	C14H8Cl4	2.9	0.3
26349	302	C18H22O4	-1.7	1.9
26692	296.33	C17H16N2O3	-1.5	2.9
26744	238	C15H10O3	-17.1	3.3
26980	334.33	C15H18N4O5	3.6	1.1
27032	223	C15H13NO	-17.1	1.1
27305	324	C13H16N4O4S	1.0	1.0
27628	208	C9H12N4S	5.4	1.9
28080	312	C19H20O4	0.5	1.9
28341	210	C12H10N4	-8.1	2.1
28377	269	C10H15N5O2S	8.2	1.4
29073	276	C16H24N2O2	-8.5	4.0
29200	357	C17H13F2N5O2	-10.7	1.5
29471	213	C10H13ClN2O	-3.6	3.5
29620	212	C11H20N2O2	8.4	0.8
30205	314.39	C21H18N2O	12.5	2.4
30260	349.42	C15H15N3O3S2	-2.4	2.2
30622	333	C18H23NO5	0.9	0.6
30625	411	C21H33NO7	-0.8	0.4
30663	405	C26H32N2O2	-0.2	1.3
30813	272	C17H12N4	6.1	0.9
30930	267.28	C16H13NO3	15.0	1.6
31069	297	C18H19NO3	2.2	4.2
31208	248	C12H12N2O2S	12.8	0.9
31664	233	C6H8AsNO4	-12.2	1.7
31698	265	C17H15NO2	7.0	2.9

Table 2.4 (cont.)

31703	295	C18H17NO3	4.5	3.4
31741	203	C5H6AsNO3	-3.1	3.1
31748	358	C7H8AsIO4	1.7	1.3
31762	529	C19H17I2NO	75.5	1.0
32673	334	C21H22N2O2	-2.3	1.9
32838	202	C11H10N2O2	3.4	0.7
32873	305	C9H12AsNO6	-1.2	1.5
32892	278	C14H12ClNO3	13.6	1.7
32984	369	C21H23NO5	-3.9	0.8
33005	243	C13H9NO2S	12.0	1.8
33010	253	C16H15NS	22.0	2.4
33173	269	C15H9ClN2O	0.1	3.8
33182	276	C11H8N4OS2	12.4	4.6
33353	337.81	C19H16ClN3O	3.3	2.3
33478	328	C19H24N2O3	-1.3	0.3
33570	321	C21H23NO2	2.6	0.4
33575	345.44	C23H23NO2	34.5	2.1
33738	339	C15H12Cl2N2O3	-1.8	0.9
34219	313	C16H21ClO4	-1.1	2.6
34488	239	C13H13N5	5.3	1.5
34769	218	C7H8ClN3O3	12.6	1.7
34774	230	C8H10N2O4S	2.5	2.9
34777	214	C8H10N2O5	3.4	2.9
34865	322	C12H11AsN2O4	-7.2	2.3
34871	364	C14H13AsN2O5	-3.0	0.8
34875	272	C15H12O5	-10.3	3.5
34879	267	C16H13NO3	-5.7	3.7
34910	291	C19H17NO2	10.9	2.0
35545	301	C18H23NO3	-4.8	0.4
35582	347	C15H10N2S4	-0.6	3.0
35676	220.18	C11H8O5	14.6	1.8
35964	238	C11H14N2O4	-9.7	1.7
36317	384	C20H24N4O4	-4.6	2.8
36425	241	C11H19N3OS	3.1	1.0
36508	471	C26H30O8	-1.8	0.8
36520	238	C10H14N4O3	6.7	0.8
36525	342.4	C18H22N4O3	1.8	0.3
36582	219	C12H13NO3	-0.8	4.1

Table 2.4 (cont.)

36586	270.24	C15H10O5	-8.5	3.8
36693	332.44	C20H28O4	1.1	1.9
36753	274	C14H14N2O4	-9.0	4.6
36758	305.82	C15H15N3S.ClH	53.7	0.6
36815	264	C12H16N4O3	4.9	2.4
36818	374.48	C19H30N6O2	-4.1	4.0
36923	317	C20H31NO2	-4.4	2.3
37003	244	C9H12N2O4S	15.5	1.6
37168	308.29	C17H12N2O4	4.6	4.3
37187	312	C18H14ClNO2	-0.3	0.2
37219	358	C24H22O3	-12.8	1.4
37553	476.58	C30H28N4O2	-5.0	0.9
37612	269.34	C17H19NO2	-10.2	4.2
37627	392.41	C26H16O4	-5.2	1.3
37641	496.57	C29H33FO6	-2.0	0.7
37812	212	C12H8N2S	2.0	4.6
37955	261	C16H23NO2	7.6	2.8
38007	256	C15H10ClNO	-15.5	9.7
38042	237	C12H15NO4	17.2	0.7
38090	333	C14H11N3O5S	11.8	2.6
38352	295	C20H25NO	-5.4	2.8
38490	249	C12H11NO3S	-5.3	0.3
38743	248	C12H12N2O4	-22.7	1.2
38845	242	C12H10N4S	2.7	1.1
38983	224	C12H16O4	5.7	2.4
39047	256	C14H12N2O3	0.9	1.2
39336	223	C9H13N5S	5.0	3.4
39938	281	C15H7NO3S	17.0	2.6
39984	314	C17H12ClNO3	2.0	0.9
40269	326	C22H18N2O	0.7	3.4
40275	263	C17H13NO2	0.0	1.7
40306	298	C17H12ClNO2	10.2	2.3
40383	226	C11H10N6	3.5	1.0
40467	224	C10H8S3	-26.8	1.6
40500	237	C12H15NO4	-4.9	8.1
40614	224	C15H12O2	-5.2	1.4
40669	209	C8H11N5S	19.2	3.2
40749	290	C16H14N6	28.6	1.0

Table 2.4 (cont.)

41066	286	C14H10N2O5	6.0	3.5
41092	215	C11H9N3O2	-19.4	0.4
41098	312	C18H14ClNO2	90.8	0.2
41148	414	C22H22O8	-3.8	0.4
41376	278	C12H11AsO3	-12.3	0.2
41378	277	C12H12AsNO2	6.1	3.6
41400	493	C24H24AsN3O4	0.2	0.1
41649	260	C16H18ClN	2.6	1.4
41805	300	C14H12N4O2S	9.5	1.2
42014	228	C9H12N2O3S	4.8	0.5
42096	294	C12H11AsO4	-6.0	3.7
42135	280	C10H10BrN5	7.3	2.4
42199	404	C21H25NO.CH4O3S	-3.7	0.7
42212	223	C14H9NO2	-4.2	1.1
42846	213	C13H15N3	7.1	0.8
43088	335	C19H13NO3S	-1.8	0.4
43271	304	C12H10BrN5	-2.3	1.1
43308	288	C18H12N2O2	10.2	1.1
43344	300	C16H13O4P	-6.3	4.4
43409	266	C11H14N4O2S	-3.7	2.3
43506	315	C14H20ClN2O2P	-3.6	2.9
43998	318	C18H14N4O2	-0.9	0.4
44556	287	C11H8Cl2N2OS	-8.4	1.1
44584	334	C12H14N8O2S	-0.7	0.3
44688	232	C12H12N2O3	5.5	2.0
44750	312	C15H8N2O6	84.0	0.3
45086	261	C12H11N3O4	3.2	4.6
45153	222	C9H10N4OS	5.8	0.2
45291	214	C12H10N2S	0.4	1.3
45384	520.5	C26H24N4O8	21.5	1.0
45527	304.37	C14H16N4O2S	6.4	3.9
45536	266	C16H11FN2O	27.6	0.9
45545	308	C16H12N4O3	-3.0	1.1
45572	386	C18H18N4O4S	2.1	2.3
45745	261	C12H11N3O4	5.6	2.9
45815	264	C13H20N4O2	3.7	3.7
46075	370	C20H20ClN3O2	-3.7	0.9
46212	298	C18H22N2O2	3.4	1.3

Table 2.4 (cont.)

46213	312	C19H24N2O2	0.5	0.9
46385	390.42	C16H18N6O4S	-5.8	1.4
46492	313	C17H19N3O3	2.3	1.6
46615	233	C11H15N5O	16.6	2.5
47522	255	C10H8Cl2N4	6.7	1.4
47617	248	C9H12O8	1.6	1.7
47619	216	C11H20O4	-20.2	1.3
47680	301	C12H10Cl2N2OS	-0.1	0.4
48388	330	C12H10N8S2	2.6	3.3
48443	332	C20H32N2O2	88.2	0.7
48617	312	C20H28N2O	16.2	0.4
48964	210	C14H14N2	-7.6	0.8
49643	292	C16H20O5	1.8	3.1
49652	225	C14H11NO2	20.3	0.6
49701	230	C12H14N4O	1.9	2.5
49847	274	C8H7AsO2S2	-1.4	1.1
49852	384	C12H9AsN2O8	-6.3	1.8
50199	260	C8H10BrN3S	0.1	2.7
50405	202	C3H6O4S3	-3.8	2.2
50572	248	C12H16N4S	10.1	1.4
50633	237	C12H15NO4	7.5	5.1
50648	308	C17H12N2O4	4.4	1.0
50650	363	C21H17NO5	-0.8	0.3
50651	336.78	C19H13ClN2O2	-5.2	1.1
50654	382.42	C24H18N2O3	-5.4	1.9
50680	293	C18H15NO3	16.3	2.1
50688	358	C19H16ClNO4	-6.2	1.9
50690	307.35	C19H17NO3	-1.3	1.4
51331	238	C14H10N2S	10.8	8.2
51349	283	C16H13NO4	0.6	3.6
51351	284	C17H16O4	7.1	3.4
51683	315.8	C17H18ClN3O	0.7	0.2
51936	214	C10H18N2O3	1.5	3.6
52241	284	C21H16O	-7.1	14.5
53275	434.45	C23H22N4O5	-5.7	1.9
53710	204	C8H12O6	-14.1	2.8
53874	327	C8H11Cl2NO3.C4H9NO	-2.0	0.9
53934	295	C13H17N3O5	12.0	2.6

Table 2.4 (cont.)

54645	283	C16H13NO4	-8.5	13.3
54709	369.55	C24H35NO2	-0.1	1.2
54860	289	C11H6Cl2OS2	-8.1	6.2
55152	346	C20H18N4O2	-1.9	3.1
55172	285	C13H19NO6	-13.4	6.3
55453	272	C13H12N4OS	-25.4	2.1
55691	493.23	C18H11Br2N3S2	-7.4	2.2
55770	206	C11H8ClNO	5.9	2.5
55845	285	C16H13ClN2O	-38.6	8.7
55862	298	C21H14O2	0.0	3.4
56287	365	C9H7BrClN5O2S	-2.7	0.8
56455	235	C10H13N5S	7.2	2.0
56779	304	C15H13N3O2.ClH	-0.2	1.5
56906	214	C7H10N4O2S	13.3	0.8
57103	235	C9H5N3O5	-7.6	0.8
57165	202	C11H10N2S	4.4	0.8
57318	225	C12H19NO3	6.1	1.5
57345	226	C13H22O3	-0.9	3.2
57608	401	C20H36N2O6	-1.0	0.6
57624	384	C22H28N2O4	-7.7	0.9
57670	230	C14H6N4	-4.3	0.7
57794	219	C10H13N5O	19.5	0.3
58347	281	C11H9ClN4O3	-13.9	9.3
58724	256	C14H12N2O3	2.0	1.0
58904	431.45	C24H21N3O5	-3.3	0.0
58907	237	C10H15N5S	14.1	1.9
59430	284	C11H10ClN3O2S	2.9	5.8
59620	413	C26H36O4	2.6	1.6
59776	220	C15H12N2	-11.5	2.0
59782	252	C15H16N4	-15.2	6.2
59814	317.34	C20H15NO3	-0.3	2.9
59984	265	C12H15N3O4	11.9	3.4
60013	307	C14H8Cl2N2O2	12.5	1.1
60034	244.29	C14H16N2O2	-4.8	3.3
60037	286	C14H18N6O	9.9	2.0
60183	310	C14H18N2O4S	4.6	1.3
60266	228	C9H12N2O3S	-26.4	3.7
60303	278.69	C13H11ClN2O3	21.4	4.4

Table 2.4 (cont.)

60339	486.96	C26H23ClN6O2	-3.2	0.7
60419	203	C15H9N	13.3	1.4
60423	321	C16H17ClN2O3	17.0	0.7
60659	312.37	C20H16N4	4.9	6.8
60785	363.54	C25H33NO	-5.8	2.8
61642	344	C18H16N8	6.7	1.3
61888	207	C15H13N	6.5	1.7
61910	231	C12H13N3O2	-32.4	0.6
61929	294	C7HCl5O2	-4.1	6.2
62375	310	C16H30N4O2	-2.6	1.5
62611	212	C12H8N2S	17.3	1.0
62665	205	C5H2Cl2N4O	-16.6	4.5
62685	353	C10H6Cl2N2O6S	2.3	4.8
62901	259	C8H10AsNO4	9.2	2.4
63001	236	C15H12N2O	4.5	4.4
63161	264	C16H16N4	1.2	1.9
63543	326	C21H26O3	-1.5	3.3
63680	376.46	C21H24N6O	0.7	0.9
63865	244	C10H16N2O3S	-14.4	1.7
63963	248	C12H16N2.C2H4O2	-7.6	2.1
64672	344	C15H16N6O4	-3.5	1.0
64859	328	C10H6Cl4N2O2	0.1	0.5
64876	495	C25H32Cl2N2O4	-4.4	0.0
65238	408	C20H31N.C7H6O2	-8.9	0.6
65537	356.4	C17H16N4O3S	72.7	2.4
65689	327	C19H21NO4	1.3	3.6
66020	259.69	C13H10ClN3O	12.1	1.4
66122	284	C20H16N2	-8.5	2.4
66695	340	C12H10BrN3O4	-4.3	3.9
66837	230	C9H14N2O3S	-18.8	1.0
67436	486.96	C26H23ClN6O2	-5.2	0.7
67546	203	C9H17NO4	6.1	0.8
68116	315	C11H21Cl2N2O2P	0.0	0.5
68841	267	C16H13NO3	4.8	9.4
68971	273	C14H11NO5	-11.7	19.1
68982	231	C8H8Cl2N4	7.2	2.7
69359	302	C19H14N2O2	17.4	1.3
69421	250	C16H14N2O	1.4	1.3

Table 2.4 (cont.)

70307	267	C12H17N3O4	-19.1	6.7
70413	327.38	C19H21NO4	3.9	3.3
70534	240	C13H12N4O	-24.3	1.8
70799	377	C22H36N2O3	-1.5	1.1
70895	316	C12H15Cl2N5O	1.1	2.7
70931	451	C29H38O4	11.4	0.4
70933	415	C18H19ClN2.C4H4O4	0.1	1.2
70959	201	C6H5ClN4O2	4.6	0.8
71097	310	C18H12ClNO2	5.2	0.7
71795	246	C17H14N2	15.7	0.8
71866	305	C11H9BrN6	-0.7	1.4
71881	314.35	C19H14N4O	4.2	1.6
72947	282	C11H10N2O7	-32.4	2.2
73053	381	C17H17NO3.H2O4S	-7.7	1.8
73054	234	C14H10N4	17.4	1.2
73170	244	C10H10ClNO4	-15.4	3.7
73254	347	C22H25N3O	-1.2	5.2
73295	252	C10H12N4O4	-1.9	4.8
73735	484.51	C28H24N2O6	20.2	0.6
73753	289	C10H6Cl2N2O2S	-2.8	4.4
75241	247	C8H11BrN2O2	13.9	3.0
75885	234	C12H18N4O	1.5	1.9
76015	344	C7H6Br3N	-5.6	4.1
76350	398	C21H22N2O6	-6.9	1.6
76478	287	C17H13N5	2.5	0.9
76549	261	C14H13ClN2O	-21.2	10.3
76747	272	C19H16N2	7.8	0.4
76988	302.24	C15H10O7	3.2	0.9
77596	244	C10H14ClN3O2	-21.1	1.4
78130	243	C12H13N5O	-7.3	1.4
78623	292	C13H12N2O6	5.2	4.2
78697	264	C14H8N4O2	-19.8	5.4
78846	359	C20H29N3O3	-1.5	0.5
79139	246	C17H14N2	4.2	2.9
79253	244	C13H12N2O3	8.0	3.4
79486	340	C21H28N2O2	1.2	2.7
79538	205	C10H11N3O2	-17.1	2.8
79559	308	C18H16N2O3	31.3	0.7

Table 2.4 (cont.)

79887	298	C14H16ClNO4	-24.3	1.8
80137	386.49	C22H30N2O4	-8.3	0.2
80141	250	C13H9Cl2N	4.9	7.7
80313	325.33	C20H11N3O2	-0.9	0.3
80731	507.37	C26H20Cl2N4O3	-1.0	0.6
80735	528.48	C26H20N6O7	1.8	2.2
80997	472.63	C30H36N2O3	-8.2	1.0
81018	242	C10H14N2O3S	2.5	4.3
81120	249.33	C16H11NS	2.9	1.3
81213	237	C6H5ClN2O4S	-15.8	1.9
81463	400	C22H28N2O5	-7.0	1.6
81493	303	C13H13N5O2S	5.3	1.5
81660	217	C9H15NO3S	-16.1	1.5
81703	224	C15H16N2	5.3	0.9
81750	329.31	C15H15N5O4	6.2	0.7
81856	327	C12H8Cl2N4O3	-4.6	1.4
81915	378	C10H10BrN5.H2O4S	1.1	1.0
82269	272	C13H12N4OS	12.1	3.4
82560	309	C10H11N7O3S	-1.0	4.6
83497	326	C19H22N2OS	37.5	2.5
83715	247	C16H13N3	13.7	0.6
83961	303	C14H11ClN4O2	-1.0	1.4
84100	392.46	C26H20N2O2	-9.5	4.7
84126	385	C11H12AsN5O4S	1.3	3.1
85179	220	C10H12ClF2N	-19.8	3.7
85326	211	C8H13N5O2	17.6	2.4
85433	424	C17H12Br2O3	-0.8	0.6
86467	328	C20H24O4	-0.6	1.4
87008	293.43	C15H23N3OS	8.0	4.7
87010	302	C16H16ClN3O	1.1	1.4
87084	331	C17H17NO4S	9.1	1.5
87136	312	C19H24N2O2	0.0	0.9
87352	212	C10H12O3S	5.5	2.4
87690	271	C12H9N5O3	8.4	2.2
87822	244	C10H17N2O3P	4.2	5.6
87838	346.43	C22H22N2O2	-3.6	3.9
88324	251	C6H5Br2N	6.5	2.8
88349	254	C5HF7N2O2	-1.8	0.5

Table 2.4 (cont.)

88402	292	C13H13N2O2PS	63.5	0.7
88600	377	C19H21ClN2O2S	0.1	0.8
88795	253	C16H15NO2	2.9	10.1
88811	212	C13H12N2O	2.9	0.5
88883	215	C12H13N3O	-13.4	2.0
88916	369.56	C23H31NOS	1.6	1.9
88962	210	C10H10O5	-0.2	1.7
88998	236	C10H15Cl2NO	1.1	1.2
89201	440.41	C23H31Cl2NO3	-8.2	1.1
89249	224	C10H12N2O4	4.8	2.9
89258	218	C16H10O	10.7	0.9
89349	284	C13H11Cl2NS	-12.9	3.5
89429	296	C14H18ClN3S	-27.4	8.2
89602	377	C20H25ClN2O3	-4.9	1.3
89723	232	C8H12N2O4S	-0.5	1.4
89759	258	C15H14O4	-31.0	0.1
89821	407	C20H27ClN4O3	-3.3	0.8
90749	303.38	C15H17N3O2S	95.4	0.1
91340	381	C19H22Cl2N2O2	1.4	2.3
91355	361	C20H25ClN2O2	-3.3	1.0
91356	361	C20H25ClN2O2	-1.4	0.6
91357	361	C20H25ClN2O2	-11.7	0.6
91368	377	C20H25ClN2O3	-6.5	1.0
91378	342	C20H26N2O3	6.1	0.6
91382	340	C21H28N2O2	5.3	2.6
91396	397	C23H25ClN2O2	2.2	1.1
91397	396.92	C23H25ClN2O2	-7.3	0.8
91516	212	C12H8N2O2	14.4	2.8
91529	516.46	C25H24O12	-8.6	1.6
92207	208	C9H5FN2O3	10.8	1.5
92794	245.24	C12H11N3O3	25.9	2.1
92849	278	C13H14N2O3S	0.5	4.4
92892	337	C13H12AsNO5	2.9	0.5
92937	261	C17H11NO2	37.1	1.1
93033	305.25	C13H11N3O6	-0.5	0.5
93427	286.33	C19H14N2O	-7.5	3.2
93817	227	C13H9NOS	42.8	2.0
93945	262	C12H10N2O5	-7.8	8.9

Table 2.4 (cont.)

94600	348	C20H16N2O4	-3.7	1.7
95204	306	C10H19N4O3PS	-5.7	0.6
95909	266	C15H10N2O3	11.3	0.7
95916	343	C16H17N5O4	-0.6	0.6
96021	455.68	C29H45NO3	-4.9	1.5
96491	241	C12H23N3O2	0.8	1.4
96541	310	C21H14N2O	-1.6	1.1
96996	339	C22H17N3O	-0.7	1.4
97865	277	C11H10F3NO2S	3.4	4.8
97920	392.5	C26H24N4	10.9	1.5
98026	300	C17H16O5	11.9	5.5
98049	262	C9H12ClN3O4	7.4	2.8
98363	342	C12H10N2O4S3	59.8	1.3
98683	211	C6H5N5O4	9.5	0.6
98857	211	C13H9NS	60.2	1.5
98938	280	C18H16O3	26.6	2.7
99634	322	C14H14N2O5S	-2.3	0.0
99657	325	C13H19N5OS2	38.4	0.7
99660	339.47	C14H21N5OS2	-3.0	1.5
99663	319	C13H13N5OS2	-3.4	1.0
99796	230	C12H6O5	1.1	1.3
99867	363	C20H25N7	-3.1	2.3
99925	383	C21H21NO6	-7.9	0.8
100058	287	C17H21NO3	11.9	1.8
100120	241	C12H11N5O	2.6	4.2
100708	385	C23H22F3NO	-0.1	0.6
100942	274	C10H14N2O3S2	-5.6	2.0
101266	219	C12H17N3O	0.2	2.7
101298	269	C16H19N3O	-0.8	1.0
101345	265	C11H19N7O	11.0	1.8
101653	209	C10H15N3O2	0.7	2.7
101679	273	C14H15N3O3	-6.1	12.4
101758	259	C8H12F3NO5	-6.6	5.7
101777	250	C8H15N2O5P	4.7	0.8
101789	311	C22H17NO	-3.8	2.9
102086	237	C10H11N3O2S	-14.1	3.0
102288	205	C11H15N3O	2.2	4.3
102314	358	C22H30O4	1.7	1.8

Table 2.4 (cont.)

102554	263	C12H13N3O2S	-38.8	14.2
103189	299	C13H12F3N3O2	-35.3	1.1
103331	399	C17H20Cl2N4OS	1.4	0.9
103520	462	C17H14Br2N6	-2.6	0.7
103770	213	C5H3N5OS2	10.3	1.3
103775	228	C5H4N6OS2	2.9	3.2
105348	330	C18H16ClNO3	-4.9	1.0
105432	284	C12H16N2O4S	2.9	3.2
105584	422	C21H26O9	-0.2	0.2
105781	304	C19H16N2O2	-1.9	0.7
105798	328	C17H16N2O5	-1.9	1.1
105827	325.34	C12H15N5O4S	33.9	0.3
106208	248	C11H10ClN5	16.4	1.5
106231	360	C23H24N2O2	-2.7	0.7
106282	249	C17H15NO	5.3	3.5
106461	240	C12H8N4S	61.1	1.7
106464	332	C17H20N2O5	-2.5	0.5
106506	224	C14H12N2O	1.0	2.6
106570	238.29	C14H14N4	-7.1	0.9
106863	242	C13H10N2O3	6.0	0.5
107022	278.17	C12H6O8	8.8	3.3
107522	499	C21H20Cl2N2O8	-0.3	0.7
107582	430	C15H7BrF3N3O4	-0.5	0.8
107677	409	C20H24N2.C4H4O4	-4.9	0.3
107679	379.88	C13H18ClN3O4S2	-4.1	0.9
107701	416	C24H21N3O2S	-0.6	0.8
108235	229	C11H11N5O	17.1	2.5
108750	250	C16H14N2O	7.7	0.2
108753	209	C13H11N3	24.1	0.7
108783	272	C13H8N2O3S	38.7	4.8
108972	223	C10H9NO3S	4.9	4.2
109084	214	C13H14N2O	12.3	0.1
109086	228	C14H16N2O	-13.1	2.3
109128	416	C25H37NO4	1.6	0.4
109174	241.25	C13H11N3O2	3.2	2.5
109466	245	C14H15NO3	-4.1	1.1
109719	204	C10H6ClN3	7.8	1.1
109747	263	C17H13NO2	-20.8	9.9

Table 2.4 (cont.)

109885	181	C7H11N5O	6.7	2.2
110300	358	C16H14N4O2S2	-2.6	2.4
110332	303	C16H21N3O3	-9.7	0.8
110562	302	C10H8BrNO3S	-4.6	0.3
110899	254	C11H10O5S	3.0	3.1
111107	184	C8H12N2OS	-16.4	8.5
111118	331	C13H8Cl2S3	-10.2	2.1
111194	347	C18H19ClN2OS	-4.8	2.5
111210	396.92	C23H25ClN2O2	-3.7	1.7
111552	202	C12H10O3	77.6	1.2
111847	263	C17H13NO2	2.2	1.8
112125	312	C18H12N6	2.8	2.3
112203	311	C15H21NO6	-7.0	1.4
112541	292	C18H16N2O2	-1.0	1.3
112547	298	C16H14N2O2S	-1.6	4.7
112677	240	C15H16N2O	10.5	1.6
112965	271	C16H14FNO2	10.5	0.5
112975	191	C11H13NO2	-27.1	4.7
113486	209	C9H15N5O	2.0	2.5
114414	357	C16H15N5O3S	-1.2	2.3
114449	338.34	C12H14N6O4S	-11.2	1.2
114490	226	C14H14N2O	3.7	0.8
114831	243	C10H13NO6	14.5	3.0
114997	326	C18H18N2O4	0.5	1.7
116339	458.55	C26H34O7	-6.6	1.4
116397	329	C20H27NO3	-3.6	1.4
116508	276	C16H24N2O2	3.3	1.6
116565	199	C6H5N3O3S	18.7	2.3
116640	295.34	C20H13N3	-1.1	0.6
116644	270	C19H14N2	14.4	2.9
116702	362.43	C25H18N2O	-7.5	1.2
116709	353	C24H19NO2	2.4	4.6
117028	398.3	C20H20BrN3O	2.1	3.7
117197	299	C14H13N5O3	29.4	0.3
117268	378.84	C15H15ClN6O2S	-0.8	1.3
117386	170	C5H6N4O3	8.6	1.6
117446	261	C11H19NO4S	4.0	1.8
117554	250	C18H18O	2.9	2.3

Table 2.4 (cont.)

117741	217	C10H7N3O3	-7.3	0.3
117908	286	C15H14N2S2	-5.7	2.0
117922	210	C7H6N4O4	-6.2	2.7
117987	360	C21H12O4S	5.3	0.7
118628	288	C16H16O5	-6.3	2.2
118723	239	C15H17N3	11.1	1.5
118818	369	C23H19N3O2	-0.8	0.7
118832	191	C10H9NOS	-31.4	5.3
119805	295	C16H13N3O3	10.5	1.6
119969	188	C11H12N2O	-9.0	1.6
120286	220	C9H8N4OS	11.7	1.6
120289	390.43	C16H14N4O4S2	1.1	0.8
120290	332	C12H8N6O2S2	-0.4	1.0
120307	227	C11H9N5O	7.6	1.8
120312	196	C10H16N2O2	-22.9	2.9
120622	316	C16H16N2O5	-9.1	1.4
120631	258	C15H14O4	10.4	2.5
120844	210	C12H22N2O	1.8	2.5
120913	262	C14H18N2O3	-6.0	0.6
120961	280	C14H20N2O4	15.4	3.0
121268	272	C16H20N2O2	8.8	2.7
121781	240	C14H12N2O2	-10.3	2.0
121868	422.53	C28H26N2O2	-1.1	1.5
121908	306	C16H22N2O2S	-0.5	2.5
122131	173	C10H7NO2	-10.0	0.5
122253	290	C18H14N2O2	-4.3	1.5
122280	204	C10H8N2OS	-7.8	3.3
122297	239	C10H13N3O2S	0.6	1.4
122376	226	C15H14O2	-23.3	2.4
122385	270	C10H10N2O3S2	-2.1	0.5
122819	656.66	C32H32O13S	-0.9	0.9
122987	212	C14H16N2	10.2	2.7
123141	214	C8H10N2O3S	9.7	1.6
123389	325	C19H19NO4	46.4	2.3
123418	441	C22H23N3O7	4.2	1.1
123458	193	C14H11N	-0.5	6.2
123527	412	C26H21NO2S	-1.9	0.7
124146	245	C13H15N3O2	-2.4	2.9

Table 2.4 (cont.)

124818	354	C12H8BrN3OS2	1.1	1.3
125043	212	C12H12N4	4.8	2.8
125095	375	C18H14FNO5S	-0.7	1.3
125197	193	C8H11N5O	13.3	6.4
125344	281	C15H17ClO3	3.7	1.6
125605	257	C14H15N3O2	1.7	4.0
125727	226	C10H14N2O2S	-12.3	1.8
126224	265	C12H11NO6	10.4	0.5
126226	302	C15H14N2O5	-6.7	0.7
126347	328	C13H16N2O2S3	0.9	1.0
126405	232	C5H2Cl4N2	4.7	1.2
126757	220.19	C8H8N6O2	-1.0	2.7
126837	391	C19H21NO6S	-2.3	1.5
127133	434.45	C27H18N2O4	-1.5	1.0
127216	162	C3H6N4S2	6.9	7.4
127458	195	C12H9N3	0.9	6.3
127886	278.31	C14H18N2O4	-12.1	4.2
127947	199	C10H17NO3	-7.1	4.1
128068	183	C12H9NO	9.0	5.3
128141	236	C13H20N2O2	-17.5	0.3
128606	435.43	C27H17NO5	-4.1	0.5
128737	210	C12H10N4	11.6	0.8
128751	229	C13H9ClN2	16.4	2.5
129220	285	C9H11N3O4.C2H4O2	2.5	3.7
129260	241	C9H8FN3S2	15.8	1.3
129536	310	C15H18O7	-0.6	0.6
129929	266	C16H14N2O2	11.1	0.3
130801	280.33	C17H16N2O2	3.9	2.9
130847	289	C17H11N3O2	3.9	1.2
130872	236	C15H12N2O	12.3	0.6
131388	209	C9H15N5O	10.2	1.8
131467	386	C23H18N2O4	-4.3	0.9
131616	354	C21H26N2O3	-9.2	0.6
131982	194	C10H14N2S	-5.0	2.3
131986	208	C11H16N2S	1.5	2.3
133002	259	C9H10NO6P	9.7	1.3
133071	512.02	C20H24ClN5O2.C2H6O3S	1.7	1.7
133075	343.36	C15H13N5O3S	4.0	1.1

Table 2.4 (cont.)

133114	346.32	C10H14N6O6S	-2.8	2.7
133195	229	C8H11N3O3S	8.9	0.4
133351	290	C12H10N4O5	10.3	3.7
133356	214	C8H6N8	9.7	1.3
134058	251	C10H9N3OS2	9.7	2.6
134137	371.37	C17H13N3O5S	33.2	1.6
134199	294	C11H10N4O4S	7.8	1.2
134577	164	C9H12N2O	-26.9	4.4
134580	167	C8H9NO3	-8.1	7.5
134674	257	C6HCl4N3	10.8	0.7
134784	182	C10H14O3	19.1	2.6
134785	197	C11H19NO2	-28.5	4.2
135168	313	C21H15NO2	-3.5	1.3
135184	308	C15H20N2O3S	-6.9	1.0
135351	151	C9H13NO	-20.6	5.3
135381	304	C17H20O3S	-5.9	1.1
135412	288	C20H20N2	7.0	2.0
135894	269	C10H12Cl3NO	9.4	0.6
136065	191	C10H13N3O	41.5	3.5
136513	410.38	C22H18O8	-0.1	0.4
137112	347	C21H21N3O2	-8.8	2.0
137399	273	C19H15NO	9.3	1.7
137577	275	C18H17N3	-9.2	3.2
138389	253	C12H13ClN2O2	7.7	0.5
138398	289	C16H23N3O2	-3.7	4.6
139021	255	C13H9N3OS	48.2	0.9
139105	539	C21H25ClN6O2.C2H6O3S	2.9	0.9
139168	390	C22H30O6	-2.0	0.8
139257	235	C10H9N3S2	9.5	3.0
140873	277.71	C13H12ClN3O2	7.0	0.8
140892	244	C13H12N2OS	13.1	3.1
140899	268	C15H12N2O3	6.1	3.4
141538	296	C16H24O5	9.2	1.5
142269	273	C14H15N3OS	-3.2	1.9
142277	320	C15H13FN2O3S	32.6	3.0
142335	398.85	C23H15ClN4O	-0.8	0.8
142446	349.82	C19H16ClN5	-0.3	1.1
143241	411	C23H25NO6	-4.6	0.5

Table 2.4 (cont.)

143348	243	C13H13N3S	0.8	0.9
143491	579	C27H30N2O10.ClH	38.8	1.2
143974	336	C15H25N6OP	-15.4	5.5
144694	274	C18H14N2O	2.7	2.1
144958	242	C13H10N2O3	2.0	2.9
144982	226	C12H18O4	7.0	1.1
145180	167	C5H5N5S	-43.3	10.3
145992	301	C12H13ClN2O5	-4.2	0.5
146071	320	C11H5Cl3N2O3	-3.0	0.9
146554	350.35	C14H14N4O5S	0.4	1.2
146557	481	C24H18BrFN2OS	2.0	0.9
146769	334	C18H14N4O3	2.8	1.1
146770	304	C18H16N4O	-0.1	1.4
146771	476.49	C27H20N6O3	3.0	0.8
147358	301	C17H17ClN2O	5.4	3.1
147829	186	C11H10N2O	-7.6	3.0
147866	282	C17H22N4	4.6	2.5
148170	227	C8H7ClN4S	77.4	1.0
148832	264	C15H20O4	9.7	2.0
149046	228	C10H10ClNO3	5.8	0.3
149054	307	C17H13N3O3	-10.3	2.0
149286	236.27	C15H12N2O	36.2	1.4
149312	266	C16H14N2O2	4.8	0.2
150114	303	C21H21NO	-5.1	2.4
150954	231	C14H17NS	14.2	1.1
150982	188	C10H8N2O2	-5.1	4.0
151262	285	C14H9BrN2	8.6	3.1
151721	354	C18H26O7	-11.7	2.7
151888	375	C25H30N2O	-8.8	1.8
151901	189	C11H11NO2	11.5	1.8
152551	236	C15H12N2O	4.4	1.5
152632	174	C6H10N2O2S	5.4	8.0
153172	272	C14H12N2O4	40.9	2.0
153330	220	C11H12N2OS	7.0	1.4
153365	249	C8H15N3O6	-1.7	1.5
153391	328.38	C17H16N2O3S	0.7	2.0
153399	237	C15H11NO2	11.2	1.7
153792	269	C15H15N3O2	28.9	0.3

Table 2.4 (cont.)

154127	281	C10H12Cl3N3	8.3	2.4
154295	231	C13H13NO3	7.0	1.5
154316	153	C4H3N5O2	-12.5	3.8
154389	396	C18H10Cl4N2	-2.9	1.0
154585	335	C19H17N3O3	-3.8	0.1
154587	219	C11H17N5	1.8	0.9
154718	183	C11H9N3	-19.9	3.7
155196	169	C10H7N3	-4.6	5.5
155698	200	C11H8N2S	-20.1	0.3
155703	196	C11H8N4	-29.2	0.9
156516	425	C26H16O2S2	10.6	1.0
156563	350.33	C19H14N2O5	26.9	0.2
156565	359.38	C22H17NO4	60.1	1.9
156571	171	C9H17NO2	-32.2	3.6
156616	215	C5H5N5O3S	9.2	1.3
156957	263	C13H13NO5	6.3	1.1
157522	275	C14H15ClN4	8.0	1.5
157725	329.74	C16H12ClN3O3	0.5	1.3
157767	211	C9H9NO5	-4.4	2.6
157940	250	C15H22O3	5.1	1.9
158413	429.91	C21H13ClFNO2S2	1.7	1.2
158549	260	C16H12N4	-1.6	4.9
158959	316	C17H11Cl2NO	-1.6	1.0
159031	223	C15H13NO	21.1	1.4
159092	332.8	C16H13ClN2O2S	-1.2	0.7
159242	463	C28H30O6	-3.0	0.7
159398	347	C5H3I2NO	-3.4	2.9
159566	351	C16H15BrO4	14.4	0.5
159632	236	C12H12O5	7.3	0.9
159686	257	C14H11NO4	15.4	0.4
160005	168	C9H16N2O	21.8	2.2
162188	275	C9H7F6NO2	-22.5	6.8
162292	196	C11H20N2O	-21.6	6.9
162915	197	C10H7N5	4.4	2.4
163104	198	C9H14N2OS	14.5	1.4
163144	211	C12H9N3O	-6.6	1.7
163158	165	C7H7N3O2	-34.5	7.3
163443	394.47	C26H22N2O2	-0.6	0.7

Table 2.4 (cont.)

163639	399	C12H12Cl2N2O7S	-3.0	1.7
163802	258	C13H10N2O4	6.4	3.6
163823	356	C14H9ClF3N5O	1.6	1.3
163910	441.31	C18H11N5O9	-6.1	2.8
163920	184	C11H8N2O	-9.5	1.9
164208	220	C13H20N2O	0.6	2.9
164435	338	C19H16ClN3O	1.2	0.9
164459	305	C15H13ClN2O3	-10.3	1.1
164464	275	C14H11ClN2O2	11.1	0.1
164511	206	C12H18N2O	7.0	1.5
164676	404	C20H25N3O4S	-6.0	0.3
164678	203	C11H13N3O	-1.2	2.3
164880	291	C19H17NO2	1.5	1.0
164965	187	C7H7ClN2S	-9.3	4.4
164991	367	C16H12Cl2N2O2S	0.3	1.6
165599	287	C10H13N3O3S2	-5.8	2.6
165701	295.4	C17H17N3S	11.0	1.1
165704	336	C19H16N2O4	-1.5	2.4
165883	227	C14H13NO2	10.3	1.7
166259	416	C19H17ClN2OS.1/2C4H6O4	0.7	0.7
166375	464	C15H25ClN2O.C6H13NO3S	-4.5	0.6
166547	229	C8H6Cl2N4	9.6	2.0
166583	219	C6H4Cl2N4O	2.0	0.4
166596	268	C13H8N4OS	-0.9	0.2
166634	267	C7H6Cl3N5	9.8	2.0
166637	384	C13H14Cl2F3N5O	-3.2	0.5
166846	266	C12H18N4O3	9.9	2.6
166900	156	C6H8N2O3	-28.7	6.5
168027	424	C21H28O9	0.9	0.4
168184	467	C12H18N6.2C2H6O3S	-10.6	3.1
168221	286	C15H14N2O2S	-4.6	2.4
168225	278	C15H14N6	13.4	0.1
169409	339	C17H25NO6	-2.4	1.2
169458	185	C8H11NO2S	9.1	6.4
169566	151	C6H5N3S	36.5	3.4
170001	206	C10H6O5	4.9	1.9
170578	245	C12H7NO3S	13.5	3.5
170621	202	C11H10N2O2	-3.6	0.2

Table 2.4 (cont.)

170637	256	C14H16N4O	67.9	1.2
170955	291	C20H21NO	1.7	1.2
172255	424	C17H23Cl2NO.CH4O3S	1.2	0.3
173101	193	C9H11N3O2	-8.1	1.9
173103	196	C6H4N4O2S	5.0	1.3
174027	212	C9H8O6	4.9	1.0
174084	295	C12H11BrN2O2	-3.5	2.3
175412	238	C9H10N4O2S	10.3	1.4
175415	216	C8H7F3N4	4.1	0.8
175743	268.32	C14H16N6	4.9	2.1
176324	195	C5H7ClN2O4	6.4	4.0
176367	257	C13H11N3OS	15.6	0.3
176736	335	C13H7Cl4NO	-6.5	0.4
176765	217	C9H10Cl2N2	2.1	2.8
177365	566.46	C23H23N7O4S.2ClH	21.7	1.3
177407	333.09	C12H5Cl2F3N4	0.9	1.2
177862	351	C21H21NO4	-6.8	1.7
177866	259.1	C13H7BrO	-6.3	4.3
177952	156	C4H4N4O3	-21.5	4.0
177989	237	C12H15NO4	8.4	1.0
178249	354	C19H14O7	-1.1	1.3
178873	268	C13H16O6	0.8	0.8
179818	214	C13H8ClN	9.6	2.2
179822	260	C14H12O5	10.7	0.7
180964	274	C16H18O4	4.8	3.0
182400	233	C6H2Cl2N4O2	1.0	4.1
186067	339.44	C20H25N3O2	-0.2	0.9
186194	324	C14H20N4O5	-1.8	1.2
186200	340	C23H20N2O	0.5	2.4
187675	323.14	C12H10AsNO5	4.5	2.3
190336	244	C8H10BrN3O	1.3	1.4
190501	326	C13H10BrClN2O	0.4	0.4
191029	183	C11H21NO	-21.2	3.5
191441	347	C21H17NO4	1.0	2.2
191454	363	C21H17NO5	-18.6	2.4
193043	221	C10H9ClN4	4.4	0.9
193528	272	C11H16N2O4S	1.5	2.2
194242	161	C8H7N3O	-10.5	1.5

Table 2.4 (cont.)

194243	176	C9H12N4	-63.5	5.8
194308	306	C12H22N2O3S2	47.6	1.2
195031	185.31	C11H23NO	-10.1	10.5
195327	271	C13H13N5S	5.3	1.5
196148	201	C7H11N3O2S	1.1	2.6
196515	476	C20H34O5.C4H11NO3	-4.0	0.5
197008	336	C18H28N2O4	-7.0	1.0
197046	252	C9H8N4O3S	3.7	0.5
197049	221	C6H7NO2S3	43.9	1.7
201631	436.44	C21H16N4O5S	-0.8	0.8
201634	274	C14H14N2O2S	10.5	2.5
201659	323	C14H11ClN2O3S	-5.8	0.7
201863	370.28	C21H17Cl2NO	-0.8	5.9
201868	318	C19H18N4O	-5.3	2.0
201989	343	C19H22N2S2	-1.2	0.8
202386	521.49	C27H19N7O5	-2.2	1.9
202705	305	C13H9ClN4OS	-1.8	3.9
202883	203	C12H13NO2	6.9	0.4
203065	191	C13H21N	21.2	1.9
203837	267	C15H13N3O2	7.6	1.4
203912	410	C14H8Cl4N2O4	-0.9	0.7
204232	406.35	C20H14N4O6	-1.8	0.8
204262	396	C17H15Cl2N3O2S	0.7	0.4
204665	376	C20H22ClNO4	-13.8	2.3
204920	226	C13H10N2O2	11.6	0.7
204939	295	C18H17NO3	2.5	2.9
204976	212	C13H12N2O	11.7	1.3
205827	301	C15H15N3O2S	5.1	0.9
205832	350	C18H20ClNO4	-3.2	3.2
205842	319	C15H17N3O3S	-1.7	1.4
205843	244	C14H16N2O2	1.6	1.4
205909	290	C14H14N2O3S	3.0	3.0
205912	325	C12H11N3O4S2	-2.5	2.2
205913	262	C12H10N2O3S	5.6	2.6
206630	172	C8H16N2O2	-60.4	9.4
207895	279.25	C11H13N5O4	50.0	0.8
209901	331	C13H6Cl3NOS	-2.6	0.4
210816	243	C12H9N3O3	4.8	1.3

Table 2.4 (cont.)

211336	273	C11H13ClN2O4	1.1	1.7
211340	303	C12H9N5O3S	-2.4	1.4
211356	346	C16H18N4O5	-6.8	1.1
211490	472.49	C28H24O7	-0.6	0.4
211787	326	C18H18N2O4	0.1	2.8
213708	253	C11H9F2N3O2	9.8	1.2
214009	362	C21H19FN4O	4.9	5.1
214029	265	C17H12FNO	3.9	0.4
215275	296	C17H16N2OS	4.7	1.4
215276	206	C12H14O3	2.1	1.1
215585	266	C12H12ClN3O2	4.3	0.2
215684	318	C15H14N2O6	-4.4	0.8
215689	345	C16H15N3O6	1.4	1.2
215718	401.28	C18H13BrN2O2S	-2.1	0.7
215721	386	C14H10BrClN2O2S	1.7	1.5
216183	289	C14H12FN3O3	6.2	0.3
216606	354	C15H13BrFNO3	1.0	1.4
216607	320	C15H13FN2O5	-3.6	0.6
216618	265	C13H19N3OS	1.0	3.3
216621	350	C20H31NO2S	-1.3	1.2
216623	301	C15H15N3O2S	0.0	0.4
216633	391	C18H16Cl2N4O2	0.4	0.9
217306	290	C16H18O5	-3.4	1.9
217697	359	C25H30N2	-8.4	0.5
217913	307	C9H8Cl2N4O2S	33.0	1.9
220030	217	C14H19NO	7.6	0.9
222362	319	C12H16AsClO3	-9.9	3.6
222365	435	C16H17AsCl2O5	0.8	0.7
227186	697.14	C35H37ClN2O11	-3.6	0.3
227309	189	C11H11NO2	-16.8	3.8
227383	211	C8H9N3O2S	7.0	1.8
228137	334	C15H14N2O5S	-1.3	1.4
228150	303	C13H9N3O4S	91.2	0.3
228155	290.25	C11H6N4O4S	42.7	0.6
234348	421	C19H21ClN4O5	-6.3	0.9
234764	196	C8H8N2O4	-3.4	4.8
234945	223	C12H9N5	22.6	0.4
236246	233	C11H11N3O3	-2.3	2.7

Table 2.4 (cont.)

236254	266	C16H14N2O2	2.8	0.9
238929	273	C10H6Cl2N2OS	1.6	2.0
240029	280	C13H16N2O5	-3.7	3.1
240502	206	C8H12ClNO3	4.6	2.6
241619	305	C14H15N3O5	-4.6	0.6
241621	279	C8H11BrN2O2S	-4.1	0.2
241624	332	C17H20N2O3S	1.1	0.9
241998	294	C14H18N2O5	8.1	2.5
242557	282	C18H22N2O	6.3	0.5
244387	328	C17H28O6	-1.2	0.5
245091	324	C22H28O2	-4.6	1.8
246415	200	C11H8N2S	-57.6	11.5
246999	331	C21H14FNS	-3.7	0.8
250429	364	C20H28O6	-1.5	1.1
252172	278	C19H18O2	38.2	1.0
252359	342.83	C17H19ClN6	-3.3	1.3
255025	226	C10H14N2O2S	7.9	0.5
260594	504.55	C29H24N6O3	1.5	0.7
261037	201	C7H11N3O4	-17.6	1.3
261610	218	C13H18N2O	7.4	2.7
263220	387.86	C14H14ClN3O4S2	-0.5	1.1
265372	264	C12H20N6O	1.3	1.5
268251	575.75	C29H49N7O5	-1.8	0.7
269904	299	C14H16Cl2N2O	0.5	0.7
269905	188	C11H12N2O	-37.1	2.9
270063	308	C15H14ClNO4	3.2	2.0
270071	391	C16H17N5O3S2	-4.0	5.2
270916	337	C22H27NO2	-1.3	0.4
271923	359.44	C14H21N3O2.CH4O3S	1.2	0.2
272275	159	C11H13N	-38.3	6.9
274905	221	C14H11N3	11.3	0.2
275266	374	C19H22N2O6	29.4	4.5
275428	361.83	C18H19N3O3.ClH	2.1	0.5
275971	365	C16H13ClN2O2S2	-0.7	1.8
276369	182	C8H10N2O3	47.5	1.9
276736	281	C17H15NO3	-3.2	0.4
277184	454	C18H20N4O4.H2O4S	-5.9	0.5
277806	230	C12H10N2O3	7.3	0.2

Table 2.4 (cont.)

278323	326	C10H18N2O6S2	-6.9	1.8
278741	177	C9H11N3O	7.9	5.1
279834	187	C11H13N3	-35.9	3.5
279895	236	C13H16O4	11.2	1.4
280058	430	C22H22O9	-0.6	0.1
280492	298	C13H18N2O2S2	-4.7	3.3
280594	400.29	C13H17N6O7P	-7.0	3.8
281307	331	C12H10Cl3N5	-3.4	3.2
281383	319	C16H21N3O2S	-4.8	3.3
281623	340	C18H16N2O3S	-1.8	0.2
281624	310	C18H18N2OS	-1.7	1.9
281639	156	C5H8N4O2	-7.8	1.8
281816	472.62	C20H24N2S2.C4H4O4	-8.1	2.0
282137	314	C17H22N4O2	-1.2	0.9
282187	248	C12H9FN2O3	5.5	1.5
283845	273.29	C18H11NO2	-0.8	0.2
283849	328	C18H20N2O4	-0.7	0.3
283856	262	C14H18N2OS	1.7	1.7
284234	245	C13H11NO4	5.5	1.4
284701	152	C9H16N2	-8.7	2.0
285669	254	C11H14N2O3S	-0.7	0.7
287065	178	C7H6N4O2	-4.9	6.2
287495	182	C8H10N2O3	-48.3	2.9
288024	297	C11H11N3O3S2	0.8	3.1
288387	348	C19H16N4O3	5.9	2.4
288519	240	C12H8N4O2	17.1	1.8
288686	189	C10H5ClN2	-14.6	3.8
289090	246	C13H12ClN3	-13.9	0.7
289359	352	C19H16N2O5	-0.3	1.3
289365	250	C12H8ClNO3	6.4	1.2
289748	262	C12H14N4OS	87.1	0.6
290307	210	C9H10N2O4	6.3	1.1
290311	421	C27H36N2O2	0.9	0.4
292140	373	C17H10Cl2N4O2	0.6	1.2
292253	464	C21H21NO5.CH4O3S	0.8	0.6
292826	250	C14H16F2N2	-0.6	1.0
292923	370	C18H12BrNO3	-2.5	1.5
293334	210	C10H14N2O3	1.3	1.7

Table 2.4 (cont.)

293360	343	C18H17NO6	-2.0	1.0
293780	209	C14H11NO	2.0	0.8
293962	366	C17H27N5O2S	-0.9	1.0
294150	291	C13H17N5O3	-3.3	0.3
294153	288	C11H8N6O4	5.2	0.2
294154	212	C8H6ClN3O2	12.4	1.9
294161	238	C14H14N4	9.5	0.4
294623	242	C13H14N4O	-3.0	3.3
294625	287	C13H13N5O3	3.6	0.2
294747	271	C11H17N3OS2	3.1	0.6
294750	310	C11H10N4O3S2	2.0	0.8
294756	333	C16H19N3OS2	-4.8	1.5
295300	330	C20H18N4O	-4.2	1.1
295358	408	C16H18F6N6	-6.7	1.0
295404	230	C12H10N2OS	-5.5	1.4
295486	359	C22H15ClN2O	-0.9	1.8
295701	189	C9H7N3S	-37.6	5.2
296934	297	C12H15N3O6	-1.6	2.4
298197	221	C9H7N3O2S	43.1	0.7
298793	233	C14H19NO2	0.7	2.7
298892	373	C20H15N5O3	-18.8	5.8
299119	312	C12H16N4O2S2	-0.1	1.0
299514	288	C13H12N4O2S	3.1	2.2
299967	287	C14H13N3O2S	-6.0	6.9
299968	270	C10H14N4O3S	4.6	1.8
300289	339.35	C18H17N3O4	-3.2	1.2
300540	331	C17H12Cl2N2O	-1.3	2.5
301167	272	C10H7Cl2N3S	-3.2	2.2
301168	236	C10H6ClN3S	0.2	0.6
302584	278	C10H6N4O4S	-6.8	0.8
302867	288	C14H16N4O3	5.6	1.8
303244	199	C12H13N3	23.2	2.5
303294	347	C15H13N3O3S2	-0.2	0.5
303304	258	C18H14N2	0.0	0.5
303603	200	C7H8N2O5	-19.7	7.2
303612	322	C20H22N2S	-5.9	2.4
303800	171	C7H9NO4	-9.9	13.9
304902	186	C12H14N2	35.8	3.7

Table 2.4 (cont.)

305329	262	C15H10N4O	8.0	2.4
305743	258	C13H8ClN3O	2.3	2.9
305780	341	C18H14N4S.1/2C2H6O	-0.9	2.2
305798	404.33	C19H18F6N2O	-1.0	1.3
306752	238	C9H8ClN5O	9.6	1.3
307703	257	C14H9ClN2O	-13.5	8.3
308814	283	C20H13NO	5.1	3.0
308835	484.59	C30H32N2O4	-3.4	0.2
308848	311	C18H21N3O2	0.0	1.1
308849	309	C18H19N3O2	-5.4	0.7
309401	377	C17H16N6.2ClH	0.3	0.5
309874	446.99	C26H23ClN2OS	-0.8	0.7
309892	407.87	C21H14ClN3O2S	-3.1	0.3
309971	242	C9H10N2O2S2	15.6	1.0
310113	278	C13H14N2O3S	-2.4	1.1
310325	502	C25H22Cl2N2OS2	0.1	0.8
310354	372	C21H29N3OS	4.3	5.3
311074	226	C6H6N6O2S	4.9	2.2
311153	433.55	C24H28N3O.C2H3O2	-0.4	0.3
311165	285	C16H19N3O2	1.0	2.0
311723	189	C9H7N3S	0.4	5.0
311727	240	C7H4N4O2S2	52.1	0.5
312606	284	C15H16N4O2	6.2	0.4
316458	263.26	C11H13N5O3	-5.9	1.0
317003	456	C18H20N2O2S.HI	9.9	1.1
317605	368	C21H22ClN3O	-3.8	1.5
318799	262	C9H12ClN3O4	-3.3	1.9
319012	321	C16H23N3O4	-4.2	0.1
319029	288	C17H24N2O2	-2.5	4.2
319034	229	C11H23N3S	14.0	1.0
319079	297	C14H17ClN2O3	-15.9	11.9
319424	309	C10H4F5N3OS	-1.4	1.7
319435	367	C19H17N3O3S	-1.0	1.8
319436	299	C16H17N3OS	-6.9	3.6
319449	341	C19H19NO3S	0.4	0.4
319471	252	C12H16N2O2S	-3.2	0.5
319709	352	C21H25N3S	-1.2	0.6
319990	474.55	C23H18N6O2S2	-0.6	0.7

Table 2.4 (cont.)

319994	362	C19H18N6O2	-1.1	1.6
320218	388	C22H20N4O3	-5.6	1.5
321484	165	C7H7N3S	-45.1	0.9
321491	383	C20H15ClN2O2S	1.9	1.5
321496	410.99	C25H31ClN2O	-4.7	1.2
321502	346	C17H9Cl2NOS	-7.1	0.9
321506	245	C9H6Cl2N2S	2.1	0.9
321517	313	C14H23N3OS2	-1.6	0.9
321792	254	C10H8ClN3OS	0.2	3.3
322661	475.3	C16H15Cl2F3N2O.CH4O3S	-8.5	0.5
324623	327	C20H13N3O2	-4.3	2.1
325014	383	C14H20Cl2N2O6	-2.7	0.9
326182	309.32	C17H15N3O3	48.1	0.9
326184	316	C15H10ClN3O3	36.0	0.3
326375	338	C23H18N2O	-6.2	0.9
326385	334	C10H5ClINO2	-1.1	2.0
326422	306	C14H18N4O2S	-4.0	1.0
326644	269	C14H9ClN4	4.6	0.4
326757	318.33	C20H14O4	-2.3	1.0
326921	274	C14H14N2S2	7.0	1.0
327444	268	C13H20N2S2	62.1	2.5
327693	248	C5H8N6O2S2	6.0	0.7
327702	353.44	C22H15N3S	-2.8	0.8
328010	336	C16H20N2O6	-3.4	1.9
328087	414	C21H17Cl2N3O2	-1.8	0.3
328111	325	C13H6Cl2N2O4	1.4	1.3
328130	261	C14H19N3S	-1.3	0.7
328403	427	C23H25NO7	-0.2	0.4
329052	322	C15H22N4O4	-2.9	1.5
329065	369	C20H23N3O2S	1.9	2.1
329249	348.76	C14H9ClN4O3S	-0.1	3.1
329250	349	C14H9ClN4O3S	-4.8	2.2
329255	329	C16H15N3OS2	-1.7	0.5
329284	212	C8H8N2O3S	3.7	2.0
329676	214	C7H10N4O4	5.5	0.6
330497	206	C12H18N2O	2.8	1.0
330500	560.69	C30H44N2O8	7.5	0.3
330770	311	C16H17N5O2	-5.3	3.5

Table 2.4 (cont.)

330796	283	C16H13NO4	5.1	1.3
331198	155	C6H9N3S	-18.6	3.6
331208	175	C8H9N5	-85.7	7.1
331968	301	C16H10Cl2N2	-3.9	1.3
331972	263	C13H17N3O3	-16.0	12.0
331977	254	C15H14N2O2	0.0	1.1
332452	286	C11H9ClFN3OS	-0.8	0.9
332473	220	C9H6ClN5	0.4	2.1
332670	310.35	C21H14N2O	-2.7	1.6
333544	336	C16H24N4O2S	-4.3	1.1
335048	239	C13H9N3O2	7.2	2.8
335504	337	C16H17ClN2O4	-0.6	1.4
335506	417.93	C18H21ClN2.C4H7NO3	-0.6	0.9
335649	166	C5H6N6O	18.0	5.0
335979	452	C25H29N3O5	-3.1	1.6
337726	304	C15H16N2O3S	0.5	0.8
337832	430	C14H20N6O3.C2H6O3S	-8.0	0.7
338042	392.46	C26H20N2O2	-1.3	0.1
338106	240	C11H8N6O	34.9	0.8
338205	175	C5H3ClN2O3	4.7	2.5
338519	355	C20H16F3N3	-0.8	1.0
338564	277	C13H13ClN4O	0.4	1.0
338578	318	C18H14N4O2	-3.4	0.9
339161	395	C20H15ClN4O3	2.5	5.3
339316	303	C15H21N5S	-2.5	0.6
339578	199	C10H9N5	-31.9	3.7
339589	322	C15H16ClN3OS	0.1	1.7
339594	339	C16H13N5O2S	-1.0	0.2
339630	339	C15H21N3.CH4O3S	-3.4	0.4
341074	241	C6H7N7O2S	5.5	3.5
341196	410.47	C22H26N4O4	1.7	0.3
341902	178	C9H10N2O2	0.8	3.3
341956	307.3	C15H17NO6	0.6	0.6
342459	469	C25H32N4O5	-2.2	0.4
342460	183	C7H9N3O3	-21.9	4.0
343230	226	C11H22N4O	6.1	0.2
343256	478	C29H35NO5	-3.4	0.8
343343	224	C10H6ClNOS	0.4	3.3

Table 2.4 (cont.)

343344	204	C10H8N2OS	14.9	0.6
343526	265	C12H11NO2S2	6.2	1.0
343549	301	C19H27NO2	-4.4	0.5
343550	309	C11H9BrN4S	-6.3	3.9
343557	281	C13H10Cl2N2O	5.9	1.5
343783	238	C9H10N4S2	3.6	1.7
344494	175	C6H4Cl2N2	36.7	6.8
345647	546.53	C30H26O10	28.2	0.4
345845	364.45	C24H20N4	-11.1	1.4
345850	332	C16H20N4O4	-1.3	1.8
346578	339	C20H18FNO3	-1.1	1.2
347463	357	C18H15NO5S	1.7	1.2
348970	258	C13H18N6	9.9	1.3
349156	325	C14H15NO8	-1.1	0.9
350187	388	C16H25N2O5PS	-1.4	1.1
351110	183	C8H9NO4	-40.6	3.3
351674	286	C20H18N2	-4.9	3.0
351691	260	C16H24N2O	-0.5	1.0
352888	279.34	C14H21N3O3	-11.1	11.4
352890	302.72	C11H14N4O4.ClH	0.1	1.9
353451	243	C7H7ClN6O2	2.3	3.8
354261	355	C19H21N3O4	0.2	0.4
354844	508.52	C28H28O9	-0.7	1.0
357683	223	C10H9NO5	0.6	0.8
358311	271	C14H13N3O3	0.8	1.2
359472	361.4	C20H19N5O2	-6.8	1.3
361056	198	C7H6N2O3S	-57.8	4.0
361570	283	C10H9N3O5S	-4.5	0.5
362093	275	C14H11ClN2O2	4.8	2.0
362639	344.24	C13H8N6O6	-4.1	1.3
363801	253	C15H15N3O	1.8	2.7
364889	299	C17H17NO4	-0.5	1.0
365560	187	C7H9NOS2	-18.7	1.1
366086	269	C9H7N3OS3	6.7	0.4
366289	303	C10H6Cl3N5	5.0	0.3
366801	333	C17H21ClN4O	-7.3	1.1
366802	298	C17H22N4O	5.5	0.3
366807	223	C9H9N3S2	9.1	0.7

Table 2.4 (cont.)

366808	197	C7H7N3S2	5.9	2.3
367306	381	C14H6Cl2F4N2O2	-5.2	0.8
367416	282	C14H10N4OS	-1.8	6.7
367428	220	C7H9FN2O5	12.2	1.6
367469	362	C14H16ClNO2S3	0.0	1.1
367474	281	C17H19N3O	-11.4	4.2
367480	298	C16H12ClN3O	-0.1	2.0
367487	205	C9H7N3OS	6.0	0.4
369066	269	C12H7N5O3	25.6	5.8
369070	299	C14H9N3O3S	-1.8	1.9
369986	329	C15H19N7O2	-4.7	1.9
370367	211	C9H7ClN2S	13.3	1.6
370383	264	C11H12N4O4	-0.8	1.0
370387	161	C6H3N5O	-10.3	2.5
371178	500	C29H33N5O3	-0.8	1.3
371765	318	C17H14N6O	-1.4	0.4
372063	191	C10H9NO3	-3.3	0.7
372134	243	C11H15ClN2O2	16.1	3.6
372146	305	C18H15N3O2	-11.9	1.1
372221	230	C12H14N4O	-2.8	2.3
372275	322	C19H18N2O3	-1.5	1.1
372287	339	C17H13N3O5	-2.1	2.8
372499	308	C18H16N2O3	-5.0	0.9
372767	345	C15H9BrN2O3	-7.0	0.4
372769	290	C15H9Cl2NO	-9.8	0.3
373427	245	C8H11N3O4S	6.4	1.1
373535	232	C12H12N2O3	-1.1	2.9
373600	401	C17H27N3O6S	-3.2	0.6
373981	257.25	C14H11NO4	-2.5	3.4
374703	298	C18H19O2P	2.1	1.2
374814	276	C15H20N2O3	-3.9	1.5
375105	285	C19H15N3	0.8	1.7
375392	210	C14H14N2	11.1	0.1
375981	337.33	C18H15N3O4	1.4	1.3
375982	344	C19H28N4O2	-2.2	2.8
375997	241	C12H11N5O	1.6	1.9
376254	447	C21H21NO8S	-0.4	0.8
378711	281	C14H17ClN2O2	-1.5	1.1

Table 2.4 (cont.)

378717	333	C17H19NO2S2	0.0	1.6
378719	404.25	C20H15Cl2NO4	-6.1	0.2
379099	402	C20H13Cl2NO4	-5.9	1.9
379388	359	C18H18FN3O2S	-3.2	0.6
379468	296	C13H11Cl2N3O	-9.9	2.7
379536	296	C10H9ClF3N3O2	-0.3	1.1
379538	304	C13H10ClN5S	-2.3	0.7
379555	357.81	C17H12ClN3O2S	-1.3	0.6
379639	245	C10H5ClN6	8.0	1.8
379651	277	C16H11N3O2	9.5	1.5
379696	499	C19H16Cl2N4O4S2	0.9	0.2
379697	343	C16H11ClN4OS	3.6	1.3
380279	295	C9H9N7O3S	-6.0	4.1
380802	363	C19H17N5O3	-5.4	2.6
382035	378.43	C20H22N6O2	0.3	0.5
382059	220	C11H12N2OS	-3.2	3.7
400770	274	C19H14O2	-2.0	0.7
400938	253	C13H11N5O	31.5	1.1
401077	334.33	C19H14N2O4	-4.9	2.4
402843	244	C8H9AsO4	12.5	2.1
403268	265	C11H7NO3S2	0.6	1.1
403374	229	C8H9ClN4S	15.8	0.9
403379	203.2	C9H9N5O	11.1	1.1
403447	304	C19H20N4	-0.1	0.6
407282	190.24	C11H14N2O	5.7	1.7
407628	302	C20H14O3	-5.7	0.7
408734	273	C11H11N7O2	-0.9	1.3
408860	286	C14H10N2O5	0.9	0.8
503425	202	C7H4ClNS2	-2.5	5.1
509563	243	C13H13N3S	3.0	3.1
513815	178	C7H6N4S	-13.6	2.3
515893	238	C13H22N2S	11.1	2.0
522131	297	C13H10Cl2N2O2	6.4	0.8
524385	268	C11H16N4O2S	-4.3	1.0
524615	278	C16H22O4	-3.6	1.1
525721	271	C15H13NO2S	-6.4	4.1
601351	240.26	C10H16N4O3	6.3	0.9
601359	392.25	C21H14BrNO2	-1.5	1.2

Table 2.4 (cont.)

603071	363.37	C20H17N3O4	0.7	0.6
605333	223	C14H9NS	10.6	0.8
607097	357.41	C19H23N3O4	-10.6	1.1
614826	361.4	C22H19NO4	-6.3	1.4
622175	203	C9H9N5O	6.5	1.9
622608	322.24	C9H11N3OS2.BrH	-2.1	2.9
622689	353	C10H10ClN3S2.BrH	24.3	0.9
622691	317	C10H11N3OS4	2.6	0.9
623109	307	C9H13BrClN5	-9.5	1.3
623638	350	C21H22N2O3	-3.0	0.9
630602	347	C22H21NO3	-1.7	1.4
631160	317	C12H11N7O2S	1.6	1.7
632536	323.48	C21H29N3	6.3	1.2
634396	347	C17H15ClN2O2S	-3.1	1.5
636717	250	C17H14O2	10.3	1.6
636718	264	C18H16O2	41.6	1.8
636734	279	C17H13NO3	25.7	0.4
637153	327	C14H15BrO4	5.6	1.1
637290	215	C13H13NO2	16.3	0.8
637317	344	C13H15BrNO3P	-8.7	5.1
637325	310	C13H15N2O5P	-3.0	2.4
637343	276	C18H16N2O	11.4	2.5
637359	258	C17H10N2O	54.9	2.2
637578	325	C20H15N5	0.5	0.9
637827	276	C19H16O2	-1.4	1.8
638080	220	C10H8N2O4	45.0	1.2
638134	203	C11H9NO3	7.8	1.0
638432	407	C24H22N2O2.ClH	-9.9	2.5
638636	257	C7H16NO.I	4.8	0.5
641396	291	C18H13NO3	31.8	0.8
643029	280	C19H20O2	-4.2	1.0
643150	222	C14H10N2O	12.9	1.3
645033	372	C18H15Cl2N5	0.3	0.7
645330	275	C18H13NO2	33.8	1.8
645987	242	C12H10N4O2	86.7	0.3
646976	233	C12H11NO4	6.8	2.6
647136	238	C15H14N2O	55.8	1.5
650438	179	C9H9NO3	77.6	0.9

Table 2.4 (cont.)

651084	347	C16H17N3O6	9.7	2.1
653004	291	C17H25NO3	-1.1	0.2
654260	549.81	C22H21BrN6O4.ClH	-2.8	0.6
659107	244	C13H12N2OS	11.3	1.0
660151	304	C15H17N2O3P	-0.3	0.2
660300	249	C11H11N3O4	11.7	2.0
661122	370	C22H26O5	-5.2	0.8
661221	275	C18H13NO2	32.0	0.2
664971	169	C8H15N3O	1.1	0.6
665497	368	C20H16O7	-2.0	0.6
670283	356.46	C25H24O2	-2.4	1.0
672441	158	C8H18N2O	-3.7	3.3
672865	367	C17H16F2NO4P	-3.0	1.4
679525	533	C27H20N2O8S	8.8	1.8
680495	312	C15H10BrN3	39.7	3.1
680515	265	C16H15N3O	19.3	1.2
680516	290	C18H18N4	16.9	0.3
689002	287	C14H9NO4S	-0.2	1.6
727038	542	C34H43N3O3	-15.1	2.1

CHAPTER 3: SYNERGISTIC ANTI-CRYPTOSPORIDIAL EFFICACY OF CPPYK AND CPLDH INHIBITORS

3.1 ABSTRACT

Cryptosporidium is an opportunistic intracellular protozoan parasite that causes serious enteric disease in humans and in a wide range of animals worldwide. Despite its high prevalence, no effective therapeutic drugs are available against life-threatening cryptosporidiosis in at-risk populations including malnourished children, immunocompromised patients, and neonatal calves. Thus, new efficacious drugs are urgently needed to treat all susceptible populations with cryptosporidiosis. Unlike other apicomplexans, *C. parvum* lacks the tricarboxylic acid cycle and the oxidative phosphorylation steps, making it solely dependent on glycolysis for metabolic energy production. We have previously reported that individual inhibitors of two unique glycolytic enzymes, the plant-like pyruvate kinase (CpPyK) and the bacterial-type lactate dehydrogenase (CpLDH), are effective against *C. parvum*, both *in vitro* and *in vivo*. Herein, we have derived combinations of CpPyK- and CpLDH-inhibitors with strong synergistic effects against the growth and survival of *C. parvum*, both *in vitro* and in an infection mouse model. In infected immunocompromised mice, compound combinations of NSC303244 + NSC158011, and NSC252172 + NSC158011, depicted enhanced efficacy against *C. parvum* reproduction, and ameliorated intestinal lesions of cryptosporidiosis at doses 4-fold lower than the total effective doses of individual compounds. Importantly, unlike individual compounds, NSC303244 + NSC158011 combination was effective in clearing the infection completely without relapse in immunocompromised mice. Collectively, our study has unveiled compound combinations that simultaneously block two essential catalytic steps for metabolic energy production in *C. parvum* to achieve improved efficacy against the parasite. These combinations are, therefore, lead-compounds for the development of a new generation of efficacious anti-cryptosporidial drugs.

3.2 INTRODUCTION

The opportunistic enteric parasite, *Cryptosporidium* is a leading cause of waterborne and foodborne outbreaks of infectious diarrhea across the globe (Zahedi and Ryan, 2020). In addition to diarrhea-related malnutrition, *Cryptosporidium* infection can result in reduced physical fitness and impaired cognitive function in early childhood (Guerrant et al., 1999). Of the currently recognized 44 *Cryptosporidium* species, the zoonotic *Cryptosporidium parvum* and the anthroponotic *Cryptosporidium hominis* are the most dominant species causing human infections (Ryan et al., 2021b). Several epidemiological studies conducted over the previous decade have reported *Cryptosporidium* to be an important cause of infectious diarrhea, growth defects, and mortality in young children living in under-developed countries (Kotloff et al., 2013; Platts-Mills et al., 2015; Khalil et al., 2018; Nasrin et al., 2021). *Cryptosporidium* generally causes a self-limiting illness in immunocompetent individuals, however, those with reduced immunity such as malnourished children or HIV-infected patients are most at risk for severe disease. In the latter group of patients, especially the ones suffering from HIV/AIDS, *Cryptosporidium* infection is chronic, difficult to treat, and often life-threatening (Desai et al., 2012). Although the use of highly active antiretroviral therapy (ART) in HIV-infected patients has significantly reduced the global frequency and severity of cryptosporidiosis in this patient population (Wang et al., 2018), advanced AIDS patients with very low CD4+ cell counts continue to show high parasite infection rates despite receiving effective ART (Tuli et al., 2008; Nsagha et al., 2016). Furthermore, the use of ART in AIDS patients with chronic diarrhea has been associated with increased early mortality (Dillingham et al., 2009). Besides humans, *C. parvum* also causes severe diarrhea in neonatal animals, especially calves, leading to impaired growth rates and ensuing high economic and production losses (Shaw et al., 2020).

Despite the strong impact of cryptosporidiosis on public health worldwide, effective control, treatment and vaccination strategies are currently lacking (Khan and Witola, 2023). Several compounds have shown good efficacy in cell culture and laboratory animal-based models of cryptosporidiosis. A few among those have advanced to clinical trials in humans and agricultural animals, but without success (Khan and Witola, 2023). Thus, there is a critical need for the development of novel anti-cryptosporidial therapeutics to ease the growing burden of cryptosporidiosis especially in low-income countries.

C. parvum seems to rely mainly on glycolysis for metabolic energy production due to the absence of functional mitochondria for the Krebs cycle and cytochrome-based electron transfer (Abrahamsen et al., 2004). Therefore, essential glycolytic enzymes such as *C. parvum* pyruvate kinase (CpPyK) and *C. parvum* lactate dehydrogenase (CpLDH) that are structurally and functionally unique to *C. parvum* are promising drug targets for this parasite (Cook et al., 2012; Cook et al., 2015). Consistent with this notion, we have previously identified small molecule inhibitors of recombinant CpPyK and CpLDH proteins' enzymatic activities and demonstrated their efficacy against *C. parvum*, both *in vitro* and *in vivo* (Li et al., 2019; Khan et al., 2022b). In *C. parvum*, glycolysis begins with the activation of glucose or fructose and ends with the production of pyruvate and ATP, the final reaction being catalyzed by CpPyK. Pyruvate is then rapidly converted to lactate (catalyzed by CpLDH) with the regeneration of cofactor NAD+, which is cycled back so that glycolysis can continue. Being cognizant of the importance of both CpPyK and CpLDH for efficient energy production in *Cryptosporidium*, we hypothesized that simultaneous inhibition of these enzymes could block glycolysis completely leading to severe growth and replication defects in the parasite. Thus, in the present study, we investigated the anti-cryptosporidial synergistic activities of CpPyK- and CpLDH-inhibitors in *C. parvum*-

infected mammalian cells and immunocompromised mice. Using multiple approaches, we endeavored to determine specific combinations and concentration ratios of CpPyK- and CpLDH-inhibitors, and tested them against *C. parvum* infection, both *in vitro* and *in vivo*, with the goal of deriving combinations with improved synergistic efficacy at relatively lower doses than those of the respective individual inhibitors.

3.3 RESULTS

3.3.1 Identification of non-toxic concentrations of compound combinations.

The half-maximal cytotoxic concentration (CC_{50}) values of CpPyK-inhibitors (NSC234945, NSC252172, NSC303244, and NSC638080) and CpLDH-inhibitors (NSC158011 and NSC10447) in human ileocecal colorectal adenocarcinoma (HCT-8) cell monolayers have been reported previously (Li et al., 2019; Khan et al., 2022b). To evaluate compound combinations for *in vitro* anti-cryptosporidial effect, we first determined specific concentration ratios of combinations of CpPyK- and CpLDH-inhibitors that were not toxic to HCT-8 cells. We used a fixed-ratio ray design (Straetemans et al., 2005) to mix individual compounds using three mixture factor (*f*) values (0.25, 0.5, and 0.75) corresponding to three different ratios of the compounds based on their previously reported anti-cryptosporidial half-maximal effective concentration (EC_{50}) values (Li et al., 2019; Khan et al., 2022b). Use of multiple combination ratios for each combination allowed us to cover a larger spectrum of interaction between the two classes of compounds. Using this method, we derived a total of 24 unique compound mixtures of CpPyK + CpLDH inhibitors (Table 3.1). We used the WST-1 assay for evaluating the cytotoxicity of the compound mixtures against the host cell line (HCT-8) used for *in vitro* culture of *C. parvum*. The WST-1 assay is based on the reduction of tetrazolium salt to formazan within the mitochondria of metabolically active cells. Each compound mixture was analyzed at several

increasing concentrations to determine its *in vitro* cytotoxicity against uninfected cells. The highest concentration of each compound mixture (Table 3.1) that did not result in more than 20% mean percent toxicity (MPT) to host cells was used as the maximum concentration limit for subsequent *in vitro* efficacy assays.

3.3.2 Synergistic *in vitro* anti-cryptosporidial efficacy of CpPyK- and CpLDH-inhibitors.

To ascertain the effect of combinations of CpPyK- and CpLDH-inhibitors on the growth and development of *C. parvum*, we performed *in vitro* parasite growth inhibition assays using infected HCT-8 cell monolayers. Increasing non-toxic concentrations of individual and mixture compounds were tested to evaluate their *in vitro* efficacy against *C. parvum*. The experimental data from test wells were normalized to that of wells treated with dimethyl sulfoxide (DMSO, negative control) and paromomycin (positive control). To demonstrate synergistic efficacy, several analytical methods such as isobologram analysis, combination-index (CI) method, curve-shift analysis, EC_{50} comparison, and dose-reduction index (DRI) analysis were utilized to analyze the concentration-response data. Figure 3.1 shows the isobologram plots of all the tested combinations. The isobologram approach is a graphical depiction of how drugs interact with each other from a pharmacological standpoint. Combination data points that fall below, on, or above the diagonal line formed by joining the individual compound EC_{75} values (line of additivity) indicate synergism, additivity, or antagonism, respectively. For the combinations of NSC252172+NSC10447 and NSC303244+NSC10447 concentration ratios of 1:6 (0.25*f*) and 1:2 (0.5*f*) were synergistic while the 3:2 concentration ratio (0.75*f*) was additive (Figure 3.1 and Table 3.1). Likewise, combinations of NSC252172+NSC158011 and NSC303244+158011 at 1:3 (0.25*f*) and 1:1 (0.5*f*) concentration ratios were synergistic and antagonistic, respectively (Figure 3.1 and Table 3.1). On the other hand, the 3:1 (0.75*f*) concentration ratio for

NSC252172+NSC158011 and NSC303244+NSC10447 was antagonistic and synergistic, respectively (Figure 3.1 and Table 3.1). Interestingly, for all the above-mentioned combinations, compound mixtures with a mixture factor of 0.25*f* demonstrated the most synergy. The remaining 4 combinations (NSC234945+NSC10447, NSC234945+NSC158011, NSC638080+NSC10447, and NSC638080+NSC158011) were mostly antagonistic, or additive at the tested combination ratios (Figure 3.1 and Table 3.1).

The synergistic activity of CpPyK- and CpLDH-inhibitor combinations was also reflected in the CI analyses of the *in vitro* concentration-response data (Figure 3.2). Unlike the isobologram approach, the CI method offers a means of quantifying the pharmacologic interaction between two drugs. We used a computer software based on the CI algorithm of Chou and Talalay (Chou and Talalay, 1984) to generate CI values for data from the parasite growth inhibition assays. In general, a CI value of 1 indicates an additive effect between two agents, whereas a CI value less than or greater than 1 indicates synergism or antagonism, respectively. The outcomes derived from the CI analyses were comparable to the results obtained from the isobologram analyses, and compounds combined in concentration ratios based on the 0.25*f* and 0.5*f* mixture factors showed the highest synergistic effects, particularly for NSC252172+NSC10447 and NSC303244+NSC10447 combinations (Figure 3.2).

The CI and the isobologram analyses were well supported by the curve-shift analyses as evidenced by a left-ward shift of concentration-response curves for synergistic combinations and a right-ward shift for the antagonistic combinations, as compared to the corresponding single compound curves (Figure 3.3). This outcome meant that synergistic combinations required relatively lower concentration values compared with individual compounds to produce the same *in vitro* anti-cryptosporidial effect. Indeed, this was also evident when we compared the EC_{50}

values of individual compounds and their combinations (Figure 3.4). We found that synergistic combinations had lower EC_{50} values than their corresponding individual compounds, and that the reverse was true for antagonistic combinations. For instance, the anti-cryptosporidial EC_{50} of the NSC303244+NSC158011 (0.25*f*) combination was almost 2-fold lower than those of the individual compounds. On the other hand, the 0.75*f* NSC638080+NSC10447 combination had a higher EC_{50} than both individual compounds (Figure 3.4).

Furthermore, we calculated DRI values for compound mixtures of CpPyK- and CpLDH-inhibitors at three parasite inhibition levels using the CompuSyn software (ComboSyn, Inc.). The DRI method assesses how much the dosage of one or more compounds in the combination can be decreased while still producing similar effects compared to using the compounds individually. Drug combinations that demonstrate substantial reduction in dosage (DRI >1) can be recognized as those that act synergistically. Table 3.2 lists the DRI values of compound mixtures at the 50%, 75%, and 90% effect levels. DRI values were found to be greater than 1 for compounds in all combinations at all effect levels with higher overall DRI values for CpPyK-inhibitors compared with CpLDH-inhibitors.

3.3.3 Anti-cryptosporidial efficacy of combinations of CpPyK- and CpLDH-inhibitors in infected mice.

Based on the results derived from the synergy assessment methods described above, the combinations of NSC252172+NSC158011, NSC252172+NSC10447, and NSC303244+NSC158011 prepared at the 0.25*f*, 0.5*f*, and 0.25*f* mixture factors, corresponding to the concentration ratios of 1:3, 1:2, and 1:3, respectively, (Table 3.1), were found to possess the most anti-cryptosporidial potency and were thus selected for further investigation in an immunocompromised mouse model of cryptosporidiosis. Before the start of efficacy experiments, we tested synergistic CpPyK- and CpLDH-inhibitors individually and in

combination at increasing doses in interferon gamma knockout (IFN-γ KO) mice to derive non-toxic doses for *in vivo* studies that did not induce any toxicity signs (changes in normal physical and mental activity, feeding pattern, body posture, body weight, fur condition, or occurrence of death) over 5 days of treatment (Table 3.3). Initially, the individual CpLDH-inhibitors were tested at doses that were 2-5-fold lower than their reported effective doses (Li et al., 2019), and were thus not expected to depict significant potency against *C. parvum* infection in mice. Additionally, individual CpPyK-inhibitors were tested at doses lower than those used for CpLDH-inhibitors since the former inhibitor class has generally been found to be more potent than the latter one in our previous study (Khan et al., 2022b). The individually evaluated treatments were NSC252172 (CpPyK-inhibitor) at 75 mg/kg, NSC303244 (CpPyK-inhibitor) at 37.5 mg/kg, NSC158011 (CpLDH-inhibitor) at 150 mg/kg, and NSC10447 (CpLDH-inhibitor) at 200 mg/kg. Then, to determine whether administering the compounds in combination (CpLDH+CpPyK inhibitors) at lower doses would confer synergistic effects and, therefore, possess potency against *C. parvum*, the combinations were tested at doses that were at least 35% lower than their individual compound doses and at least 4-fold lower than the combined reported effective doses of individual compounds (Li et al., 2019; Khan et al., 2022b). Those evaluated combination treatments were NSC252172+NSC158011 (100 mg/kg, 1:3 ratio), NSC252172+NSC10447 (150 mg/kg, 1:2 ratio), and NSC303244+NSC158011 (100 mg/kg, 1:3 ratio). Paromomycin was used as a positive control at 1000 mg/kg once daily orally (Griffiths et al., 1998). Fecal oocyst shedding was confirmed by quantitative real time PCR (qPCR) on day 3 post-infection, following which oral gavage treatment of mice with compounds, paromomycin or vehicle control commenced.

As expected, vehicle control treatment group mice showed a progressive increase in oocysts shedding, with a peak load of about 5×10^7 oocysts per gram of feces (OPG) being attained by day 9 post-infection (Figure 3.5). Treatments with individual compound NSC252172 (75 mg/kg) and paromomycin showed sustained lower ($P < 0.05$) oocysts counts than the vehicle control treatment until the end of treatment (Figure 3.5). On the other hand, treatment with individual compound NSC10447 (200 mg/kg) had no notable effect on oocysts shedding when compared to the vehicle control treatment (Figure 3.5). Further, combination treatment with NSC252172+NSC10447 (at lower combined dose than that of individual compounds) also did not have effect on oocysts shedding (Figure 3.5), implying that this particular combination was not synergistic *in vivo*.

Post-treatment, all groups of mice were observed for an additional 11 days for disease progression or relapse of infection. During this period, the average oocyst loads in the vehicle control-, the NSC252172+NSC10447 combination-, and the individual NSC10447-treatment groups rose to higher peaks at day 16 post-infection than those observed earlier at day 9 post-infection (Figure 3.5). Interestingly, the oocyst loads in the NSC252172- and paromomycin-treatment groups (that had earlier been lower than in the vehicle control group) had started to rebound (Figure 3.5). This indicated that the *C. parvum* infection in mice treated with NSC252172 or paromomycin relapsed promptly after treatment withdrawal, suggesting that these compounds inhibited parasite reproduction without killing the parasite.

Next, we tested the effect of NSC252172+NSC158011 combination in comparison to the individual compounds. Treatment of mice with NSC158011 (150 mg/kg) resulted in lowered oocysts load in feces of infected mice at the end of the treatment period, although not statistically significant ($P > 0.05$), when compared to the vehicle control group (Figure 3.6). Notably,

NSC252172+NSC158011 combination treatment, and individual NSC25172 and paromomycin treatments resulted in significant ($P < 0.05$) reductions in oocysts loads starting at day 9 until the end of treatment (Figure 3.6). But as earlier observed for paromomycin and NSC158011, cessation of treatment with NSC252172+NSC158011 combination or individual NSC158011 led to a relapse of infection (Figure 3.6).

In the third treatment trial, we compared the effects of combination of NSC303244+NSC158011 to the respective individual compounds, paromomycin and vehicle control treatments on oocysts load in *C. parvum*-infected mice. In a similar manner to individual treatment with NSC158011, treatment with individual NSC303244 led to reduced oocysts loads that relapsed after treatment was withdrawn (Figure 3.7). Intriguingly, NSC303244+NSC158011 combination treatment resulted in sustained very low oocysts counts in feces, that continued to decline even after cessation of treatment, reaching nearly zero count by day 22 post-infection when the oocysts loads in other treatment groups were rapidly increasingly exponentially (Figure 3.7). This strongly indicated that combination of NSC303244 (CpPyK-inhibitor) and NSC158011 (CpLDH-inhibitor) resulted in a synergistic effect that was parasiticidal. Corroboratively, when the entire shedding-monitoring period was considered, the combination of NSC303244 and NSC158011 was the only treatment observed to significantly decrease ($P < 0.01$) the average fecal oocysts count in infected mice in comparison to the vehicle control (Table 3.4).

Analysis of the daily changes in the body weight of mice showed that the mean weight of the untreated mice decreased by 22% (from 24.3 g on day 3 to 19 g on day 22 post-infection) (Figure 3.8). In contrast, the average weight of the mice treated with the NSC303244+NSC158011 combination only dropped by 3% (from 24.4 g on day 3 to 23.6 g on

day 22 post-infection), a nearly seven-fold difference compared to the vehicle control group ($P < 0.01$) (Figure 3.8). Interestingly, paromomycin-treated mice despite shedding considerable numbers of oocysts during the monitoring phase; showed no apparent clinical signs of infection and minimal loss of body weight from day 3 until day 22 (1.5 g, ~6%). Griffiths et al. reported a similar finding after treating *C. parvum*-infected IFN-γ KO mice with a lower dose of paromomycin (Griffiths et al., 1998). All other treatment groups lost body weight comparable to the untreated group of mice by the end of the experiment (Figure 3.8).

One day after cessation of treatment, two mice per treatment group were randomly selected and sacrificed for intestinal histopathological examination. As expected, the uninfected control group samples showed a healthy intestinal mucosa with prominent villi. There were no obvious differences in the structure and organization of the intestinal mucosa of mice that were treated with NSC252172, NSC303244, NSC252172+NSC158011, NSC303244+NSC158011, or the positive control paromomycin, when compared to the uninfected mice (Figure 3.9). These findings were consistent with the significantly reduced number of oocysts detected in these groups during the treatment phase. On the contrary, mice treated with the vehicle control had lesions characterized by mucosal erosion, villous atrophy, hypertrophy of the crypts, and inflammation. Similar but milder lesions were observed in the intestinal mucosa of mice treated with NSC158011, NSC10447, and the NSC252172+NSC10447 combination (Figure 3.9).

To evaluate the impact of treatment discontinuation on the recurrence or advancement of the disease, we sacrificed all the remaining mice on day 23 and performed histopathological analysis of intestinal tissue samples. As anticipated, at this stage, the vehicle control mice depicted pronounced pathological lesions of severe illness including denudation and blunting of intestinal villi, severe mucosal erosion, and marked widespread infiltration of inflammatory cells

(Figure 3.10). Similar to the vehicle control, mice from the NSC158011, NSC10447, and NSC252172+NSC10447 treatment groups showed an escalation of pathological changes in the small intestinal mucosa by day 23 (Figure 3.10). Likewise, on day 23, we observed microscopic intestinal lesions of cryptosporidiosis in mice treated with NSC252172, NSC303244, NSC252172+NSC158011, or paromomycin, suggesting a relapse of infection, which correlated with the elevated oocyst load observed after treatment was discontinued on day 12. However, these lesions were milder than the ones observed in the vehicle control on that day. In contrast, the NSC303244+NSC158011 combination had a noticeable effect in preventing intestinal pathology in infected mice even after treatment cessation, as evidenced by the preservation of the intestinal epithelium with intact villi on day 23 (Figure 3.10).

3.4 DISCUSSION

Cryptosporidiosis is a leading cause of diarrheal illness worldwide. Yet, the development of efficacious therapies for this important parasitic infection remains a significant challenge in public health. Currently, there are no effective treatments for cryptosporidiosis, especially in vulnerable populations including children, immunocompromised individuals, and neonatal calves. Nitazoxanide is the only drug approved by FDA for treating cryptosporidiosis in immunocompetent humans, but it remains ineffective for those who are susceptible to the disease (Checkley et al., 2015). Although halofuginone lactate is licensed for treating calf cryptosporidiosis in Europe and Canada, it is not approved for use in the United States. Regardless, halofuginone lactate has a limited safety margin and is contraindicated in dehydrated animals with diarrhea, a clinical finding consistent with cryptosporidiosis in neonatal calves (Santin, 2020). Thus, finding effective treatments for this human and animal disease continues to be a top priority. We provide compelling evidence for the effectiveness of combination therapy

in the treatment of cryptosporidiosis by deriving specific combinations of compounds that target two unique enzymes in the glycolytic pathway for the generation of metabolic energy for the parasite, leading to greater efficacy than individual compounds in cell culture and animal models at reduced doses.

C. parvum lacks functional mitochondria along with the genes encoding enzymes of the Krebs cycle and the electron transport chain (Abrahamsen et al., 2004). Consequently, the glycolytic pathway is a critical metabolic pathway in this parasite and is believed to be essential for parasite survival and pathogenesis. By simultaneously targeting two enzymes in this pathway, we aimed to completely disrupt the energy production in the parasite and eventually kill it. While glycolysis is a conserved metabolic pathway in most eukaryotic organisms, making it challenging to develop drugs that selectively target the parasite without affecting the host, the cryptosporidial glycolytic enzymes are, nevertheless, significantly different from those found in mammals. Further, our previous studies have demonstrated that inhibitors against two of these enzymes, CpPyK and CpLDH, possess high therapeutic indices for treating experimental *C. parvum* infections (Li et al., 2019; Khan et al., 2022b). Therefore, in the present study, we tested the efficacy of various combinations of CpPyK- and CpLDH-inhibitors against *C. parvum* in cell culture and animal models. Our results showed that CpPyK- and CpLDH-inhibitors, when combined at suboptimal concentrations, were able to effectively inhibit the growth and proliferation of these parasites compared to the use of either of the compounds alone. Of particular significance, the combination of NSC303244 (CpPyK-inhibitor) and NSC158011 (CpLDH-inhibitor) was successful in preventing relapse of infection in IFN-γ knockout mice, a suitable and widely used immunodeficient model of cryptosporidiosis (Griffiths et al., 1998), even after discontinuation of treatment. This is a promising finding as relapse is a common

problem in the treatment of cryptosporidiosis in susceptible individuals, and management of the disease often requires extended treatment periods or multiple rounds of treatment (Maggi et al., 2000; Lanternier et al., 2017).

Most drug discovery efforts for cryptosporidiosis have historically relied on testing individual compounds and none of these studies has been able to translate the research findings into an effective cure for cryptosporidiosis to date (Love and Choy, 2021). Some *Cryptosporidium* drug discovery efforts, however, have screened a combination of two or more drugs and noted a marked improvement in efficacy against the parasite in cell culture (You et al., 1998; Giacometti et al., 2000; Hommer et al., 2003). Moreover, several combination therapies have been shown to improve clinical outcomes compared with monotherapy in immunocompromised humans and animals with *Cryptosporidium* infections (Khan and Witola, 2023). However, these potential anti-cryptosporidial therapies have not been followed up in large controlled clinical trials despite the increasing importance of combination therapies for the treatment other related apicomplexan protozoan infections including *Plasmodium*, *Babesia* and *Toxoplasma*.

Combination therapy has several advantages over monotherapy, including increased efficacy, reduced toxicity, and decreased risk of drug resistance. The effectiveness of the combination therapy in our study can be attributed to the fact that targeting two important enzymes in the glycolytic pathway effectively disrupts the generation of metabolic energy for the parasite. CpPyK plays a central role in the energy metabolism of *C. parvum* and serves as a key metabolic control point as both the substrate (phosphoenolpyruvate) and the product (pyruvate) of this enzyme feed into several metabolic pathways essential to the parasite. Similarly, CpLDH plays a critical role in glycolysis, allowing for the interconversion of pyruvate and lactate and the

regeneration of NAD+ from NADH which is required for glycolysis to continue. In *C. parvum*, CpPyK is constitutively expressed in the cytosol during all parasite stages (Mauzy et al., 2012) with relatively higher expression seen in intracellular stages than oocysts and sporozoites (Mirhashemi et al., 2018; Tandel et al., 2019), suggesting that this enzyme is vital for energy production during intracellular parasite growth. In contrast, CpLDH is localized mainly in the cytosol in extracellular parasites including sporozoites within oocysts, free sporozoites, and merozoites but becomes associated with the parasitophorous vacuole membrane (PVM) during intracellular development, suggesting involvement of the PVM in the energy metabolism of *C. parvum* (Zhang et al., 2015). Moreover, CpLDH expression in intracellular parasites is significantly weaker than that observed in extracellular parasite stages (Mirhashemi et al., 2018; Tandel et al., 2019), indicating that this enzyme is mainly utilized for energy metabolism in the invading life cycle stages. Concurrent inhibition of these enzymes, therefore, produces strong synergistic inhibitory effects on the energy metabolism of all parasite stages by shutting down ATP generation through the glycolytic cycle. Our findings are significant in light of the worrying emergence of drug resistant parasites during anti-cryptosporidial treatment as recently evidenced using a promising tRNA synthetase inhibitor (Hasan et al., 2021).

The effectiveness of drug combinations may vary depending on the individual properties of each drug, their dosages, drug ratios, and potential drug-drug interactions. For some classes of compounds, certain ratios may have a synergistic effect while others might be antagonistic, a widely acknowledged phenomenon in pharmacology (Tallarida, 2011). Thus, when combining drugs, multiple ratios should be used to achieve the desired therapeutic effect while minimizing side effects. In this study, we used a fixed-ratio design based on individual EC_{50} values for combining CpPyK- and CpLDH-inhibitors. Moreover, we used 3 values of the mixture factor to

design different compound mixtures for each combination and assessed synergy by multiple approaches. By using multiple fixed-ratios, we were able to explore different combinations and concentrations of compounds and test them independently for both cytotoxicity and anti-cryptosporidial efficacy in mammalian cells. We observed that different concentration-ratio mixtures within the same combination showed markedly different responses to each other. Importantly, the various synergy-assessment methods used in our study demonstrated this crucial outcome, with the ability to identify effective and safe compound mixtures with the greatest synergistic interaction for *in vivo* studies.

The NSC251272+NSC10447 combination, although found to be synergistic *in vitro*, showed reduced efficacy in infected mice. There are several possible reasons to explain this unexpected outcome. For example, the pharmacokinetics of the individual drugs in this combination may differ, and their levels and distribution *in vivo* could be impacted differently, leading to a reduced effect compared to *in vitro*. Other factors that may be responsible for reduced *in vivo* efficacy include drug-drug interactions and differences in cellular environment at the target site. Meanwhile, based on the monitoring of relapse of infection in infected mice, the NSC303244+NSC158011 combination was apparently parasiticidal for *C. parvum* while most individual compounds, paromomycin, and the combination of NSC252172 and NSC158011 were parasitistatic. A “cidal” antiparasitic agent is one that kills parasites without depending on the patient's immune system for assistance. On the other hand, a “static” agent is one that inhibits the growth and multiplication of the parasite without necessarily killing it, thus allowing the patient’s immune system to kill off the parasite leading to recovery from the infection. Clearly, parasiticidal agents are more desirable for treating cryptosporidiosis in malnourished children, immunocompromised humans, and neonatal calves, a patient population in which there is

minimal host defense. In addition, the development of such drugs is essential in the fight against the inevitable rise of resistance to anti-cryptosporidial drugs. Thus, the parasiticidal nature of the NSC303244+NSC158011 combination is extremely valuable for our efforts to find a much-needed cure for cryptosporidiosis.

3.5 MATERIAL AND METHODS

3.5.1 Parasites and host cells.

The *C. parvum* AUCP-1 isolate was maintained and propagated in male Holstein calves. *C. parvum* oocysts were extracted and purified from freshly collected calf feces by sequential sieve filtration, Sheather's sugar flotation, and discontinuous sucrose density gradient centrifugation (Arrowood and Sterling, 1987; Current, 1990). Purified oocysts were washed and stored in phosphate-buffered saline (PBS) at 4°C and used within 3 months to ensure maximum viability as judged by excystation. *C. parvum* sporozoites were excysted from oocysts as previously described (Kuhlenschmidt et al., 2016), but with slight modifications. Briefly, 1×10^8 purified *C. parvum* oocysts were suspended in 500 µl of PBS and treated with an equal volume of 40% commercial laundry bleach for 10 min on ice, followed by four washes in PBS containing 1% bovine serum albumin. Oocysts were suspended in Hanks balanced salt solution (HBSS, Corning), incubated for 60 min at 37°C, and mixed with an equal volume of warm 1.5% sodium taurocholate in HBSS, followed by further incubation for 60 min at 37°C. The excysted sporozoites were pelleted by centrifugation and resuspended in RPMI-1640 medium containing 1% heat-inactivated fetal bovine serum (Hi-FBS; Gibco). The sporozoites were separated from oocyst shells and unexcysted oocysts by passing the suspension through a sterile 5 µm syringe filter (Millex™; Millipore). Purified sporozoites were enumerated with a hemocytometer and used immediately for infection of cell monolayers.

For *in vitro* studies, HCT-8 cells (HCT-8 [HRT-18]; ATCC® CCL-244™, RRID:CVCL_2478) were used. Cells were cultured and maintained in RPMI-1640 medium (Gibco) supplemented with 2.5 g/L of glucose, 1 mM sodium pyruvate, 1.5 g/L of sodium bicarbonate, 10% Hi-FBS (Gibco), and 1× Antibiotic-Antimycotic (Gibco) at 37°C with 5% CO_2 in a humidified incubator.

3.5.2 Chemical compounds.

Compounds, originally from the National Cancer Institute (NCI) Diversity Set VI chemical library, were procured from different chemical vendors: NSC234945 and NSC10447 were obtained from A2B Chem LLC USA; NSC158011 and NSC252172 were acquired from AKos Consulting & Solutions GmbH Germany; NSC303244 and NSC638080 were purchased from ChemSpace LLC USA. All compounds were ≥95% pure as determined by liquid chromatography-mass spectrometry (LC-MS) and/or proton nuclear magnetic resonance (proton NMR) analysis and were shipped as powder. Upon receipt, compounds were individually reconstituted in cell culture grade DMSO (ATCC) and stored as stock solutions at -20°C. For *in vitro* experiments, stock solutions of compounds and their combinations were diluted in RPMI-1640 medium to produce working solutions for testing cytotoxicity and anti-cryptosporidial efficacy. For *in vivo* studies, stock solutions of individual compounds and their combinations were diluted in 100% (v/v) polyethylene glycol 400 (PEG 400; Rigaku Reagents) to a final DMSO concentration of 25%. Paromomycin sulfate (Thermo Scientific) was used as a control for *in vitro* and *in vivo* studies because of its previously reported activity against *C. parvum* (Griffiths et al., 1998; Khan et al., 2022a).

3.5.3 Compound combination model.

The fixed-ratio or ray design model of drug combination (Straetemans et al., 2005) was used for combination of compounds for *in vitro* studies. Briefly, two classes of compounds (CpPyK- and CpLDH-inhibitors) were combined to prepare a compound mixture *Z* according to the formula:

$$Z = fA + (1 - f)\,B,$$

where A and B are *in vitro* anti-cryptosporidial half-maximal effective concentration (EC_{50}) values of individual CpPyK- and CpLDH-inhibitors respectively, and *f* is the mixture factor. Compounds were combined in concentration ratios based on 3 values of *f* (0.25, 0.5, and 0.75) to prepare 3 compound mixtures for each compound combination. Each compound mixture was considered as a new compound and tested *in vitro* for cytotoxicity and anti-*Cryptosporidium* efficacy.

3.5.4 *In vitro* cytotoxicity assay.

A colorimetric assay using the cell proliferation reagent WST-1 (Roche) was performed for the quantification of *in vitro* cytotoxicity of compound combinations in HCT-8 cells. About 5×10^4 HCT-8 cells were seeded per well in flat-bottomed 96-well plates and grown overnight in 200 µl of supplemented RPMI-1640 medium. Upon reaching 80 - 90% confluency, cells were treated in quadruplicate with increasing concentrations of each fixed-ratio chemical compound mixture (reconstituted in DMSO) for 48 hours. The volume of DMSO did not exceed 1% of the total culture volume in any of the wells to avoid DMSO toxicity to the cells. Control wells received equivalent volumes of DMSO instead of the compounds. Ten microliters of the WST-1 reagent were added to each well after 48 h of culture, and the plates were incubated for 30 min at 37°C with 5% CO_2 under dark conditions. Following incubation, the plates were shaken thoroughly and 150 µl of the medium from each well was transferred to a new clear flat-

bottomed black 96-well plate (Corning). Absorbance was read at a test wavelength of 440 nm and a reference wavelength of 690 nm using a multi-mode microplate reader (Spectra Max iD5; Molecular Devices). Mean percent toxicity (MPT) of each compound mixture was derived by dividing the difference in absorbance between the compound-treated cells and the DMSO-treated cells by the absorbance from the DMSO-treated cells and multiplying the product by 100:

$$MPT = [(\text{Mean } OD_{\text{DMSO-treated}} - \text{Mean } OD_{\text{compound-treated}}) \div \text{Mean } OD_{\text{DMSO-treated}}] \times 100.$$

Where

- MPT is the mean percent toxicity of compound.
- Mean $OD_{\text{DMSO-treated}}$ is the average absorbance value of quadruplicate wells treated with volumes of DMSO equivalent to that of the compound-treated wells.
- Mean $OD_{\text{compound-treated}}$ is the average absorbance value of quadruplicate wells treated with the compound.

3.5.5 *In vitro Cryptosporidium* growth inhibition assay.

HCT-8 cells were seeded and grown to confluency in supplemented RPMI-1640 medium in flat-bottomed 96-well plates. After replacing the old medium with fresh RPMI-1640 medium containing 1% Hi-FBS (infection medium), plates were inoculated with 10^5 freshly excysted *C. parvum* sporozoites per well. Immediately after infection, HCT-8 monolayers were treated with two-fold dilution series of the highest sub-toxic (<20% MPT) concentration of individual compounds and compound mixtures. Control infected cells were treated with volumes of DMSO (up to a maximum final concentration of 1%) equivalent to those used for the compound-treated cultures. Paromomycin reconstituted in sterile distilled water was added to a separate set of wells as a positive control at a final concentration of 400 μM. Control wells with uninfected

monolayers were also included for background subtraction. After 48 h of culture at 37°C with 5% CO_2, the cultures were analyzed for parasite infectivity and proliferation by a direct immunofluorescence assay. The medium was removed from the culture wells, and the cell monolayer was rinsed two times with PBS before fixation with pre-chilled methanol-acetic acid (9:1) for 5 min. The wells were rinsed with PBS to remove traces of fixative followed by successive washes with buffer containing 0.1% Triton X-100, 0.35 M NaCl, and 0.13 M Tris-base, pH 7.6 to rehydrate and permeabilize the cells. Normal goat serum (5%) in PBS was used as a blocking solution, and the cell monolayer was stained with a fluorescein-labeled anti-*C. parvum* polyclonal antibody (Sporo-Glo™; Waterborne, Inc.) overnight at 4°C. The stained cells were washed with PBS, followed by rinsing with water, and then imaged with an inverted EVOS™ M7000 Imaging System (Invitrogen) using a fully automated scan protocol. The EVOS™ M7000 software was used to program the microscope to autofocus on the center of each well using a 20× objective and then acquire images from multiple fields with overlapping edges to build a single tile-stitched image per well, equating to approximately 40% of the total well area. Celleste™ Imaging Analysis software (Invitrogen) was used to count the number of intracellular *C. parvum* parasites in each stitched image using the smart segmentation feature to distinguish between objects (parasites) and background (host cells). Experiments were performed in triplicate and repeated three times.

3.5.6 Synergy analyses.

Concentration-response data of each compound mixture and individual compounds obtained from the *in vitro C. parvum* growth inhibition assays were analyzed by multiple approaches to determine the synergistic activity of compound combinations. Dose-response curves were plotted in GraphPad PRISM® v8 for curve-shift analysis and calculation of anti-

Cryptosporidium EC_{50} values by non-linear regression analysis of the mean dose-response curve data normalized to DMSO- and paromomycin-treated wells that represented negative and positive treatment controls, respectively. The combination-index (CI) values for the actual experimental data points, as well as the dose-reduction index (DRI_x) values at various parasite inhibition levels (x = 50 - 90%), were derived from the median-effect equation of Chou and Talalay (Chou and Talalay, 1984) using the CompuSyn software. Compound concentrations for single agents and combinations required to produce a 75% inhibition of the growth of *Cryptosporidium* parasites in cell culture were also calculated by CompuSyn and plotted for isobologram analysis. CI plots and isobolograms were created with GraphPad PRISM® v8.

3.5.7 Testing of the *in vivo* anti-*Cryptosporidium* efficacy of compound combinations.

Male IFN-γ KO mice (B6.129S7-*Ifng*^{tm1Ts}/J), aged 7 weeks, were procured from The Jackson Laboratory, USA, and housed for 1 week before the start of experiments for acclimatization. Prior to the testing of anti-cryptosporidial efficacy of compounds in mice, groups of mice (n = 3 per group) were treated by daily oral gavage with varying dosages of individual compounds and compound combinations for 5 days using a 20G × 1.5-inch animal feeding needle. During this period, mice were monitored daily for any signs of toxicity including loss of appetite and body weight. Changes in physical and mental activity, body posture, and fur condition were quantified according to a scoring rubric. Once non-toxic doses were determined, a newly procured batch of 50 mice were separated into 10 groups (n = 5 per group) for efficacy studies. Except for the uninfected control group, all other groups of mice were infected by oral gavage with 5×10^4 *C. parvum* AUCP-1 isolate oocysts suspended in 100 µl of PBS on day 0. Immediately after infection, each individual mouse was housed in a separate cage lined with sterile gauze bedding. On day 3 post-infection, infected groups of mice were orally treated with

CpPyK (NSC252172 and NSC303244) and CpLDH (NSC158011 and NSC10447) inhibitors either individually or in combination at the indicated doses, 1000 mg/kg paromomycin in sterile water (positive control), or vehicle (100 µl of 25% DMSO in PEG 400), once daily until day 12. Uninfected control mice were also orally gavaged with the compound vehicle during the treatment period. Mice were weighed daily till study completion. Starting on day 3 after infection, fecal pellets were collected daily in individual sterile 15-ml tubes from each cage and stored at -80°C, until use. After treatment discontinuation, 2 mice from each group were randomly selected and sacrificed on day 13 to assess the effect of compounds on disease development. A small portion (~ 5 cm) of the distal small intestine just anterior to the cecum was resected from each sacrificed mouse and preserved in 10% neutral buffered formalin for histopathological processing. The remaining mice were maintained up until the termination of study (day 23 post-infection) to assess the effect of compound withdrawal on survival and disease relapse/progression. On day 23, all surviving mice were sacrificed, and intestinal tissue samples were collected for histopathological analysis, as described above. Harvested intestinal tissues were paraffin-embedded and sectioned transversely at a thickness of 5 µm. Sections stained with hematoxylin and eosin were imaged using the EVOS™ M7000 Imaging System (Invitrogen).

3.5.8 Quantification of oocyst shedding in fecal samples.

Genomic DNA was extracted from 150 mg of feces collected from individual mice by using the QIAamp® PowerFecal® Pro DNA kit (Qiagen) following the manufacturer's protocol. Quantification of the oocysts load per gram of feces was performed by qPCR analysis of the Cp18S rRNA gene (GenBank accession number AF164102) using gene-specific primers: 5'-CTGCGAATGGCTCATTATAACA-3' (Forward) and 5'-AGGCCAATACCCTACCGTCT-3'

(Reverse), described previously (Parr et al., 2007). To generate quantification standards for qPCR, fecal samples were obtained from uninfected mice and spiked with 10^8 *C. parvum* oocysts per gram of feces, followed by extraction of DNA as described above. The extracted genomic DNA was then 10-fold serially diluted to generate standard curve quantification standards for qPCR. *C. parvum* oocyst load was quantified for the test mice by using DNA samples from the infected feces in triplicate reactions. Each 20 µl qPCR reaction contained 10 µl of PowerUp™ SYBR™ Green Master Mix (Applied Biosystems), 500 nM of each primer, and 2 µl of DNA template. After an initial 5 min denaturation step at 95°C, 40 cycles of denaturation at 95°C for 15 seconds and annealing/extension at 60°C for 1 min were performed in a QuantStudio™3 Real-Time PCR System (Applied Biosystems). The oocyst load per gram of feces was derived by the QuantStudio™3-system software using the generated quantification standard curves.

3.5.9 Statistical analyses.

All statistical analyses were performed using GraphPad PRISM® v8. Normality of data distribution was assessed using Q-Q normal probability plots and the Shapiro-Wilk normality test. Statistical comparisons between the treatment groups and the vehicle control group were done by a non-parametric Kruskal-Wallis test or a parametric one-way analysis of variance (ANOVA) test with the Dunn's or the Dunnett's multiple comparison *post hoc* tests respectively, as appropriate for the data. *P* values of 0.05 or less were considered significant. For animal studies, a sample size of five mice per group was found to be sufficient to have a high confidence of detecting a difference in means of at least 25% between treated and untreated groups (two-tailed test using $P < 0.05$) with a power of 90%, as determined by power analyses using the G*Power software (Faul et al., 2007). This number was consistent with numbers that we have

used in the past for similar studies and accounted for animal attrition due to mortality during the study duration.

3.5.10 Ethics.

All experiments involving the use of animals in this study were carried out in strict compliance with the recommendations and guidelines of the United States Department of Agriculture Animal Welfare Act and the National Institute of Health Public Health Service Policy on the Humane Care and Use of Animals. The protocol numbers 22236 and 21091 used were approved by the University of Illinois Institutional Animal Care and Use Committee for conducting research with mice and calves, respectively. All efforts were made to reduce the pain and suffering of animals.

3.6 FIGURES AND TABLES

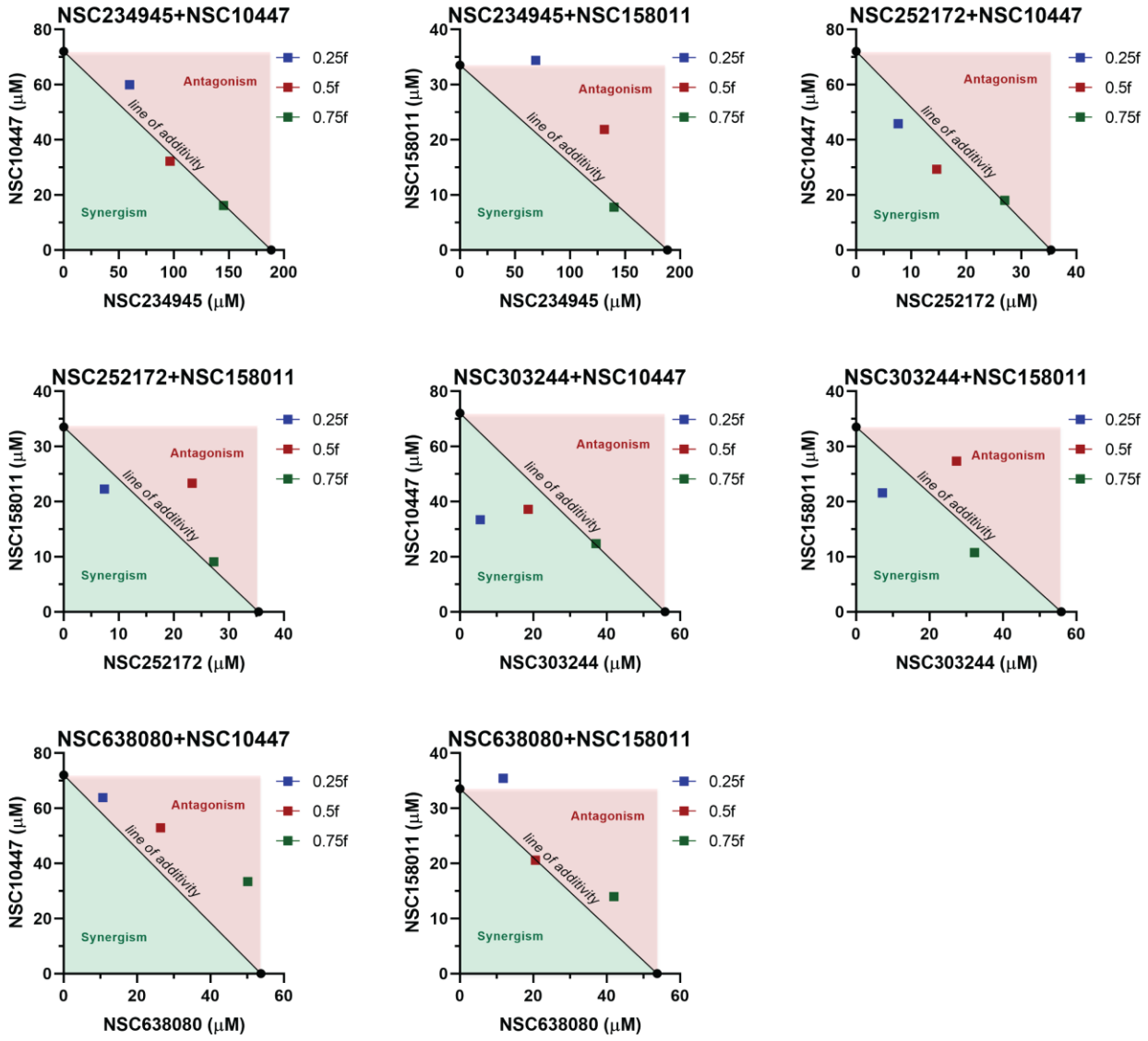

Figure 3.1: Isobolograms of multiple combination ratios of CpPyK- and CpLDH-inhibitors at the 75% parasite inhibition level. CpPyK- and CpLDH-inhibitors were combined in concentration ratios determined by 3 values of mixture factor (*f*) to prepare 3 different compound mixtures (0.25*f*, 0.5*f*, and 0.75*f*) for each combination. Concentration-response data of each compound mixture and individual compounds obtained from the *in vitro* parasite growth inhibition assays were analyzed by CompuSyn software to compute anti-*Cryptosporidium* EC_{75} values. The EC_{75} of CpPyK-inhibitor plotted on the x-axis and the EC_{75} of CpLDH-inhibitor plotted on the y-axis were joined to construct the line of additivity. Combination data points that fall below, on, or above the line of additivity indicate synergism, additivity, or antagonism, respectively. The data shown represents the mean of three independent experiments.

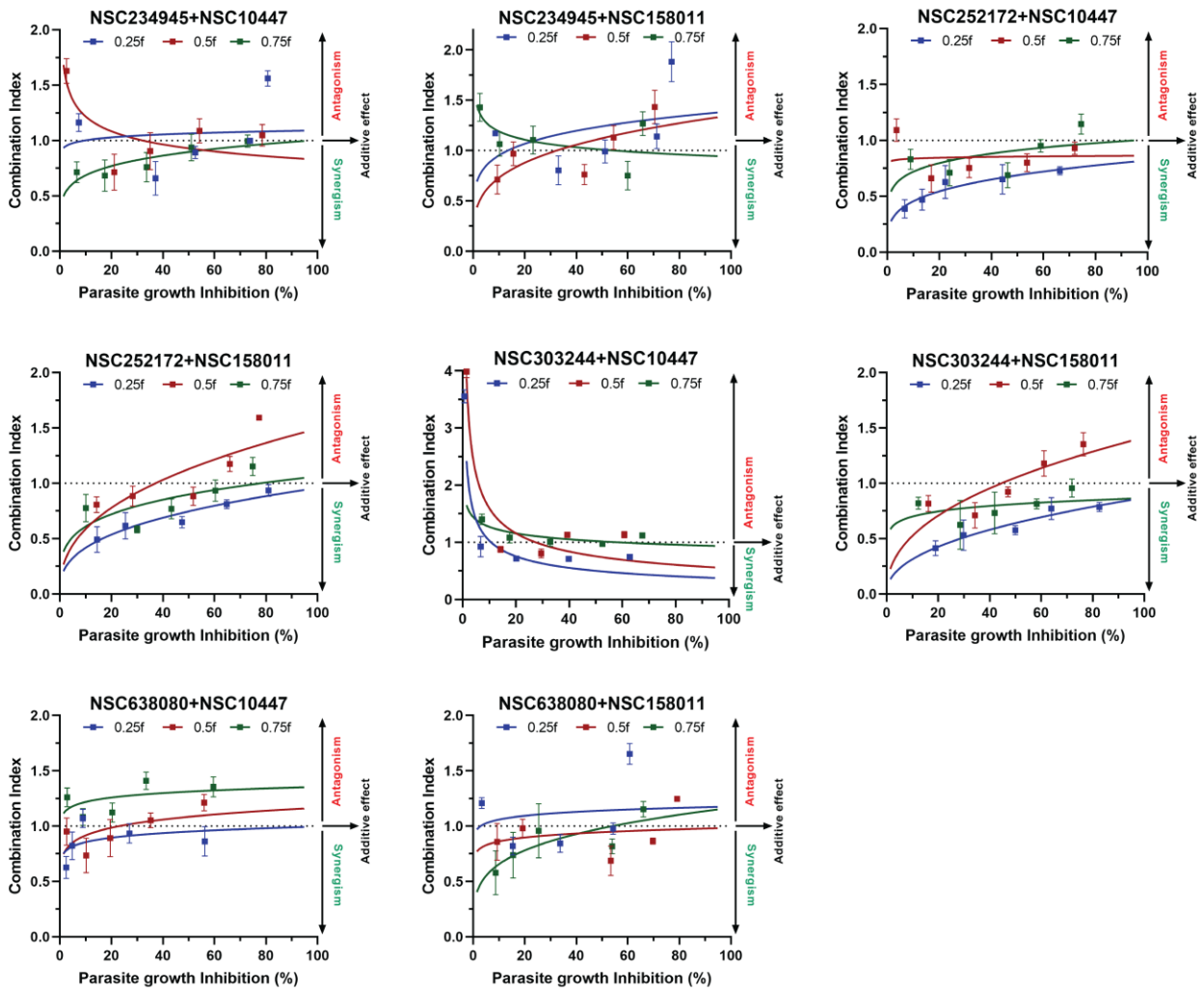

Figure 3.2: Combination index (CI) plots for combinations of CpPyK- and CpLDH-inhibitors at different combination ratios. CpPyK- and CpLDH-inhibitors were combined in concentration ratios determined by 3 values of mixture factor (*f*) to prepare 3 different compound mixtures (0.25*f*, 0.5*f*, and 0.75*f*) for each combination. Concentration-response data points of each compound mixture acquired from the *in vitro C. parvum* growth inhibition assays were analyzed by CompuSyn software to calculate CI values. To construct CI plots, CI values of each compound mixture were plotted against the respective parasite growth inhibition levels. A CI of 1 (dotted line) indicates an additive effect between two agents, whereas values that fall below and above the line indicate synergism and antagonism, respectively. Data are presented as mean ± standard deviation of the mean (SD) of three independent experiments.

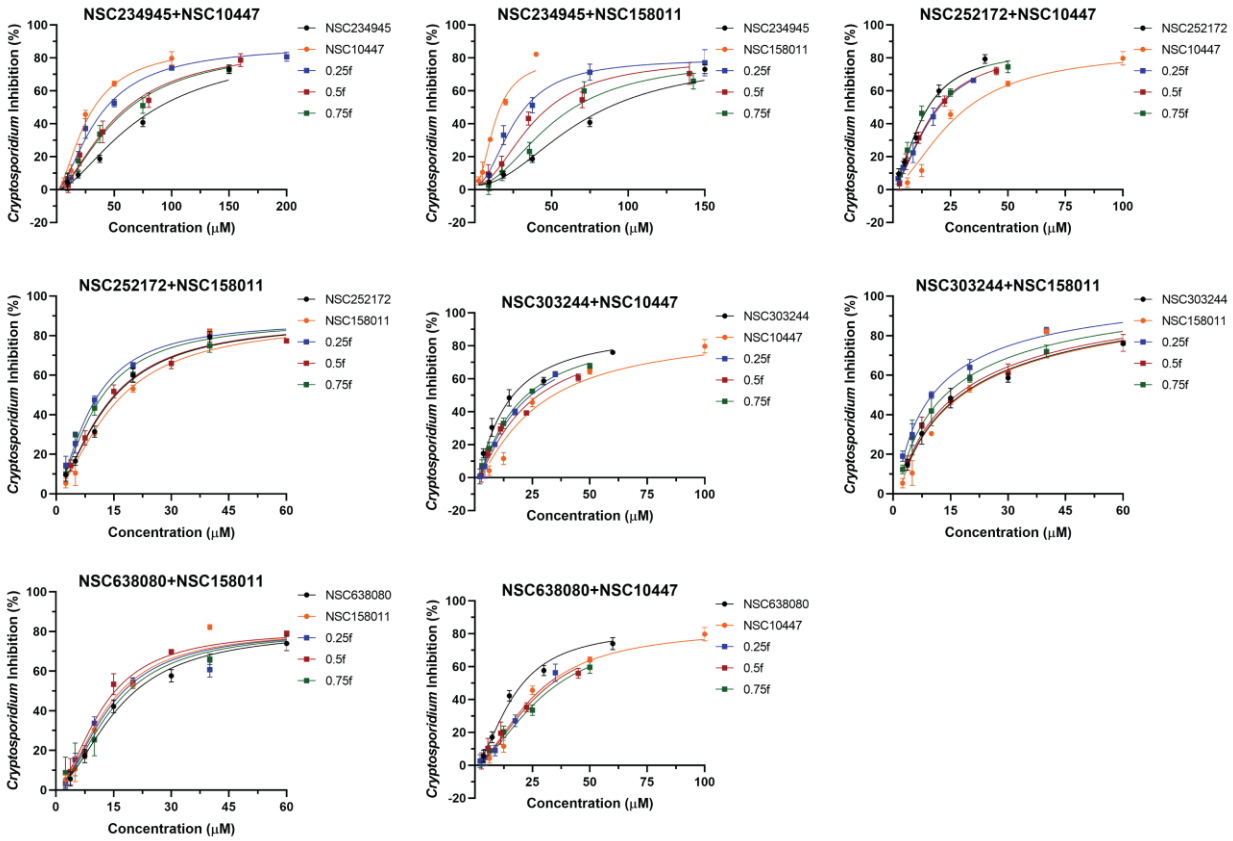

Figure 3.3: Curve-shift analyses of individual CpPyK- and CpLDH-inhibitors and their combinations at different combination ratios. CpPyK- and CpLDH-inhibitors were combined in concentration ratios determined by 3 values of mixture factor (*f*) to prepare 3 different compound mixtures (0.25*f*, 0.5*f*, and 0.75*f*) for each combination. Concentration-response data of each compound mixture and individual compounds acquired from the *in vitro* parasite growth inhibition assays were plotted in GraphPad PRISM® v8. A leftward shift of curves for combinations compared with individual compound curves indicates synergism and a rightward shift indicates antagonism. Data are presented as mean ± standard deviation of the mean (SD) of three independent experiments.

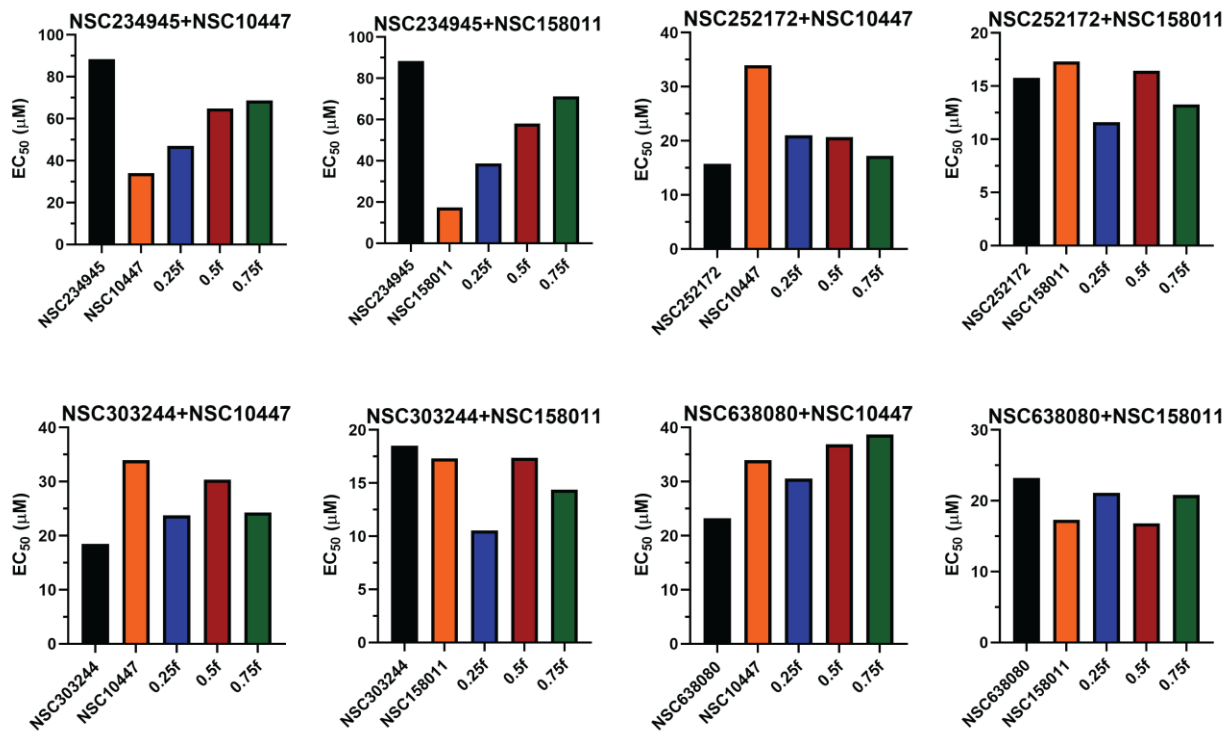

Figure 3.4: Comparison of anti-*Cryptosporidium* EC_{50} values of individual CpPyK- and CpLDH-inhibitors and their combinations at different combination ratios. CpPyK- and CpLDH-inhibitors were combined in concentration ratios determined by 3 values of mixture factor (*f*) to prepare 3 different compound mixtures (0.25*f*, 0.5*f*, and 0.75*f*) for each combination. Concentration-response data points of each compound mixture and individual compounds obtained from the *in vitro C. parvum* growth inhibition assays were analyzed by the non-linear regression equation in GraphPad PRISM® v8 software to calculate EC_{50} values. The EC_{50} of the individual drugs were compared to the resulting EC_{50} after combination treatments. The data shown represents the mean EC_{50} values of three independent experiments.

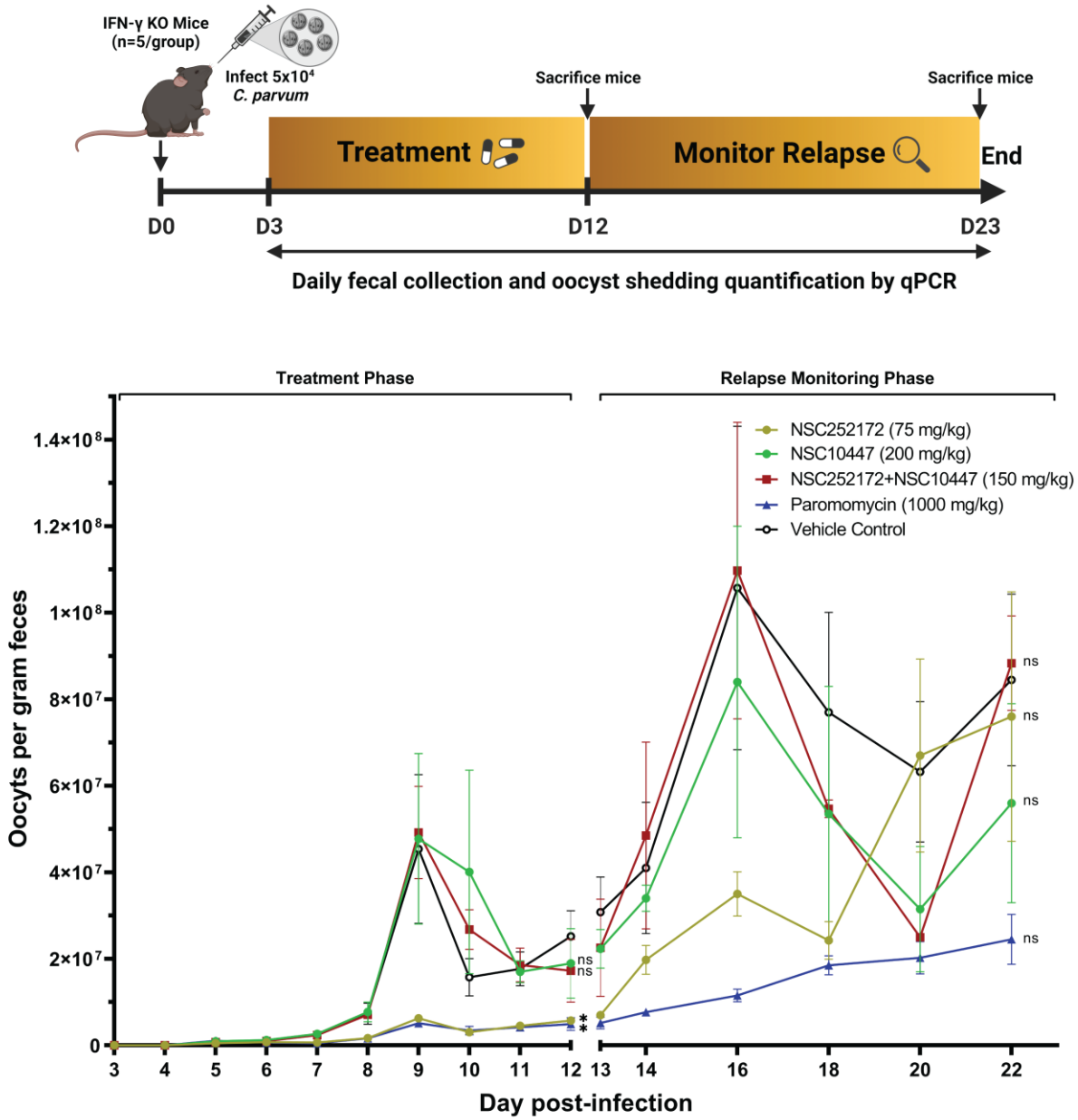

Figure 3.5: Analysis of the efficacy of NSC252172 and NSC10447 combination treatment against cryptosporidiosis. Male IFN-γ KO mice were infected by oral gavage with 5×10^4 *C. parvum* oocysts on day 0. Beginning at day 3 post-infection, groups of mice were treated with NSC252172 (75 mg/kg), NSC10447 (200 mg/kg), NSC252172+NSC10447 (150 mg/kg), paromomycin (1000 mg/kg) in sterile water (positive control), or vehicle (100 µl of 25% DMSO in PEG 400), once daily until day 12. Oocyst shedding per gram of feces was determined by quantitative PCR on different days post-infection. The data shown represents means for fecal samples from 5 mice (days 3-13 post-infection) and 3 mice (days 14-22 post-infection) per group. On days 12 and 22 post-infection, parasite load in different treatment groups was compared to the oocyst shedding in the vehicle control group by a non-parametric Kruskal-Wallis test with the Dunn's multiple comparison test (ns, not significant; *, $P < 0.05$). Created with BioRender.com.

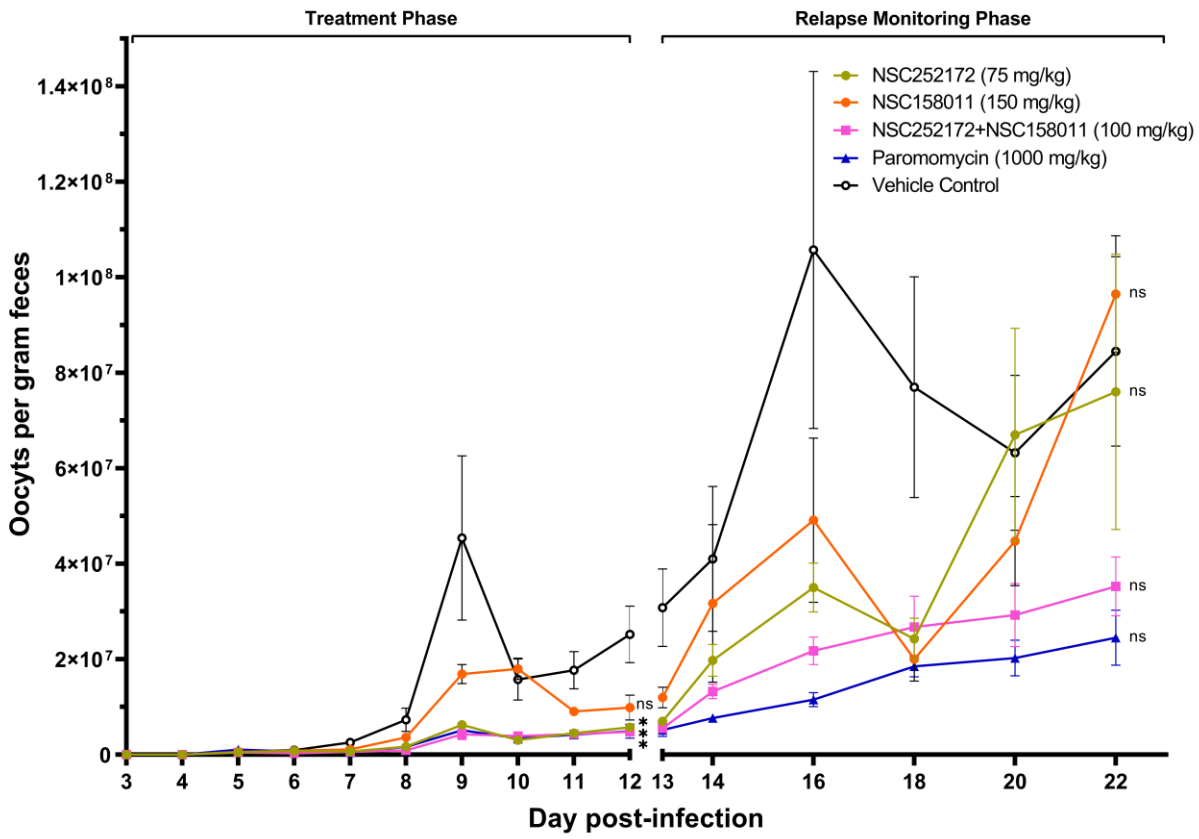

Figure 3.6: Analysis of the efficacy of NSC252172 and NSC158011 combination treatment against cryptosporidiosis. Male IFN-γ KO mice were infected by oral gavage with 5×10^4 *C. parvum* oocysts on day 0. Beginning at day 3 post-infection, groups of mice were treated with NSC252172 (75 mg/kg), NSC158011 (150 mg/kg), NSC252172+NSC158011 (100 mg/kg), paromomycin (1000 mg/kg) in sterile water (positive control), or vehicle (100 µl of 25% DMSO in PEG 400), once daily until day 12. Oocyst shedding per gram of feces was determined by quantitative PCR on different days post-infection. The data shown represents means for fecal samples from 5 mice (days 3-13 post-infection) and 3 mice (days 14-22 post-infection) per group. Bars represent standard errors of the mean (SEM). On days 12 and 22 post-infection, parasite load in different treatment groups was compared to the oocyst shedding in the vehicle control group by a non-parametric Kruskal-Wallis test with the Dunn's multiple comparison test (ns, not significant; *, $P < 0.05$).

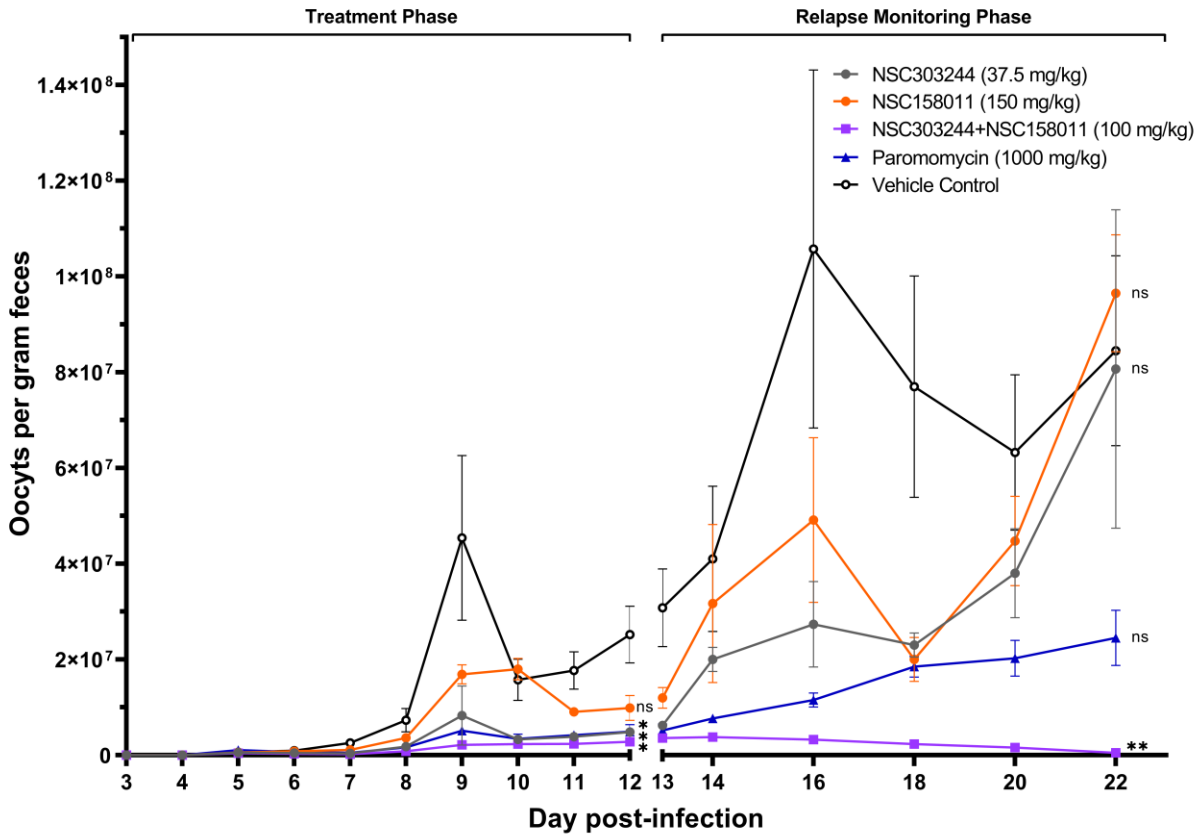

Figure 3.7: Analysis of the efficacy of NSC303244 and NSC158011 combination treatment against cryptosporidiosis. Male IFN-γ KO mice were infected by oral gavage with 5×10^4 *C. parvum* oocysts on day 0. Beginning at day 3 post-infection, groups of mice were treated with NSC303244 (37.5 mg/kg), NSC158011 (150 mg/kg), NSC303244+NSC158011 (100 mg/kg), paromomycin (1000 mg/kg) in sterile water (positive control), or vehicle (100 µl of 25% DMSO in PEG 400), once daily until day 12. Oocyst shedding per gram of feces was determined by quantitative PCR on different days post-infection. The data shown represents means for fecal samples from 5 mice (days 3-13 post-infection) and 3 mice (days 14-22 post-infection) per group. Bars represent standard errors of the mean (SEM). On days 12 and 22 post-infection, parasite load in different treatment groups was compared to the oocyst shedding in the vehicle control group by a non-parametric Kruskal-Wallis test with the Dunn's multiple comparison test (ns, not significant; *, $P < 0.05$; **, $P < 0.01$).

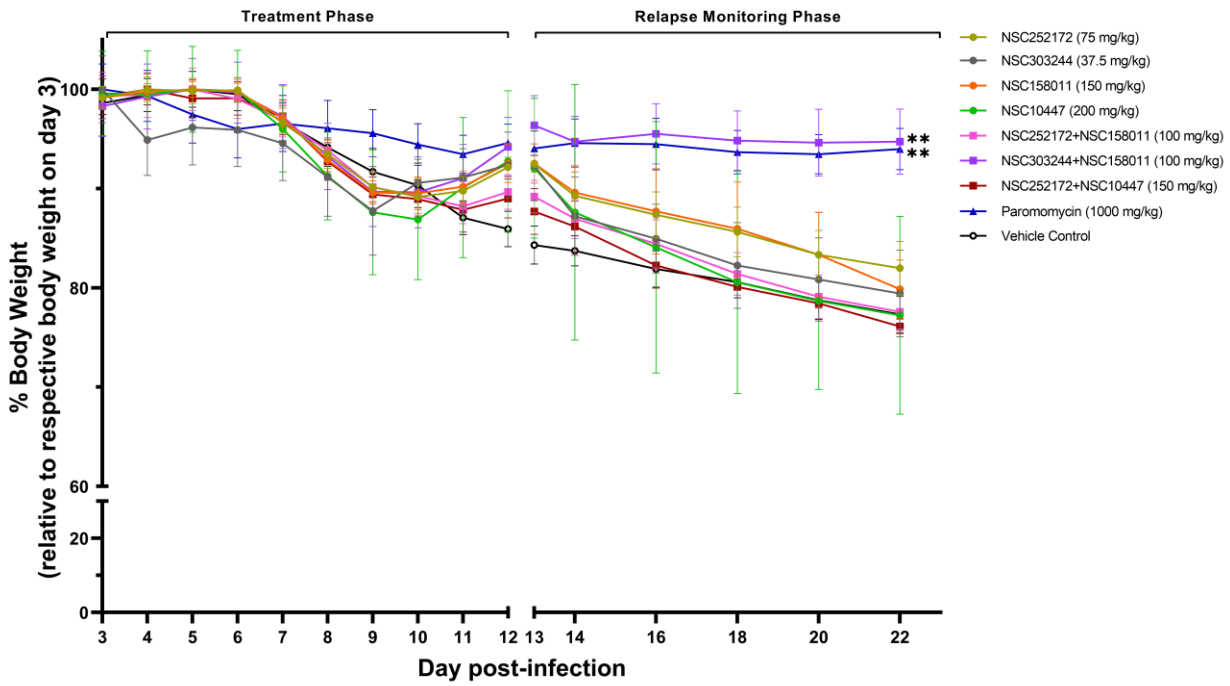

Figure 3.8: Determination of average body weight of mice during and after treatment against cryptosporidiosis. Male IFN-γ KO mice were infected by oral gavage with 5×10^4 *C. parvum* oocysts on day 0. Beginning day 3 post-infection, groups of mice were treated with CpPyK- and CpLDH-inhibitors either individually or in combination at the indicated doses, paromomycin (1000 mg/kg) in sterile water (positive control), or vehicle (100 µl of 25% DMSO in PEG 400), once daily until day 12. Body weight was recorded daily during and after the treatment period and is shown on the y-axis representing the average body weight of each treatment group normalized to the respective mean body weight on day 3. The data shown represents means for fecal samples from 5 mice (days 3-13 post-infection) and 3 mice (days 14-22 post-infection) per group. Bars represent standard errors of the mean (SEM). On day 22 post-infection, mean body weights of various treatment groups were compared to that of the vehicle control group by a parametric one-way analysis of variance (ANOVA) test with the Dunnett's multiple comparison test (**, $P < 0.01$).

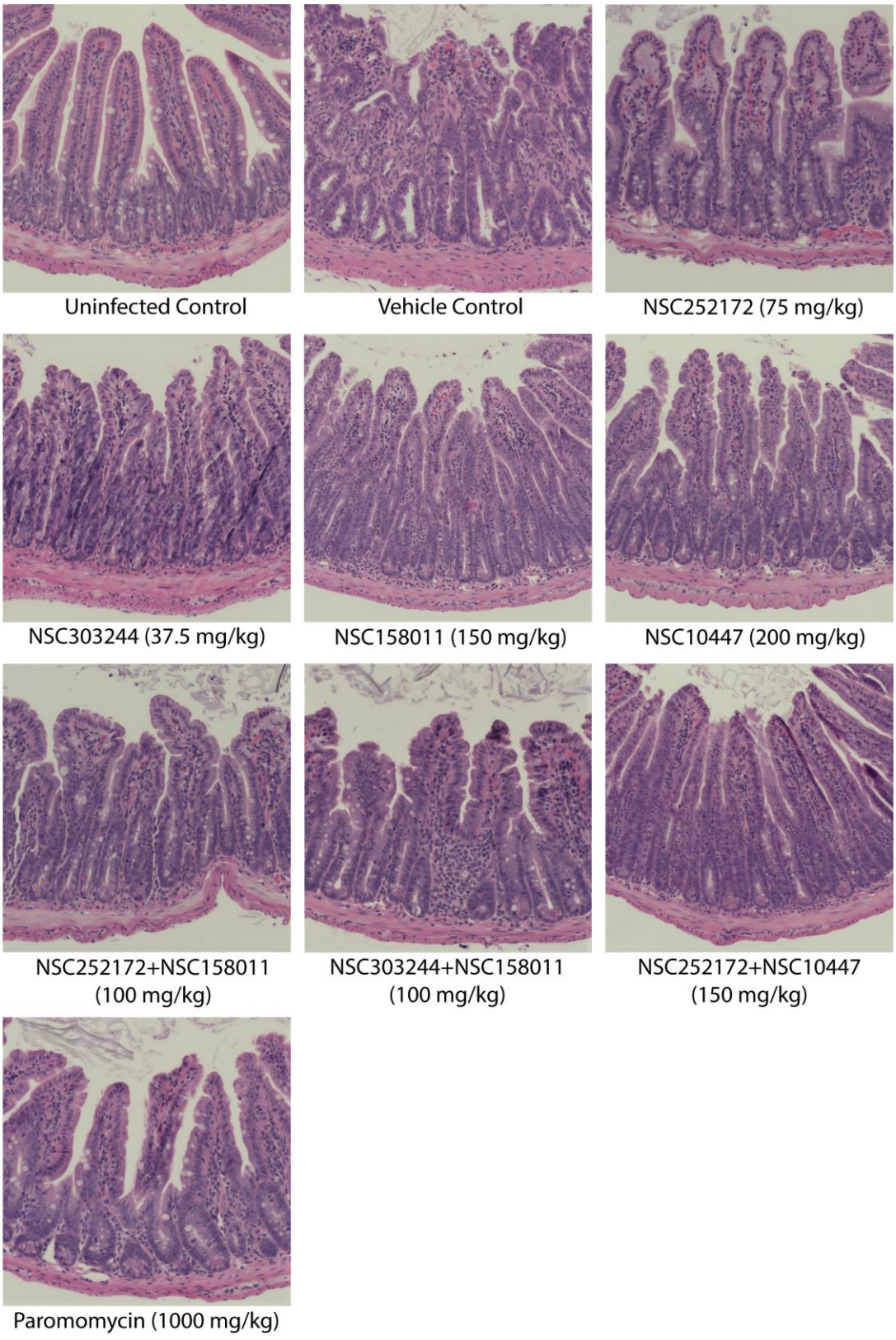

Figure 3.9: Hematoxylin- and eosin-stained histological sections from the distal small intestines of *C. parvum*-infected mice with or without treatment. Male IFN-γ KO mice were infected by

Figure 3.9 (cont.)

oral gavage with 5×10^4 *C. parvum* oocysts on day 0. Beginning day 3 post-infection, groups of mice were treated with NSC272172 (75 mg/kg), NSC303244 (37.5 mg/kg), NSC158011 (150 mg/kg), NSC10447 (200 mg/kg), NSC252172+NSC158011 (100 mg/kg), NSC303244+NSC158011 (100 mg/kg), NSC252172+NSC10447 (150 mg/kg), paromomycin (1000 mg/kg) in sterile water (positive control), or vehicle (100 µl of 25% DMSO in PEG 400), once daily until day 12. The uninfected control group of mice was administered an equivalent volume of the compound vehicle. On day 13 post-infection, randomly selected mice were sacrificed, and the distal small intestines were processed for histology and stained with hematoxylin and eosin. Representative microscopy images of samples harvested from at least 2 mice per treatment group on day 13 after infection are shown here.

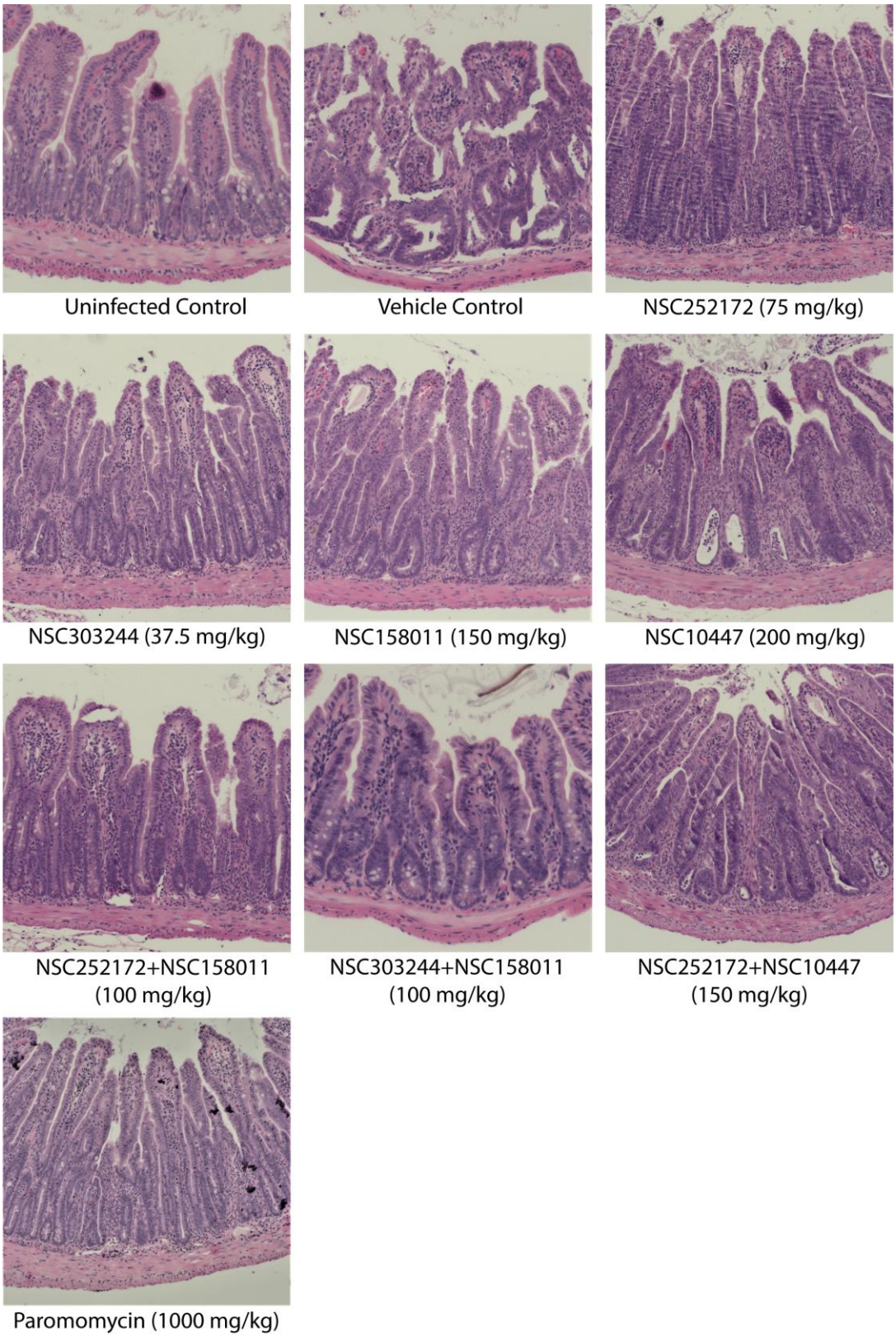

Figure 3.10: Hematoxylin- and eosin-stained histological sections from the distal small intestines of *C. parvum*-infected mice with or without treatment. Male IFN-γ KO mice were

Figure 3.10 (cont.)

infected by oral gavage with 5×10^4 *C. parvum* oocysts on day 0. Beginning day 3 post-infection, groups of mice were treated with NSC272172 (75 mg/kg), NSC303244 (37.5 mg/kg), NSC158011 (150 mg/kg), NSC10447 (200 mg/kg), NSC252172+NSC158011 (100 mg/kg), NSC303244+NSC158011 (100 mg/kg), NSC252172+NSC10447 (150 mg/kg), paromomycin (1000 mg/kg) in sterile water (positive control), or vehicle (100 µl of 25% DMSO in PEG 400), once daily until day 12. The uninfected control group of mice was administered an equivalent volume of the compound vehicle. On day 23 post-infection, randomly selected mice were sacrificed, and the distal small intestines were processed for histology and stained with hematoxylin and eosin. Representative microscopy images of samples harvested from at least 2 mice per treatment group on day 23 after infection are shown here.

Table 3.1: Combination of inhibitors of *C. parvum* pyruvate kinase (CpPyKi) and *C. parvum* lactate dehydrogenase (CpLDHi) according to the ray design model.

Compound mixture (CpPyKi + CpLDHi)	**Mixture factor (*f*)**	**Mix ratio**	**Highest concentration mix (µM:µM)**
NSC234945 + NSC10447	0.25	1:1	100:100
	0.50	3:1	120:40
	0.75	9:1	135:15
NSC234945 + NSC158011	0.25	2:1	100:50
	0.50	6:1	120:20
	0.75	18:1	135:7.5
NSC252172 + NSC10447	0.25	1:6	5:30
	0.50	1:2	15:30
	0.75	3:2	30:20
NSC252172 + NSC158011	0.25	1:3	10:30
	0.50	1:1	30:30
	0.75	3:1	30:10
NSC303244 + NSC10447	0.25	1:6	5:30
	0.50	1:2	15:30
	0.75	3:2	30:20
NSC303244 + NSC158011	0.25	1:3	10:30
	0.50	1:1	30:30
	0.75	3:1	30:10
NSC638080 + NSC10447	0.25	1:6	5:30
	0.50	1:2	15:30
	0.75	3:2	30:20
NSC638080 + NSC158011	0.25	1:3	10:30
	0.50	1:1	30:30
	0.75	3:1	30:10

Table 3.2: Dose-reduction index (DRI) values of compound mixtures at the parasite inhibition effective concentration (EC) of 50%, 75%, and 90% (EC_{50}, EC_{75}, and EC_{90}, respectively).

Compound mixture (CpPyKi + CpLDHi)	**Mixture factor (*f*)**	**DRI value of CpPyKi and CpLDHi at**					
		EC_{50}		**EC_{75}**		**EC_{90}**	
		CpPyKi	**CpLDHi**	**CpPyKi**	**CpLDHi**	**CpPyKi**	**CpLDHi**
NSC234945 + NSC10447	0.25	3.29	1.39	1.79	2.27	1.44	5.47
	0.50	3.15	1.20	1.95	2.24	1.30	4.47
	0.75	3.01	1.04	2.13	2.20	1.17	3.64
NSC234945 + NSC158011	0.25	3.06	1.17	1.71	1.96	1.25	4.30
	0.50	2.74	0.98	1.44	1.53	1.35	4.31
	0.75	2.45	0.81	1.20	1.20	1.45	4.32
NSC252172 + NSC10447	0.25	5.09	2.05	2.22	2.69	1.43	5.20
	0.50	4.64	1.57	2.42	2.46	1.31	4.00
	0.75	4.22	1.21	2.63	2.25	1.20	3.08
NSC252172 + NSC158011	0.25	5.31	1.93	1.80	1.96	1.50	4.91
	0.50	4.77	1.51	1.52	1.44	1.30	3.69
	0.75	4.28	1.17	1.28	1.05	1.12	2.77
NSC303244 + NSC10447	0.25	5.96	1.98	2.06	2.05	1.28	3.82
	0.50	5.03	2.15	3.01	1.94	1.51	2.91
	0.75	4.87	2.35	3.39	1.83	1.77	2.22
NSC303244 + NSC158011	0.25	7.29	2.18	2.14	1.91	1.72	4.62
	0.50	7.77	1.55	2.05	1.23	1.73	3.12
	0.75	8.28	1.11	1.96	0.79	1.75	2.11
NSC638080 + NSC10447	0.25	4.96	1.27	2.10	1.61	1.08	2.50
	0.50	5.05	1.13	2.03	1.36	1.07	2.15
	0.75	5.14	1.00	1.97	1.15	1.06	1.86
NSC638080 + NSC158011	0.25	4.60	1.06	2.64	1.83	1.53	3.17
	0.50	4.55	0.95	2.61	1.63	1.28	2.40
	0.75	4.50	0.84	2.59	1.45	1.08	1.82

Table 3.3: Effect of oral administration of CpPyK- and CpLDH-inhibitors on the physical indicators of health in mice.

Treatment	Dose (mg/kg)	Day	Average Body Weight (g)	Average Score*			
				Activity	Skin/ Fur	Posture	Mental State
NSC252172	50	1	23.7	4	4	4	4
		2	24.4	4	4	4	4
		3	24.7	4	4	4	4
		4	24.9	4	4	4	4
		5	24.8	4	4	4	4
	75	1	24.4	4	4	4	4
		2	24.6	4	4	4	4
		3	24.5	4	4	4	4
		4	24.7	4	4	4	4
		5	24.9	4	4	4	4
	100	1	24.6	4	4	4	4
		2	24.6	4	4	4	4
		3	25.1	4	4	4	4
		4	25.1	4	4	4	4
		5	25.3	4	4	4	4
NSC303244	50	1	21.9	4	4	4	4
		2	21.6	4	4	4	4
		3	22.2	4	4	4	4
		4	22.4	4	4	4	4
		5	22.4	4	4	4	4
	75	1	23.7	4	4	4	4
		2	23.6	4	4	4	4
		3	23.5	4	4	4	4
		4	23.2	4	4	4	4
		5	22.7	3	3	4	4
	100	1	23.1	4	4	4	4
		2	22.9	4	4	4	4
		3	22.7	4	4	4	4
		4	22	3	3	4	3
		5	20.9	3	2	3	3
NSC158011	75	1	22	4	4	4	4
		2	22.2	4	4	4	4
		3	22.2	4	4	4	4
		4	22.1	4	4	4	4
		5	22.4	4	4	4	4
	150	1	22.4	4	4	4	4
		2	22.6	4	4	4	4
		3	22.8	4	4	4	4
		4	22.9	4	4	4	4
		5	23.4	4	4	4	4

Table 3.3 (cont.)

NSC158011	200	1	22.9	4	4	4	4
		2	22.7	4	4	4	4
		3	22.9	4	4	4	4
		4	23.2	4	4	4	4
		5	23.3	4	4	4	4
NSC10447	100	1	22.7	4	4	4	4
		2	22.9	4	4	4	4
		3	22.8	4	4	4	4
		4	22.9	4	4	4	4
		5	23	4	4	4	4
	200	1	24.4	4	4	4	4
		2	24.9	4	4	4	4
		3	24.9	4	4	4	4
		4	25	4	4	4	4
		5	25.3	4	4	4	4
	400	1	22.6	4	4	4	4
		2	23	4	4	4	4
		3	23.2	4	4	4	4
		4	23	4	4	4	4
		5	23	4	4	4	4
NSC252172 + NSC10447 (1:2)	75	1	22.9	4	4	4	4
		2	23.3	4	4	4	4
		3	23.3	4	4	4	4
		4	23.5	4	4	4	4
		5	23.9	4	4	4	4
	150	1	24.6	4	4	4	4
		2	24.5	4	4	4	4
		3	24.4	4	4	4	4
		4	24.5	4	4	4	4
		5	24.4	4	4	4	4
	300	1	22.4	4	4	4	4
		2	22.7	4	4	4	4
		3	22.5	4	4	4	4
		4	22.6	4	4	4	4
		5	22.7	4	4	4	4
NSC252172 + NSC158011 (1:3)	50	1	23.9	4	4	4	4
		2	23.9	4	4	4	4
		3	24.1	4	4	4	4
		4	23.9	4	4	4	4
		5	24	4	4	4	4
	100	1	24.7	4	4	4	4
		2	24.9	4	4	4	4
		3	24.7	4	4	4	4
		4	25	4	4	4	4
		5	24.9	4	4	4	4

Table 3.3 (cont.)

NSC252172 + NSC158011 (1:3)	200	1	23.5	4	4	4	4
		2	23.8	4	4	4	4
		3	23.7	4	4	4	4
		4	23.9	4	4	4	4
		5	24.1	4	4	4	4
NSC303244 + NSC158011 (1:3)	50	1	25.1	4	4	4	4
		2	25.4	4	4	4	4
		3	25.6	4	4	4	4
		4	25.5	4	4	4	4
		5	25.5	4	4	4	4
	100	1	23.4	4	4	4	4
		2	23.6	4	4	4	4
		3	23.8	4	4	4	4
		4	23.7	4	4	4	4
		5	23.9	4	4	4	4
	200	1	24	4	4	4	4
		2	23.8	4	4	4	4
		3	24	4	4	4	4
		4	23.9	4	4	4	4
		5	23.9	4	4	4	4

* Criteria used for scoring changes in physical activity, fur condition, body posture, and mental state due to compound toxicity in mice:

Score	**Physical activity**	**Skin/ Fur**	**Posture**	**Mental State**
1	immobile	sparse	lying flat	lifeless/ trembling
2	bradykinesia	rough/ lackluster	hunched	depressed
3	slightly sluggish	little rough/ lackluster	slightly hunched	agitated
4	fully active	smooth/ glossy	normal standing	good spirit

Table 3.4: Average counts of oocyst shedding per gram of feces in infected mice from day 3 to day 22 post-infection as measured by qPCR quantification.

Treatment group	Average oocyst count per gram feces
NSC252172 (75 mg/kg)	15766647[#]
NSC303244 (37.5 mg/kg)	13674439[#]
NSC158011 (150 mg/kg)	19632226[#]
NSC10447 (200 mg/kg)	26110916[#]
NSC252172 + NSC158011 (100 mg/kg)	9466084[#]
NSC303244 + NSC158011 (100 mg/kg)	1664310[**]
NSC252172 + NSC10447 (150 mg/kg)	29490632[#]
Paromomycin (1000 mg/kg)	6832361[#]
Vehicle control	32364839

#, not significantly different from vehicle control; **, $P < 0.01$ by a non-parametric Kruskal-Wallis test with the Dunn's test for multiple comparisons between the treatments and the vehicle control.

CHAPTER 4: CONCLUSIONS AND FUTURE DIRECTIONS

Cryptosporidium parvum is a significant cause of waterborne diseases worldwide and can affect both humans and animals (Chalmers, 2014). Developing effective drugs to treat cryptosporidiosis has been challenging due to the complex life cycle of the parasite and its ability to form a protective outer shell, known as an oocyst, which makes it resistant to many traditional antiprotozoal treatments and disinfection methods. Nitazoxanide is an antiparasitic drug that has been approved by the FDA for the treatment of *Cryptosporidium* infections in children and adults. While it has shown some efficacy, it may not be effective in all cases, particularly in individuals with weakened immune systems. Moreover, currently there are no specific antiparasitic drugs approved in the US for the treatment of cryptosporidiosis in animals. Thus, there is an urgent and critical need for the discovery and/or development of improved drugs with universal efficacy to treat all the susceptible populations suffering from cryptosporidial infections.

Modern drug-discovery projects utilize either a phenotype-based or target-based screening approach to identify lead candidate compounds for further development. *Cryptosporidium* drug discovery programs in the recent past have mostly used phenotypic screening methods to successfully discover or repurpose compounds with *in vitro* and *in vivo* activity against the parasite (Love et al., 2017; Jumani et al., 2018; Lunde et al., 2019; Li et al., 2020; Khan et al., 2022a). However, such an approach invariably results in the identification of candidate compounds that are difficult to optimize as their molecular mechanism of action (MMOA) and structure-activity relationships (SAR) are generally unknown. This inflexibility typically leads to higher failure rates once a roadblock is reached in the drug development process. As such, molecular target identification and validation by various genetic and molecular

"target deconvolution" methodologies are essential for hits identified from phenotype-based screens (Swinney and Anthony, 2011).

Another approach to anti-cryptosporidial drug discovery is to target biochemical pathways that are unique to the parasite and at the same time, essential for its survival, infection, or multiplication within the host. This strategy has also been used for anti-*Cryptosporidium* drug discovery, albeit less commonly than the phenotypic one. In the last few years, several enzymes have been identified as potential drug targets, including calcium-dependent protein kinases (Van Voorhis et al., 2021), aminoacyl-tRNA synthetases (Jain et al., 2017; Baragana et al., 2019; Buckner et al., 2019; Vinayak et al., 2020), lipid kinase PI(4)K (Manjunatha et al., 2017), and glycolytic enzymes (Witola et al., 2017; Eltahan et al., 2018; Zhang et al., 2018; Eltahan et al., 2019; Li et al., 2019; Velez et al., 2021), among others. The advantage of this approach is that discovery of drug candidates with known MMOA and clearer SAR can create better opportunities for structure-based drug optimization. Indeed, while phenotypic screening has historically had more success in identifying first-in-class drugs, target-based screening has produced more best-in-class drugs (Swinney and Anthony, 2011). However, both approaches need to go hand in hand to identify safe and efficacious anti-*Cryptosporidium* lead compounds for further development.

C. parvum possesses an extensively simplified metabolism and does not possess several metabolic pathways, including the mannitol cycle, shikimate pathway, Krebs cycle, and electron transport chains (Zhu, 2007). As a result, the parasite relies significantly on the glycolytic pathway for generating metabolic energy. The glycolytic enzymes, therefore, are excellent targets for developing therapeutics against this human and veterinary pathogen. It has been previously reported that specific inhibitors of the *C. parvum* lactate dehydrogenase (CpLDH)

enzyme exhibit both *in vitro* and *in vivo* efficacy against *C. parvum* (Li et al., 2019). In the current study, we characterized the biochemical features of the recombinant *C. parvum* pyruvate kinase (CpPyK) enzyme. We found that the putative CpPyK protein indeed possessed pyruvate kinase catalytic activity and depicted Michaelis-Menten kinetics. Using a validated *in vitro* CpPyK enzymatic assay, we screened 1424 chemical compounds and discovered 70 compounds that showed more than 30% inhibition of the *in vitro* enzymatic activity of CpPyK at 50 μM concentration. To filter out compounds with potential toxicity issues, we tested these CpPyK-inhibitors for cytotoxicity in mammalian cells and found 44 compounds with low or no toxicity (<25%) at a test concentration of 50 μM. Among them, 6 compounds (NSC234945, NSC252172, NSC636718, NSC303244, NSC638080, and NSC11437) significantly inhibited the growth and proliferation of *C. parvum* in mammalian cells in the primary screen at 25 μM. In the secondary analysis, all 6 compounds showed concentration-dependent inhibitory effect against *C. parvum* with low micromolar EC_{50} values and high SI values. Importantly, oral treatment of infected IFN-γ KO mice with low non-toxic doses of NSC252172, NSC303244, NSC638080, or NSC234945 caused significant decreases in the fecal shedding of oocysts and prevented the development of intestinal lesions as compared to untreated infected mice. Treatment with higher doses of the most efficacious compounds, NSC234945 and NSC252172, produced a better dose-dependent response compared to the paromomycin positive control.

Combination therapy is the first-line treatment recommended for tuberculosis, HIV/AIDS, cancer, and apicomplexan diseases such as malaria, babesiosis, and toxoplasmosis. The use of combination therapy for cryptosporidiosis can help to 1) increase the efficacy of treatment, 2) reduce the chances of host toxicity, and 3) prevent the inevitable rise of drug resistance in the future. Yet, limited attempts have been undertaken in the past to assess drug

combinations for the treatment of cryptosporidiosis as pointed out earlier in Chapter 1 of this dissertation (Table 1.3). Interestingly, both glycolytic enzymes, CpLDH and CpPyK, are differentially expressed across the different stages of the *Cryptosporidium* life cycle suggesting that this parasite is capable of metabolic adjustments when it transitions from one developmental form to another during its life cycle. Therefore, concurrent inhibition of these essential parasite enzymes can be detrimental to the parasite's survival and multiplication within the host. To test this hypothesis, we combined CpLDH- and CpPyK-inhibitors in multiple combination ratios to form 24 compound mixtures and evaluated their cytotoxicity in mammalian cells. Non-toxic concentrations of individual compounds and combinations were subsequently tested for *in vitro* anti-cryptosporidial efficacy using *C. parvum* growth inhibition assays. We analyzed the *in vitro* dose-response data by multiple synergy-assessment methods and selected 3 synergistic compound combinations for *in vivo* studies. Interestingly, the *in vivo* efficacy of the tested combinations varied substantially in immunocompromised mice infected with *C. parvum*. While the NSC252172+NSC10447 combination showed reduced efficacy in treating cryptosporidiosis in infected mice, the NSC252172+NSC158011 combination depicted enhanced efficacy only during the treatment period. In contrast, the combination of NSC303244 and NSC158011 cured the disease and prevented relapse in mice after the termination of treatment, suggesting that this combination was parasiticidal against *C. parvum* in mice.

After successfully completing this dissertation work, we believe that we have laid a strong foundation for finding the much-needed cure for cryptosporidiosis. The next logical step would be to utilize the neonatal dairy calf animal model (a natural animal host for the parasite) of the disease to test the most efficacious compounds/combinations obtained in the study. *C. parvum*-infected newborn calves, unlike mice, exhibit a watery diarrheal disease like the one

seen in infected human infants (Zambriski et al., 2013). Thus, neonatal calves provide an excellent clinically relevant natural host for both animal and human cryptosporidiosis. However, prior to testing in calves, it will be necessary to acquire an understanding of the *in vivo* pharmacokinetic (PK) behavior of CpLDH- and CpPyK-inhibitors that will allow SAR investigation and management of undesirable PK properties related to solubility, bioavailability, metabolic stability, toxicity, and other important drug factors. The target patient population for anti-*Cryptosporidium* drug development is mainly comprised of young children, neonatal calves, and immunocompromised patients. These groups frequently suffer from co-morbidities due to their underdeveloped immunity or immunodeficiency and thus, there is an increased likelihood of such patients receiving other treatments. A highly safe pharmacological profile with a minimal risk of drug-drug interactions is, therefore, a key selection criterion for anti-*Cryptosporidium* drug candidates. In addition to safety-related pharmacological properties, assessment of the absorption, distribution, metabolism, and excretion (ADME) properties of a lead compound is also critical to its initial selection and clinical success. Failure of translation of excellent *in vitro* efficacy into *in vivo* clinical potency may be caused by insufficient drug concentrations at the target site. Because cryptosporidiosis is primarily an enteric disease, optimal local gastrointestinal concentrations, in addition to systemic concentrations, might be essential for *in vivo* anti-*Cryptosporidium* efficacy of the compounds (Hulverson et al., 2017; Manjunatha et al., 2017; Stebbins et al., 2018; Lunde et al., 2019).

Identification of novel and effective anti-cryptosporidial compounds/combinations in the current investigation has also enabled us to test various structural modifications to identify core compound pharmacophores associated with anti-parasitic activity against *C. parvum*. Together, all outcomes of this study will guide further structure-guided lead optimization efforts, for design

and synthesis of superior pre-clinical drug candidates with high potency, improved target selectivity, and attractive *in vivo* PK profiles. Ultimately, our research will help us move a step closer toward our goal of developing a gold standard therapy for human and animal cryptosporidiosis.

REFERENCES

Abaza, B.E., Hamza, R.S., Farag, T.I., Abdel-Hamid, M.A., and Moustafa, R.A. (2016). Assessing the Efficacy of Nitazoxanide in Treatment of Cryptosporidiosis Using Pcr Examination. *J Egypt Soc Parasitol* 46(3)**,** 683-692.

Abraham, D.R., Rabie, H., and Cotton, M.F. (2008). Nitazoxanide for severe cryptosporidial diarrhea in human immunodeficiency virus infected children. *Pediatr Infect Dis J* 27(11)**,** 1040-1041. doi: 10.1097/inf.0b013e318186257b.

Abrahamsen, M.S., Templeton, T.J., Enomoto, S., Abrahante, J.E., Zhu, G., Lancto, C.A., et al. (2004). Complete genome sequence of the apicomplexan, *Cryptosporidium parvum*. *Science* 304(5669)**,** 441-445. doi: 10.1126/science.1094786.

Abubakar, I., Aliyu, S.H., Arumugam, C., Hunter, P.R., and Usman, N.K. (2007). Prevention and treatment of cryptosporidiosis in immunocompromised patients. *Cochrane Database Syst Rev* (1)**,** CD004932. doi: 10.1002/14651858.CD004932.pub2.

Acikgoz, Y., Ozkaya, O., Bek, K., Genc, G., Sensoy, S.G., and Hokelek, M. (2012). Cryptosporidiosis: a rare and severe infection in a pediatric renal transplant recipient. *Pediatr Transplant* 16(4)**,** E115-119. doi: 10.1111/j.1399-3046.2011.01473.x.

Adamu, H., Wegayehu, T., and Petros, B. (2013). High prevalence of diarrhoegenic intestinal parasite infections among non-ART HIV patients in Fitche Hospital, Ethiopia. *PLoS One* 8(8)**,** e72634. doi: 10.1371/journal.pone.0072634.

Aggarwal, R., and Sumran, G. (2020). An insight on medicinal attributes of 1,2,4-triazoles. *Eur J Med Chem* 205**,** 112652. doi: 10.1016/j.ejmech.2020.112652.

Alagarsamy, V., Chitra, K., Saravanan, G., Solomon, V.R., Sulthana, M.T., and Narendhar, B. (2018). An overview of quinazolines: Pharmacological significance and recent developments. *Eur J Med Chem* 151**,** 628-685. doi: 10.1016/j.ejmech.2018.03.076.

Ali, S., Mumar, S., Kalam, K., Raja, K., and Baqi, S. (2014). Prevalence, clinical presentation and treatment outcome of cryptosporidiosis in immunocompetent adult patients presenting with acute diarrhoea. *J Pak Med Assoc* 64(6)**,** 613-618.

Allam, A.F., and Shehab, A.Y. (2002). Efficacy of azithromycin, praziquantel and mirazid in treatment of cryptosporidiosis in school children. *J Egypt Soc Parasitol* 32(3)**,** 969-978.

Almawly, J., Prattley, D., French, N.P., Lopez-Villalobos, N., Hedgespeth, B., and Grinberg, A. (2013). Utility of halofuginone lactate for the prevention of natural cryptosporidiosis of calves, in the presence of co-infection with rotavirus and *Salmonella* Typhimurium. *Vet Parasitol* 197(1-2)**,** 59-67. doi: 10.1016/j.vetpar.2013.04.029.

Amadi, B., Mwiya, M., Musuku, J., Watuka, A., Sianongo, S., Ayoub, A., et al. (2002). Effect of nitazoxanide on morbidity and mortality in Zambian children with cryptosporidiosis: a randomised controlled trial. *Lancet* 360(9343)**,** 1375-1380. doi: 10.1016/S0140-6736(02)11401-2.

Amadi, B., Mwiya, M., Sianongo, S., Payne, L., Watuka, A., Katubulushi, M., et al. (2009). High dose prolonged treatment with nitazoxanide is not effective for cryptosporidiosis in HIV positive Zambian children: a randomised controlled trial. *BMC Infect Dis* 9(1)**,** 195. doi: 10.1186/1471-2334-9-195.

Amenta, M., Dalle Nogare, E.R., Colomba, C., Prestileo, T.S., Di Lorenzo, F., Fundaro, S., et al. (1999). Intestinal protozoa in HIV-infected patients: effect of rifaximin in *Cryptosporidium parvum* and *Blastocystis hominis* infections. *J Chemother* 11(5)**,** 391-395. doi: 10.1179/joc.1999.11.5.391.

Amer, S., Zidan, S., Adamu, H., Ye, J., Roellig, D., Xiao, L., et al. (2013). Prevalence and characterization of *Cryptosporidium* spp. in dairy cattle in Nile River delta provinces, Egypt. *Exp Parasitol* 135(3)**,** 518-523. doi: 10.1016/j.exppara.2013.09.002.

Amoo, J.K., Akindele, A.A., Amoo, A.O.J., Efunshile, A.M., Ojurongbe, T.A., Fayemiwo, S.A., et al. (2018). Prevalence of enteric parasitic infections among people living with HIV in Abeokuta, Nigeria. *Pan Afr Med J* 30**,** 66. doi: 10.11604/pamj.2018.30.66.13160.

Angus, K.W., Tzipori, S., and Gray, E.W. (1982). Intestinal lesions in specific-pathogen-free lambs associated with a cryptosporidium from calves with diarrhea. *Vet Pathol* 19(1)**,** 67-78. doi: 10.1177/030098588201900110.

Armitage, K., Flanigan, T., Carey, J., Frank, I., MacGregor, R.R., Ross, P., et al. (1992). Treatment of cryptosporidiosis with paromomycin. A report of five cases. *Arch Intern Med* 152(12)**,** 2497-2499. doi: 10.1001/archinte.1992.00400240111018.

Arrowood, M.J., and Sterling, C.R. (1987). Isolation of *Cryptosporidium* oocysts and sporozoites using discontinuous sucrose and isopycnic Percoll gradients. *J Parasitol* 73(2)**,** 314-319. doi: Doi 10.2307/3282084.

Artursson, P., and Karlsson, J. (1991). Correlation between Oral-Drug Absorption in Humans and Apparent Drug Permeability Coefficients in Human Intestinal Epithelial (Caco-2) Cells. *Biochemical and Biophysical Research Communications* 175(3)**,** 880-885. doi: Doi 10.1016/0006-291x(91)91647-U.

Askari, N., Shayan, P., Mokhber-Dezfouli, M.R., Ebrahimzadeh, E., Lotfollahzadeh, S., Rostami, A., et al. (2016). Evaluation of recombinant P23 protein as a vaccine for passive immunization of newborn calves against *Cryptosporidium parvum*. *Parasite Immunol* 38(5)**,** 282-289. doi: 10.1111/pim.12317.

Aydogdu, U., Coskun, A., Atas, A.D., Basbug, O., and Agaoglu, Z.T. (2019). The determination of treatment effect of chitosan oligosaccharide in lambs with experimentally cryptosporidiosis. *Small Rumin Res* 180**,** 27-34. doi: 10.1016/j.smallrumres.2019.09.021.

Aydogdu, U., Isik, N., Ekici, O.D., Yildiz, R., Sen, I., and Coskun, A. (2018). Comparison of the Effectiveness of Halofuginone Lactate and Paromomycin in the Treatment of Calves Naturally Infected with *Cryptosporidium parvum*. *Acta Scientiae Veterinariae* 46(1)**,** 9. doi: 10.22456/1679-9216.81809.

Babiker, A., Darbyshire, J., Pezzotti, P., Porter, K., Rezza, G., Walker, S.A., et al. (2002). Changes over calendar time in the risk of specific first AIDS-defining events following HIV seroconversion, adjusting for competing risks. *Int J Epidemiol* 31(5)**,** 951-958. doi: 10.1093/ije/31.5.951.

Bachur, T.P., Vale, J.M., Coelho, I.C., Queiroz, T.R., and Chaves Cde, S. (2008). Enteric parasitic infections in HIV/AIDS patients before and after the highly active antiretroviral therapy. *Braz J Infect Dis* 12(2)**,** 115-122. doi: 10.1590/s1413-86702008000200004.

Bakliwal, A., Nath, U.K., Mohanty, A., and Gupta, P. (2021). Life-Threatening *Cryptosporidium* Diarrhea in a Child on Induction Chemotherapy for Acute Lymphoblastic Leukemia. *Cureus* 13(9)**,** e18340. doi: 10.7759/cureus.18340.

Baragana, B., Forte, B., Choi, R., Nakazawa Hewitt, S., Bueren-Calabuig, J.A., Pisco, J.P., et al. (2019). Lysyl-tRNA synthetase as a drug target in malaria and cryptosporidiosis. *Proc Natl Acad Sci U S A* 116(14)**,** 7015-7020. doi: 10.1073/pnas.1814685116.

Bellini, V., Swale, C., Brenier-Pinchart, M.P., Pezier, T., Georgeault, S., Laurent, F., et al. (2020). Target Identification of an Antimalarial Oxaborole Identifies AN13762 as an

Alternative Chemotype for Targeting CPSF3 in Apicomplexan Parasites. *iScience* 23(12)**,** 101871. doi: 10.1016/j.isci.2020.101871.

Benson, J.E., Ensley, S.M., Carson, T.L., Halbur, P.G., Janke, B.H., and Quinn, W.J. (1998). Lasalocid toxicosis in neonatal calves. *J Vet Diagn Invest* 10(2)**,** 210-214. doi: 10.1177/104063879801000224.

Berg, J.M., Tymoczko, J.L., and Stryer, L. (2002). "The Glycolytic Pathway Is Tightly Controlled," in *Biochemistry*. 5th ed: W H Freeman).

Bhadauria, D., Goel, A., Kaul, A., Sharma, R.K., Gupta, A., Ruhela, V., et al. (2015). *Cryptosporidium* infection after renal transplantation in an endemic area. *Transpl Infect Dis* 17(1)**,** 48-55. doi: 10.1111/tid.12336.

Bissuel, F., Cotte, L., Rabodonirina, M., Rougier, P., Piens, M.A., and Trepo, C. (1994). Paromomycin: an effective treatment for cryptosporidial diarrhea in patients with AIDS. *Clin Infect Dis* 18(3)**,** 447-449. doi: 10.1093/clinids/18.3.447.

Blanshard, C., Shanson, D.C., and Gazzard, B.G. (1997). Pilot studies of azithromycin, letrazuril and paromomycin in the treatment of cryptosporidiosis. *Int J STD AIDS* 8(2)**,** 124-129. doi: 10.1258/0956462971919543.

Bobin, S., Bouhour, D., Durupt, S., Boibieux, A., Girault, V., and Peyramond, D. (1998). [Importance of antiproteases in the treatment of microsporidia and/or cryptosporidia infections in HIV-seropositive patients]. *Pathol Biol (Paris)* 46(6)**,** 418-419.

Borowitz, S.M., and Saulsbury, F.T. (1991). Treatment of chronic cryptosporidial infection with orally administered human serum immune globulin. *J Pediatr* 119(4)**,** 593-595. doi: 10.1016/s0022-3476(05)82412-6.

Braga, S.S. (2019). Cyclodextrins: Emerging Medicines of the New Millennium. *Biomolecules* 9(12)**,** 801. doi: 10.3390/biom9120801.

Brainard, J., Hammer, C.C., Hunter, P.R., Katzer, F., Hurle, G., and Tyler, K. (2021). Efficacy of halofuginone products to prevent or treat cryptosporidiosis in bovine calves: a systematic review and meta-analyses. *Parasitology* 148(4)**,** 408-419. doi: 10.1017/S0031182020002267.

Buckner, F.S., Ranade, R.M., Gillespie, J.R., Shibata, S., Hulverson, M.A., Zhang, Z., et al. (2019). Optimization of Methionyl tRNA-Synthetase Inhibitors for Treatment of *Cryptosporidium* Infection. *Antimicrob Agents Chemother* 63(4)**,** e02061-02018. doi: 10.1128/AAC.02061-18.

Burdese, M., Veglio, V., Consiglio, V., Soragna, G., Mezza, E., Bergamo, D., et al. (2005). A dance teacher with kidney-pancreas transplant and diarrhoea: what is the cause? *Nephrol Dial Transplant* 20(8)**,** 1759-1761. doi: 10.1093/ndt/gfh881.

Call, S.A., Heudebert, G., Saag, M., and Wilcox, C.M. (2000). The changing etiology of chronic diarrhea in HIV-infected patients with CD4 cell counts less than 200 cells/mm3. *Am J Gastroenterol* 95(11)**,** 3142-3146. doi: 10.1111/j.1572-0241.2000.03285.x.

Carr, A., Marriott, D., Field, A., Vasak, E., and Cooper, D.A. (1998). Treatment of HIV-1-associated microsporidiosis and cryptosporidiosis with combination antiretroviral therapy. *Lancet* 351(9098)**,** 256-261. doi: 10.1016/S0140-6736(97)07529-6.

Castro-Hermida, J.A., Garcia-Presedo, I., Gonzalez-Warleta, M., Mezo, M., Fenoy, S., Rueda, C., et al. (2008). Activity of an anti-inflammatory drug against cryptosporidiosis in neonatal lambs. *Vet Parasitol* 155(3-4)**,** 308-313. doi: 10.1016/j.vetpar.2008.05.012.

Castro-Hermida, J.A., Gonzalez-Losada, Y., Freire-Santos, F., Mezo-Menendez, M., and Ares-Mazas, E. (2001a). Evaluation of beta-cyclodextrin against natural infections of

cryptosporidiosis in calves. *Vet Parasitol* 101(2)**,** 85-89. doi: 10.1016/s0304-4017(01)00505-2.

Castro-Hermida, J.A., Gonzalez-Warleta, M., and Mezo, M. (2007). Natural infection by *Cryptosporidium parvum* and *Giardia duodenalis* in sheep and goats in Galicia (NW Spain). *Small Ruminant Research* 72(2-3)**,** 96-100. doi: 10.1016/j.smallrumres.2006.08.008.

Castro-Hermida, J.A., Pors, I., Otero-Espinar, F., Luzardo-Alvarez, A., Ares-Mazas, E., and Chartier, C. (2004). Efficacy of alpha-cyclodextrin against experimental cryptosporidiosis in neonatal goats. *Vet Parasitol* 120(1-2)**,** 35-41. doi: 10.1016/j.vetpar.2003.12.012.

Castro-Hermida, J.A., Quilez-Cinca, J., Lopez-Bernad, F., Sanchez-Acedo, C., Freire-Santos, F., and Ares-Mazas, E. (2001b). Treatment with beta-cyclodextrin of natural *Cryptosporidium parvum* infections in lambs under field conditions. *Int J Parasitol* 31(10)**,** 1134-1137. doi: 10.1016/s0020-7519(01)00220-x.

Causape, A.C., Quilez, J., Sanchez-Acedo, C., del Cacho, E., and Lopez-Bernad, F. (2002). Prevalence and analysis of potential risk factors for *Cryptosporidium parvum* infection in lambs in Zaragoza (northeastern Spain). *Vet Parasitol* 104(4)**,** 287-298. doi: 10.1016/s0304-4017(01)00639-2.

Causapé, A.C., Sanchez-Acedo, C., Quilez, J., Del Cacho, E., and Viu, M. (1999). Efficacy of halofuginone lactate against natural *Cryptosporidium parvum* infections in lambs. *Res Rev Parasitol* 59**,** 41-46.

CDC (2019). *DPDx Cryptosporidiosis* [Online]. Centers for Disease Control and Prevention (CDC). Available: https://www.cdc.gov/dpdx/cryptosporidiosis/index.html [Accessed December 30 2022].

Cello, J.P., Grendell, J.H., Basuk, P., Simon, D., Weiss, L., Wittner, M., et al. (1991). Effect of octreotide on refractory AIDS-associated diarrhea. A prospective, multicenter clinical trial. *Ann Intern Med* 115(9)**,** 705-710. doi: 10.7326/0003-4819-115-9-705.

Cerveja, B.Z., Tucuzo, R.M., Madureira, A.C., Nhacupe, N., Langa, I.A., Buene, T., et al. (2017). Prevalence of Intestinal Parasites Among HIV Infected and HIV Uninfected Patients Treated at the 1 degrees De Maio Health Centre in Maputo, Mozambique. *EC Microbiol* 9(6)**,** 231-240.

Chalmers, R.M. (2012). Waterborne outbreaks of cryptosporidiosis. *Ann Ist Super Sanita* 48(4)**,** 429-446. doi: 10.4415/ANN_12_04_10.

Chalmers, R.M. (2014). "*Cryptosporidium*," in *Microbiology of Waterborne Diseases*, eds. S.L. Percival, M.V. Yates, D.W. Williams, R.M. Chalmers & N.F. Gray. Elsevier Ltd.), 287-326.

Chartier, C., Mallereau, M.P., and Lenfant, D. (1999). Halofuginone lactate in the control of cryptosporidiosis in neonate kids. *Revue De Medecine Veterinaire* 150(4)**,** 341-346.

Chartier, C., Mallereau, M.P., and Naciri, M. (1996). Prophylaxis using paromomycin of natural cryptosporidial infection in neonatal kids. *Preventive Veterinary Medicine* 25(3-4)**,** 357-361. doi: Doi 10.1016/0167-5877(95)00511-0.

Checkley, W., White, A.C., Jr., Jaganath, D., Arrowood, M.J., Chalmers, R.M., Chen, X.M., et al. (2015). A review of the global burden, novel diagnostics, therapeutics, and vaccine targets for cryptosporidium. *Lancet Infect Dis* 15(1)**,** 85-94. doi: 10.1016/S1473-3099(14)70772-8.

Cho, Y.I., Han, J.I., Wang, C., Cooper, V., Schwartz, K., Engelken, T., et al. (2013). Case-control study of microbiological etiology associated with calf diarrhea. *Vet Microbiol* 166(3-4)**,** 375-385. doi: 10.1016/j.vetmic.2013.07.001.

Chou, T.C., and Talalay, P. (1984). Quantitative analysis of dose-effect relationships: the combined effects of multiple drugs or enzyme inhibitors. *Adv Enzyme Regul* 22(C)**,** 27-55. doi: 10.1016/0065-2571(84)90007-4.

Clezy, K., Gold, J., Blaze, J., and Jones, P. (1991). Paromomycin for the treatment of cryptosporidial diarrhoea in AIDS patients. *AIDS* 5(9)**,** 1146-1147.

Clotet, B., Sirera, G., Cofan, F., Monterola, J.M., Tortosa, F., and Fox, M. (1989). Efficacy of the somatostatin analogue (SMS-201-995), Sandostatin, for cryptosporidial diarrhoea in patients with AIDS. *AIDS* 3(12)**,** 857-858. doi: 10.1097/00002030-198912000-00016.

Collaborators, G.B.D.D.D. (2018). Estimates of the global, regional, and national morbidity, mortality, and aetiologies of diarrhoea in 195 countries: a systematic analysis for the Global Burden of Disease Study 2016. *Lancet Infect Dis* 18(11)**,** 1211-1228. doi: 10.1016/S1473-3099(18)30362-1.

Connolly, G.M., Youle, M., and Gazzard, B.G. (1990). Diclazuril in the treatment of severe cryptosporidial diarrhoea in AIDS patients. *AIDS* 4(7)**,** 700-701. doi: 10.1097/00002030-199007000-00020.

Connor, E.E., Wall, E.H., Bravo, D.M., Evock-Clover, C.M., Elsasser, T.H., Baldwin, R.L.t., et al. (2017). Reducing gut effects from *Cryptosporidium parvum* infection in dairy calves through prophylactic glucagon-like peptide 2 therapy or feeding of an artificial sweetener. *J Dairy Sci* 100(4)**,** 3004-3018. doi: 10.3168/jds.2016-11861.

Conti, S., Masocco, M., Pezzotti, P., Toccaceli, V., Vichi, M., Boros, S., et al. (2000). Differential impact of combined antiretroviral therapy on the survival of italian patients with specific AIDS-defining illnesses. *J Acquir Immune Defic Syndr* 25(5)**,** 451-458. doi: 10.1097/00042560-200012150-00011.

Cook, D.J., Kelton, J.G., Stanisz, A.M., and Collins, S.M. (1988). Somatostatin treatment for cryptosporidial diarrhea in a patient with the acquired immunodeficiency syndrome (AIDS). *Ann Intern Med* 108(5)**,** 708-709. doi: 10.7326/0003-4819-108-5-708.

Cook, W.J., Senkovich, O., Aleem, K., and Chattopadhyay, D. (2012). Crystal structure of *Cryptosporidium parvum* pyruvate kinase. *PLoS One* 7(10)**,** e46875. doi: 10.1371/journal.pone.0046875.

Cook, W.J., Senkovich, O., Hernandez, A., Speed, H., and Chattopadhyay, D. (2015). Biochemical and structural characterization of *Cryptosporidium parvum* Lactate dehydrogenase. *Int J Biol Macromol* 74**,** 608-619. doi: 10.1016/j.ijbiomac.2014.12.019.

Corso, P.S., Kramer, M.H., Blair, K.A., Addiss, D.G., Davis, J.P., and Haddix, A.C. (2003). Cost of illness in the 1993 waterborne *Cryptosporidium* outbreak, Milwaukee, Wisconsin. *Emerg Infect Dis* 9(4)**,** 426-431. doi: 10.3201/eid0904.020417.

Current, W.L. (1990). "Techniques and laboratory maintenance of *Cryptosporidium*," in *Cryptosporidiosis of Man and Animals*, eds. J.P. Dubey, C.A. Speer & R. Fayer. CRC Press, Boca Raton, Fla), 44-77.

Current, W.L. (2018). "Techniques and Laboratory Maintenance of *Cryptosporidium*," in *Cryptosporidiosis of Man and Animals*. CRC Press), 31-50.

Current, W.L., and Garcia, L.S. (1991). Cryptosporidiosis. *Clin Microbiol Rev* 4(3)**,** 325-358. doi: 10.1128/CMR.4.3.325.

Current, W.L., and Reese, N.C. (1986). A comparison of endogenous development of three isolates of *Cryptosporidium* in suckling mice. *J Protozool* 33(1)**,** 98-108. doi: 10.1111/j.1550-7408.1986.tb05567.x.

Current, W.L., Reese, N.C., Ernst, J.V., Bailey, W.S., Heyman, M.B., and Weinstein, W.M. (1983). Human cryptosporidiosis in immunocompetent and immunodeficient persons. Studies of an outbreak and experimental transmission. *N Engl J Med* 308(21)**,** 1252-1257. doi: 10.1056/NEJM198305263082102.

D'Antonio, R.G., Winn, R.E., Taylor, J.P., Gustafson, T.L., Current, W.L., Rhodes, M.M., et al. (1985). A waterborne outbreak of cryptosporidiosis in normal hosts. *Ann Intern Med* 103(6 (Pt 1))**,** 886-888. doi: 10.7326/0003-4819-103-6-886.

Danziger-Isakov, L. (2014). Gastrointestinal infections after transplantation. *Curr Opin Gastroenterol* 30(1)**,** 40-46. doi: 10.1097/MOG.0000000000000016.

Danziger, L.H., Kanyok, T.P., and Novak, R.M. (1993). Treatment of cryptosporidial diarrhea in an AIDS patient with paromomycin. *Ann Pharmacother* 27(12)**,** 1460-1462. doi: 10.1177/106002809302701209.

de Graaf, D.C., Vanopdenbosch, E., Ortega-Mora, L.M., Abbassi, H., and Peeters, J.E. (1999). A review of the importance of cryptosporidiosis in farm animals. *Int J Parasitol* 29(8)**,** 1269-1287. doi: 10.1016/s0020-7519(99)00076-4.

de Oliveira-Silva, M.B., de Oliveira, L.R., Resende, J.C., Peghini, B.C., Ramirez, L.E., Lages-Silva, E., et al. (2007). Seasonal profile and level of CD4+ lymphocytes in the occurrence of cryptosporidiosis and cystoisosporidiosis in HIV/AIDS patients in the Triangulo Mineiro region, Brazil. *Rev Soc Bras Med Trop* 40(5)**,** 512-515. doi: 10.1590/s0037-86822007000500004.

De Waele, V., Speybroeck, N., Berkvens, D., Mulcahy, G., and Murphy, T.M. (2010). Control of cryptosporidiosis in neonatal calves: use of halofuginone lactate in two different calf rearing systems. *Prev Vet Med* 96(3-4)**,** 143-151. doi: 10.1016/j.prevetmed.2010.06.017.

Demonchy, J., Cordier, C., Frealle, E., Demarquette, H., Herbaux, C., Escure, G., et al. (2021). Case Report: Two Cases of Cryptosporidiosis in Heavily Pretreated Patients With Myeloma. *Clin Lymphoma Myeloma Leuk* 21(6)**,** e545-e547. doi: 10.1016/j.clml.2021.01.019.

Denkinger, C.M., Harigopal, P., Ruiz, P., and Dowdy, L.M. (2008). *Cryptosporidium parvum*-associated sclerosing cholangitis in a liver transplant patient. *Transpl Infect Dis* 10(2)**,** 133-136. doi: 10.1111/j.1399-3062.2007.00245.x.

Denton, H., Brown, S.M., Roberts, C.W., Alexander, J., McDonald, V., Thong, K.W., et al. (1996). Comparison of the phosphofructokinase and pyruvate kinase activities of *Cryptosporidium parvum*, *Eimeria tenella* and *Toxoplasma gondii*. *Mol Biochem Parasitol* 76(1-2)**,** 23-29. doi: 10.1016/0166-6851(95)02527-8.

Desai, N.T., Sarkar, R., and Kang, G. (2012). Cryptosporidiosis: An under-recognized public health problem. *Trop Parasitol* 2(2)**,** 91-98. doi: 10.4103/2229-5070.105173.

Dillingham, R.A., Pinkerton, R., Leger, P., Severe, P., Guerrant, R.L., Pape, J.W., et al. (2009). High early mortality in patients with chronic acquired immunodeficiency syndrome diarrhea initiating antiretroviral therapy in Haiti: a case-control study. *Am J Trop Med Hyg* 80(6)**,** 1060-1064.

Dinler Ay, C., Voyvoda, H., Ulutas, P.A., Karagenc, T., and Ulutas, B. (2021). Prophylactic and therapeutic efficacy of clinoptilolite against *Cryptosporidium parvum* in experimentally

challenged neonatal lambs. *Vet Parasitol* 299**,** 109574. doi: 10.1016/j.vetpar.2021.109574.

Dionisio, D., Orsi, A., Sterrantino, G., Meli, M., Di Lollo, S., Ibba Manneschi, L., et al. (1998). Chronic cryptosporidiosis in patients with AIDS: stable remission and possible eradication after long-term, low dose azithromycin. *J Clin Pathol* 51(2)**,** 138-142. doi: 10.1136/jcp.51.2.138.

Doumbo, O., Rossignol, J.F., Pichard, E., Traore, H.A., Dembele, T.M., Diakite, M., et al. (1997). Nitazoxanide in the treatment of cryptosporidial diarrhea and other intestinal parasitic infections associated with acquired immunodeficiency syndrome in tropical Africa. *Am J Trop Med Hyg* 56(6)**,** 637-639. doi: 10.4269/ajtmh.1997.56.637.

Dupuy, F., Valot, S., Dalle, F., Sterin, A., and L'Ollivier, C. (2021). Disseminated *Cryptosporidium* infection in an infant with CD40L deficiency. *IDCases* 24**,** e01115. doi: 10.1016/j.idcr.2021.e01115.

Duru, S.Y., Öcal, N., Yağcİ, B.B., Gazyağcİ, S., Duru, Ö., and Yİldİz, K. (2013). The therapeutic efficacy of tylosin in calf cryptosporidiosis. *Kafkas Üniversitesi Veteriner Fakültesi Dergisi* 19(Supplement A)**,** A175-A180.

Elitok, B., Elitok, O.M., and Pulat, H. (2005). Efficacy of azithromycin dihydrate in treatment of cryptosporidiosis in naturally infected dairy calves. *J Vet Intern Med* 19(4)**,** 590-593. doi: 10.1892/0891-6640(2005)19[590:eoadit]2.0.co;2.

Eltahan, R., Guo, F., Zhang, H., Xiang, L., and Zhu, G. (2018). Discovery of ebselen as an inhibitor of *Cryptosporidium parvum* glucose-6-phosphate isomerase (CpGPI) by high-throughput screening of existing drugs. *Int J Parasitol Drugs Drug Resist* 8(1)**,** 43-49. doi: 10.1016/j.ijpddr.2018.01.003.

Eltahan, R., Guo, F., Zhang, H., and Zhu, G. (2019). The Action of the Hexokinase Inhibitor 2-deoxy-d-glucose on *Cryptosporidium parvum* and the Discovery of Activities against the Parasite Hexokinase from Marketed Drugs. *J Eukaryot Microbiol* 66(3)**,** 460-468. doi: 10.1111/jeu.12690.

English, E.D., Guerin, A., Tandel, J., and Striepen, B. (2022). Live imaging of the *Cryptosporidium parvum* life cycle reveals direct development of male and female gametes from type I meronts. *PLoS Biol* 20(4)**,** e3001604. doi: 10.1371/journal.pbio.3001604.

Entrala, E., and Mascaro, C. (1997). Glycolytic enzyme activities in *Cryptosporidium parvum* oocysts. *FEMS Microbiol Lett* 151(1)**,** 51-57. doi: 10.1016/s0378-1097(97)00136-5.

Faul, F., Erdfelder, E., Lang, A.G., and Buchner, A. (2007). G*Power 3: a flexible statistical power analysis program for the social, behavioral, and biomedical sciences. *Behav Res Methods* 39(2)**,** 175-191. doi: 10.3758/bf03193146.

Fayer, R. (1992). Activity of sulfadimethoxine against cryptosporidiosis in dairy calves. *J Parasitol* 78(3)**,** 534-537.

Fayer, R., Andrews, C., Ungar, B.L., and Blagburn, B. (1989). Efficacy of hyperimmune bovine colostrum for prophylaxis of cryptosporidiosis in neonatal calves. *J Parasitol* 75(3)**,** 393-397. doi: 10.2307/3282595.

Fayer, R., and Ellis, W. (1993). Paromomycin is effective as prophylaxis for cryptosporidiosis in dairy calves. *J Parasitol* 79(5)**,** 771-774.

Fayer, R., and Fetterer, R. (1995). Activity of benzimidazoles against cryptosporidiosis in neonatal BALB/c mice. *J Parasitol* 81(5)**,** 794-795.

Fayer, R., Klesius, P.H., and Andrews, C. (1987). Efficacy of bovine transfer factor to protect neonatal calves against experimentally induced clinical cryptosporidiosis. *J Parasitol* 73(5)**,** 1061-1062.

Fayer, R., and Leek, R.G. (1984). The effects of reducing conditions, medium, pH, temperature, and time on in vitro excystation of *Cryptosporidium*. *J Protozool* 31(4)**,** 567-569. doi: 10.1111/j.1550-7408.1984.tb05504.x.

Fayer, R., Morgan, U., and Upton, S.J. (2000). Epidemiology of *Cryptosporidium*: transmission, detection and identification. *Int J Parasitol* 30(12-13)**,** 1305-1322. doi: 10.1016/s0020-7519(00)00135-1.

Fayer, R., and Santin, M. (2009). *Cryptosporidium xiaoi* n. sp. (Apicomplexa: Cryptosporidiidae) in sheep (*Ovis aries*). *Vet Parasitol* 164(2-4)**,** 192-200. doi: 10.1016/j.vetpar.2009.05.011.

Fayer, R., Santin, M., and Macarisin, D. (2010). *Cryptosporidium ubiquitum* n. sp. in animals and humans. *Vet Parasitol* 172(1-2)**,** 23-32. doi: 10.1016/j.vetpar.2010.04.028.

Fayer, R., Santin, M., and Trout, J.M. (2008). *Cryptosporidium ryanae* n. sp. (Apicomplexa: Cryptosporidiidae) in cattle (*Bos taurus*). *Vet Parasitol* 156(3-4)**,** 191-198. doi: 10.1016/j.vetpar.2008.05.024.

Fayer, R., Santin, M., Trout, J.M., and Greiner, E. (2006). Prevalence of species and genotypes of *Cryptosporidium* found in 1-2-year-old dairy cattle in the eastern United States. *Vet Parasitol* 135(2)**,** 105-112. doi: 10.1016/j.vetpar.2005.08.003.

Fayer, R., Santin, M., and Xiao, L. (2005). *Cryptosporidium bovis* n. sp. (Apicomplexa: Cryptosporidiidae) in cattle (*Bos taurus*). *J Parasitol* 91(3)**,** 624-629. doi: 10.1645/GE-3435.

FDA (2012). *21CFR530.41 Drugs prohibited for extralabel use in animals* [Online]. Food and Drug Administration. Available: https://www.accessdata.fda.gov/scripts/cdrh/cfdocs/cfCFR/CFRSearch.cfm?fr=530.41 [Accessed 19 November 2022].

Fernandez, S., Fraga, M., Castells, M., Colina, R., and Zunino, P. (2020). Effect of the administration of *Lactobacillus* spp. strains on neonatal diarrhoea, immune parameters and pathogen abundance in pre-weaned calves. *Benef Microbes* 11(5)**,** 477-488. doi: 10.3920/BM2019.0167.

Ferre, I., Benito-Pena, A., Garcia, U., Osoro, K., and Ortega-Mora, L.M. (2005). Effect of different decoquinate treatments on cryptosporidiosis in naturally infected cashmere goat kids. *Vet Rec* 157(9)**,** 261-262. doi: 10.1136/vr.157.9.261.

Fichtenbaum, C.J., Ritchie, D.J., and Powderly, W.G. (1993). Use of paromomycin for treatment of cryptosporidiosis in patients with AIDS. *Clin Infect Dis* 16(2)**,** 298-300. doi: 10.1093/clind/16.2.298.

Fichtenbaum, C.J., Zackin, R., Feinberg, J., Benson, C., Griffiths, J.K., and Team, A.C.T.G.N.W.C.S. (2000). Rifabutin but not clarithromycin prevents cryptosporidiosis in persons with advanced HIV infection. *AIDS* 14(18)**,** 2889-2893. doi: 10.1097/00002030-200012220-00010.

Fischer, O. (1983). Attempted Therapy and Prophylaxis of Cryptosporidiosis in Calves by Administration of Sulphadimidine. *Acta Veterinaria Brno* 52(3-4)**,** 183-190. doi: 10.2754/avb198352030183.

Flanigan, T., Whalen, C., Turner, J., Soave, R., Toerner, J., Havlir, D., et al. (1992). *Cryptosporidium* infection and CD4 counts. *Ann Intern Med* 116(10)**,** 840-842. doi: 10.7326/0003-4819-116-10-840.

Flanigan, T.P., Ramratnam, B., Graeber, C., Hellinger, J., Smith, D., Wheeler, D., et al. (1996). Prospective trial of paromomycin for cryptosporidiosis in AIDS. *Am J Med* 100(3)**,** 370-372. doi: 10.1016/S0002-9343(97)89499-5.

Floren, C.H., Chinenye, S., Elfstrand, L., Hagman, C., and Ihse, I. (2006). ColoPlus, a new product based on bovine colostrum, alleviates HIV-associated diarrhoea. *Scand J Gastroenterol* 41(6)**,** 682-686. doi: 10.1080/00365520500380817.

Fothergill-Gilmore, L.A., and Michels, P.A. (1993). Evolution of glycolysis. *Prog Biophys Mol Biol* 59(2)**,** 105-235. doi: 10.1016/0079-6107(93)90001-z.

Foudraine, N.A., Weverling, G.J., van Gool, T., Roos, M.T., de Wolf, F., Koopmans, P.P., et al. (1998). Improvement of chronic diarrhoea in patients with advanced HIV-1 infection during potent antiretroviral therapy. *AIDS* 12(1)**,** 35-41. doi: 10.1097/00002030-199801000-00005.

Gathe, J., Piot, D., Hawkins, K., Bernal, A., Clemmons, J., and Stool, E. (1990). "Treatment of gastrointestinal cryptosporidiosis with paromomycin (abstract 2121)", in: *International Conference on AIDS.* (San Francisco, CA).

Gathe, J.C., Jr., Mayberry, C., Clemmons, J., and Nemecek, J. (2008). Resolution of severe cryptosporidial diarrhea with rifaximin in patients with AIDS. *J Acquir Immune Defic Syndr* 48(3)**,** 363-364. doi: 10.1097/QAI.0b013e31817beb78.

Geurden, T., Thomas, P., Casaert, S., Vercruysse, J., and Claerebout, E. (2008). Prevalence and molecular characterisation of *Cryptosporidium* and *Giardia* in lambs and goat kids in Belgium. *Vet Parasitol* 155(1-2)**,** 142-145. doi: 10.1016/j.vetpar.2008.05.002.

Gharpure, R., Perez, A., Miller, A.D., Wikswo, M.E., Silver, R., and Hlavsa, M.C. (2019). Cryptosporidiosis Outbreaks - United States, 2009-2017. *MMWR Morb Mortal Wkly Rep* 68(25)**,** 568-572. doi: 10.15585/mmwr.mm6825a3.

Giacometti, A., Cirioni, O., Barchiesi, F., Ancarani, F., and Scalise, G. (2000). Activity of nitazoxanide alone and in combination with azithromycin and rifabutin against *Cryptosporidium parvum* in cell culture. *J Antimicrob Chemother* 45(4)**,** 453-456. doi: 10.1093/jac/45.4.453.

Giadinis, N.D., Papadopoulos, E., Lafi, S.Q., Panousis, N.K., Papazahariadou, M., and Karatzias, H. (2008). Efficacy of halofuginone lactate for the treatment and prevention of cryptosporidiosis in goat kids: An extensive field trial. *Small Ruminant Research* 76(3)**,** 195-200. doi: 10.1016/j.smallrumres.2008.01.007.

Giadinis, N.D., Papadopoulos, E., Panousis, N., Papazahariadou, M., Lafi, S.Q., and Karatzias, H. (2007). Effect of halofuginone lactate on treatment and prevention of lamb cryptosporidiosis: an extensive field trial. *J Vet Pharmacol Ther* 30(6)**,** 578-582. doi: 10.1111/j.1365-2885.2007.00900.x.

Girard, P.M., Goldschmidt, E., Vittecoq, D., Massip, P., Gastiaburu, J., Meyohas, M.C., et al. (1992). Vapreotide, a somatostatin analogue, in cryptosporidiosis and other AIDS-related diarrhoeal diseases. *AIDS* 6(7)**,** 715-718. doi: 10.1097/00002030-199207000-00015.

Gobel, E. (1987a). Diagnosis and treatment of acute cryptosporidiosis in the calf. *Tieraerztliche Umschau* 42**,** 863-869.

Gobel, E. (1987b). Possibilities of therapy of cryptosporidiosis in calves in problematic farms. *Zentralblatt für Bakteriologie, Mikrobiologie und Hygiene. Series A: Medical Microbiology, Infectious Diseases, Virology, Parasitology* 265(3-4)**,** 490-490.

Goma, F.Y., Geurden, T., Siwila, J., Phiri, I.G.K., Gabriel, S., Claerebout, E., et al. (2007). The prevalence and molecular characterisation of *Cryptosporidium* spp. in small ruminants in Zambia. *Small Ruminant Research* 72(1)**,** 77-80. doi: 10.1016/j.smallrumres.2006.08.010.

Greenberg, P.D., and Cello, J.P. (1996). Treatment of severe diarrhea caused by *Cryptosporidium parvum* with oral bovine immunoglobulin concentrate in patients with AIDS. *J Acquir Immune Defic Syndr Hum Retrovirol* 13(4)**,** 348-354. doi: 10.1097/00042560-199612010-00008.

Griffiths, J.K., Theodos, C., Paris, M., and Tzipori, S. (1998). The gamma interferon gene knockout mouse: a highly sensitive model for evaluation of therapeutic agents against *Cryptosporidium parvum*. *J Clin Microbiol* 36(9)**,** 2503-2508. doi: 10.1128/JCM.36.9.2503-2508.1998.

Grinberg, A., Markovics, A., Galindez, J., Lopez-Villalobos, N., Kosak, A., and Tranquillo, V.M. (2002). Controlling the onset of natural cryptosporidiosis in calves with paromomycin sulphate. *Vet Rec* 151(20)**,** 606-608. doi: 10.1136/vr.151.20.606.

Grube, H., Ramratnam, B., Ley, C., and Flanigan, T.P. (1997). Resolution of AIDS associated cryptosporidiosis after treatment with indinavir. *Am J Gastroenterol* 92(4)**,** 726.

Guerin, A., and Striepen, B. (2020). The Biology of the Intestinal Intracellular Parasite *Cryptosporidium*. *Cell Host Microbe* 28(4)**,** 509-515. doi: 10.1016/j.chom.2020.09.007.

Guerrant, D.I., Moore, S.R., Lima, A.A., Patrick, P.D., Schorling, J.B., and Guerrant, R.L. (1999). Association of early childhood diarrhea and cryptosporidiosis with impaired physical fitness and cognitive function four-seven years later in a poor urban community in northeast Brazil. *Am J Trop Med Hyg* 61(5)**,** 707-713. doi: 10.4269/ajtmh.1999.61.707.

Harp, J.A., Jardon, P., Atwill, E.R., Zylstra, M., Checel, S., Goff, J.P., et al. (1996). Field testing of prophylactic measures against *Cryptosporidium parvum* infection in calves in a California dairy herd. *Am J Vet Res* 57(11)**,** 1586-1588.

Harris, M., Deutsch, G., MacLean, J.D., and Tsoukas, C.M. (1994). A phase I study of letrazuril in AIDS-related cryptosporidiosis. *AIDS* 8(8)**,** 1109-1113. doi: 10.1097/00002030-199408000-00011.

Hartmann, G., Honikel, K.O., Knusel, F., and Nuesch, J. (1967). The specific inhibition of the DNA-directed RNA synthesis by rifamycin. *Biochim Biophys Acta* 145(3)**,** 843-844. doi: 10.1016/0005-2787(67)90147-5.

Hasan, M.M., Stebbins, E.E., Choy, R.K.M., Gillespie, J.R., de Hostos, E.L., Miller, P., et al. (2021). Spontaneous Selection of *Cryptosporidium* Drug Resistance in a Calf Model of Infection. *Antimicrob Agents Chemother* 65(6). doi: 10.1128/AAC.00023-21.

Hashmey, R., Smith, N.H., Cron, S., Graviss, E.A., Chappell, C.L., and White, A.C., Jr. (1997). Cryptosporidiosis in Houston, Texas. A report of 95 cases. *Medicine (Baltimore)* 76(2)**,** 118-139. doi: 10.1097/00005792-199703000-00004.

Hatam-Nahavandi, K., Ahmadpour, E., Carmena, D., Spotin, A., Bangoura, B., and Xiao, L. (2019). *Cryptosporidium* infections in terrestrial ungulates with focus on livestock: a systematic review and meta-analysis. *Parasit Vectors* 12(1)**,** 453. doi: 10.1186/s13071-019-3704-4.

Hayes, E.B., Matte, T.D., O'Brien, T.R., McKinley, T.W., Logsdon, G.S., Rose, J.B., et al. (1989). Large community outbreak of cryptosporidiosis due to contamination of a filtered

public water supply. *N Engl J Med* 320(21)**,** 1372-1376. doi: 10.1056/NEJM198905253202103.

Henry, R.J. (1943). The Mode of Action of Sulfonamides. *Bacteriol Rev* 7(4)**,** 175-262. doi: 10.1128/br.7.4.175-262.1943.

Hewitt, R.G., Yiannoutsos, C.T., Higgs, E.S., Carey, J.T., Geiseler, P.J., Soave, R., et al. (2000). Paromomycin: no more effective than placebo for treatment of cryptosporidiosis in patients with advanced human immunodeficiency virus infection. AIDS Clinical Trial Group. *Clin Infect Dis* 31(4)**,** 1084-1092. doi: 10.1086/318155.

Hicks, P., Zwiener, R.J., Squires, J., and Savell, V. (1996). Azithromycin therapy for *Cryptosporidium parvum* infection in four children infected with human immunodeficiency virus. *J Pediatr* 129(2)**,** 297-300. doi: 10.1016/s0022-3476(96)70258-5.

Hoffman, P.S., Sisson, G., Croxen, M.A., Welch, K., Harman, W.D., Cremades, N., et al. (2007). Antiparasitic drug nitazoxanide inhibits the pyruvate oxidoreductases of *Helicobacter pylori*, selected anaerobic bacteria and parasites, and *Campylobacter jejuni*. *Antimicrob Agents Chemother* 51(3)**,** 868-876. doi: 10.1128/AAC.01159-06.

Holmberg, S.D., Moorman, A.C., Von Bargen, J.C., Palella, F.J., Loveless, M.O., Ward, D.J., et al. (1998). Possible effectiveness of clarithromycin and rifabutin for cryptosporidiosis chemoprophylaxis in HIV disease. HIV Outpatient Study (HOPS) Investigators. *JAMA* 279(5)**,** 384-386. doi: 10.1001/jama.279.5.384.

Hommer, V., Eichholz, J., and Petry, F. (2003). Effect of antiretroviral protease inhibitors alone, and in combination with paromomycin, on the excystation, invasion and *in vitro* development of *Cryptosporidium parvum*. *J Antimicrob Chemother* 52(3)**,** 359-364. doi: 10.1093/jac/dkg357.

Hong, D.K., Wong, C.J., and Gutierrez, K. (2007). Severe cryptosporidiosis in a seven-year-old renal transplant recipient: case report and review of the literature. *Pediatr Transplant* 11(1)**,** 94-100. doi: 10.1111/j.1399-3046.2006.00593.x.

Hoxie, N.J., Davis, J.P., Vergeront, J.M., Nashold, R.D., and Blair, K.A. (1997). Cryptosporidiosis-associated mortality following a massive waterborne outbreak in Milwaukee, Wisconsin. *Am J Public Health* 87(12)**,** 2032-2035. doi: 10.2105/ajph.87.12.2032.

Huang, M.Z., Li, J., Guan, L., Li, D.Q., Nie, X.M., Gui, R., et al. (2015). Therapeutic effects of acetylspiramycin and garlicin on cryptosporidiosis among drug users. *Int J Parasitol Drugs Drug Resist* 5(3)**,** 185-190. doi: 10.1016/j.ijpddr.2015.09.002.

Huang, W., Hulverson, M.A., Choi, R., Arnold, S.L.M., Zhang, Z., McCloskey, M.C., et al. (2019). Development of 5-Aminopyrazole-4-carboxamide-based Bumped-Kinase Inhibitors for Cryptosporidiosis Therapy. *J Med Chem* 62(6)**,** 3135-3146. doi: 10.1021/acs.jmedchem.9b00069.

Hulverson, M.A., Choi, R., Arnold, S.L.M., Schaefer, D.A., Hemphill, A., McCloskey, M.C., et al. (2017). Advances in bumped kinase inhibitors for human and animal therapy for cryptosporidiosis. *Int J Parasitol* 47(12)**,** 753-763. doi: 10.1016/j.ijpara.2017.08.006.

Hunt, E., Fu, Q., Armstrong, M.U., Rennix, D.K., Webster, D.W., Galanko, J.A., et al. (2002). Oral bovine serum concentrate improves cryptosporidial enteritis in calves. *Pediatr Res* 51(3)**,** 370-376. doi: 10.1203/00006450-200203000-00017.

Hussien, S.M., Abdella, O.H., Abu-Hashim, A.H., Aboshiesha, G.A., Taha, M.A., El-Shemy, A.S., et al. (2013). Comparative study between the effect of nitazoxanide and

paromomycine in treatment of cryptosporidiosis in hospitalized children. *J Egypt Soc Parasitol* 43(2)**,** 463-470.

Innes, E.A., Chalmers, R.M., Wells, B., and Pawlowic, M.C. (2020). A One Health Approach to Tackle Cryptosporidiosis. *Trends Parasitol* 36(3)**,** 290-303. doi: 10.1016/j.pt.2019.12.016.

Iroh Tam, P., Arnold, S.L.M., Barrett, L.K., Chen, C.R., Conrad, T.M., Douglas, E., et al. (2021). Clofazimine for Treatment of Cryptosporidiosis in Human Immunodeficiency Virus Infected Adults: An Experimental Medicine, Randomized, Double-blind, Placebo-controlled Phase 2a Trial. *Clin Infect Dis* 73(2)**,** 183-191. doi: 10.1093/cid/ciaa421.

Ives, N.J., Gazzard, B.G., and Easterbrook, P.J. (2001). The changing pattern of AIDS-defining illnesses with the introduction of highly active antiretroviral therapy (HAART) in a London clinic. *J Infect* 42(2)**,** 134-139. doi: 10.1053/jinf.2001.0810.

Jacobson, C., Al-Habsi, K., Ryan, U., Williams, A., Anderson, F., Yang, R., et al. (2018). *Cryptosporidium* infection is associated with reduced growth and diarrhoea in goats beyond weaning. *Vet Parasitol* 260**,** 30-37. doi: 10.1016/j.vetpar.2018.07.005.

Jacobson, C., Williams, A., Yang, R., Ryan, U., Carmichael, I., Campbell, A.J., et al. (2016). Greater intensity and frequency of *Cryptosporidium* and *Giardia* oocyst shedding beyond the neonatal period is associated with reductions in growth, carcase weight and dressing efficiency in sheep. *Vet Parasitol* 228**,** 42-51. doi: 10.1016/j.vetpar.2016.08.003.

Jain, V., Yogavel, M., Kikuchi, H., Oshima, Y., Hariguchi, N., Matsumoto, M., et al. (2017). Targeting Prolyl-tRNA Synthetase to Accelerate Drug Discovery against Malaria, Leishmaniasis, Toxoplasmosis, Cryptosporidiosis, and Coccidiosis. *Structure* 25(10)**,** 1495-1505 e1496. doi: 10.1016/j.str.2017.07.015.

Jarvie, B.D., Trotz-Williams, L.A., McKnight, D.R., Leslie, K.E., Wallace, M.M., Todd, C.G., et al. (2005). Effect of halofuginone lactate on the occurrence of *Cryptosporidium parvum* and growth of neonatal dairy calves. *J Dairy Sci* 88(5)**,** 1801-1806. doi: 10.3168/jds.S0022-0302(05)72854-X.

Jasenosky, L.D., Cadena, C., Mire, C.E., Borisevich, V., Haridas, V., Ranjbar, S., et al. (2019). The FDA-Approved Oral Drug Nitazoxanide Amplifies Host Antiviral Responses and Inhibits Ebola Virus. *iScience* 19**,** 1279-1290. doi: 10.1016/j.isci.2019.07.003.

Joachim, A., Krull, T., Schwarzkopf, J., and Daugschies, A. (2003). Prevalence and control of bovine cryptosporidiosis in German dairy herds. *Vet Parasitol* 112(4)**,** 277-288. doi: 10.1016/s0304-4017(03)00006-2.

Johnson, E.H., Windsor, J.J., Muirhead, D.E., King, G.J., and Al-Busaidy, R. (2000). Confirmation of the prophylactic value of paromomycin in a natural outbreak of caprine cryptosporidiosis. *Vet Res Commun* 24(1)**,** 63-67. doi: 10.1023/a:1006381522986.

Jordan, W.C. (1996). Clarithromycin prophylaxis against *Cryptosporidium* enteritis in patients with AIDS. *J Natl Med Assoc* 88(7)**,** 425-427.

Jumani, R.S., Bessoff, K., Love, M.S., Miller, P., Stebbins, E.E., Teixeira, J.E., et al. (2018). A Novel Piperazine-Based Drug Lead for Cryptosporidiosis from the Medicines for Malaria Venture Open-Access Malaria Box. *Antimicrob Agents Chemother* 62(4)**,** e01505-01517. doi: 10.1128/AAC.01505-17.

Kacar, Y., Baykal, A.T., Aydin, L., and Batmaz, H. (2022). Evaluation of the efficacy of cow colostrum in the treatment and its effect on serum proteomes in calves with cryptosporidiosis. *Vet Immunol Immunopathol* 248**,** 110429. doi: 10.1016/j.vetimm.2022.110429.

Kadappu, K., Nagaraja, M., Rao, P., and Shastry, B. (2002). Azithromycin as treatment for cryptosporidiosis in human immunodeficiency virus disease. *Journal of Postgraduate Medicine* 48(3)**,** 179-181.

Kaminsky, R., Schmid, C., and Brun, R. (1996). An 'in vitro selectivity index' for evaluation of cytotoxicity of antitrypanosomal compounds. *Tropical Medicine & International Health* 1(6)**,** A36-A36.

Karanis, P. (2018). "*Cryptosporidium*: Waterborne and Foodborne Transmission and Worldwide Outbreaks," in *Recent Advances in Environmental Science from the Euro-Mediterranean and Surrounding Regions*. (Cham: Springer), 41-44.

Katsoulos, P.D., Karatzia, M.A., Dovas, C.I., Filioussis, G., Papadopoulos, E., Kiossis, E., et al. (2017). Evaluation of the in-field efficacy of oregano essential oil administration on the control of neonatal diarrhea syndrome in calves. *Res Vet Sci* 115**,** 478-483. doi: 10.1016/j.rvsc.2017.07.029.

Katz, M.D., Erstad, B.L., and Rose, C. (1988). Treatment of severe cryptosporidium-related diarrhea with octreotide in a patient with AIDS. *Drug Intell Clin Pharm* 22(2)**,** 134-136. doi: 10.1177/106002808802200206.

Keidel, J., and Daugschies, A. (2013). Integration of halofuginone lactate treatment and disinfection with p-chloro-m-cresol to control natural cryptosporidiosis in calves. *Vet Parasitol* 196(3-4)**,** 321-326. doi: 10.1016/j.vetpar.2013.03.003.

Kelly, P., Lungu, F., Keane, E., Baggaley, R., Kazembe, F., Pobee, J., et al. (1996). Albendazole chemotherapy for treatment of diarrhoea in patients with AIDS in Zambia: a randomised double blind controlled trial. *BMJ* 312(7040)**,** 1187-1191. doi: 10.1136/bmj.312.7040.1187.

Khalil, I.A., Troeger, C., Rao, P.C., Blacker, B.F., Brown, A., Brewer, T.G., et al. (2018). Morbidity, mortality, and long-term consequences associated with diarrhoea from *Cryptosporidium* infection in children younger than 5 years: a meta-analyses study. *Lancet Glob Health* 6(7)**,** e758-e768. doi: 10.1016/S2214-109X(18)30283-3.

Khan, S.M., Debnath, C., Pramanik, A.K., Xiao, L., Nozaki, T., and Ganguly, S. (2010). Molecular characterization and assessment of zoonotic transmission of *Cryptosporidium* from dairy cattle in West Bengal, India. *Vet Parasitol* 171(1-2)**,** 41-47. doi: 10.1016/j.vetpar.2010.03.008.

Khan, S.M., Garcia Hernandez, A., Allaie, I.M., Grooms, G.M., Li, K., Witola, W.H., et al. (2022a). Activity of (1-benzyl-4-triazolyl)-indole-2-carboxamides against *Toxoplasma gondii* and *Cryptosporidium parvum*. *Int J Parasitol Drugs Drug Resist* 19**,** 6-20. doi: 10.1016/j.ijpddr.2022.04.001.

Khan, S.M., and Witola, W.H. (2023). Past, current, and potential treatments for cryptosporidiosis in humans and farm animals: A comprehensive review. *Front Cell Infect Microbiol* 13**,** 1115522. doi: 10.3389/fcimb.2023.1115522.

Khan, S.M., Zhang, X., and Witola, W.H. (2022b). *Cryptosporidium parvum* Pyruvate Kinase Inhibitors With *in vivo* Anti-cryptosporidial Efficacy. *Front Microbiol* 12**,** 800293. doi: 10.3389/fmicb.2021.800293.

Klein, P. (2008). Preventive and therapeutic efficacy of halofuginone-lactate against *Cryptosporidium parvum* in spontaneously infected calves: a centralised, randomised, double-blind, placebo-controlled study. *Vet J* 177(3)**,** 429-431. doi: 10.1016/j.tvjl.2007.05.007.

Kotloff, K.L., Nataro, J.P., Blackwelder, W.C., Nasrin, D., Farag, T.H., Panchalingam, S., et al. (2013). Burden and aetiology of diarrhoeal disease in infants and young children in developing countries (the Global Enteric Multicenter Study, GEMS): a prospective, case-control study. *Lancet* 382(9888)**,** 209-222. doi: 10.1016/S0140-6736(13)60844-2.

Koudela, B., and Bokova, A. (1997). The effect of cotrimoxazole on experimental *Cryptosporidium parvum* infection in kids. *Vet Res* 28(4)**,** 405-412.

Krause, I., Amir, J., Cleper, R., Dagan, A., Behor, J., Samra, Z., et al. (2012). Cryptosporidiosis in children following solid organ transplantation. *Pediatr Infect Dis J* 31(11)**,** 1135-1138. doi: 10.1097/INF.0b013e31826780f7.

Kuhlenschmidt, T.B., Rutaganira, F.U., Long, S., Tang, K., Shokat, K.M., Kuhlenschmidt, M.S., et al. (2016). Inhibition of Calcium-Dependent Protein Kinase 1 (CDPK1) *In Vitro* by Pyrazolopyrimidine Derivatives Does Not Correlate with Sensitivity of *Cryptosporidium parvum* Growth in Cell Culture. *Antimicrob Agents Chemother* 60(1)**,** 570-579. doi: 10.1128/AAC.01915-15.

Lacey, E. (1988). The role of the cytoskeletal protein, tubulin, in the mode of action and mechanism of drug resistance to benzimidazoles. *Int J Parasitol* 18(7)**,** 885-936. doi: 10.1016/0020-7519(88)90175-0.

Lallemand, M., Villeneuve, A., Belda, J., and Dubreuil, P. (2006). Field study of the efficacy of halofuginone and decoquinate in the treatment of cryptosporidiosis in veal calves. *Vet Rec* 159(20)**,** 672-676. doi: 10.1136/vr.159.20.672.

Lanternier, F., Amazzough, K., Favennec, L., Mamzer-Bruneel, M.F., Abdoul, H., Tourret, J., et al. (2017). *Cryptosporidium* spp. Infection in Solid Organ Transplantation: The Nationwide "TRANSCRYPTO" Study. *Transplantation* 101(4)**,** 826-830. doi: 10.1097/TP.0000000000001503.

Larkin, M.A., Blackshields, G., Brown, N.P., Chenna, R., McGettigan, P.A., McWilliam, H., et al. (2007). Clustal W and Clustal X version 2.0. *Bioinformatics* 23(21)**,** 2947-2948. doi: 10.1093/bioinformatics/btm404.

Le Moing, V., Bissuel, F., Costagliola, D., Eid, Z., Chapuis, F., Molina, J.-M., et al. (1998). Decreased prevalence of intestinal cryptosporidiosis in HIV-infected patients concomitant to the widespread use of protease inhibitors. *AIDS* 12(11)**,** 1395-1397.

Lee, S., Ginese, M., Beamer, G., Danz, H.R., Girouard, D.J., Chapman-Bonofiglio, S.P., et al. (2018). Therapeutic Efficacy of Bumped Kinase Inhibitor 1369 in a Pig Model of Acute Diarrhea Caused by *Cryptosporidium hominis*. *Antimicrob Agents Chemother* 62(7)**,** e00147-00118. doi: 10.1128/AAC.00147-18.

Lee, S., Ginese, M., Girouard, D., Beamer, G., Huston, C.D., Osbourn, D., et al. (2019). Piperazine-Derivative MMV665917: An Effective Drug in the Diarrheic Piglet Model of *Cryptosporidium hominis*. *J Infect Dis* 220(2)**,** 285-293. doi: 10.1093/infdis/jiz105.

Lee, S., Harwood, M., Girouard, D., Meyers, M.J., Campbell, M.A., Beamer, G., et al. (2017). The therapeutic efficacy of azithromycin and nitazoxanide in the acute pig model of *Cryptosporidium hominis*. *PLoS One* 12(10)**,** e0185906. doi: 10.1371/journal.pone.0185906.

Lefay, D., Naciri, M., Poirier, P., and Chermette, R. (2001). Efficacy of halofuginone lactate in the prevention of cryptosporidiosis in suckling calves. *Vet Rec* 148(4)**,** 108-112. doi: 10.1136/vr.148.4.108.

Legrand, F., Grenouillet, F., Larosa, F., Dalle, F., Saas, P., Millon, L., et al. (2011). Diagnosis and treatment of digestive cryptosporidiosis in allogeneic haematopoietic stem cell

transplant recipients: a prospective single centre study. *Bone Marrow Transplant* 46(6)**,** 858-862. doi: 10.1038/bmt.2010.200.

Lendner, M., Bottcher, D., Delling, C., Ojo, K.K., Van Voorhis, W.C., and Daugschies, A. (2015). A novel CDPK1 inhibitor--a potential treatment for cryptosporidiosis in calves? *Parasitol Res* 114(1)**,** 335-336. doi: 10.1007/s00436-014-4228-7.

Li, K., Grooms, G.M., Khan, S.M., Hernandez, A.G., Witola, W.H., and Stec, J. (2020). Novel acyl carbamates and acyl / diacyl ureas show in vitro efficacy against *Toxoplasma gondii* and *Cryptosporidium parvum*. *Int J Parasitol Drugs Drug Resist* 14**,** 80-90. doi: 10.1016/j.ijpddr.2020.08.006.

Li, K., Nader, S.M., Zhang, X., Ray, B.C., Kim, C.Y., Das, A., et al. (2019). Novel lactate dehydrogenase inhibitors with *in vivo* efficacy against *Cryptosporidium parvum*. *PLoS Pathog* 15(7)**,** e1007953. doi: 10.1371/journal.ppat.1007953.

Liberti, A., Bisogno, A., and Izzo, E. (1992). Octreotide treatment in secretory and cyrptosporidial diarrhea in patients with acquired immunodeficiency syndrome (AIDS): clinical evaluation. *J Chemother* 4(5)**,** 303-305. doi: 10.1080/1120009x.1992.11739182.

Lin, J., Zhou, D., Steitz, T.A., Polikanov, Y.S., and Gagnon, M.G. (2018). Ribosome-Targeting Antibiotics: Modes of Action, Mechanisms of Resistance, and Implications for Drug Design. *Annu Rev Biochem* 87(1)**,** 451-478. doi: 10.1146/annurev-biochem-062917-011942.

Lindsay, D.S., Upton, S.J., Owens, D.S., Morgan, U.M., Mead, J.R., and Blagburn, B.L. (2000). *Cryptosporidium andersoni* n. sp. (Apicomplexa: Cryptosporiidae) from cattle, *Bos taurus*. *J Eukaryot Microbiol* 47(1)**,** 91-95. doi: 10.1111/j.1550-7408.2000.tb00016.x.

Lipinski, C.A., Lombardo, F., Dominy, B.W., and Feeney, P.J. (2001). Experimental and computational approaches to estimate solubility and permeability in drug discovery and development settings. *Adv Drug Deliv Rev* 46(1-3)**,** 3-26. doi: 10.1016/s0169-409x(00)00129-0.

Loeb, M., Walach, C., Phillips, J., Fong, I., Salit, I., Rachlis, A., et al. (1995). Treatment with letrazuril of refractory cryptosporidial diarrhea complicating AIDS. *J Acquir Immune Defic Syndr Hum Retrovirol* 10(1)**,** 48-53.

Louie, E., Borkowsky, W., Klesius, P.H., Haynes, T.B., Gordon, S., Bonk, S., et al. (1987). Treatment of cryptosporidiosis with oral bovine transfer factor. *Clin Immunol Immunopathol* 44(3)**,** 329-334. doi: 10.1016/0090-1229(87)90077-8.

Love, M.S., Beasley, F.C., Jumani, R.S., Wright, T.M., Chatterjee, A.K., Huston, C.D., et al. (2017). A high-throughput phenotypic screen identifies clofazimine as a potential treatment for cryptosporidiosis. *PLoS Negl Trop Dis* 11(2)**,** e0005373. doi: 10.1371/journal.pntd.0005373.

Love, M.S., and Choy, R.K.M. (2021). Emerging treatment options for cryptosporidiosis. *Curr Opin Infect Dis* 34(5)**,** 455-462. doi: 10.1097/QCO.0000000000000761.

Lunde, C.S., Stebbins, E.E., Jumani, R.S., Hasan, M.M., Miller, P., Barlow, J., et al. (2019). Identification of a potent benzoxaborole drug candidate for treating cryptosporidiosis. *Nat Commun* 10(1)**,** 2816. doi: 10.1038/s41467-019-10687-y.

Mac Kenzie, W.R., Hoxie, N.J., Proctor, M.E., Gradus, M.S., Blair, K.A., Peterson, D.E., et al. (1994). A massive outbreak in Milwaukee of cryptosporidium infection transmitted through the public water supply. *N Engl J Med* 331(3)**,** 161-167. doi: 10.1056/NEJM199407213310304.

Maddox-Hyttel, C., Langkjaer, R.B., Enemark, H.L., and Vigre, H. (2006). *Cryptosporidium* and *Giardia* in different age groups of Danish cattle and pigs--occurrence and management associated risk factors. *Vet Parasitol* 141(1-2)**,** 48-59. doi: 10.1016/j.vetpar.2006.04.032.

Maggi, P., Larocca, A.M., Quarto, M., Serio, G., Brandonisio, O., Angarano, G., et al. (2000). Effect of antiretroviral therapy on cryptosporidiosis and microsporidiosis in patients infected with human immunodeficiency virus type 1. *Eur J Clin Microbiol Infect Dis* 19(3)**,** 213-217. doi: 10.1007/s100960050461.

Malik, E.M., and Muller, C.E. (2016). Anthraquinones As Pharmacological Tools and Drugs. *Med Res Rev* 36(4)**,** 705-748. doi: 10.1002/med.21391.

Mancassola, R., Reperant, J.M., Naciri, M., and Chartier, C. (1995). Chemoprophylaxis of *Cryptosporidium parvum* infection with paromomycin in kids and immunological study. *Antimicrob Agents Chemother* 39(1)**,** 75-78. doi: 10.1128/AAC.39.1.75.

Mancassola, R., Richard, A., and Naciri, M. (1997). Evaluation of decoquinate to treat experimental cryptosporidiosis in kids. *Vet Parasitol* 69(1-2)**,** 31-37. doi: 10.1016/s0304-4017(96)01094-1.

Manjunatha, U.H., Vinayak, S., Zambriski, J.A., Chao, A.T., Sy, T., Noble, C.G., et al. (2017). A *Cryptosporidium* PI(4)K inhibitor is a drug candidate for cryptosporidiosis. *Nature* 546(7658)**,** 376-380. doi: 10.1038/nature22337.

Marshall, R.J., and Flanigan, T.P. (1992). Paromomycin inhibits *Cryptosporidium* infection of a human enterocyte cell line. *J Infect Dis* 165(4)**,** 772-774. doi: 10.1093/infdis/165.4.772.

Maurya, P.S., Sahu, S., Sudhakar, N.R., Jaiswal, V., Prashant, D.G., Rawat, S., et al. (2016). Cryptosporidiosis in a buffalo calf at Meerut, Uttar Pradesh and its successful therapeutic management. *J Parasit Dis* 40(4)**,** 1583-1585. doi: 10.1007/s12639-015-0734-5.

Mauzy, M.J., Enomoto, S., Lancto, C.A., Abrahamsen, M.S., and Rutherford, M.S. (2012). The *Cryptosporidium parvum* transcriptome during *in vitro* development. *PLoS One* 7(3)**,** e31715. doi: 10.1371/journal.pone.0031715.

McDonald, V., Korbel, D.S., Barakat, F.M., Choudhry, N., and Petry, F. (2013). Innate immune responses against *Cryptosporidium parvum* infection. *Parasite Immunol* 35(2)**,** 55-64. doi: 10.1111/pim.12020.

McMeeking, A., Borkowsky, W., Klesius, P.H., Bonk, S., Holzman, R.S., and Lawrence, H.S. (1990). A controlled trial of bovine dialyzable leukocyte extract for cryptosporidiosis in patients with AIDS. *J Infect Dis* 161(1)**,** 108-112. doi: 10.1093/infdis/161.1.108.

Mead, J.R. (2014). Prospects for immunotherapy and vaccines against *Cryptosporidium*. *Hum Vaccin Immunother* 10(6)**,** 1505-1513. doi: 10.4161/hv.28485.

Meamar, A.R., Rezaian, M., Rezaie, S., Mohraz, M., Kia, E.B., Houpt, E.R., et al. (2006). *Cryptosporidium parvum* bovine genotype oocysts in the respiratory samples of an AIDS patient: efficacy of treatment with a combination of azithromycin and paromomycin. *Parasitol Res* 98(6)**,** 593-595. doi: 10.1007/s00436-005-0097-4.

Meganck, V., Hoflack, G., Piepers, S., and Opsomer, G. (2015). Evaluation of a protocol to reduce the incidence of neonatal calf diarrhoea on dairy herds. *Prev Vet Med* 118(1)**,** 64-70. doi: 10.1016/j.prevetmed.2014.11.007.

Meisel, J.L., Perera, D.R., Meligro, C., and Rubin, C.E. (1976). Overwhelming watery diarrhea associated with a cryptosporidium in an immunosuppressed patient. *Gastroenterology* 70(6)**,** 1156-1160.

Mele, R., Morales, M.A.G., Tosini, F., and Pozio, E. (2003). Indinavir reduces *Cryptosporidium parvum* infection in both in vitro and in vivo models. *International Journal for Parasitology* 33(7)**,** 757-764. doi: 10.1016/S0020-7519(03)00093-6.

Mendonca, F.L.M., Carvalho, J.G., Silva, R.J., Ferreira, L.C.A., Cerqueira, D.M., Rogge, H.I., et al. (2021). Use of a natural herbal-based feed additive containing isoquinoline alkaloids in newborn calves with cryptosporidiosis. *Vet Parasitol* 300**,** 109615. doi: 10.1016/j.vetpar.2021.109615.

Menichetti, F., Moretti, M.V., Marroni, M., Papili, R., and Di Candilo, F. (1991). Diclazuril for cryptosporidiosis in AIDS. *Am J Med* 90(2)**,** 271-272. doi: https://doi.org/10.1016/0002-9343(91)80174-K.

Meuten, D.J., Van Kruiningen, H.J., and Lein, D.H. (1974). Cryptosporidiosis in a calf. *J Am Vet Med Assoc* 165(10)**,** 914-917.

Miao, Y.M., Awad-El-Kariem, F.M., Franzen, C., Ellis, D.S., Muller, A., Counihan, H.M., et al. (2000). Eradication of cryptosporidia and microsporidia following successful antiretroviral therapy. *J Acquir Immune Defic Syndr* 25(2)**,** 124-129. doi: 10.1097/00042560-200010010-00006.

Miao, Y.M., Awad-El-Kariem, F.M., Gibbons, C.L., and Gazzard, B.G. (1999). Cryptosporidiosis: eradication or suppression with combination antiretroviral therapy? *AIDS* 13(6)**,** 734-735. doi: 10.1097/00002030-199904160-00019.

Mirhashemi, M.E., Noubary, F., Chapman-Bonofiglio, S., Tzipori, S., Huggins, G.S., and Widmer, G. (2018). Transcriptome analysis of pig intestinal cell monolayers infected with *Cryptosporidium parvum* asexual stages. *Parasit Vectors* 11(1)**,** 176. doi: 10.1186/s13071-018-2754-3.

Missaye, A., Dagnew, M., Alemu, A., and Alemu, A. (2013). Prevalence of intestinal parasites and associated risk factors among HIV/AIDS patients with pre-ART and on-ART attending dessie hospital ART clinic, Northeast Ethiopia. *AIDS Res Ther* 10(1)**,** 7. doi: 10.1186/1742-6405-10-7.

Moling, O., Avi, A., Rimenti, G., and Mian, P. (2005). Glutamine supplementation for patients with severe cryptosporidiosis. *Clin Infect Dis* 40(5)**,** 773-774. doi: 10.1086/427948.

Moon, H.W., and Bemrick, W.J. (1981). Fecal transmission of calf cryptosporidia between calves and pigs. *Vet Pathol* 18(2)**,** 248-255. doi: 10.1177/030098588101800213.

Moon, H.W., Woode, G.N., and Ahrens, F.A. (1982). Attempted chemoprophylaxis of cryptosporidiosis in calves. *Vet Rec* 110(8)**,** 181. doi: 10.1136/vr.110.8.181-a.

Moore, D.A., Atwill, E.R., Kirk, J.H., Brahmbhatt, D., Herrera Alonso, L., Hou, L., et al. (2003). Prophylactic use of decoquinate for infections with *Cryptosporidium parvum* in experimentally challenged neonatal calves. *J Am Vet Med Assoc* 223(6)**,** 839-845. doi: 10.2460/javma.2003.223.839.

Moroni, M., Esposito, R., Cernuschi, M., Franzetti, F., Carosi, G.P., and Fiori, G.P. (1993). Treatment of AIDS-related refractory diarrhoea with octreotide. *Digestion* 54 Suppl 1(Suppl. 1)**,** 30-32. doi: 10.1159/000201073.

Moskovitz, B.L., Stanton, T.L., and Kusmierek, J.J. (1988). Spiramycin therapy for cryptosporidial diarrhoea in immunocompromised patients. *J Antimicrob Chemother* 22 Suppl B(Supplement_B)**,** 189-191. doi: 10.1093/jac/22.supplement_b.189.

Murakoshi, F., Takeuchi, M., Inomata, A., Horimoto, T., Ito, M., Suzuki, Y., et al. (2014). Administration of lasalocid-NA is preventive against cryptosporidiosis of newborn calves. *Vet Rec* 175(14)**,** 353. doi: 10.1136/vr.102508.

Murdoch, D.A., Bloss, D.E., and Glover, S.C. (1993). Successful treatment of cryptosporidiosis in an AIDS patient with letrazuril. *AIDS* 7(9)**,** 1279-1280. doi: 10.1097/00002030-199309000-00026.

Naciri, M., Mancassola, R., Reperant, J.M., Canivez, O., Quinque, B., and Yvore, P. (1994). Treatment of Experimental Ovine Cryptosporidiosis with Ovine or Bovine Hyperimmune Colostrum. *Veterinary Parasitology* 53(3-4)**,** 173-190. doi: Doi 10.1016/0304-4017(94)90181-3.

Naciri, M., Mancassola, R., Yvore, P., and Peeters, J.E. (1993). The effect of halofuginone lactate on experimental *Cryptosporidium parvum* infections in calves. *Vet Parasitol* 45(3-4)**,** 199-207. doi: 10.1016/0304-4017(93)90075-x.

Naciri, M., and Yvore, P. (1989). Efficiency of Halofuginone Lactate in the Treatment of Experimental Cryptosporidiosis in Lambs. *Recueil De Medecine Veterinaire* 165(10)**,** 823-826.

Naciri, M., Yvoré, P., and Levieux, D. (1984). Cryptosporidiose expérimentale du chevreau. Influence de la prise du colostrum. Essais de traitements. *Les maladies de la chèvre. INRA Publications, Les colloques de l'INRA* (28)**,** 465-471.

Nasir, A., Avais, M., Khan, M.S., Khan, J.A., Hameed, S., and Reichel, M.P. (2013). Treating *Cryptosporidium parvum* infection in calves. *J Parasitol* 99(4)**,** 715-717. doi: 10.1645/12-42.1.

Nasrin, D., Blackwelder, W.C., Sommerfelt, H., Wu, Y., Farag, T.H., Panchalingam, S., et al. (2021). Pathogens Associated With Linear Growth Faltering in Children With Diarrhea and Impact of Antibiotic Treatment: The Global Enteric Multicenter Study. *J Infect Dis* 224(12 Suppl 2)**,** S848-S855. doi: 10.1093/infdis/jiab434.

Navin, T.R., and Juranek, D.D. (1984). Cryptosporidiosis: clinical, epidemiologic, and parasitologic review. *Rev Infect Dis* 6(3)**,** 313-327. doi: 10.1093/clinids/6.3.313.

Niine, T., Dorbek-Kolin, E., Lassen, B., and Orro, T. (2018). *Cryptosporidium* outbreak in calves on a large dairy farm: Effect of treatment and the association with the inflammatory response and short-term weight gain. *Res Vet Sci* 117**,** 200-208. doi: 10.1016/j.rvsc.2017.12.015.

Nime, F.A., Burek, J.D., Page, D.L., Holscher, M.A., and Yardley, J.H. (1976). Acute Enterocolitis in a Human Being Infected with the Protozoan *Cryptosporidium*. *Gastroenterology* 70(4)**,** 592-598. doi: 10.1016/s0016-5085(76)80503-3.

Noordeen, F., Faizal, A.C., Rajapakse, R.P., Horadagoda, N.U., and Arulkanthan, A. (2001). Excretion of *Cryptosporidium* oocysts by goats in relation to age and season in the dry zone of Sri Lanka. *Vet Parasitol* 99(1)**,** 79-85. doi: 10.1016/s0304-4017(01)00449-6.

Nord, J., Ma, P., DiJohn, D., Tzipori, S., and Tacket, C.O. (1990). Treatment with bovine hyperimmune colostrum of cryptosporidial diarrhea in AIDS patients. *AIDS* 4(6)**,** 581-584. doi: 10.1097/00002030-199006000-00015.

Nsagha, D.S., Njunda, A.L., Assob, N.J.C., Ayima, C.W., Tanue, E.A., Kibu, O.D., et al. (2016). Intestinal parasitic infections in relation to CD4(+) T cell counts and diarrhea in HIV/AIDS patients with or without antiretroviral therapy in Cameroon. *BMC Infect Dis* 16**,** 9. doi: 10.1186/s12879-016-1337-1.

O'Connor R, M., Shaffie, R., Kang, G., and Ward, H.D. (2011). Cryptosporidiosis in patients with HIV/AIDS. *AIDS* 25(5)**,** 549-560. doi: 10.1097/QAD.0b013e3283437e88.

Oboh, E., Schubert, T.J., Teixeira, J.E., Stebbins, E.E., Miller, P., Philo, E., et al. (2021). Optimization of the Urea Linker of Triazolopyridazine MMV665917 Results in a New

Anticryptosporidial Lead with Improved Potency and Predicted hERG Safety Margin. *J Med Chem* 64(15)**,** 11729-11745. doi: 10.1021/acs.jmedchem.1c01136.

Okhuysen, P.C., Chappell, C.L., Crabb, J., Valdez, L.M., Douglass, E.T., and DuPont, H.L. (1998). Prophylactic effect of bovine anti-*Cryptosporidium* hyperimmune colostrum immunoglobulin in healthy volunteers challenged with *Cryptosporidium parvum*. *Clin Infect Dis* 26(6)**,** 1324-1329. doi: 10.1086/516374.

Ollivett, T.L., Nydam, D.V., Bowman, D.D., Zambriski, J.A., Bellosa, M.L., Linden, T.C., et al. (2009). Effect of nitazoxanide on cryptosporidiosis in experimentally infected neonatal dairy calves. *J Dairy Sci* 92(4)**,** 1643-1648. doi: 10.3168/jds.2008-1474.

Olson, E.J., Epperson, W.B., Zeman, D.H., Fayer, R., and Hildreth, M.B. (1998). Effects of an allicin-based product on cryptosporidiosis in neonatal calves. *J Am Vet Med Assoc* 212(7)**,** 987-990.

Palmieri, F., Cicalini, S., Froio, N., Rizzi, E.B., Goletti, D., Festa, A., et al. (2005). Pulmonary cryptosporidiosis in an AIDS patient: successful treatment with paromomycin plus azithromycin. *Int J STD AIDS* 16(7)**,** 515-517. doi: 10.1258/0956462054308332.

Panciera, R.J., Garner, F.M., and Thomassen, R.W. (1971). Cryptosporidial Infection in a Calf. *Veterinary Pathology* 8(5)**,** 479-+. doi: Doi 10.1177/0300985871008005-00610.

Pantenburg, B., Cabada, M.M., and White, A.C., Jr. (2009). Treatment of cryptosporidiosis. *Expert Rev Anti Infect Ther* 7(4)**,** 385-391. doi: 10.1586/eri.09.24.

Paraud, C., and Chartier, C. (2012). Cryptosporidiosis in small ruminants. *Small Rumin Res* 103(1)**,** 93-97. doi: 10.1016/j.smallrumres.2011.10.023.

Paraud, C., Pors, I., and Chartier, C. (2010). Evaluation of oral tilmicosin efficacy against severe cryptosporidiosis in neonatal kids under field conditions. *Vet Parasitol* 170(1-2)**,** 149-152. doi: 10.1016/j.vetpar.2010.01.024.

Paraud, C., Pors, I., Journal, J.P., Besnier, P., Reisdorffer, L., and Chartier, C. (2011). Control of cryptosporidiosis in neonatal goat kids: efficacy of a product containing activated charcoal and wood vinegar liquid (Obionekk) in field conditions. *Vet Parasitol* 180(3-4)**,** 354-357. doi: 10.1016/j.vetpar.2011.03.022.

Parr, J.B., Sevilleja, J.E., Samie, A., Alcantara, C., Stroup, S.E., Kohli, A., et al. (2007). Detection and quantification of *Cryptosporidium* in HCT-8 cells and human fecal specimens using real-time polymerase chain reaction. *Am J Trop Med Hyg* 76(5)**,** 938-942.

Pasquali, P., Fayer, R., Zarlenga, D., Canals, A., Marez, T., Gomez Munoz, M.T., et al. (2006). Recombinant bovine interleukin-12 stimulates a gut immune response but does not provide resistance to *Cryptosporidium parvum* infection in neonatal calves. *Vet Parasitol* 135(3-4)**,** 259-268. doi: 10.1016/j.vetpar.2005.05.062.

Peeters, J.E., Villacorta, I., Naciri, M., and Vanopdenbosch, E. (1993). Specific serum and local antibody responses against *Cryptosporidium parvum* during medication of calves with halofuginone lactate. *Infect Immun* 61(10)**,** 4440-4445. doi: 10.1128/iai.61.10.4440-4445.1993.

Perryman, L.E., Kapil, S.J., Jones, M.L., and Hunt, E.L. (1999). Protection of calves against cryptosporidiosis with immune bovine colostrum induced by a *Cryptosporidium parvum* recombinant protein. *Vaccine* 17(17)**,** 2142-2149. doi: 10.1016/s0264-410x(98)00477-0.

Petermann, J., Paraud, C., Pors, I., and Chartier, C. (2014). Efficacy of halofuginone lactate against experimental cryptosporidiosis in goat neonates. *Vet Parasitol* 202(3-4)**,** 326-329. doi: 10.1016/j.vetpar.2014.02.027.

Petersen, H.H., Jianmin, W., Katakam, K.K., Mejer, H., Thamsborg, S.M., Dalsgaard, A., et al. (2015). *Cryptosporidium* and *Giardia* in Danish organic pig farms: Seasonal and age-related variation in prevalence, infection intensity and species/genotypes. *Vet Parasitol* 214(1-2)**,** 29-39. doi: 10.1016/j.vetpar.2015.09.020.

Platts-Mills, J.A., Babji, S., Bodhidatta, L., Gratz, J., Haque, R., Havt, A., et al. (2015). Pathogen-specific burdens of community diarrhoea in developing countries: a multisite birth cohort study (MAL-ED). *Lancet Glob Health* 3(9)**,** e564-575. doi: 10.1016/S2214-109X(15)00151-5.

Plettenberg, A., Stoehr, A., Stellbrink, H.J., Albrecht, H., and Meigel, W. (1993). A preparation from bovine colostrum in the treatment of HIV-positive patients with chronic diarrhea. *Clin Investig* 71(1)**,** 42-45. doi: 10.1007/BF00210962.

Puiu, D., Enomoto, S., Buck, G.A., Abrahamsen, M.S., and Kissinger, J.C. (2004). CryptoDB: the *Cryptosporidium* genome resource. *Nucleic Acids Res* 32(Database issue)**,** D329-331. doi: 10.1093/nar/gkh050.

Raabis, S.M., Ollivett, T.L., Cook, M.E., Sand, J.M., and McGuirk, S.M. (2018). Health benefits of orally administered anti-IL-10 antibody in milk-fed dairy calves. *J Dairy Sci* 101(8)**,** 7375-7382. doi: 10.3168/jds.2017-14270.

Redman, D.R., and Fox, J.E. (Year). "The Effect of Varying Levels of DECCOX® on Experimental Cryptosporidia Infections in Holstein Bull Calves", in: *American Association of Bovine Practitioners Proceedings of the Annual Conference*, (Stillwater, OK: Frontiers Printers, Inc.), 157-159.

Reduker, D.W., and Speer, C.A. (1985). Factors influencing excystation in *Cryptosporidium* oocysts from cattle. *J Parasitol* 71(1)**,** 112-115.

Robertson, L.J., Björkman, C., Axén, C., and Fayer, R. (2014). "Cryptosporidiosis in Farmed Animals," in *Cryptosporidium: parasite and disease*. Springer Vienna), 149-235.

Romeu, J., Miro, J.M., Sirera, G., Mallolas, J., Arnal, J., Valls, M.E., et al. (1991). Efficacy of octreotide in the management of chronic diarrhoea in AIDS. *AIDS* 5(12)**,** 1495-1499. doi: 10.1097/00002030-199112000-00012.

Ross, J., Schatz, C., Beaugrand, K., Zuidhof, S., Ralston, B., Allan, N., et al. (2021). Evaluation of Activated Charcoal as an Alternative to Antimicrobials for the Treatment of Neonatal Calf Diarrhea. *Vet Med (Auckl)* 12**,** 359-369. doi: 10.2147/VMRR.S337698.

Rossignol, J.F. (2006). Nitazoxanide in the treatment of acquired immune deficiency syndrome-related cryptosporidiosis: results of the United States compassionate use program in 365 patients. *Aliment Pharmacol Ther* 24(5)**,** 887-894. doi: 10.1111/j.1365-2036.2006.03033.x.

Rossignol, J.F., Ayoub, A., and Ayers, M.S. (2001). Treatment of diarrhea caused by *Cryptosporidium parvum*: a prospective randomized, double-blind, placebo-controlled study of Nitazoxanide. *J Infect Dis* 184(1)**,** 103-106. doi: 10.1086/321008.

Rossignol, J.F., Hidalgo, H., Feregrino, M., Higuera, F., Gomez, W.H., Romero, J.L., et al. (1998). A double-'blind' placebo-controlled study of nitazoxanide in the treatment of cryptosporidial diarrhoea in AIDS patients in Mexico. *Trans R Soc Trop Med Hyg* 92(6)**,** 663-666. doi: 10.1016/s0035-9203(98)90804-5.

Rossignol, J.F., Kabil, S.M., el-Gohary, Y., and Younis, A.M. (2006). Effect of nitazoxanide in diarrhea and enteritis caused by *Cryptosporidium* species. *Clin Gastroenterol Hepatol* 4(3)**,** 320-324. doi: 10.1016/j.cgh.2005.12.020.

Rotte, C., Stejskal, F., Zhu, G., Keithly, J.S., and Martin, W. (2001). Pyruvate : NADP+ oxidoreductase from the mitochondrion of *Euglena gracilis* and from the apicomplexan *Cryptosporidium parvum*: a biochemical relic linking pyruvate metabolism in mitochondriate and amitochondriate protists. *Mol Biol Evol* 18(5)**,** 710-720. doi: 10.1093/oxfordjournals.molbev.a003853.

Rump, J.A., Arndt, R., Arnold, A., Bendick, C., Dichtelmuller, H., Franke, M., et al. (1992). Treatment of diarrhoea in human immunodeficiency virus-infected patients with immunoglobulins from bovine colostrum. *Clin Investig* 70(7)**,** 588-594. doi: 10.1007/BF00184800.

Ryan, U., Fayer, R., and Xiao, L. (2014). *Cryptosporidium* species in humans and animals: current understanding and research needs. *Parasitology* 141(13)**,** 1667-1685. doi: 10.1017/S0031182014001085.

Ryan, U., Zahedi, A., Feng, Y., and Xiao, L. (2021a). An Update on Zoonotic *Cryptosporidium* Species and Genotypes in Humans. *Animals (Basel)* 11(11)**,** 3307. doi: 10.3390/ani11113307.

Ryan, U.M., Bath, C., Robertson, I., Read, C., Elliot, A., McInnes, L., et al. (2005). Sheep may not be an important zoonotic reservoir for *Cryptosporidium* and *Giardia* parasites. *Appl Environ Microbiol* 71(9)**,** 4992-4997. doi: 10.1128/AEM.71.9.4992-4997.2005.

Ryan, U.M., Feng, Y., Fayer, R., and Xiao, L. (2021b). Taxonomy and molecular epidemiology of *Cryptosporidium* and *Giardia* - a 50 year perspective (1971-2021). *Int J Parasitol* 51(13-14)**,** 1099-1119. doi: 10.1016/j.ijpara.2021.08.007.

Saez-Llorens, X., Odio, C.M., Umana, M.A., and Morales, M.V. (1989). Spiramycin vs. placebo for treatment of acute diarrhea caused by *Cryptosporidium*. *Pediatr Infect Dis J* 8(3)**,** 136-140.

Sahal, M., Karaer, Z., Yasa Duru, S., Cizmeci, S., and Tanyel, B. (2005). [Cryptosporidiosis in newborn calves in Ankara region: clinical, haematological findings and treatment with Lasalocid-NA]. *Dtsch Tierarztl Wochenschr* 112(6)**,** 203-208, 210.

Sallon, S., Deckelbaum, R.J., Schmid, II, Harlap, S., Baras, M., and Spira, D.T. (1988). *Cryptosporidium*, malnutrition, and chronic diarrhea in children. *Am J Dis Child* 142(3)**,** 312-315. doi: 10.1001/archpedi.1988.02150030086027.

Santin, M. (2020). *Cryptosporidium* and *Giardia* in Ruminants. *Vet Clin North Am Food Anim Pract* 36(1)**,** 223-238. doi: 10.1016/j.cvfa.2019.11.005.

Santín, M., and Trout, J.M. (2007). "Livestock," in *Cryptosporidium and Cryptosporidiosis*, eds. R. Fayer & L. Xiao. (Boca Raton, FL: CRC Press), 451-484.

Santin, M., Trout, J.M., and Fayer, R. (2007). Prevalence and molecular characterization of *Cryptosporidium* and *Giardia* species and genotypes in sheep in Maryland. *Vet Parasitol* 146(1-2)**,** 17-24. doi: 10.1016/j.vetpar.2007.01.010.

Santin, M., Trout, J.M., and Fayer, R. (2008). A longitudinal study of cryptosporidiosis in dairy cattle from birth to 2 years of age. *Vet Parasitol* 155(1-2)**,** 15-23. doi: 10.1016/j.vetpar.2008.04.018.

Santin, M., Trout, J.M., Xiao, L., Zhou, L., Greiner, E., and Fayer, R. (2004). Prevalence and age-related variation of *Cryptosporidium* species and genotypes in dairy calves. *Vet Parasitol* 122(2)**,** 103-117. doi: 10.1016/j.vetpar.2004.03.020.

Scaglia, M., Atzori, C., Marchetti, G., Orso, M., Maserati, R., Orani, A., et al. (1994). Effectiveness of aminosidine (paromomycin) sulfate in chronic *Cryptosporidium* diarrhea

in AIDS patients: an open, uncontrolled, prospective clinical trial. *J Infect Dis* 170(5)**,** 1349-1350. doi: 10.1093/infdis/170.5.1349.

Schaefer, D.A., Betzer, D.P., Smith, K.D., Millman, Z.G., Michalski, H.C., Menchaca, S.E., et al. (2016). Novel Bumped Kinase Inhibitors Are Safe and Effective Therapeutics in the Calf Clinical Model for Cryptosporidiosis. *J Infect Dis* 214(12)**,** 1856-1864. doi: 10.1093/infdis/jiw488.

Schmidt, W., Wahnschaffe, U., Schafer, M., Zippel, T., Arvand, M., Meyerhans, A., et al. (2001). Rapid increase of mucosal CD4 T cells followed by clearance of intestinal cryptosporidiosis in an AIDS patient receiving highly active antiretroviral therapy. *Gastroenterology* 120(4)**,** 984-987. doi: 10.1053/gast.2001.22557.

Schnyder, M., Kohler, L., Hemphill, A., and Deplazes, P. (2009). Prophylactic and therapeutic efficacy of nitazoxanide against *Cryptosporidium parvum* in experimentally challenged neonatal calves. *Vet Parasitol* 160(1-2)**,** 149-154. doi: 10.1016/j.vetpar.2008.10.094.

Shaw, H.J., Innes, E.A., Morrison, L.J., Katzer, F., and Wells, B. (2020). Long-term production effects of clinical cryptosporidiosis in neonatal calves. *Int J Parasitol* 50(5)**,** 371-376. doi: 10.1016/j.ijpara.2020.03.002.

Shield, J., Melville, C., Novelli, V., Anderson, G., Scheimberg, I., Gibb, D., et al. (1993). Bovine colostrum immunoglobulin concentrate for cryptosporidiosis in AIDS. *Arch Dis Child* 69(4)**,** 451-453. doi: 10.1136/adc.69.4.451.

Shirley, D.A., Moonah, S.N., and Kotloff, K.L. (2012). Burden of disease from cryptosporidiosis. *Curr Opin Infect Dis* 25(5)**,** 555-563. doi: 10.1097/QCO.0b013e328357e569.

Sinkala, E., Katubulushi, M., Sianongo, S., Obwaller, A., and Kelly, P. (2011). In a trial of the use of miltefosine to treat HIV-related cryptosporidiosis in Zambian adults, extreme metabolic disturbances contribute to high mortality. *Ann Trop Med Parasitol* 105(2)**,** 129-134. doi: 10.1179/136485911X12899838683160.

Slacek, B., Ankenbauer-Perkins, K.L., and Tunnicliffe, A. (1996). Evaluation of colostrum and whey-derived gamma globulins for prevention of cryptosporidiosis in artificially infected neonatal calves. *N Z Vet J* 44(4)**,** 158-160. doi: 10.1080/00480169.1996.35962.

Smith, N.H., Cron, S., Valdez, L.M., Chappell, C.L., and White, A.C., Jr. (1998). Combination drug therapy for cryptosporidiosis in AIDS. *J Infect Dis* 178(3)**,** 900-903. doi: 10.1086/515352.

Soave, R., Danner, R.L., Honig, C.L., Ma, P., Hart, C.C., Nash, T., et al. (1984). Cryptosporidiosis in homosexual men. *Ann Intern Med* 100(4)**,** 504-511. doi: 10.7326/0003-4819-100-4-504.

Soave, R., Havlir, D., Lancaster, D., Joseph, P., Leedom, J., Clough, W., et al. (1993). "Azithromycin therapy of AIDS-related cryptosporidial diarrhea: A multi-center, placebo-controlled, double-blind study (abstract 405)", in: *33rd Interscience Conference on Antimicrobial Agents and Chemotherapy*. (New Orleans, LA).

Sprinz, E., Mallman, R., Barcellos, S., Silbert, S., Schestatsky, G., and Bem David, D. (1998). AIDS-related cryptosporidial diarrhoea: an open study with roxithromycin. *J Antimicrob Chemother* 41 Suppl B(suppl 2)**,** 85-91. doi: 10.1093/jac/41.suppl_2.85.

Stebbins, E., Jumani, R.S., Klopfer, C., Barlow, J., Miller, P., Campbell, M.A., et al. (2018). Clinical and microbiologic efficacy of the piperazine-based drug lead MMV665917 in the dairy calf cryptosporidiosis model. *PLoS Negl Trop Dis* 12(1)**,** e0006183. doi: 10.1371/journal.pntd.0006183.

Stefańska, B., Sroka, J., Katzer, F., Goliński, P., and Nowak, W. (2021). The effect of probiotics, phytobiotics and their combination as feed additives in the diet of dairy calves on performance, rumen fermentation and blood metabolites during the preweaning period. *Animal Feed Science and Technology* 272**,** 114738. doi: 10.1016/j.anifeedsci.2020.114738.

Straetemans, R., O'Brien, T., Wouters, L., Van Dun, J., Janicot, M., Bijnens, L., et al. (2005). Design and analysis of drug combination experiments. *Biom J* 47(3)**,** 299-308. doi: 10.1002/bimj.200410124.

Swale, C., Bougdour, A., Gnahoui-David, A., Tottey, J., Georgeault, S., Laurent, F., et al. (2019). Metal-captured inhibition of pre-mRNA processing activity by CPSF3 controls *Cryptosporidium* infection. *Sci Transl Med* 11(517)**,** eaax7161. doi: 10.1126/scitranslmed.aax7161.

Swinney, D.C., and Anthony, J. (2011). How were new medicines discovered? *Nat Rev Drug Discov* 10(7)**,** 507-519. doi: 10.1038/nrd3480.

Tallarida, R.J. (2011). Quantitative methods for assessing drug synergism. *Genes Cancer* 2(11)**,** 1003-1008. doi: 10.1177/1947601912440575.

Tamura, K., Stecher, G., and Kumar, S. (2021). MEGA11: Molecular Evolutionary Genetics Analysis Version 11. *Mol Biol Evol* 38(7)**,** 3022-3027. doi: 10.1093/molbev/msab120.

Tandel, J., English, E.D., Sateriale, A., Gullicksrud, J.A., Beiting, D.P., Sullivan, M.C., et al. (2019). Life cycle progression and sexual development of the apicomplexan parasite *Cryptosporidium parvum*. *Nat Microbiol* 4(12)**,** 2226-2236. doi: 10.1038/s41564-019-0539-x.

Theodos, C.M., Griffiths, J.K., D'Onfro, J., Fairfield, A., and Tzipori, S. (1998). Efficacy of nitazoxanide against *Cryptosporidium parvum* in cell culture and in animal models. *Antimicrob Agents Chemother* 42(8)**,** 1959-1965. doi: 10.1128/AAC.42.8.1959.

Thomson, S., Hamilton, C.A., Hope, J.C., Katzer, F., Mabbott, N.A., Morrison, L.J., et al. (2017). Bovine cryptosporidiosis: impact, host-parasite interaction and control strategies. *Vet Res* 48(1)**,** 42. doi: 10.1186/s13567-017-0447-0.

Tomczak, E., McDougal, A.N., and White, A.C., Jr. (2022). Resolution of Cryptosporidiosis in Transplant Recipients: Review of the Literature and Presentation of a Renal Transplant Patient Treated With Nitazoxanide, Azithromycin, and Rifaximin. *Open Forum Infect Dis* 9(1)**,** ofab610. doi: 10.1093/ofid/ofab610.

Trad, O., Jumaa, P., Uduman, S., and Nawaz, A. (2003). Eradication of *Cryptosporidium* in four children with acute lymphoblastic leukemia. *J Trop Pediatr* 49(2)**,** 128-130. doi: 10.1093/tropej/49.2.128.

Trotz-Williams, L.A., Jarvie, B.D., Peregrine, A.S., Duffield, T.F., and Leslie, K.E. (2011). Efficacy of halofuginone lactate in the prevention of cryptosporidiosis in dairy calves. *Vet Rec* 168(19)**,** 509. doi: 10.1136/vr.d1492.

Trotz-Williams, L.A., Wayne Martin, S., Leslie, K.E., Duffield, T., Nydam, D.V., and Peregrine, A.S. (2007). Calf-level risk factors for neonatal diarrhea and shedding of *Cryptosporidium parvum* in Ontario dairy calves. *Prev Vet Med* 82(1-2)**,** 12-28. doi: 10.1016/j.prevetmed.2007.05.003.

Tuli, L., Gulati, A.K., Sundar, S., and Mohapatra, T.M. (2008). Correlation between CD4 counts of HIV patients and enteric protozoan in different seasons - an experience of a tertiary care hospital in Varanasi (India). *BMC Gastroenterol* 8**,** 36. doi: 10.1186/1471-230X-8-36.

Tyzzer, E.E. (1907). A sporozoan found in the peptic glands of the common mouse. *Experimental Biology and Medicine* 5(1)**,** 12-13. doi: 10.3181/00379727-5-5.

Tyzzer, E.E. (1910). An extracellular Coccidium, *Cryptosporidium muris* (Gen. Et Sp. Nov.), of the gastric Glands of the Common Mouse. *J Med Res* 23(3)**,** 487-510 483.

Tyzzer, E.E. (1912). *Cryptosporidium parvum* (sp. nov.), a coccidium found in the small intestine of the common mouse. *Arch Protistenkd* 26**,** 394-412.

Tzipori, S., Campbell, I., Sherwood, D., Snodgrass, D.R., and Whitelaw, A. (1980). An outbreak of calf diarrhoea attributed to cryptosporidial infection. *Vet Rec* 107(25-26)**,** 579-580.

Tzipori, S., Rand, W., Griffiths, J., Widmer, G., and Crabb, J. (1994). Evaluation of an animal model system for cryptosporidiosis: therapeutic efficacy of paromomycin and hyperimmune bovine colostrum-immunoglobulin. *Clin Diagn Lab Immunol* 1(4)**,** 450-463. doi: 10.1128/cdli.1.4.450-463.1994.

Tzipori, S., Roberton, D., Cooper, D.A., and White, L. (1987). Chronic cryptosporidial diarrhoea and hyperimmune cow colostrum. *Lancet* 2(8554)**,** 344-345. doi: 10.1016/s0140-6736(87)90944-5.

Tzipori, S., Smith, M., Halpin, C., Angus, K.W., Sherwood, D., and Campbell, I. (1983). Experimental cryptosporidiosis in calves: clinical manifestations and pathological findings. *Vet Rec* 112(6)**,** 116-120. doi: 10.1136/vr.112.6.116.

Uip, D.E., Lima, A.L., Amato, V.S., Boulos, M., Neto, V.A., and Bem David, D. (1998). Roxithromycin treatment for diarrhoea caused by *Cryptosporidium* spp. in patients with AIDS. *J Antimicrob Chemother* 41 Suppl B(suppl 2)**,** 93-97. doi: 10.1093/jac/41.suppl_2.93.

Ungar, B.L., Ward, D.J., Fayer, R., and Quinn, C.A. (1990). Cessation of *Cryptosporidium*-associated diarrhea in an acquired immunodeficiency syndrome patient after treatment with hyperimmune bovine colostrum. *Gastroenterology* 98(2)**,** 486-489. doi: 10.1016/0016-5085(90)90842-o.

Urie, N.J., Lombard, J.E., Shivley, C.B., Adams, A.E., Kopral, C.A., and Santin, M. (2018a). Preweaned heifer management on US dairy operations: Part III. Factors associated with *Cryptosporidium* and *Giardia* in preweaned dairy heifer calves. *J Dairy Sci* 101(10)**,** 9199-9213. doi: 10.3168/jds.2017-14060.

Urie, N.J., Lombard, J.E., Shivley, C.B., Kopral, C.A., Adams, A.E., Earleywine, T.J., et al. (2018b). Preweaned heifer management on US dairy operations: Part I. Descriptive characteristics of preweaned heifer raising practices. *J Dairy Sci* 101(10)**,** 9168-9184. doi: 10.3168/jds.2017-14010.

Van Voorhis, W.C., Hulverson, M.A., Choi, R., Huang, W., Arnold, S.L.M., Schaefer, D.A., et al. (2021). One health therapeutics: Target-Based drug development for cryptosporidiosis and other apicomplexa diseases. *Vet Parasitol* 289**,** 109336. doi: 10.1016/j.vetpar.2020.109336.

Vandenberg, O., Robberecht, F., Dauby, N., Moens, C., Talabani, H., Dupont, E., et al. (2012). Management of a *Cryptosporidium hominis* outbreak in a day-care center. *Pediatr Infect Dis J* 31(1)**,** 10-15. doi: 10.1097/INF.0b013e318235ab64.

Vargas, S.L., Shenep, J.L., Flynn, P.M., Pui, C.H., Santana, V.M., and Hughes, W.T. (1993). Azithromycin for treatment of severe *Cryptosporidium* diarrhea in two children with cancer. *J Pediatr* 123(1)**,** 154-156. doi: 10.1016/s0022-3476(05)81562-8.

Veber, D.F., Johnson, S.R., Cheng, H.Y., Smith, B.R., Ward, K.W., and Kopple, K.D. (2002). Molecular properties that influence the oral bioavailability of drug candidates. *J Med Chem* 45(12)**,** 2615-2623. doi: 10.1021/jm020017n.

Velez, J., Lange, M.K., Zieger, P., Yoon, I., Failing, K., and Bauer, C. (2019). Long-term use of yeast fermentation products in comparison to halofuginone for the control of cryptosporidiosis in neonatal calves. *Vet Parasitol* 269**,** 57-64. doi: 10.1016/j.vetpar.2019.04.008.

Velez, J., Velasquez, Z., Silva, L.M.R., Gartner, U., Failing, K., Daugschies, A., et al. (2021). Metabolic Signatures of *Cryptosporidium parvum*-Infected HCT-8 Cells and Impact of Selected Metabolic Inhibitors on *C. parvum* Infection under Physioxia and Hyperoxia. *Biology (Basel)* 10(1)**,** 1-24. doi: 10.3390/biology10010060.

Vermeulen, L.C., Benders, J., Medema, G., and Hofstra, N. (2017). Global *Cryptosporidium* Loads from Livestock Manure. *Environ Sci Technol* 51(15)**,** 8663-8671. doi: 10.1021/acs.est.7b00452.

Viel, H., Rocques, H., Martin, J., and Chartier, C. (2007). Efficacy of nitazoxanide against experimental cryptosporidiosis in goat neonates. *Parasitol Res* 102(1)**,** 163-166. doi: 10.1007/s00436-007-0744-z.

Villacorta, I., Peeters, J.E., Vanopdenbosch, E., Ares-Mazas, E., and Theys, H. (1991). Efficacy of halofuginone lactate against *Cryptosporidium parvum* in calves. *Antimicrob Agents Chemother* 35(2)**,** 283-287. doi: 10.1128/AAC.35.2.283.

Vinayak, S., Jumani, R.S., Miller, P., Hasan, M.M., McLeod, B.I., Tandel, J., et al. (2020). Bicyclic azetidines kill the diarrheal pathogen *Cryptosporidium* in mice by inhibiting parasite phenylalanyl-tRNA synthetase. *Sci Transl Med* 12(563)**,** eaba8412-eaba8412. doi: 10.1126/scitranslmed.aba8412.

Vinayak, S., Pawlowic, M.C., Sateriale, A., Brooks, C.F., Studstill, C.J., Bar-Peled, Y., et al. (2015). Genetic modification of the diarrhoeal pathogen *Cryptosporidium parvum*. *Nature* 523(7561)**,** 477-480. doi: 10.1038/nature14651.

Viu, M., Quilez, J., Sanchez-Acedo, C., del Cacho, E., and Lopez-Bernad, F. (2000). Field trial on the therapeutic efficacy of paromomycin on natural *Cryptosporidium parvum* infections in lambs. *Vet Parasitol* 90(3)**,** 163-170. doi: 10.1016/s0304-4017(00)00241-7.

Volpato, A., Crecencio, R.B., Tomasi, T., Galli, G.M., Griss, L.G., Da Silva, A.D., et al. (2019). Phytogenic as feed additive for suckling dairy calves' has a beneficial effect on animal health and performance. *Anais Da Academia Brasileira De Ciencias* 91(4). doi: ARTN e20180747

10.1590/0001-3765201920180747.

Wallace, M.R., Nguyen, M.T., and Newton, J.A., Jr. (1993). Use of paromomycin for the treatment of cryptosporidiosis in patients with AIDS. *Clin Infect Dis* 17(6)**,** 1070-1071. doi: 10.1093/clinids/17.6.1070.

Wang, C.C. (1976). Inhibition of the respiration of *Eimeria tenella* by quinolone coccidiostats. *Biochem Pharmacol* 25(3)**,** 343-349. doi: 10.1016/0006-2952(76)90225-2.

Wang, R.J., Li, J.Q., Chen, Y.C., Zhang, L.X., and Xiao, L.H. (2018). Widespread occurrence of *Cryptosporidium* infections in patients with HIV/AIDS: Epidemiology, clinical feature, diagnosis, and therapy. *Acta Trop* 187**,** 257-263. doi: 10.1016/j.actatropica.2018.08.018.

Watanabe, Y., Yang, C.H., and Ooi, H.K. (2005). *Cryptosporidium* infection in livestock and first identification of *Cryptosporidium parvum* genotype in cattle feces in Taiwan. *Parasitol Res* 97(3)**,** 238-241. doi: 10.1007/s00436-005-1428-1.

Watarai, S., Tana, and Koiwa, M. (2008). Feeding activated charcoal from bark containing wood vinegar liquid (Nekka-Rich) is effective as treatment for cryptosporidiosis in calves. *J Dairy Sci* 91(4)**,** 1458-1463. doi: 10.3168/jds.2007-0406.

Weikel, C., Lazenby, A., Belitsos, P., McDewitt, M., Fleming, H.E., Jr., and Barbacci, M. (1991). Intestinal injury associated with spiramycin therapy of *Cryptosporidium* infection in AIDS. *J Protozool* 38(6)**,** 147S.

Welsch, M.E., Snyder, S.A., and Stockwell, B.R. (2010). Privileged scaffolds for library design and drug discovery. *Curr Opin Chem Biol* 14(3)**,** 347-361. doi: 10.1016/j.cbpa.2010.02.018.

Wetzel, D.M., Schmidt, J., Kuhlenschmidt, M.S., Dubey, J.P., and Sibley, L.D. (2005). Gliding motility leads to active cellular invasion by *Cryptosporidium parvum* sporozoites. *Infect Immun* 73(9)**,** 5379-5387. doi: 10.1128/IAI.73.9.5379-5387.2005.

Weyl-Feinstein, S., Markovics, A., Eitam, H., Orlov, A., Yishay, M., Agmon, R., et al. (2014). Short communication: effect of pomegranate-residue supplement on *Cryptosporidium parvum* oocyst shedding in neonatal calves. *J Dairy Sci* 97(9)**,** 5800-5805. doi: 10.3168/jds.2013-7136.

White, A.C., Jr., Chappell, C.L., Hayat, C.S., Kimball, K.T., Flanigan, T.P., and Goodgame, R.W. (1994). Paromomycin for cryptosporidiosis in AIDS: a prospective, double-blind trial. *J Infect Dis* 170(2)**,** 419-424. doi: 10.1093/infdis/170.2.419.

WHO (2009). *Risk assessment of Cryptosporidium in drinking water* [Online]. World Health Organization. Available: https://www.who.int/publications/i/item/WHO-HSE-WSH-09.04 [Accessed October 26 2022].

Wilke, G., Funkhouser-Jones, L.J., Wang, Y., Ravindran, S., Wang, Q., Beatty, W.L., et al. (2019). A Stem-Cell-Derived Platform Enables Complete *Cryptosporidium* Development *In Vitro* and Genetic Tractability. *Cell Host Microbe* 26(1)**,** 123-134 e128. doi: 10.1016/j.chom.2019.05.007.

Wilke, G., Wang, Y., Ravindran, S., Stappenbeck, T., Witola, W.H., and Sibley, L.D. (2020). "*In Vitro* Culture of *Cryptosporidium parvum* Using Stem Cell-Derived Intestinal Epithelial Monolayers," in *Methods in Molecular Biology*. Springer New York), 351-372.

Witchel, H.J. (2011). Drug-induced hERG block and long QT syndrome. *Cardiovasc Ther* 29(4)**,** 251-259. doi: 10.1111/j.1755-5922.2010.00154.x.

Witola, W.H., Zhang, X., and Kim, C.Y. (2017). Targeted gene knockdown validates the essential role of lactate dehydrogenase in *Cryptosporidium parvum*. *Int J Parasitol* 47(13)**,** 867-874. doi: 10.1016/j.ijpara.2017.05.002.

Wittenberg, D.F., Miller, N.M., and van den Ende, J. (1989). Spiramycin is not effective in treating cryptosporidium diarrhea in infants: results of a double-blind randomized trial. *J Infect Dis* 159(1)**,** 131-132. doi: 10.1093/infdis/159.1.131.

Woolf, G.M., Townsend, M., and Guyatt, G. (1987). Treatment of cryptosporidiosis with spiramycin in AIDS. An "N of 1" trial. *J Clin Gastroenterol* 9(6)**,** 632-634. doi: 10.1097/00004836-198712000-00005.

Wright, S.E., and Coop, R.L. (2007). "Cryptosporidiosis and Coccidiosis," in *Diseases of Sheep*. Blackwell Publishing), 179-185.

Xiao, L., Fayer, R., Ryan, U., and Upton, S.J. (2004). *Cryptosporidium* taxonomy: recent advances and implications for public health. *Clin Microbiol Rev* 17(1)**,** 72-97. doi: 10.1128/CMR.17.1.72-97.2004.

Xu, P., Widmer, G., Wang, Y., Ozaki, L.S., Alves, J.M., Serrano, M.G., et al. (2004). The genome of *Cryptosporidium hominis*. *Nature* 431(7012)**,** 1107-1112. doi: 10.1038/nature02977.

You, X., Schinazi, R.F., Arrowood, M.J., Lejkowski, M., Juodawlkis, A.S., and Mead, J.R. (1998). In-vitro activities of paromomycin and lasalocid evaluated in combination against *Cryptosporidium parvum*. *J Antimicrob Chemother* 41(2)**,** 293-296. doi: 10.1093/jac/41.2.293.

Zahedi, A., and Ryan, U. (2020). *Cryptosporidium* - An update with an emphasis on foodborne and waterborne transmission. *Res Vet Sci* 132**,** 500-512. doi: 10.1016/j.rvsc.2020.08.002.

Zambriski, J.A., Nydam, D.V., Wilcox, Z.J., Bowman, D.D., Mohammed, H.O., and Liotta, J.L. (2013). *Cryptosporidium parvum*: determination of ID_{50} and the dose-response relationship in experimentally challenged dairy calves. *Vet Parasitol* 197(1-2)**,** 104-112. doi: 10.1016/j.vetpar.2013.04.022.

Zhang, H., Guo, F., and Zhu, G. (2015). *Cryptosporidium* Lactate Dehydrogenase Is Associated with the Parasitophorous Vacuole Membrane and Is a Potential Target for Developing Therapeutics. *PLoS Pathog* 11(11)**,** e1005250. doi: 10.1371/journal.ppat.1005250.

Zhang, X., Kim, C.Y., Worthen, T., and Witola, W.H. (2018). Morpholino-mediated in vivo silencing of *Cryptosporidium parvum* lactate dehydrogenase decreases oocyst shedding and infectivity. *Int J Parasitol* 48(8)**,** 649-656. doi: 10.1016/j.ijpara.2018.01.005.

Zhu, G. (2007). "Biochemistry," in *Cryptosporidium and Cryptosporidiosis*, eds. R. Fayer & L. Xiao. Second ed (Boca Raton, FL: CRC Press), 57-78.

Zulu, I., Kelly, P., Njobvu, L., Sianongo, S., Kaonga, K., McDonald, V., et al. (2005). Nitazoxanide for persistent diarrhoea in Zambian acquired immune deficiency syndrome patients: a randomized-controlled trial. *Aliment Pharmacol Ther* 21(6)**,** 757-763. doi: 10.1111/j.1365-2036.2005.02394.x.

Zulu, I., Veitch, A., Sianongo, S., McPhail, G., Feakins, R., Farthing, M.J., et al. (2002). Albendazole chemotherapy for AIDS-related diarrhoea in Zambia--clinical, parasitological and mucosal responses. *Aliment Pharmacol Ther* 16(3)**,** 595-601. doi: 10.1046/j.1365-2036.2002.01182.x.